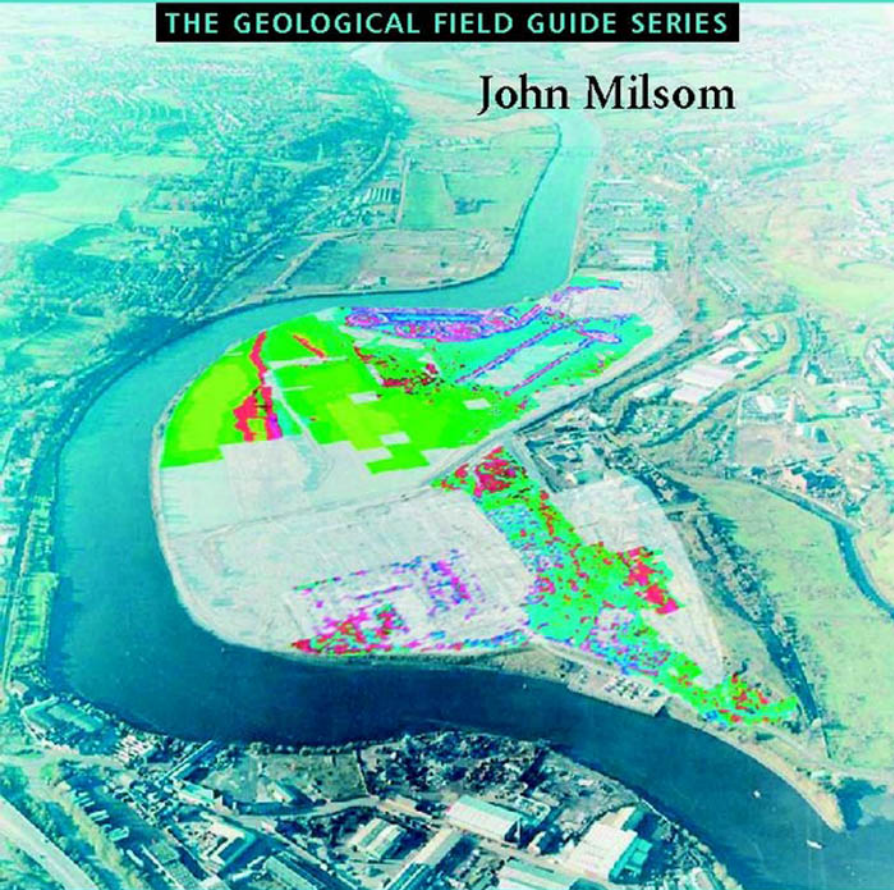


# Field Geophysics

THE GEOLOGICAL FIELD GUIDE SERIES

John Milsom



 WILEY

THIRD EDITION

# Field Geophysics

THIRD EDITION

John Milsom

*University College London*



WILEY



# **Field Geophysics**

## **The Geological Field Guide Series**

*Basic Geological Mapping, Third edition* John Barnes

*The Field Description of Metamorphic Rocks* Norman Fry

*The Mapping of Geological Structures* Ken McClay

*Field Geophysics, Third edition* John Milsom

*The Field Description of Igneous Rocks* Richard Thorpe & Geoff Brown

*Sedimentary Rocks in the Field, Second edition* Maurice Tucker

# Field Geophysics

THIRD EDITION

John Milsom

*University College London*



WILEY

Copyright © 2003 by

John Milsom

Published 2003 by

John Wiley & Sons Ltd,  
The Atrium, Southern Gate, Chichester,  
West Sussex PO19 8SQ, England

Telephone (+44) 1243 779777

Email (for orders and customer service enquiries): [cs-books@wiley.co.uk](mailto:cs-books@wiley.co.uk)

Visit our Home Page on [www.wileyeurope.com](http://www.wileyeurope.com) or [www.wiley.com](http://www.wiley.com)

First edition first published in 1989 by Open University Press, and Halsted Press (a division of John Wiley Inc.) in the USA, Canada and Latin America. Copyright © J. Milsom 1989.

Second edition first published in 1996 by John Wiley & Sons Ltd. Copyright © 1996 John Wiley & Sons Ltd.

All Rights Reserved. No part of this publication may be reproduced, stored in a retrieval system or transmitted in any form or by any means, electronic, mechanical, photocopying, recording, scanning or otherwise, except under the terms of the Copyright, Designs and Patents Act 1988 or under the terms of a licence issued by the Copyright Licensing Agency Ltd, 90 Tottenham Court Road, London W1T 4LP, UK, without the permission in writing of the Publisher. Requests to the Publisher should be addressed to the Permissions Department, John Wiley & Sons Ltd, The Atrium, Southern Gate, Chichester, West Sussex PO19 8SQ, England, or emailed to [permreq@wiley.co.uk](mailto:permreq@wiley.co.uk), or faxed to (+44) 1243 770620.

This publication is designed to provide accurate and authoritative information in regard to the subject matter covered. It is sold on the understanding that the Publisher is not engaged in rendering professional services. If professional advice or other expert assistance is required, the services of a competent professional should be sought.

### ***Other Wiley Editorial Offices***

John Wiley & Sons Inc., 111 River Street, Hoboken, NJ 07030, USA

Jossey-Bass, 989 Market Street, San Francisco, CA 94103-1741, USA

Wiley-VCH Verlag GmbH, Boschstr. 12, D-69469 Weinheim, Germany

John Wiley & Sons Australia Ltd, 33 Park Road, Milton, Queensland 4064, Australia

John Wiley & Sons (Asia) Pte Ltd, 2 Clementi Loop #02-01, Jin Xing Distripark, Singapore 129809

John Wiley & Sons Canada Ltd, 22 Worcester Road, Etobicoke, Ontario, Canada M9W 1L1

Wiley also publishes its books in a variety of electronic formats. Some content that appears in print may not be available in electronic books.

### ***Library of Congress Cataloging-in-Publication Data***

Milsom, John, 1939–

Field geophysics / John Milsom.—3rd ed.

p. cm. — (The geological field guide series)

Includes bibliographical references and index.

ISBN 0-470-84347-0 (alk. paper)

1. Prospecting—Geophysical methods. I. Title. II. Series.

TN269 .F445 2002

622'.15—dc21

2002191039

### ***British Library Cataloguing in Publication Data***

A catalogue record for this book is available from the British Library

ISBN 0-470-84347-0

Typeset in 8.5/10.5pt Times by Laserwords Private Limited, Chennai, India

Printed and bound in Great Britain by Antony Rowe Ltd, Chippenham, Wiltshire

This book is printed on acid-free paper responsibly manufactured from sustainable forestry in which at least two trees are planted for each one used for paper production.

# Contents

---

<b>Preface to the First Edition</b>	<b>vii</b>
<b>Preface to the Second Edition</b>	<b>ix</b>
<b>Preface to the Third Edition</b>	<b>xi</b>
<b>1 Introduction</b>	<b>1</b>
1.1 Fields	1
1.2 Geophysical Fieldwork	5
1.3 Geophysical Data	10
1.4 Bases and Base Networks	22
1.5 Global Positioning Satellites	25
<b>2 Gravity Method</b>	<b>29</b>
2.1 Physical Basis of the Gravity Method	29
2.2 Gravity Meters	31
2.3 Gravity Reductions	38
2.4 Gravity Surveys	41
2.5 Field Interpretation	46
<b>3 Magnetic Method</b>	<b>51</b>
3.1 Magnetic Properties	51
3.2 The Magnetic Field of the Earth	53
3.3 Magnetic Instruments	58
3.4 Magnetic Surveys	62
3.5 Simple Magnetic Interpretation	67
<b>4 Radiometric Surveys</b>	<b>71</b>
4.1 Natural Radiation	71
4.2 Radiation Detectors	75
4.3 Radiometric Surveys	78
<b>5 Electric Current Methods – General Considerations</b>	<b>83</b>
5.1 Resistivity and Conductivity	83
5.2 DC Methods	88
5.3 Varying Current Methods	91
<b>6 Resistivity Methods</b>	<b>97</b>
6.1 DC Survey Fundamentals	97
6.2 Resistivity Profiling	107
6.3 Resistivity Depth-sounding	108
6.4 Capacitative Coupling	113



<b>7</b>	<b>SP and IP</b>	<b>117</b>
7.1	SP Surveys	117
7.2	Polarization Fundamentals	120
7.3	Time-domain IP Surveys	122
7.4	Frequency-domain Surveys	124
7.5	IP Data	126
<b>8</b>	<b>Electromagnetic Methods</b>	<b>129</b>
8.1	Two-coil CW Systems	129
8.2	Other CWEM Techniques	140
8.3	Transient Electromagnetics	144
<b>9</b>	<b>VLF and CSAMT/MT</b>	<b>149</b>
9.1	VLF Radiation	149
9.2	VLF Instruments	155
9.3	Presentation of VLF Results	158
9.4	Natural and Controlled-source Audio-magnetotellurics	162
<b>10</b>	<b>Ground Penetrating Radar</b>	<b>167</b>
10.1	Radar Fundamentals	167
10.2	GPR Surveys	171
10.3	Data Processing	175
<b>11</b>	<b>Seismic Methods – General Considerations</b>	<b>179</b>
11.1	Seismic Waves	179
11.2	Seismic Sources	183
11.3	Detection of Seismic Waves	188
11.4	Recording Seismic Signals	192
<b>12</b>	<b>Seismic Reflection</b>	<b>197</b>
12.1	Reflection Theory	197
12.2	Reflection Surveys	201
<b>13</b>	<b>Seismic Refraction</b>	<b>207</b>
13.1	Refraction Surveys	207
13.2	Field Interpretation	211
13.3	Limitations of the Refraction Method	216
<b>Appendix Terrain Corrections for Hammer Zones B to M</b>		<b>223</b>
<b>Bibliography</b>		<b>225</b>
<b>Index</b>		<b>229</b>

## PREFACE TO THE FIRST EDITION

---

The purpose of this book is to help anyone involved in small-scale geophysical surveys. It is not a textbook in the traditional sense, in that it is designed for use in the field and concerns itself with practical matters – with theory taking second place. Where theory determines field practice, it is stated, not developed or justified. For example, no attempt is made to explain why four-electrode resistivity works where two-electrode surveys do not.

The book does not deal with marine, airborne or downhole geophysics, nor with deep seismic reflection work. In part this is dictated by the space available, but also by the fact that such surveys are usually carried out by quite large field crews, at least some of whom, it is to be hoped, are both experienced and willing to spread the benefit of that experience more widely.

Where appropriate, some attention is given to jargon. A field observer needs not only to know what to do but also the right words to use, and right in this context means the words which will be understood by others in the same line of business, if not by the compilers of standard dictionaries.

A word of apology is necessary. The field observer is sometimes referred to as ‘he’. This is unfortunately realistic, as ‘she’ is still all too rare, but is not intended to indicate that ‘she’ is either unknown or unwelcome in the geophysical world. It is hoped that all geophysical field workers, whether male or female and whether geophysicists, geologists or unspecialized field hands, will find something useful in this book.

Finally, a word of thanks. Paul Hayston of BP Minerals and Tim Langdale-Smith of Terronics read early drafts of the text and made numerous invaluable suggestions. To them, to Janet Baker, who drew many of the sketches, and to the companies which provided data and illustrations, I am extremely grateful.



## PREFACE TO THE SECOND EDITION

---

Since the first edition of this book was published in 1989, there have been some changes in the world of field geophysics, not least in its frequent appearance in television coverage of archaeological 'digs'. In this work, and in surveys of contaminated ground and landfill sites (the archaeological treasure houses of the future), very large numbers of readings are taken at very small spacings and writing down the results could absorb a major part of the entire time in the field. Automatic data logging has therefore become much more important and is being made ever easier as personal computers become smaller and more powerful. New field techniques have been developed and image processing methods are now routinely used to handle the large volumes of data. Comments made in the first edition on the need to record information about the survey area as well as geophysical data have equal, and perhaps even more, force in these instances, but it is obviously usually not practical or appropriate to make individual notes relating to individual readings.

The increase in the number of geophysical surveys directed at the very shallow subsurface (1–5 m) has also led to the increasing use of noncontacting (electromagnetic) methods of conductivity mapping. Moreover, the increased computing power now at every geophysicist's disposal has introduced inversion methods into the interpretation of conventional direct current resistivity soundings and has required corresponding modifications to field operations. It is hoped that these changes are adequately covered in this new edition. A further development has been the much wider availability of ground penetrating radar systems and a recent and fairly rapid fall in their cost. A chapter has been added to cover this relatively new method.

Much else has remained unchanged, and advances in airborne techniques have actually inhibited research into improving ground-based instrumentation for mineral exploration. Automatic and self-levelling gravity meters are becoming more widely available, but are still fairly uncommon. Magnetometers more sensitive than the conventional proton precession or fluxgate instruments are widely advertised, but in most circumstances provide more precision than can be readily used, except in the measurement of field gradients. VLF methods are enjoying something of a revival in exploration for fracture aquifers in basement rocks, and the importance of ease of use is being recognized by manufacturers. Instruments for induced polarization and time-domain electromagnetic surveys also continue to be improved, but their

basic principles remain unchanged. More use is being made of reflected seismic waves, partly because of the formerly undreamed of processing power now available in portable field seismographs, but refraction still dominates seismic studies of the shallow subsurface.

Inevitably, not all the methods currently in use could be covered in the space available. Seismo-electrical methods, in which the source pulses are mechanical and the signal pulses are electrical, are beginning to make their presence felt and may demand a place in textbooks in the future. Few case histories have yet been published. Magnetotelluric methods have a much longer history and continue to be developed, in conjunction with developments in the use of controlled (CSAMT) rather than natural sources, but many general purpose geophysicists will go through their entire careers without being involved in one such survey.

Despite the considerable rewriting, and the slight increase in size (for which I am immensely grateful to the new publishers), the aim of the book remains the same. Like its predecessor it is not a textbook in the conventional sense, but aims to provide practical information and assistance to anyone engaged in small-scale surveys on the ground. In helping me towards this objective, I am grateful particularly to Paul Hayston (RTZ) for introducing me to mineral exploration in a new and exciting area, to Asgeir Eriksen of Geophysical Services International (UK) for keeping me in touch with the realities of engineering and ground-water geophysics, and to my students for reminding me every year of where the worst problems lie. I am also grateful to all those who have given their permission for illustrations to be reproduced (including my daughter, Kate, whose view of field geophysics is shown in Fig. 5.1), and most especially to my wife, Pam, for retyping the original text and for putting up with this all over again.

John Milsom

## PREFACE TO THE THIRD EDITION

---

In the decade and a half since the preparation of the first edition of this handbook there have been few fundamental changes in the methods used in small-scale ground geophysical surveys. There have, however, been radical changes in instrumentation, and far-reaching developments in applications. The use of geophysics in mineral exploration has declined, both in absolute terms (along with the world-wide decline in the mining industry itself), and relative to other uses. What is loosely termed environmental, engineering or industrial geophysics has taken up much of the slack. Sadly, the search for unexploded ordnance (UXO) is also assuming ever-increasing importance as more and more parts of the world become littered with the detritus of military training and military operations (the much more lethal search for landmines which, unlike UXO, are deliberately designed to escape detection, also uses geophysical methods but is emphatically *not* covered in this book). Archaeological usage is also increasing, although still inhibited in many cases by the relatively high cost of the equipment.

In instrumentation, the automation of reading and data storage, which was only just becoming significant in the late 1980s, has proceeded apace. Virtually all the new instruments coming on to the market incorporate data loggers and many include devices (such as automatic levelling) to make operations quicker and easier. This, and the fact that virtually every field crew now goes into the field equipped with at least one laptop PC, has had two main, and contrasting, consequences. On the one hand, the need for specialist skills in the field personnel actually operating the instruments has been reduced, and this is leading to a general decline in the quality of field notes. On the other hand, much more can now be done in the field by way of processing and data display, and even interpretation. The change is exemplified by ground radar units, which provide users with visual (even though distorted) pictures of the subsurface while the survey is actually under way. Interestingly, the trend towards instruments that provide effectively continuous coverage as they are dragged or carried along lines has led to the emergence in ground surveys of errors that have long plagued airborne surveys but have now been largely eliminated there. Comments made in the first edition on the need to record information about the survey area as well as geophysical data have equal, and perhaps even more, force in these instances, but it is obviously usually neither practical nor appropriate to make individual notes relating to individual readings.

The increase in the number of geophysical surveys directed at the very shallow subsurface (1–5 m) has also led to the increasing use of electromagnetic methods of conductivity mapping and the development of non-contacting electrical methods which use capacitative rather than inductive coupling. A chapter section has been added to cover this latter, relatively new, method. Other new sections deal with GPS navigation, which has become immensely more useful to geophysicists since the removal of ‘selective availability’ and with audio-magnetotellurics (AMT), largely considered in the context of controlled sources (CSAMT) that mimic the natural signals but provide greater consistency.

There has also been a slight change in the notes and bibliography. Providing references to individual papers is a problem in a book of this size, and I have actually reduced the number of such references, confining myself to older papers containing some fundamental discussion, and to papers that are the sources of illustrations used. I have also eliminated the section on manufacturers’ literature, not because this literature is any less voluminous or important, but because it is now largely available through the Internet. A number of key URLs are therefore given.

Despite the considerable rewriting, and the slight increase in size (for which I am again immensely grateful to the publishers), the aim of the book remains unchanged. Like its predecessors, it is not a textbook in the conventional sense, but aims to provide practical information and assistance to anyone engaged in small-scale surveys on the ground. In helping me towards achieving this objective, I am grateful particularly to Chris Leech of Geomatrix for involving me in some of his training and demonstration surveys, to Asgeir Eriksen of Geophysical Services International (UK) for keeping me in touch with the realities of engineering and groundwater geophysics, and to my students for incisive and uninhibited criticisms of earlier editions. I am also grateful to all those who have given their permission for illustrations to be reproduced (including my daughter, Kate, whose view of field geophysics is shown in Figure 5.1), and most especially to my wife, Pam, for exhaustive (and exhausting) proofreading and for putting up with this for a third time.

# 1

## INTRODUCTION

---

### 1.1 Fields

Although there are many different geophysical methods, small-scale surveys all tend to be rather alike and involve similar, and sometimes ambiguous, jargon. For example, the word *base* has three different common meanings, and *stacked* and *field* have two each.

Measurements in geophysical surveys are made *in the field* but, unfortunately, many are also *of* fields. Field theory is fundamental to gravity, magnetic and electromagnetic work, and even particle fluxes and seismic wavefronts can be described in terms of radiation fields. Sometimes ambiguity is unimportant, and sometimes both meanings are appropriate (and intended), but there are occasions when it is necessary to make clear distinctions. In particular, the term *field reading* is almost always used to identify readings made *in* the field, i.e. not at a base station.

The fields used in geophysical surveys may be natural ones (e.g. the Earth's magnetic or gravity fields) but may be created artificially, as when alternating currents are used to generate electromagnetic fields. This leads to the broad classification of geophysical methods into *passive* and *active* types, respectively.

Physical fields can be illustrated by lines of force that show the field direction at any point. Intensity can also be indicated, by using more closely spaced lines for strong fields, but it is difficult to do this quantitatively where three-dimensional situations are being illustrated on two-dimensional media.

#### 1.1.1 Vector addition

Vector addition (Figure 1.1) must be used when combining fields from different sources. In passive methods, knowledge of the principles of vector addition is needed to understand the ways in which measurements of local anomalies are affected by regional backgrounds. In active methods, a local anomaly (*secondary* field) is often superimposed on a *primary* field produced by a transmitter. In either case, if the local field is much the weaker of the two (in practice, less than one-tenth the strength of the primary or background field), then the measurement will, to a first approximation, be made in the direction of the stronger field and only the component in this direction of the secondary field ( $c_a$  in Figure 1.1) will be measured. In most surveys the slight difference in direction between the resultant and the background or primary field can be ignored.



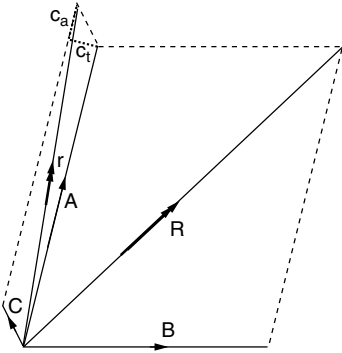


**Figure 1.1** Vector addition by the parallelogram rule. Fields represented in magnitude and direction by the vectors  $A$  and  $B$  combine to give the resultant  $R$ . The resultant  $r$  of  $A$  and the smaller field  $C$  is approximately equal in length to the sum of  $A$  and the component  $c_a$  of  $C$  in the direction of  $A$ . The transverse component  $c_t$  rotates the resultant but has little effect on its magnitude.

effect), and the interactions between fields and currents in electrical and electromagnetic surveys can be very complex.

If the two fields are similar in strength, there will be no simple relationship between the magnitude of the anomalous field and the magnitude of the observed anomaly. However, variations in any given component of the secondary field can be estimated by taking all measurements in an appropriate direction and assuming that the component of the background or primary field in this direction is constant over the survey area. Measurements of vertical rather than total fields are sometimes preferred in magnetic and electromagnetic surveys for this reason.

The fields due to multiple sources are not necessarily equal to the vector sums of the fields that would have existed had those sources been present in isolation. A strong magnetic field from one body can affect the magnetization in another, or even in itself (*demagnetization*

### 1.1.2 The inverse-square law

Inverse-square law attenuation of signal strength occurs in most branches of applied geophysics. It is at its simplest in gravity work, where the field due to a point mass is inversely proportional to the square of the distance from the mass, and the constant of proportionality (the *gravitational constant*  $G$ ) is invariant. Magnetic fields also obey an inverse-square law. The fact that their strength is, in principle, modified by the permeability of the medium is irrelevant in most geophysical work, where measurements are made in either air or water. Magnetic sources are, however, essentially bipolar, and the modifications to the simple inverse-square law due to this fact are much more important (Section 1.1.5).

Electric current flowing from an isolated point electrode embedded in a continuous homogeneous ground provides a physical illustration of the

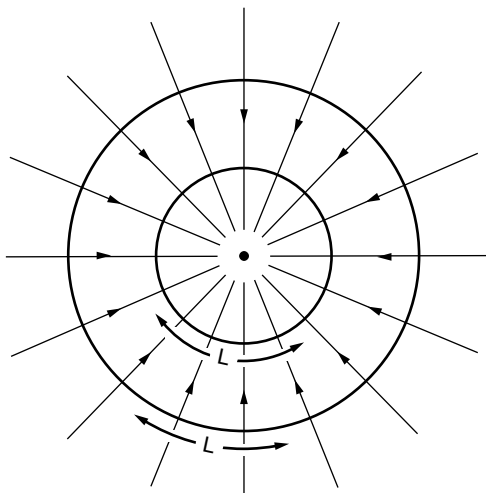


**Figure 1.2** Lines of force from an infinite line source (viewed end on). The distance between the lines increases linearly with distance from the source so that an arc of length  $L$  on the inner circle is cut by four lines but an arc of the same length on the outer circle, with double the radius, is cut by only two.

significance of the inverse-square law. All of the current leaving the electrode must cross any closed surface that surrounds it. If this surface is a sphere concentric with the electrode, the same fraction of the total current will cross each unit area on the surface of the sphere. The current *per unit area* will therefore be inversely proportional to the *total* surface area, which is in turn proportional to the square of the radius. Current flow in the real Earth is, of course, drastically modified by conductivity variations.

### 1.1.3 Two-dimensional sources

Rates of decrease in field strengths depend on source shapes as well as on the inverse-square law. Infinitely long sources of constant cross-section are termed *two-dimensional (2D)* and are often used in computer modelling to approximate bodies of large strike extent. If the source ‘point’ in Figure 1.2 represents an infinite line source seen end on, the area of the enclosing (cylindrical) surface is proportional to the radius. The argument applied in the previous section to a point source implies that in this case the field strength is inversely proportional to distance and not to its square. In 2D situations, lines of force drawn on pieces of paper illustrate field magnitude (by their separation) as well as direction.

## 1.1.4 One-dimensional sources

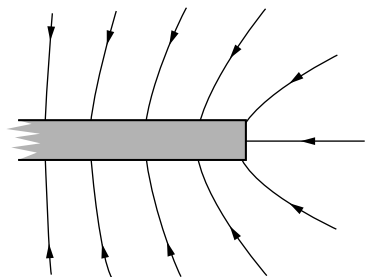


**Figure 1.3** Lines of force from a semi-infinite slab. The lines diverge appreciably only near the edge of the slab, implying that towards the centre of the slab the field strength will decrease negligibly with distance.

The lines of force or radiation intensity from a source consisting of a homogeneous layer of constant thickness diverge only near its edges (Figure 1.3). The *Bouguer plate* of gravity reductions (Section 2.5.1) and the radioactive source with  $2\pi$  geometry (Section 4.3.3) are examples of infinitely extended layer sources, for which field strengths are independent of distance. This condition is approximately achieved if a detector is only a short distance above an extended source and a long way from its edges.

## 1.1.5 Dipoles

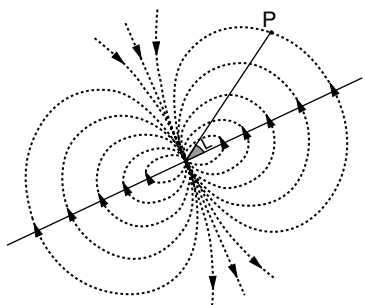


**Figure 1.4** The dipole field. The plane through the dipole at right angles to its axis is known as the equatorial plane, and the angle ( $L$ ) between this plane and the line joining the centre of the dipole to any point ( $P$ ) is sometimes referred to as the latitude of  $P$ .

A dipole consists of equal-strength positive and negative point sources a very small distance apart. Field strength decreases as the inverse cube of distance and both strength and direction change with 'latitude' (Figure 1.4). The intensity of the field at a point on a dipole axis is double the intensity at a point the same distance away on the dipole 'equator', and in the opposite direction.

Electrodes are used in some electrical surveys in approximately dipolar pairs and magnetization is fundamentally dipolar. Electric currents circulating in small loops are dipolar sources of magnetic field.

## 1.1.6 Exponential decay

Radioactive particle fluxes and seismic and electromagnetic waves are subject to absorption as well as geometrical attenuation, and the energy crossing

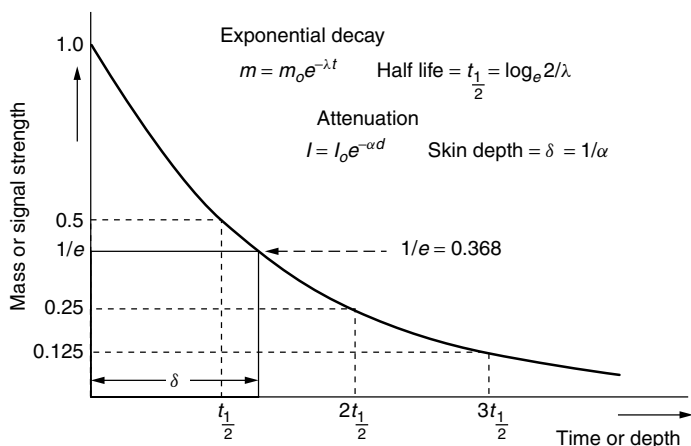


**Figure 1.5** The exponential law, illustrating the parameters used to characterize radioactive decay and radio wave attenuation.

closed surfaces is then less than the energy emitted by the sources they enclose. In homogeneous media, the percentage loss of signal is determined by the path length and the *attenuation constant*. The absolute loss is proportional also to the signal strength. A similar *exponential law* (Figure 1.5), governed by a *decay constant*, determines the rate of loss of mass by a radioactive substance.

Attenuation rates are alternatively characterized by *skin depths*, which are the reciprocals of attenuation constants. For each skin depth travelled, the signal strength decreases to  $1/e$  of its original value, where  $e$  ( $= 2.718$ ) is the base of natural logarithms. Radioactivity decay rates are normally described in terms of the *half-lives*, equal to  $\log_e 2$  ( $= 0.693$ ) divided by the decay constant. During each half-life period, one half of the material present at its start is lost.

## 1.2 Geophysical Fieldwork

Geophysical instruments vary widely in size and complexity but all are used to make physical measurements, of the sort commonly made in laboratories, at temporary sites in sometimes hostile conditions. They should be economical in power use, portable, rugged, reliable and simple. These criteria are satisfied to varying extents by the commercial equipment currently available.

### 1.2.1 Choosing geophysical instruments

Few instrument designers can have tried using their own products for long periods in the field, since operator comfort seldom seems to have been

considered. Moreover, although many real improvements have been made in the last 30 years, design features have been introduced during the same period, for no obvious reasons, that have actually made fieldwork more difficult. The proton magnetometer staff, discussed below, is a case in point.

If different instruments can, in principle, do the same job to the same standards, practical considerations become paramount. Some of these are listed below.

*Serviceability:* Is the manual comprehensive and comprehensible? Is a breakdown likely to be repairable in the field? Are there facilities for repairing major failures in the country of use or would the instrument have to be sent overseas, risking long delays en route and in customs? Reliability is vital but some manufacturers seem to use their customers to evaluate prototypes.

*Power supplies:* If dry batteries are used, are they of types easy to replace or will they be impossible to find outside major cities? If rechargeable batteries are used, how heavy are they? In either case, how long will the batteries last at the temperatures expected in the field? Note that battery life is reduced in cold climates. The reduction can be dramatic if one of the functions of the battery is to keep the instrument at a constant temperature.

*Data displays:* Are these clearly legible under all circumstances? A torch is needed to read some in poor light and others are almost invisible in bright sunlight. Large displays used to show continuous traces or profiles can exhaust power supplies very quickly.

*Hard copy:* If hard copy records can be produced directly from the field instrument, are they of adequate quality? Are they truly permanent, or will they become illegible if they get wet, are abraded or are exposed to sunlight?

*Comfort:* Is prolonged use likely to cripple the operator? Some instruments are designed to be suspended on a strap passing across the back of the neck. This is tiring under any circumstances and can cause serious medical problems if the instrument has to be levelled by bracing it against the strap. Passing the strap over one shoulder and under the other arm may reduce the strain but not all instruments are easy to use when carried in this way.

*Convenience:* If the instrument is placed on the ground, will it stand upright? Is the cable then long enough to reach the sensor in its normal operating position? If the sensor is mounted on a tripod or pole, is this strong enough? The traditional proton magnetometer poles, in sections that screwed together and ended in spikes that could be stuck into soft ground, have now been largely replaced by unspiked hinged rods that are more awkward to stow away, much more fragile (the hinges can twist and break), can only be used if fully extended and must be supported at all times.

*Fieldworthiness:* Are the control knobs and connectors protected from accidental impact? Is the casing truly waterproof? Does protection from damp

grass depend on the instrument being set down in a certain way? Are there depressions on the console where moisture will collect and then inevitably seep inside?

*Automation:* Computer control has been introduced into almost all the instruments in current production (although older, less sophisticated models are still in common use). Switches have almost vanished, and every instruction has to be entered via a keypad. This has reduced the problems that used to be caused by electrical spikes generated by switches but, because the settings are often not permanently visible, unsuitable values may be repeatedly used in error. Moreover, simple operations have sometimes been made unduly complicated by the need to access nested menus. Some instruments do not allow readings to be taken until line and station numbers have been entered and some even demand to know the distance to the next station and to the next line!

The computer revolution has produced real advances in field geophysics, but it has its drawbacks. Most notably, the ability to store data digitally in data loggers has discouraged the making of notes on field conditions where these, however important, do not fall within the restricted range of options the logger provides. This problem is further discussed in Section 1.3.2.

### 1.2.2 Cables

Almost all geophysical work involves cables, which may be short, linking instruments to sensors or batteries, or hundreds of metres long. Electrical induction between cables (electromagnetic coupling, also known as *cross-talk*) can be a serious source of noise (see also Section 11.3.5).

Efficiency in cable handling is an absolute necessity. Long cables always tend to become tangled, often because of well-intentioned attempts to make neat coils using hand and elbow. Figures of eight are better than simple loops, but even so it takes an expert to construct a coil from which cable can be run freely once it has been removed from the arm. On the other hand, a seemingly chaotic pile of wire spread loosely on the ground can be quite trouble-free. The basic rule is that cable must be fed on and off the pile in opposite directions, i.e. the last bit of cable fed on must be the first to be pulled off. Any attempts to pull cable from the bottom will almost certainly end in disaster.

Cable piles are also unlikely to cause the permanent kinks which are often features of neat and tidy coils and which may have to be removed by allowing the cable to hang freely and untwist naturally. Places where this is possible with 100-metre lengths are rare.

Piles can be made portable by feeding cables into open boxes, and on many seismic surveys the shot-firers carried their firing lines in this way in old gellignite boxes. Ideally, however, if cables are to be carried from place

to place, they should be wound on properly designed drums. Even then, problems can occur. If cable is unwound by pulling on its free end, the drum will not stop simply because the pull stops, and a free-running drum is an effective, but untidy, knitting machine.

A drum carried as a back-pack should have an efficient brake and should be reversible so that it can be carried across the chest and be wound from a standing position. Some drums sold with geophysical instruments combine total impracticality with inordinate expense and are inferior to home-made or garden-centre versions.

Geophysical lines exert an almost hypnotic influence on livestock. Cattle have been known to desert lush pastures in favour of midnight treks through hedges and across ditches in search of juicy cables. Not only can a survey be delayed but a valuable animal may be killed by biting into a live conductor, and constant vigilance is essential.

### 1.2.3 Connections

Crocodile clips are usually adequate for electrical connections between single conductors. Heavy plugs must be used for multi-conductor connections and are usually the weakest links in the entire field system. They should be placed on the ground very gently and as seldom as possible and, if they do not have screw-on caps, be protected with plastic bags or 'clingfilm'. They must be shielded from grit as well as moisture. Faults are often caused by dirt increasing wear on the contacts in socket units, which are almost impossible to clean.

Plugs should be clamped to their cables, since any strain will otherwise be borne by the weak soldered connections to the individual pins. Inevitably, the cables are flexed repeatedly just beyond the clamps, and wires may break within the insulated sleeving at these points. Any break there, or a broken or dry joint inside the plug, means work with a soldering iron. This is never easy when connector pins are clotted with old solder, and is especially difficult if many wires crowd into a single plug.

Problems with plugs can be minimized by ensuring that, when moving, they are always carried, never dragged along the ground. Two hands should always be used, one holding the cable to take the strain of any sudden pull, the other to support the plug itself. The rate at which cable is reeled in should never exceed a comfortable walking pace, and especial care is needed when the last few metres are being wound on to a drum. Drums should be fitted with clips or sockets where the plugs can be secured when not in use.

### 1.2.4 Geophysics in the rain

A geophysicist, huddled over his instruments, is a sitting target for rain, hail, snow and dust, as well as mosquitoes, snakes and dogs. His most useful piece

of field clothing is often a large waterproof cape which he can not only wrap around himself but into which he can retreat, along with his instruments, to continue work (Figure 1.6).

Electrical methods that rely on direct or close contact with the ground generally do not work in the rain, and heavy rain can be a source of seismic noise. Other types of survey can continue, since most geophysical instruments are supposed to be waterproof and some actually are. However, unless dry weather can be guaranteed, a field party should be plentifully supplied with plastic bags and sheeting to protect instruments, and paper towels for



**Figure 1.6** *The geophysical cape in action. Magnetometer and observer are both dry, with only the sensor bottle exposed to the elements.*



drying them. Large transparent plastic bags can often be used to enclose instruments completely while they are being used, but even then condensation may create new conductive paths, leading to drift and erratic behaviour. Silica gel within instruments can absorb minor traces of moisture but cannot cope with large amounts, and a portable hair-drier held at the base camp may be invaluable.

### 1.2.5 A geophysical toolkit

Regardless of the specific type of geophysical survey, similar tools are likely to be needed. A field toolkit should include the following:

- Long-nose pliers (the longer and thinner the better)
- Slot-head screwdrivers (one very fine, one normal)
- Phillips screwdriver
- Allen keys (metric and imperial)
- Scalpels (light, expendable types are best)
- Wire cutters/strippers
- Electrical contact cleaner (spray)
- Fine-point 12V soldering iron
- Solder and ‘Solder-sucker’
- Multimeter (mainly for continuity and battery checks, so small size and durability are more important than high sensitivity)
- Torch (preferably of a type that will stand unsupported and double as a table lamp. A ‘head torch’ can be very useful)
- Hand lens
- Insulating tape, preferably self-amalgamating
- Strong epoxy glue/‘super-glue’
- Silicone grease
- Waterproof sealing compound
- Spare insulated and bare wire, and connectors
- Spare insulating sleeving
- Kitchen cloths and paper towels
- Plastic bags and ‘clingfilm’

A comprehensive first-aid kit is equally vital.

## 1.3 Geophysical Data

Some geophysical readings are of true *point data* but others are obtained using sources that are separated from detectors. Where values are determined *between* rather than *at* points, readings will be affected by orientation. Precise field notes are always important but especially so in these cases, since reading points must be defined and orientations must be recorded.

If transmitters, receivers and/or electrodes are laid out in straight lines and the whole system can be reversed without changing the reading, the mid-point should be considered the reading point. Special notations are needed for asymmetric systems, and the increased probability of positioning error is in itself a reason for avoiding asymmetry. Especial care must be taken when recording the positions of sources and detectors in seismic work.

### 1.3.1 Station numbering

Station numbering should be logical and consistent. Where data are collected along traverses, numbers should define positions in relation to the traverse grid. Infilling between traverse stations 3 and 4 with stations  $3\frac{1}{4}$ ,  $3\frac{1}{2}$  and  $3\frac{3}{4}$  is clumsy and may create typing problems, whereas defining as 325E a station halfway between stations 300E and 350E, which are 50 metres apart, is easy and unambiguous. The fashion for labelling such a station 300+25E has no discernible advantages and uses a plus sign which may be needed, with digital field systems or in subsequent processing, to stand for N or E. It may be worth defining the grid origin in such a way that S or W stations do not occur, and this may be essential with data loggers that cannot cope with either negatives or points of the compass.

Stations scattered randomly through an area are best numbered sequentially. Positions can be recorded in the field by pricking through maps or air-photos and labelling the reverse sides. Estimating coordinates in the field from maps may seem desirable but mistakes are easily made and valuable time is lost. Station coordinates are now often obtained from GPS receivers (Section 1.5), but differential GPS may be needed to provide sufficient accuracy for detailed surveys.

If several observers are involved in a single survey, numbers can easily be accidentally duplicated. All field books and sheets should record the name of the observer. The interpreter or data processor will need to know who to look for when things go wrong.

### 1.3.2 Recording results

Geophysical results are primarily numerical and must be recorded even more carefully than qualitative observations of field geology. Words, although sometimes difficult to read, can usually be deciphered eventually, but a set of numbers may be wholly illegible or, even worse, may be misread. The need for extra care has to be reconciled with the fact that geophysical observers are usually in more of a hurry than are geologists, since their work may involve instruments that are subject to drift, draw power from batteries at frightening speed or are on hire at high daily rates.

Numbers may, of course, not only be misread but miswritten. The circumstances under which data are recorded in the field are varied but seldom

ideal. Observers are usually either too hot, too cold, too wet or too thirsty. Under such conditions, they may delete correct results and replace them with incorrect ones, in moments of confusion or temporary dyslexia. Data on geophysical field sheets should therefore never be erased. Corrections should be made by crossing out the incorrect items, preserving their legibility, and writing the correct values alongside. Something may then be salvaged even if the correction is wrong. Precise reporting standards must be enforced and strict routines must be followed if errors are to be minimized. Reading the instrument twice at each occupation of a station, and recording both values, reduces the incidence of major errors.

Loss of geophysical data tends to be final. Some of the qualitative observations in a geological notebook might be remembered and re-recorded, but not strings of numbers. Copies are therefore essential and should be made in the field, using duplicating sheets or carbon paper, or by transcribing the results each evening. Whichever method is used, originals and duplicates must be separated immediately and stored separately thereafter. Duplication is useless if copies are stored, and lost, together. This, of course, applies equally to data stored in a data logger incorporated in, or linked to, the field instrument. Such data should be checked, and backed up, each evening.

Digital data loggers are usually poorly adapted to storing non-numeric information, but observers are uniquely placed to note and comment on a multitude of topographic, geological, manmade (*cultural*) and climatic factors that may affect the geophysical results. If they fail to do so, the data that they have gathered may be interpreted incorrectly. If data loggers are not being used, comments should normally be recorded in notebooks, alongside the readings concerned. If they are being used, adequate supplementary positional data must be stored elsewhere. In archaeological and site investigation surveys, where large numbers of readings are taken in very small areas, annotated sketches are always useful and may be essential. Sketch maps should be made wherever the distances of survey points or lines from features in the environment are important. Geophysical field workers may also have a responsibility to pass on to their geological colleagues information of interest about places that only they may visit. They should at least be willing to record dips and strikes, and perhaps to return with rock samples where these would be useful.

### 1.3.3 Accuracy, sensitivity, precision

Accuracy must be distinguished from sensitivity. A standard gravity meter, for example, is sensitive to field changes of one-tenth of a gravity unit but an equivalent level of accuracy will be achieved only if readings are carefully made and drift and tidal corrections are correctly applied. Accuracy is thus limited, but not determined, by instrument sensitivity. Precision,

which is concerned only with the numerical presentation of results (e.g. the number of decimal places used), should always be appropriate to accuracy (Example 1.1). Not only does superfluous precision waste time but false conclusions may be drawn from the high implied accuracy.

---

### Example 1.1

Gravity reading = 858.3 scale units

Calibration constant = 1.0245 g.u. per scale division (see Section 2.1)

Converted reading = 879.32835 g.u.

But reading accuracy is only 0.1 g.u. (approximately), and therefore:

Converted reading = 879.3 g.u.

(Four decimal place precision is needed in the calibration constant, because 858.3 multiplied by 0.0001 is equal to almost 0.1 g.u.)

---

Geophysical measurements can sometimes be made to a greater accuracy than is needed, or even usable, by the interpreters. However, the highest possible accuracy should always be sought, as later advances may allow the data to be analysed more effectively.

### 1.3.4 Drift

A geophysical instrument will usually not record the same results if read repeatedly at the same place. This may be due to changes in background field but can also be caused by changes in the instrument itself, i.e. to *drift*. Drift correction is often the essential first stage in data analysis, and is usually based on repeat readings at *base stations* (Section 1.4).

Instrument drift is often related to temperature and is unlikely to be linear between two readings taken in the relative cool at the beginning and end of a day if temperatures are 10 or 20 degrees higher at noon. Survey *loops* may therefore have to be limited to periods of only one or two hours.

Drift calculations should be made whilst the field crew is still in the survey area so that readings may be repeated if the drift-corrected results appear questionable. Changes in background field are sometimes treated as drift but in most cases the variations can either be monitored directly (as in magnetics) or calculated (as in gravity). Where such alternatives exist, it is preferable they be used, since poor instrument performance may otherwise be overlooked.

### 1.3.5 Signal and noise

To a geophysicist, *signal* is the object of the survey and *noise* is anything else that is measured but is considered to contain no useful information. One observer's signal may be another's noise. The magnetic effect of a buried

pipe is a nuisance when interpreting magnetic data in geological terms but may be invaluable to a site developer. Much geophysical field practice is dictated by the need to improve signal-to-noise ratios. In many cases, as in magnetic surveys, variations in a background field are a source of noise and must be precisely monitored.

The statistics of random noise are important in seismic, radiometric and induced polarization (IP) surveys. Adding together  $N$  statistically long random series, each of average amplitude  $A$ , produces a random series with average amplitude  $A \times \sqrt{N}$ . Since  $N$  identical signals of average amplitude  $A$  treated in the same way produce a signal of amplitude  $A \times N$ , adding together (*stacking*)  $N$  signals containing some random noise should improve signal-to-noise ratios by a factor of  $\sqrt{N}$ .

## 1.3.6 Variance and standard deviation

Random variations often follow a *normal* or *Gaussian* distribution law, described by a bell-shaped probability curve. Normal distributions can be characterized by *means* (equal to the sums of all the values divided by the total number of values) and *variances* (defined in Figure 1.7) or their square-roots, the *standard deviations* (SD). About two-thirds of the readings in a

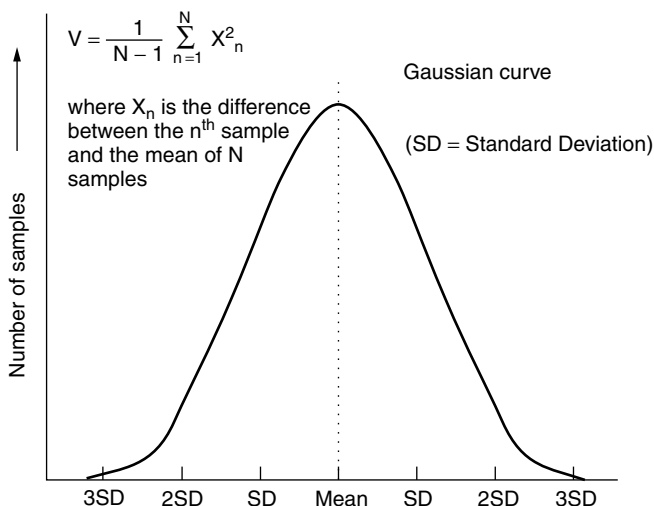


**Figure 1.7** Gaussian distribution. The curve is symmetric, and approximately two-thirds of the area beneath it (i.e. two-thirds of the total number of samples) lies within one standard deviation (SD) of the mean.

normal distribution lie within 1 SD of the mean, and less than 0.3% differ from it by more than 3 SDs. The SD is popular with contractors when quoting survey reliability, since a small value can efficiently conceal several major errors. Geophysical surveys rarely provide enough field data for statistical methods to be validly applied, and distributions are more often assumed to be normal than proven to be so.

### 1.3.7 Anomalies

Only rarely is a single geophysical observation significant. Usually, many readings are needed, and regional background levels must be determined, before interpretation can begin. Interpreters tend to concentrate on *anomalies*, i.e. on differences from a constant or smoothly varying background. Geophysical anomalies take many forms. A massive sulphide deposit containing pyrrhotite would be dense, magnetic and electrically conductive. Typical anomaly profiles recorded over such a body by various types of geophysical survey are shown in Figure 1.8. A wide variety of possible contour patterns correspond to these differently shaped profiles.

Background fields also vary and may, at different scales, be regarded as anomalous. A 'mineralization' gravity anomaly, for example, might lie on a broader high due to a mass of basic rock. Separation of regionals from residuals is an important part of geophysical data processing and even in the field it may be necessary to estimate background so that the significance of local anomalies can be assessed. On profiles, background fields estimated by eye may be more reliable than those obtained using a computer, because of the virtual impossibility of writing a computer program that will produce a background field uninfluenced by the anomalous values (Figure 1.9). Computer methods are, however, essential when deriving backgrounds from data gathered over an area rather than along a single line.

The existence of an anomaly indicates a difference between the real world and some simple model, and in gravity work the terms *free air*, *Bouguer* and *isostatic anomaly* are commonly used to denote derived quantities that represent differences from gross Earth models. These so-called anomalies are sometimes almost constant within a small survey area, i.e. the area is not anomalous! Use of terms such as *Bouguer gravity* (rather than *Bouguer anomaly*) avoids this confusion.

### 1.3.8 Wavelengths and half-widths

Geophysical anomalies in profile often resemble transient waves but vary in space rather than time. In describing them the terms *frequency* and *frequency content* are often loosely used, although *wavenumber* (the number of complete waves in unit distance) is pedantically correct. *Wavelength* may be quite properly used of a spatially varying quantity, but is imprecise where

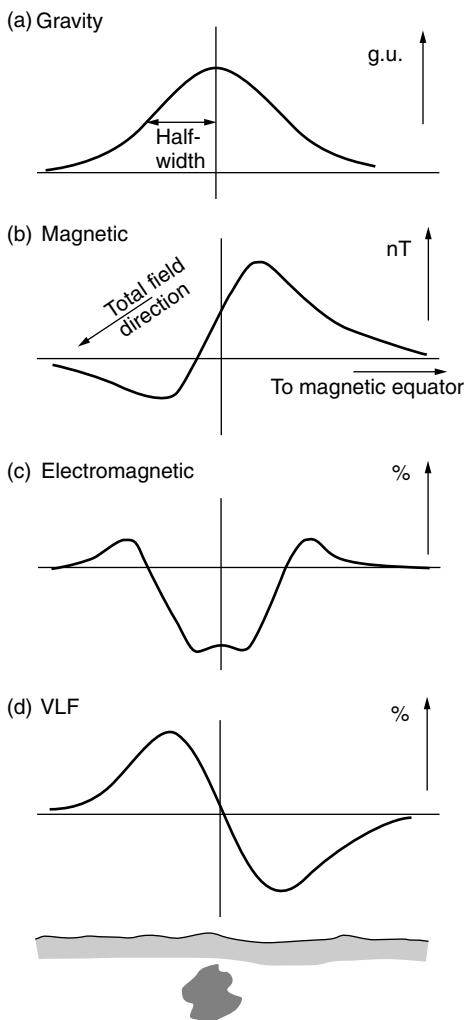


**Figure 1.8** Geophysical profiles across a pyrrhotite-bearing sulphide mass. The amplitude of the gravity anomaly (a) might be a few g.u. and of the magnetic anomaly (b) a few hundred nT. The electromagnetic anomalies are for (c) a two-coil co-planar system and (d) a VLF dip-angle system. Neither of these is likely to have an amplitude of more than about 20%.

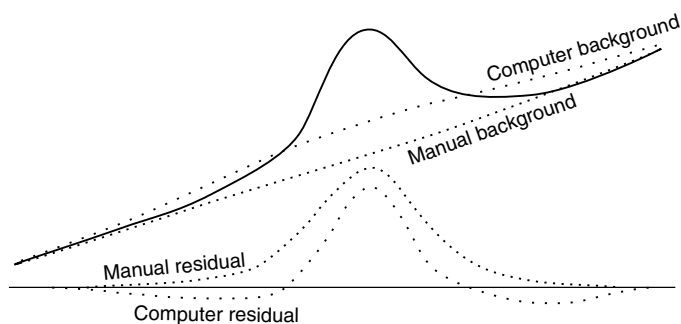


**Figure 1.9** *Computer and manual residuals. The background field drawn by eye recognizes the separation between regional and local anomaly, and the corresponding residual anomaly is probably a good approximation to the actual effect of the local source. The computer-drawn background field is biased by the presence of the local anomaly, and the corresponding residual anomaly is therefore flanked by troughs.*

geophysical anomalies are concerned because an anomaly described as having a single ‘wavelength’ would be resolved by Fourier analysis into a number of components of different wavelengths.

A more easily estimated quantity is the *half-width*, which is equal to half the distance between the points at which the amplitude has fallen to half the anomaly maximum (cf. Figure 1.8a). This is roughly equal to a quarter of the wavelength of the dominant sinusoidal component, but has the advantage of being directly measurable on field data. Wavelengths and half-widths are important because they are related to the depths of sources. Other things being equal, the deeper the source, the broader the anomaly.

### 1.3.9 Presentation of results

The results of surveys along traverse lines can be presented in profile form, as in Figure 1.8. It is usually possible to plot profiles in the field, or at least each evening, as work progresses, and such plots are vital for quality control. A laptop computer can reduce the work involved, and many modern instruments and data loggers are programmed to display profiles in ‘real time’ as work proceeds.

A traverse line drawn on a topographic map can be used as the baseline for a geophysical profile. This type of presentation is particularly helpful in identifying anomalies due to manmade features, since correlations with features such as roads and field boundaries are obvious. If profiles along a number of different traverses are plotted in this way on a single map they are



said to be *stacked*, a word otherwise used for the addition of multiple data sets to form a single output set (see Section 1.3.5).

Contour maps used to be drawn in the field only if the strike of some feature had to be defined quickly so that infill work could be planned, but once again the routine use of laptop computers has vastly reduced the work involved. However, information is lost in contouring because it is not generally possible to choose a contour interval that faithfully records all the features of the original data. Also, contour lines are drawn in the areas between traverses, where there are no data, and inevitably introduce a form of noise. Examination of contour patterns is not, therefore, the complete answer to field quality control.

Cross-sectional contour maps (*pseudo-sections*) are described in Sections 6.3.5 and 7.4.2.

In engineering site surveys, pollution monitoring and archaeology, the objects of interest are generally close to the surface and their positions in plan are usually much more important than their depths. They are, moreover, likely to be small and to produce anomalies detectable only over very small areas. Data have therefore to be collected on very closely spaced grids and can often be presented most effectively if background-adjusted values are used to determine the colour or grey-scale shades of picture elements (*pixels*) that can be manipulated by image-processing techniques. Interpretation then relies on pattern recognition and a single pixel value is seldom important. Noise is eliminated by eye, i.e. patterns such as those in Figure 1.10 are easily recognized as due to human activity.



**Figure 1.10** Image-processed magnetic data over an archaeological site. (Reproduced by permission of Professor Irwin Scollar.)

### 1.3.10 Data loggers

During the past decade, automation of geophysical equipment in small-scale surveys has progressed from a rarity to a fact of life. Although many of the older types of instrument are still in use, and giving valuable service, they now compete with variants containing the sort of computer power employed, 30 years ago, to put a man on the moon. At least one manufacturer now proudly boasts ‘no notebook’, even though the instrument in question is equipped with only a numerical key pad so that there is no possibility of entering text comments into the (more than ample) memory. On other automated instruments the data display is so small and so poorly positioned that the possibility that the observer might actually want to look at, and even think about, his observations as he collects them has clearly not been considered. Unfortunately, this pessimism may all too often be justified, partly because of the speed with which readings, even when in principle discontinuous, can now be taken and logged. Quality control thus often depends on the subsequent playback and display of whole sets of data, and it is absolutely essential that this is done on, at the most, a daily basis. As Oscar Wilde might have said (had he opted for a career in field geophysics), to spend a few hours recording rubbish might be accounted a misfortune. To spend anything more than a day doing so looks suspiciously like carelessness.

Automatic data loggers, whether ‘built-in’ or separate, are particularly useful where instruments can be dragged, pushed or carried along traverse to provide virtually continuous readings. Often, all that is required of the operators is that they press a key to initiate the reading process, walk along the traverse at constant speed and press the key again when the traverse is completed. On lines more than about 20 m long, additional keystrokes can be used to ‘mark’ intermediate survey points.

One consequence of continuous recording has been the appearance in ground surveys of errors of types once common in airborne surveys which have now been almost eliminated by improved compensation methods and GPS navigation. These were broadly divided into *parallax* errors, *heading* errors, ground clearance/coupling errors and errors due to speed variations.

With the system shown in Figure 1.11, parallax errors can occur because the magnetic sensor is about a metre ahead of the GPS sensor. Similar errors can occur in surveys where positions are recorded by key strokes on a data logger. If the key is depressed by the operator when he, rather than the sensor, passes a survey peg, all readings will be displaced from their true positions. If, as is normal practice, alternate lines on the grid are traversed in opposite directions, a *herringbone* pattern will be imposed on a linear anomaly, with the position of the peak fluctuating backwards and forwards according to the direction in which the operator was walking (Figure 1.12a).



**Figure 1.11** Magnetometer coupled to a differential GPS navigation system. Unless allowance is made in processing for the offset between the GPS aerial (behind the operator's head) and the magnetometer sensor (at the end of the horizontal bar), anomalies will be incorrectly located on detailed maps (photo courtesy Geometrics Inc.)

False anomalies can also be produced in airborne surveys if ground clearance is allowed to vary, and similar effects can now be observed in ground surveys. Keeping the sensor shown in Figure 1.11 at a constant height above the ground is not easy (although a light flexible 'spacer' hanging from it can help). On level ground there tends to be a rhythmic effect associated with the operator's motion, and this can sometimes appear on contour maps as 'striping' at right angles to the traverse when minor peaks and troughs on adjacent lines are linked to each other by the contouring algorithm. On slopes there will, inevitably, be a tendency for a sensor in front of the observer to be closer to the ground when going uphill than when going down. How this will affect the final maps will vary with the nature of the terrain, but in an area with constant slope there will a tendency for background levels to be different on parallel lines traversed in opposite directions. This can produce herringbone effects on individual contour lines in low gradient areas (Figure 1.12b).

*Heading errors* occurred in airborne (especially aeromagnetic) surveys because the effect of the aircraft on the sensor depended on aircraft orientation.

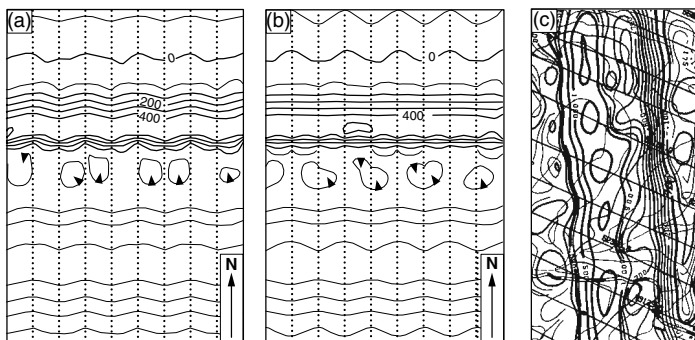


**Figure 1.12** Distortions in automatic contouring of linear anomalies. (a) Herringbone pattern due to a parallax error, i.e. to a consistent offset between geophysical and positional control, with alternate lines measured in opposite directions. (b) Herringbone pattern due to a consistent difference in background levels on lines measured in opposite directions (see discussion in text). Note that in this case the effect is barely visible on the large anomaly indicated by thick contour lines at 100 nT intervals, but is very obvious in the low-gradient areas where contours are shown by thinner lines at 10 and 50 nT intervals. (c) Introduction of closures on the peak of a linear anomaly by an automatic contouring program seeking (as most do) to equalize gradients in all directions. A similar effect can be seen in the ‘bubbling’ of the very closely spaced contour lines on the south side of the anomaly in (b). In neither case are the features necessitated by the data, which exists only along the traverse lines indicated by points in (b) and continuous lines in (c).

A similar effect can occur in a ground magnetic survey if the observer is carrying any iron or steel material. The induced magnetization in these objects will vary according to the facing direction, producing effects similar to those produced by constant slopes, i.e. similar to those in Figure 1.12b.

Before the introduction of GPS navigation, flight path recovery in airborne surveys relied on interpolation between points identified photographically. Necessarily, ground speed was assumed constant between these points, and anomalies were displaced if this was not the case. Similar effects can now be seen in datalogged ground surveys. Particularly common reasons for slight displacements of anomalies are that the observer either presses the key to start recording at the start of the traverse, and then starts walking or, at the end of the traverse, stops walking and only then presses the key to stop recording. These effects can be avoided by insisting that observers begin walking before the start of the traverse and continue walking until the end point has been

safely passed. If, however, speed changes are due to rugged ground, all that can be done is to increase the number of 'marked' points.

Many data loggers not only record data but have screens large enough to show individual and multiple profiles, allowing a considerable degree of quality control in the field. Further quality control will normally be done each evening, using automatic contouring programs on laptop PCs, but allowance must be made for the fact that automatic contouring programs tend to introduce their own distortions (Figure 1.12c).

### 1.4 Bases and Base Networks

*Bases (base stations)* are important in gravity and magnetic surveys, and in some electrical and radiometric work. They may be:

1. *Drift bases* – Repeat stations that mark the starts and ends of sequences of readings and are used to control drift.
2. *Reference bases* – Points where the value of the field being measured has already been established.
3. *Diurnal bases* – Points where regular measurements of background are made whilst field readings are taken elsewhere.

A single base may fulfil more than one of these functions. The reliability of a survey, and the ease with which later work can be tied to it, will often depend on the quality of the base stations. Base-station requirements for individual geophysical methods are considered in the appropriate chapters, but procedures common to more than one type of survey are discussed below.

#### 1.4.1 Base station principles

There is no absolute reason why any of the three types of base should coincide, but surveys tend to be simpler and fewer errors are made if every *drift base* is also a *reference base*. If, as is usually the case, there are too few existing reference points for this to be done efficiently, the first step in a survey should be to establish an adequate base network.

It is not essential that the *diurnal base* be part of this network and, because two instruments cannot occupy exactly the same point at the same time, it may actually be inconvenient for it to be so. However, if a diurnal monitor has to be used, work will normally be begun each day by setting it up and end with its removal. It is good practice to read the field instruments at a drift base at or near the monitor position on these occasions, noting any differences between the simultaneous readings of the base and field instruments.

#### 1.4.2 ABAB ties

Bases are normally linked together using ABAB ties (Figure 1.13). A reading is made at Base A and the instrument is then taken as quickly as possible

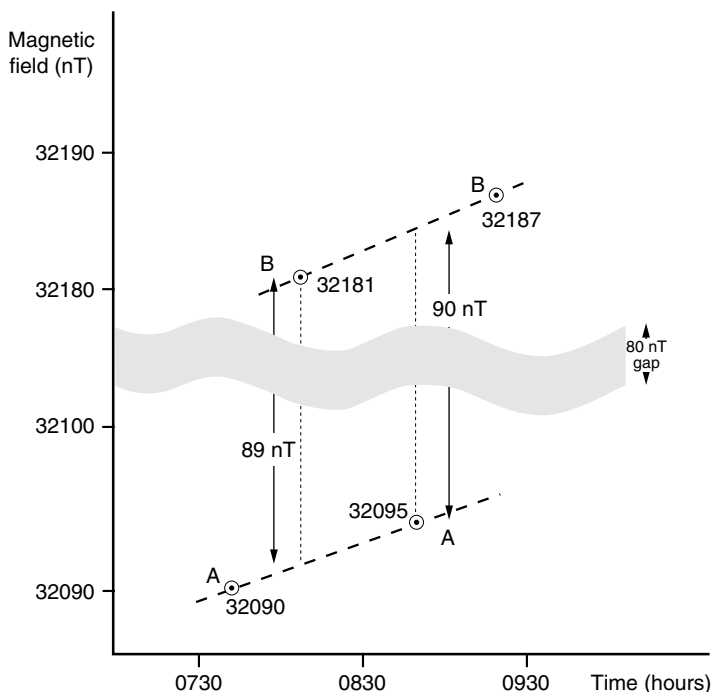


**Figure 1.13** ABAB tie between bases in a magnetic survey with a 1 nT instrument. The estimated difference between the two stations would be 89 nT. Note that the plotting scale should be appropriate to instrument sensitivity and that it may be necessary to ‘remove’ some of the range of the graph to allow points to be plotted with sufficient precision.

to Base B. Repeat readings are then made at A and again at B. The times between readings should be short so that drift, and sometimes also diurnal variation, can be assumed linear. The second reading at B may also be the first in a similar set linking B to a Base C, in a process known as *forward looping*.

Each set of four readings provides two estimates of the difference in field strength between the two bases, and if these do not agree within the limits of instrument accuracy ( $\pm 1$  nT in Figure 1.13), further ties should be made. Differences should be calculated in the field so that any necessary extra links can be added immediately.

### 1.4.3 Base networks

Most modern geophysical instruments are accurate and quite easy to read, so that the error in any ABAB estimate of the difference in value between two points should be trivial. However, a final value obtained at the end of an extended series of links could include quite large accumulated errors. The integrity of a system of bases can be assured if they form part of a network in which each base is linked to at least two others. *Misclosures* are calculated by summing differences around each loop, with due regard to sign, and are then reduced to zero by making the smallest possible adjustments to individual differences. The network in Figure 1.14 is sufficiently simple to be adjusted

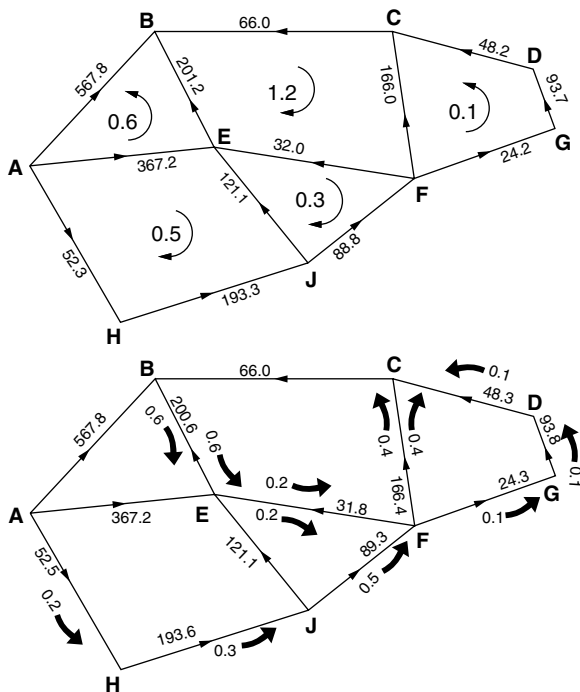


**Figure 1.14** Network adjustment. (a) The 1.2 unit misclosure in loop BCFE suggests a large error in either the 'unsupported' link BC or in BE, the only link shared with another loop with a large misclosure. (b) Adjustments made on the assumption that BC was checked and found to be correct but that no other checks could be made.

by inspection. A more complicated network could be adjusted by computer, using least-squares or other criteria, but this is not generally necessary in small-scale surveys.

### 1.4.4 Selecting base stations

It is important that bases be adequately described and, where possible, permanently marked, so that extensions or infills can be linked to previous work by exact re-occupations. Concrete or steel markers can be quickly destroyed, either deliberately or accidentally, and it is usually better to describe station locations in terms of existing features that are likely to be permanent. In any survey area there will be points that are distinctive because of the presence of manmade or natural features. Written descriptions and sketches are the best way to preserve information about these points for the future. Good sketches are usually better than photographs, because they can emphasize salient points.

Permanence can be a problem, e.g. maintaining gravity bases at international airports is almost impossible because building work is almost always under way. Geodetic survey markers are usually secure but may be in isolated and exposed locations. Statues, memorials and historic or religious buildings often provide sites that are not only quiet and permanent but also offer some shelter from sun, wind and rain.

## 1.5 Global Positioning Satellites

Small, reasonably cheap, hand-held GPS receivers have been available since about 1990. Until May 2000, however, their accuracy was no better than a few hundred metres in position and even less in elevation, because of deliberate signal degradation for military reasons ('selective availability' or SA). The instruments were thus useful only for the most regional of surveys. For more accurate work, differential GPS (DGPS) was required, involving a base station and recordings, both in the field and at the base, of the estimated ranges to individual satellites. Transmitted corrections that could be picked up by the field receiver allowed *real-time kinetic positioning (RTKP)*. Because of SA, differential methods were essential if GPS positioning was to replace more traditional methods in most surveys, even though the accuracies obtainable in differential mode were usually greater than needed for geophysical purposes.

### 1.5.1 Accuracies in hand-held GPS receivers

The removal of SA dramatically reduced the positional error in non-differential GPS, and signals also became easier to acquire. It is often now possible to obtain fixes through forest canopy, although buildings or solid rock between



receiver and satellite still present insuperable obstacles. The precision of the readouts on small hand-held instruments, for both elevations and co-ordinates, is generally to the nearest metre, or its rough equivalent in latitude and longitude ( $0.00001^\circ$ ). Accuracies are considerably less, because of *multi-path errors* (i.e. reflections from topography or buildings providing alternative paths of different lengths) and because of variations in the properties of the atmosphere. The main atmospheric effects occur in the ionosphere and depend on the magnitude and variability of the ionization. They are thus most severe during periods of high solar activity, and particularly during magnetic storms (Section 3.2.4).

Because of atmospheric variations, all three co-ordinates displayed on a hand-held GPS will usually vary over a range of several metres within a period of a few minutes, and by several tens of metres over longer time intervals. Despite this, it is now feasible to use a hand-held GPS for surveys with inter-station separations of 100 m or even less because GPS errors, even if significant fractions of station spacing, are not, as are so many other errors, cumulative. Moreover, rapid movement from station to station is, in effect, a primitive form of DGPS, and if fixes at adjacent stations are taken within a few minutes of each other, the error in determining the intervening distance will be of the order of 5 metres or less. (In theory, this will not work, because corrections for transmission path variations should be made individually for each individual satellite used, and this cannot be done with the hand-held instruments currently available. However, if distances and time intervals between readings are both small, it is likely that the same satellite constellation will have been used for all estimates and that the atmospheric changes will also be small.)

### 1.5.2 Elevations from hand-held GPS receivers

In some geophysical work, errors of the order of 10 metres may be acceptable for horizontal co-ordinates but not for elevations, and DGPS is then still needed. There is a further complication with ‘raw’ GPS elevations, since these are referenced to an ellipsoid. A national elevation datum is, however, almost always based on the local position of the *geoid* via the mean sea level at some selected port. Differences of several tens of metres between geoid and ellipsoid are common, and the source of frequent complaints from users that their instruments never show zero at sea level! In extreme cases, the difference may exceed 100 m.

Most hand-held instruments give reasonable positional fixes using three satellites but need four to even attempt an elevation. This is because the unknown quantities at each fix include the value of the offset between the instrument’s internal clock and the synchronized clocks of the satellite

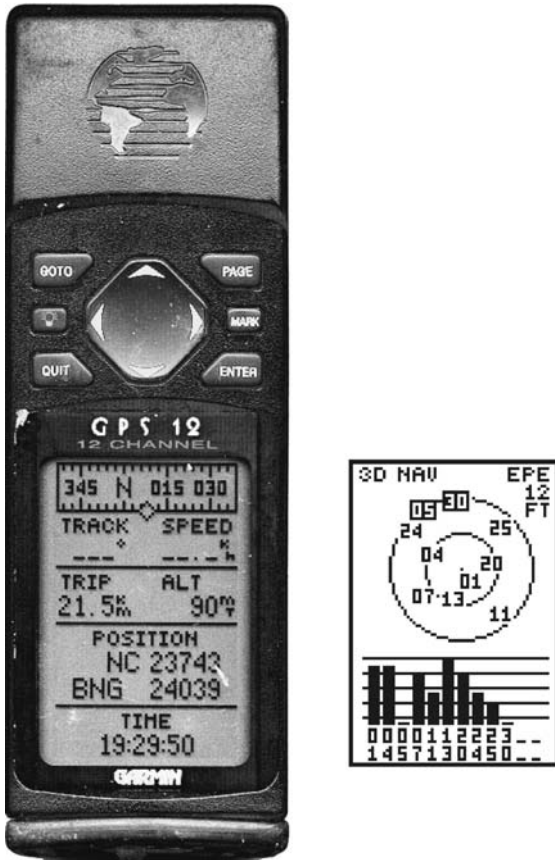


**Figure 1.15** Garmin 12 hand-held GPS, showing 'navigation' window, which gives position (in UK National Grid co-ordinates in this instance), altitude to the foot or metre, time and (for use in continuous tracking mode) track orientation and speed. The inset shows the 'satellite' window. Satellites potentially available are shown in the main display. Signal strengths are indicated by black columns but no indication is given as to which four are actually being used to calculate position. Satellites not acquired (05 and 30) are highlighted. Note that the 2D/3D NAV indicator is on this display and that there is no warning on the navigation display when only 2D navigation is being achieved (with only three satellites) and the elevation estimate is therefore not usable.

constellation. Four unknowns require four measurements. Unfortunately, in some cases the information as to whether '3D navigation' is being achieved is not included on the display that shows the co-ordinates (e.g. Figure 1.15), and the only indication that the fourth satellite has been 'lost' may be a suspicious lack of variation in the elevation reading.

Differences in rock density produce small changes in the Earth's gravity field that can be measured using portable instruments known as gravity meters or gravimeters.

## 2.1 Physical Basis of the Gravity Method

The gravitational constant,  $G$ , has a value of  $6.67 \times 10^{-11} \text{ N m}^2 \text{ kg}^{-2}$ . Gravity fields are equivalent to accelerations, for which the SI unit is the  $\text{m s}^{-2}$  (alternatively written as the  $\text{N kg}^{-1}$ ). This is inconveniently large for geophysical work and the gravity unit (g.u. or  $\mu\text{m s}^{-2}$ ) is generally used. The cgs unit, the milligal, equal to 10 g.u., is still also very popular.

### 2.1.1 Gravity field of the Earth

The Earth's gravity field is almost the same as that of a sphere having the same average radius and total mass but increases slightly towards the poles. The difference between polar and equatorial fields is about 0.5% or 50 000 g.u. The rate of change is zero at the poles and equator and reaches a maximum of about 8 g.u. per kilometre north or south at  $45^\circ$  latitude (Figure 2.1). The relationship between normal sea-level gravity and latitude ( $\lambda$ ) is described by the *International Gravity Formula*, adopted in 1967:

$$g_{\text{norm}} = 9\,780\,318.5 + 51629.27 \sin^2 \lambda + 229.5 \sin^4 \lambda$$

The theoretical sea-level gravity at the equator is thus 9 780 318.5 g.u. This formula replaced an earlier, 1930, version with slightly different constants (including an equatorial sea-level gravity of 9 780 490 g.u.). The change of formula was necessitated by the recognition that the absolute gravity values at the 'Potsdam' system of base stations were in error by some 160 g.u., and that correcting this error, and allowing for an improved knowledge of the shape of the Earth, required a corresponding change in formula. The network of international base stations compatible with the 1967 IGF is known as IGSN71 (see Notes to Bibliography). It is still all too common to find surveys in which the 1930 IGF has been applied to data referenced to IGSN71 bases or that the 1967 IGF has been applied to Potsdam values, leading to errors of up to 160 g.u. in latitude-corrected values.

Recently there has been a move towards using an updated formula that is fully compatible with the World Geodetic System 1984 (WGS84). The equation is more complicated than that defining IGF67, and an additional,

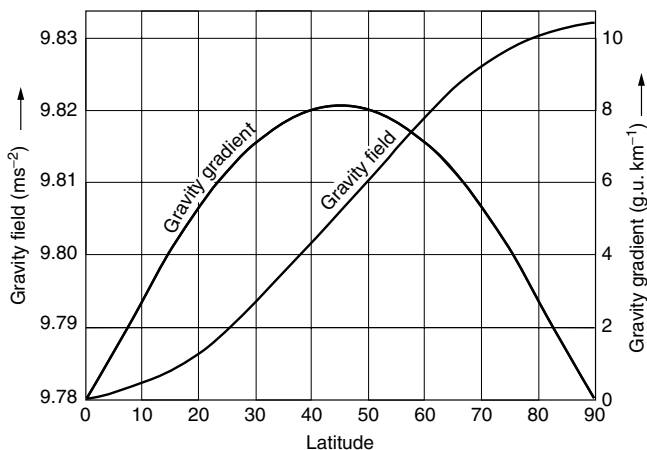


**Figure 2.1** Variation in theoretical sea-level gravity field and in corresponding north–south horizontal gradient with latitude. There is no east–west gradient in the theoretical field.

elevation dependent, correction is needed for the mass of the atmosphere (see Notes to Bibliography). Since the actual changes implied in theoretical gravity are often smaller than the errors in absolute gravity of individual gravity stations, and no changes in base-station values are required, the changeover is widely regarded as not urgent and is proceeding only slowly.

A major sedimentary basin can reduce the gravity field by more than 1000 g.u., but many other common targets, such as massive ore bodies, produce anomalies of only a few g.u. Caves and artificial cavities such as mine workings usually produce even smaller (and negative) effects, even when very close to the surface. Topographic effects may be much larger. Elevation difference alone produces a gravity difference of nearly 20 000 g.u. between the summit of Mount Everest and sea-level. For engineering and geological purposes, gravity changes must often be measured to an accuracy of 0.1 g.u. (approximately one-hundred millionth of the Earth's field), and this is the sensitivity of virtually all modern gravity meters. The so-called 'microgravity meters' have readout precisions of 0.01 g.u. but not even their manufacturers claim accuracies of better than about 0.03 g.u.

### 2.1.2 Rock density

The SI unit of density is the  $\text{kg m}^{-3}$  but the  $\text{Mg m}^{-3}$  is widely used since the values are, numerically, the same as those in the old cgs system in which water has unit density. Most crustal rocks have densities of between 2.0 and

**Table 2.1** *Densities of common rocks and ore minerals ( $\text{Mg m}^{-3}$ )*

<i>Common rocks</i>	
Dry sand	1.4–1.65
Serpentinite	2.5–2.6
Wet sand	1.95–2.05
Gneiss	2.65–2.75
Coal	1.2–1.5
Granite	2.5–2.7
Chalk	1.9–2.1
Dolerite	2.5–3.1
Salt	2.1–2.4
Basalt	2.7–3.1
Limestone	2.6–2.7
Gabbro	2.7–3.3
Quartzite	2.6–2.7
Peridotite	3.1–3.4
<i>Ore minerals</i>	
Sphalerite	3.8–4.2
Galena	7.3–7.7
Chalcopyrite	4.1–4.3
Chromite	4.5–4.8
Pyrrhotite	4.4–4.7
Hematite	5.0–5.2
Pyrite	4.9–5.2
Magnetite	5.1–5.3

$2.9 \text{ Mg m}^{-3}$ . In the early days of gravity work a density of  $2.67 \text{ Mg m}^{-3}$  was adopted as standard for the upper crust and is still widely used in modelling and in calculating elevation corrections for standardized gravity maps. Density ranges for some common rocks are shown in Table 2.1.

## 2.2 Gravity Meters

For the past 50 years the vast majority of gravity measurements have been made using meters with unstable (*astatic*) spring systems, and this seems likely to remain the case for the foreseeable future. Gravity surveys are complicated by the fact that such meters measure gravity differences, not absolute field strengths.

### 2.2.1 Astatic spring systems

Astatic systems use *zero-length* main springs, in which tension is proportional to actual length. With the geometry shown in Figure 2.2 and for one particular

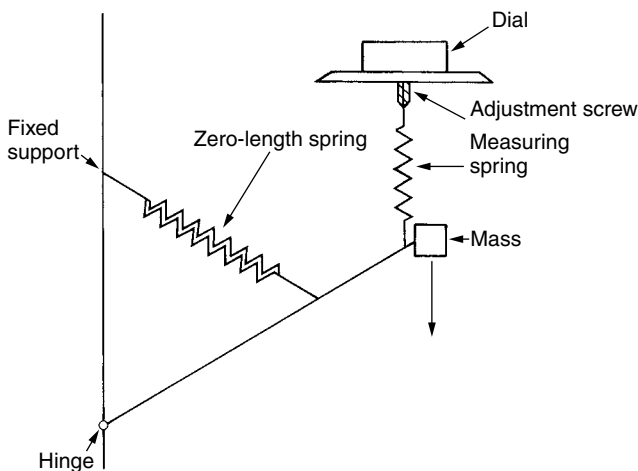


**Figure 2.2** Astatic gravity meter. The tension in the zero-length spring is proportional to its length. Measurements are made by rotating the dial, which raises or lowers the measuring spring to return the mass to a standard position.

value of gravity field, the spring will support the balance arm in any position. In stronger fields, a much weaker auxiliary spring can be used to support the increase in weight, which will be equal to the product of the total mass and the increase in gravity field. To use an expression common in other geophysical methods, the zero-length spring *backs off* a constant weight so that the measuring spring can respond to small changes in gravity field.

None of the meters described below (and illustrated in Figure 2.3) uses exactly the system of Figure 2.2. The Worden and Sodin have two auxiliary springs, one for fine and one for coarse adjustments, attached to balance arms of more complicated design, while in the later Scintrex meters (CG-3 and CG-5) the restoring force is electrostatic. LaCoste meters have no auxiliary springs and measurements are made by adjusting the point of support of the main spring.

Because spring systems are mechanical, they are subject to drift. Short-period drift is largely due to temperature changes that affect the elastic constants of the springs despite the compensation devices that are usually included. There is also longer term extensional *creep* of springs under continual tension. Repeated readings at base stations are required to monitor drift and to allow the necessary corrections to be calculated.



**Figure 2.3** ‘Manual’ gravity meters. From left to right, LaCoste ‘G’ (geodetic), Worden ‘Student’ and Sodin.

Although gravity meters remained essentially unchanged for almost 50 years, major moves were made in the last decade of the twentieth century towards automating readings and reducing the need for skilled operators. The LaCoste G and D meters were fitted with electronic readouts and the Scintrex CG-3 pioneered automated tilt correction and reading. The basic LaCoste meter was then completely redesigned as the fully automatic Graviton-EG, in which actual levelling, rather than merely the levelling correction, is automated. Inevitably, data loggers have also been added and can be directly downloaded to laptop PCs. The Graviton-EG, the CG-3 and its successor, the CG-5 Autograv, are also sufficiently rugged to be transported in the field without additional protective cases. However, despite the advantages of the newer models, the longevity (and, to some extent, the high cost) of gravity meters ensures that the less sophisticated versions will be around for many years to come. Much of the discussion below refers principally to these older meters.

### 2.2.2 Quartz astatic meters

Worden, Sodin and Scintrex meters have springs of fused quartz, enclosed in vacuum chambers that provide a high degree of thermal insulation. Some also have electrical thermostats, implying a need for heavier batteries, and



the Scintrex meters have a temperature sensor that allows corrections for temperature-induced drift to be made by software. Vacuum-chamber meters are pressure sensitive, the effect with older meters amounting to as much as 2 g.u. for a kilometre elevation change, although in the CG-3/CG-5 this has been reduced by a factor of four or five. None of the quartz meters can be clamped, so the spring systems are all to some degree vulnerable when in transit. In some cases, if a meter suffers sharp sideways acceleration or is tilted, even gently, through more than about  $45^\circ$ , the springs may become tangled, and have to be unknotted by the manufacturer.

Worden and Sodin quartz meters have limited ranges on their direct-reading scales, of generally between 500 and 2000 g.u., and must be reset if a limit is reached. Some meters can be reset with a second dial calibrated to a lower degree of accuracy but in others an uncalibrated adjustment screw is used. It is always advisable to allow several hours for the system to settle after reset, and surveys of areas with large elevation changes need to be carefully planned to allow for this.

The level bubbles of Sodin meters are mounted deep within the instrument to shield them from the direct rays of the sun, which in other meters can cause levelling errors due to uneven heating of the fluid. They therefore need to be illuminated and are much less easy to check during reading than are levels on the top of the meter. It seems probable that more readings are taken off-level with Sodins than with other meters. With all the manual quartz meters it takes an experienced and conscientious observer to maintain the theoretical reading accuracy of 0.1 g.u.

### 2.2.3 Steel astatic meters

LaCoste meters (Figure 2.4) use steel springs. Because steel conducts heat well, these cannot be effectively insulated and thermostatic control is essential. The meter weight, of about 5 kg, is roughly doubled by the necessary rechargeable battery. Some form of charger is needed in the field since a single charge lasts only one or two days, depending on thermostat setting and external temperature. For two or three hours after reaching operating temperature, the drift is so high that the instrument is unusable. Drift is then very low, and can even be extrapolated linearly across intervals during which the meter has been off-heat. However, discontinuous *tares*, of perhaps several g.u., can occur at any time. These are the main form of drift in LaCoste meters and if they happen more than about once a month the instrument should be checked by the manufacturer.

With spring clamped, a LaCoste meter is reputedly able to survive any shock that does not fracture the outer casing. The springs are also less affected by vibration and the optical systems are generally clearer than those of most quartz meters. Even quite inexperienced observers have little difficulty in

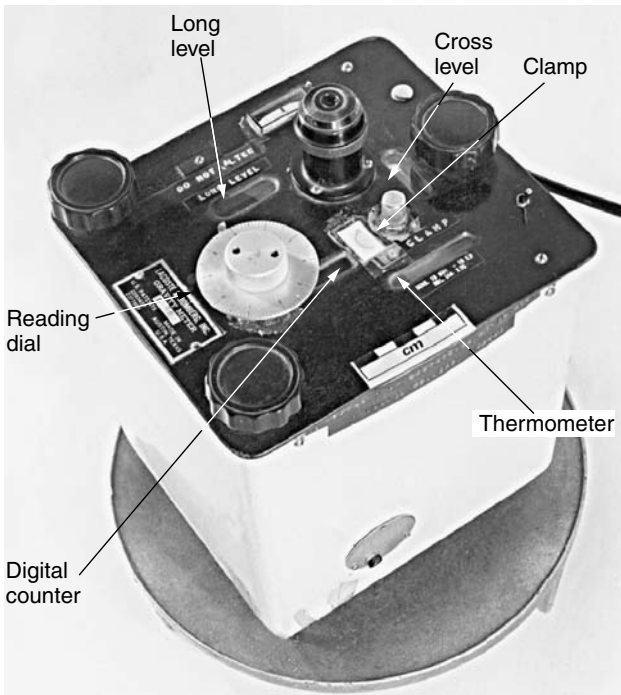


**Figure 2.4** Controls of the LaCoste 'G' meter. Note the two level bubbles at right angles, the clamp and the aluminium reading dial. The digital counter is behind the small window between the clamp and the dial. The thermometer, viewed through a window in front of the clamp, monitors internal temperature and must show the pre-set operating temperature if the instrument is to be usable.

achieving accuracies of 0.1 g.u., particularly if aided by the optional (and expensive) electronic repeater needle.

A major advantage of the LaCoste G (geodetic) meter over the Worden and Sodin quartz meters is that a single long measuring screw is used to give readings world-wide without resetting (the D-meter, used for microgravity surveys, sacrifices this advantage in the interests of greater reading precision). Calibration factors vary slightly over the range, being tabulated for 1000 g.u. intervals. The G-meter thus has considerable advantages over quartz equivalents, but costs about twice as much.

### 2.2.4 Setting up a gravity meter

Gravity meters are normally read on concave dishes supported by three short stubs to which longer legs can be attached. The stubs are usually used alone, pressed firmly but not too deeply into the ground. The under surface of the dish must not touch the ground since a fourth support point allows 'rocking' back and forth. Thick grass under the dish may have to be removed before a reading can be taken. Extension legs may also be used but readings will then take longer, the dish itself may have to be levelled (some incorporate a bull's-eye bubble) and the height above ground will have to be measured.

The meters themselves rest on three adjustable, screw-threaded feet and are levelled using two horizontal spirit-levels (see Figure 2.4), initially by being moved around the dish until both level bubbles are 'floating'. The temptation to hurry this stage and use the footscrews almost immediately should be resisted.

Usually one of the levels (probably the *cross-level*, at right angles to the plane of movement of the balance arm) is set parallel to a line joining two of the feet. Adjustments to the third foot then scarcely affect this level. The quickest method of levelling is to centre the cross-level bubble, using one or both of the two footscrews that control it, and then use the third screw to set the *long-level*. Some meters can rotate in their casings and level bubbles and feet may become misaligned, but levelling is very much easier if any such slippage is corrected. Experienced observers often use two screws simultaneously but the ability to do this efficiently comes only with practice.

Once a meter is level, a reading can be obtained. With most gravity meters, this is done by rotating a calibrated dial to bring a pointer linked to the spring system to a fixed point on a graduated scale. Because the alignment is rather subjective if the pointer is viewed directly through an eyepiece, all readings in a single loop should be made by the same observer. The subjective element is then eliminated when the base reading is subtracted. Subjectivity is much reduced when instruments are fitted with electronic repeaters.

It is vital that the level bubbles are checked whilst the dial is being adjusted, and especially immediately after a supposedly satisfactory reading has been taken. Natural surfaces subside slowly under the weight of observers, off-levelling the meter. On snow or ice the levels have to be adjusted almost continuously as the dish melts its way down, unless it is insulated from the surface by being placed on a small piece of plywood.

All mechanical measuring systems suffer from *whiplash* and two readings will differ, even if taken within seconds of each other, if the final adjustments are made by opposite rotations of the reading dial. The only remedy is total consistency in the direction of the final adjustment.

Earthquakes can make the pointer swing slowly from side to side across the field of view and survey work must be stopped until the disturbance

is over. Fortunately, this effect is rare in most parts of the world, although very large earthquakes can affect gravity meters at distances of more than 10 000 km. Severe continuous vibration, as from nearby machinery or the roots of trees moved by the wind, can make reading difficult and may even displace the reading point.

### 2.2.5 Meter checks

A series of checks should be made each day before beginning routine survey work. The meter should first be *shaken down* by tapping the dish gently with a pencil between readings until a constant value is recorded. This method can also be used if, as sometimes happens, the pointer ‘sticks’ at one side of the scale.

The levelling system should then be checked. Because astatic systems are asymmetric, the effect of a levelling error depends on the direction of tilt. A slight off-levelling at right angles to the balance arm gives a reading of gravity field multiplied by the cosine of the tilt angle (an error of about 0.15 g.u. for a tilt of  $0.01^\circ$ ). If the tilt is in the plane of movement, reading *sensitivity* (the amount the pointer moves for a given rotation of the dial) is also affected.

Off-levelling a correctly adjusted cross-level will reduce the reading, regardless of the direction of offset. To check that this actually happens, the meter should be set up and read normally and the cross-level should then be offset by equal amounts in both directions. The pointer should move roughly the same distance in the same direction in each case. Meters are usually considered usable provided that the movements are at least in the same direction, but otherwise the level must be adjusted.

The long-level affects reading sensitivity, i.e. the distance the pointer moves for a given dial rotation. The recommended sensitivity and instructions for resetting will be found in the manufacturer’s handbook. The actual sensitivity can be estimated by moving the dial by a set amount and noting the pointer movement. After adjustment, levels often take a few days to settle in their new positions, during which time they must be rechecked with special care.

### 2.2.6 Meter calibration

Readings on non-automatic meters are usually combinations of values read from a dial and numbers displayed on a mechanical counter. The sensitivity of most such meters is such that the final figure on the dial corresponds to approximately 0.1 g.u.

Readings are converted to gravity units using calibration factors specific to the individual instrument. These are usually quoted by manufacturers in milligals, not g.u., per scale division and involve the arbitrary insertion of a decimal point somewhere in the reading. The factors are not affected by

changes in reading sensitivity but may alter slowly with time and should be checked regularly. This can be done by the manufacturers or by using calibration ranges of known gravity interval. Calibration ranges usually involve gravity changes of about 500 g.u., which is within the range of even the most limited-range meters, and almost always make use of the rapid change of gravity field with elevation. A height change of about 250 metres is generally necessary, although in some cases local gravity gradients can also play a part. Travel times between top and bottom stations should normally be less than 15 minutes and the two stations should be well marked and described. A *run* should consist of at least an ABAB tie (Section 1.4.2), giving two estimates of gravity difference. If these differ by more than 0.1 g.u., more links should be added.

Meters with separate fine and coarse adjustments can be checked over different sections of their fine ranges by slightly altering the coarse setting. Most meters need a little time to stabilize after coarse adjustment, but if this is allowed it may be possible to identify minor irregularities in a calibration curve. This cannot be done with LaCoste G-meters, since only one part of the curve can be monitored on any one calibration range. Because of slight irregularities in the pitch of the adjustment screws, different meters may give results on the same range which differ consistently by a few tenths of a g.u.

## 2.3 Gravity Reductions

In gravity work, more than in any other branch of geophysics, large and (in principle) calculable effects are produced by sources which are not of direct geological interest. These effects are removed by *reductions* involving sequential calculation of a number of recognized quantities. In each case the sign of the reduction is opposite to that of the effect it is designed to remove. A positive effect is one that increases the magnitude of the measured field.

### 2.3.1 Latitude correction

Latitude corrections are usually made by subtracting the *normal* gravity, calculated from the International Gravity Formula, from the *observed* or absolute gravity. For surveys not tied to the absolute reference system, local latitude corrections may be made by selecting an arbitrary base and using the theoretical north–south gradient of  $8.12 \sin 2\lambda$  g.u./km.

### 2.3.2 Free-air correction

The remainder left after subtracting the normal from the observed gravity will be due in part to the height of the gravity station above the sea-level reference surface. An increase in height implies an increase in distance from the Earth's centre of mass and the effect is negative for stations above sea level. The *free-air correction* is thus positive, and for all practical purposes is equal to

3.086 g.u./metre. The quantity obtained after applying both the latitude and free-air corrections is termed the *free-air anomaly* or *free-air gravity*.

### 2.3.3 Bouguer correction

Since topographic masses are irregularly distributed, their effects are difficult to calculate precisely and approximation is necessary. The simplest approach assumes that topography can be represented by a flat plate extending to infinity in all directions, with constant density and a thickness equal to the height of the gravity station above the reference surface. This *Bouguer plate* produces a gravity field equal to  $2\pi\rho Gh$ , where  $h$  is the plate thickness and  $\rho$  the density (1.1119 g.u./metre for the standard  $2.67 \text{ Mg m}^{-3}$  density).

The Bouguer effect is positive and the correction is therefore negative. Since it is only about one-third of the size of the free-air correction, the net effect of an increase in height is a reduction in field. The combined correction is positive and equal to about 2 g.u. per metre, so elevations must be known to 5 cm to make full use of meter sensitivity.

Because Bouguer corrections depend on assumed densities as well as measured heights, they are fundamentally different from free-air corrections, and combining the two into unified elevation corrections can be misleading. It is also sometimes stated that the combined corrections reduce gravity values to those that would be obtained were the reading made on the reference surface, with all the topography removed. This is not true. In Figure 2.5, the

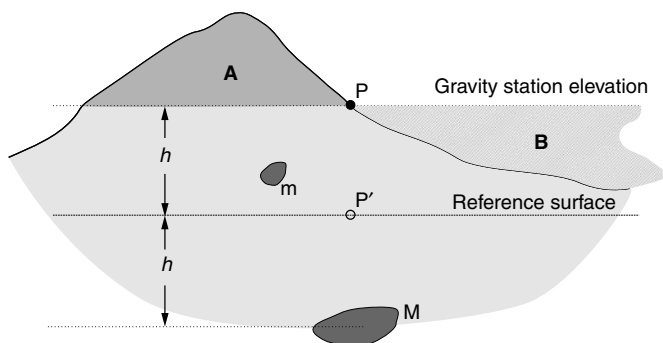


**Figure 2.5** Terrain corrections. The corrections are for the deviations of the topography from a surface parallel to sea level through the gravity station, and not from sea level itself, and are always positive (see discussion in text). Even after application of the Bouguer and free-air corrections, the gravity effects of the masses  $M$  and  $m$  will appear on the maps as they are measured at the station point  $P$ , and not as they would be measured at the point  $P'$  on the reference surface.

effect of the mass  $M$  recorded at the observation point  $P$  is unaltered by these corrections. It remains the effect of a body a distance  $2h$  below  $P$ , not at the point  $P'$  a distance  $h$  below it. Still more obviously, the corrections do not mysteriously eliminate the effect of the mass  $m$ , above the reference surface, since the Bouguer correction assumes constant density. Bouguer gravity is determined at the points where measurements are made, a fact that has to be taken into account in interpretation.

## 2.3.4 Terrain corrections

In areas of high relief, detailed topographic corrections must be made. Although it would be possible to correct directly for the entire topography above the reference surface in one pass without first making the Bouguer correction, it is simpler to calculate the *Bouguer gravity* and then correct for deviations from the Bouguer plate.

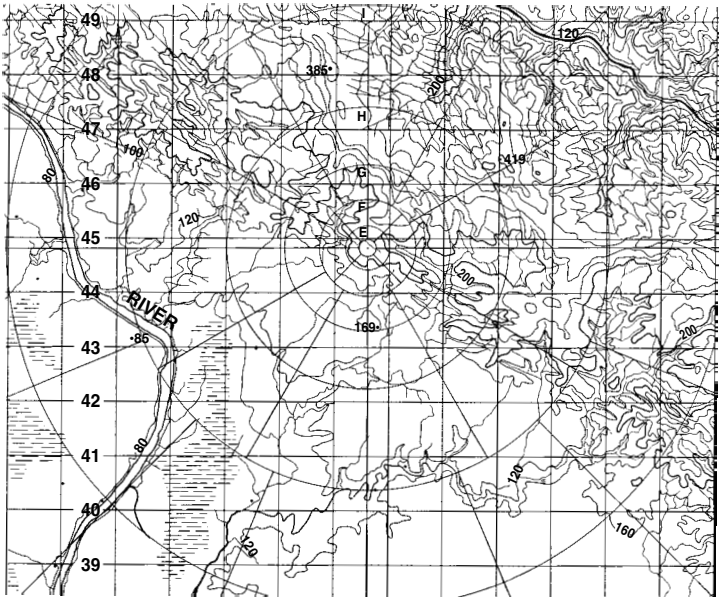


**Figure 2.6** Hammer chart (Zones E to I) overlaid on a topographic map. The difficulties in estimating average heights in the larger compartments are easily appreciated. The letters identifying the zones are difficult to see in this example but are clear when the overlay is removed from the map and viewed on its own.

A peculiarity of the two-stage approach is that the second-stage corrections are always positive. In Figure 2.5, the topographic mass (A) above the gravity station exerts an upward pull on the gravity meter, the effect is negative and the correction is positive. The valley (B), on the other hand, occupies a region that the Bouguer correction assumed to be filled with rock that would exert a downwards gravitational pull. This rock does not exist. The terrain correction must compensate for an over-correction by the Bouguer plate and is again positive.

Terrain corrections can be extremely tedious. To make them manually, a transparent *Hammer chart* is centred on the gravity station on the topographic map (Figure 2.6) and the difference between the average height of the terrain and the height of the station is estimated for each compartment. The corresponding corrections are then obtained from tables (see Appendix). Computers can simplify this process but require terrain data in digital form and may be equally time consuming unless a digital terrain model (DTM) already exists.

Adding terrain corrections to the simple Bouguer gravity produces a quantity often known as the *extended* or *complete Bouguer gravity*. Topographic densities are sometimes varied with geology in attempts to still further reduce terrain dependence.

## 2.4 Gravity Surveys

A gravity survey is a basically simple operation but few are completed wholly without problems, and in some cases the outcomes can only be described as disastrous. Most of the difficulties arise because gravity meters measure only differences in gravity field and readings have to be interrelated by links to a common reference system.

### 2.4.1 Survey principles

A gravity survey consists of a number of *loops*, each of which begins and ends with readings at the same point, the *drift base* (Section 1.4). The size of the loop is usually dictated by the need to monitor drift and will vary with the mode of transport being used; two-hour loops are common in detailed work. At least one station of the reference network must be occupied in the course of each loop and operations are simplified if this is also the drift base for that loop. In principle, a base network can be allowed to emerge gradually as the work proceeds but if it is completed and adjusted early, absolute values can be calculated as soon as each field station has been occupied, allowing possible errors to be identified while there is still time for checks to be made. There is also much to be gained from the early overview of the whole survey area that can be obtained while the network is being set up, and practical advantages in establishing bases while not under the pressure to maximize



the daily total of new stations that characterizes the routine production phase of most surveys.

A small survey may use an arbitrary base without any tie to an absolute system. Problems will arise only if such a survey has later to be linked to others or added to a national database. This nearly always happens eventually and the use of a purely local reference is often a false economy.

## 2.4.2 Base stations

The criteria used in siting reference bases differ from those for normal stations. Provided that exact reoccupation is possible, large terrain effects can be tolerated. These may make it inadvisable to use the gravity value in interpretation, in which case the elevation is not needed either. On the other hand, since the overall survey accuracy depends on repeated base readings, quiet environments and easy access are important. Traffic noise and other strong vibrations can invalidate base (or any other) readings. Also, the general principles outlined in Section 1.4 apply to gravity bases, and descriptions should be provided in the form of sketch plans permitting reoccupation exactly in elevation and to within a few centimetres in position (Figure 2.7).

## 2.4.3 Station positioning

The sites of field stations must also be chosen with care. Except in detailed surveys where stations are at fixed intervals along traverses, observers in the field have some, and often considerable, freedom of choice. They also have the responsibility for estimating terrain corrections within the area, up to

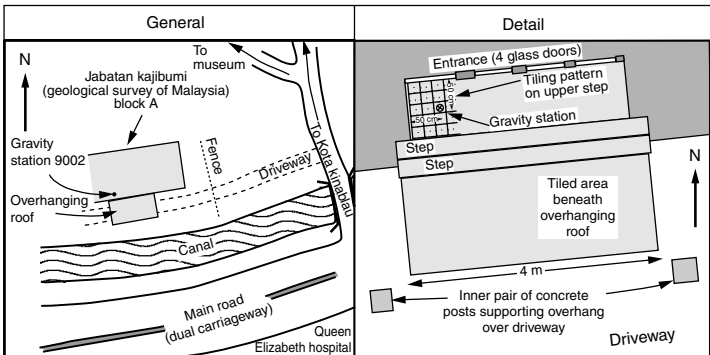
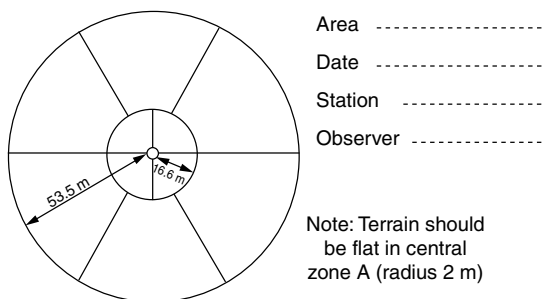


**Figure 2.7** Gravity base-station sketches. Two sketches, at different scales, together with a short written description, are usually needed to ensure the station can be reoccupied quickly and accurately.



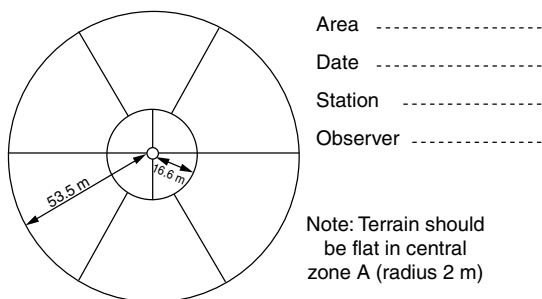
Zone B (2.0–16.6 m)	
Terrain correction (g.u.)	Height difference (metres)
0.01	0.3–0.6
0.02	0.6–0.8
0.03	0.8–0.9
0.04	0.9–1.0
0.05	1.0–1.1
0.1	1.1–2.1
0.2	2.1–2.7
0.3	2.7–3.6
0.4	3.6–4.3
0.5	4.3–4.9

Zone C (16.6–53.5 m)	
Terrain correction (g.u.)	Height difference (metres)
0.01	1.3–2.3
0.02	2.3–3.0
0.03	3.0–3.5
0.04	3.5–4.0
0.05	4.0–4.4
0.1	4.4–7.3
0.2	7.3–9.7
0.3	9.7–11.9
0.4	11.9–13.7
0.5	13.7–15.5

**Figure 2.8** Field observer's Hammer chart, for Zones B and C.

about 50 metres from the reading point, where features too small to be shown on any topographic map can be gravitationally significant. Corrections can be estimated in the field using a truncated graticule such as that in Figure 2.8, which covers the Hammer zones B and C only. Height differences of less than 30 cm in Zone B and 130 cm in Zone C can be ignored since they produce effects of less than 0.01 g.u. per compartment. The charts can also be used qualitatively, to select reading points where overall terrain corrections will be small.

The effect of a normal survey vehicle is detectable only if the observer actually crawls underneath it, and most modern buildings produce similarly small effects. Old, thick-walled structures may need to be treated with more respect (Figure 2.9). Subsurface cavities, whether cellars, mine-workings or natural caverns, can produce anomalies amounting to several g.u. The gravity method is sometimes used in cavity detection but where this is not the object



Zone B (2.0–16.6 m)	
Terrain correction (g.u.)	Height difference (metres)
0.01	0.3–0.6
0.02	0.6–0.8
0.03	0.8–0.9
0.04	0.9–1.0
0.05	1.0–1.1
0.1	1.1–2.1
0.2	2.1–2.7
0.3	2.7–3.6
0.4	3.6–4.3
0.5	4.3–4.9

Zone C (16.6–53.5 m)	
Terrain correction (g.u.)	Height difference (metres)
0.01	1.3–2.3
0.02	2.3–3.0
0.03	3.0–3.5
0.04	3.5–4.0
0.05	4.0–4.4
0.1	4.4–7.3
0.2	7.3–9.7
0.3	9.7–11.9
0.4	11.9–13.7
0.5	13.7–15.5

**Figure 2.8** Field observer's Hammer chart, for Zones B and C.

about 50 metres from the reading point, where features too small to be shown on any topographic map can be gravitationally significant. Corrections can be estimated in the field using a truncated graticule such as that in Figure 2.8, which covers the Hammer zones B and C only. Height differences of less than 30 cm in Zone B and 130 cm in Zone C can be ignored since they produce effects of less than 0.01 g.u. per compartment. The charts can also be used qualitatively, to select reading points where overall terrain corrections will be small.

The effect of a normal survey vehicle is detectable only if the observer actually crawls underneath it, and most modern buildings produce similarly small effects. Old, thick-walled structures may need to be treated with more respect (Figure 2.9). Subsurface cavities, whether cellars, mine-workings or natural caverns, can produce anomalies amounting to several g.u. The gravity method is sometimes used in cavity detection but where this is not the object

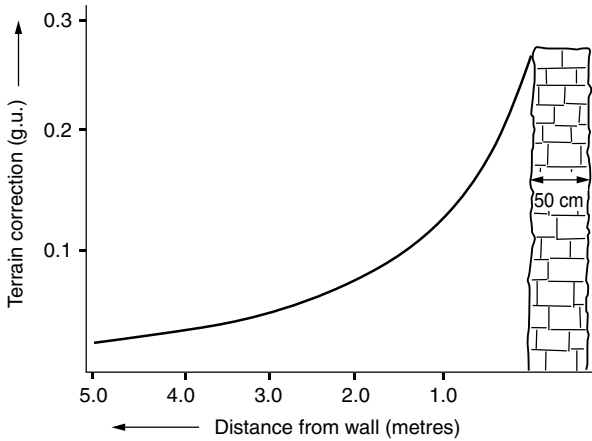


**Figure 2.9** Effect of a half-metre thick stone wall on the gravity field.

of the survey it is obviously important that stations are not sited where such effects may occur.

## 2.4.4 Tidal effects

Before meter drift can be estimated, allowance must be made for *Earth tides*. These are background variations due to changes in the relative positions of the Earth, moon and sun, and follow linked 12- and 24-hour cycles superimposed on a cycle related to the lunar month (Figure 2.10). Swings are largest at new and full moons, when the Earth, moon and sun are in line. Changes of more than 0.5 g.u. may then occur within an hour and total changes may exceed

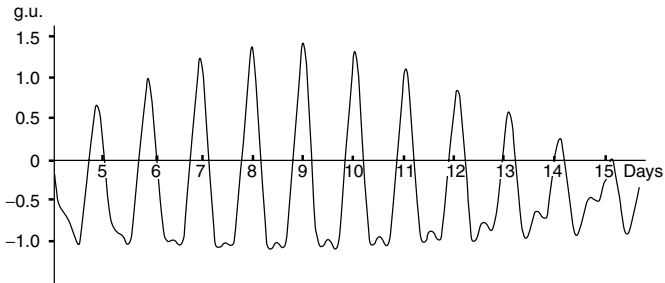


**Figure 2.10** Tidal variations, 5 to 15 January 1986, in g.u.

2.5 g.u. The assumption of linearity made in correcting for drift may fail if tidal effects are not first removed.

Earth tides are predictable, at least at the 0.1 g.u. level required for gravity survey, and corrections can be calculated using widely available computer programs. Meter readings must be converted to gravity units before corrections are applied.

### 2.4.5 Drift corrections

The assumption that instrument drift has been linear in the time between two base readings is unlikely to be true if drift is dependent mainly on external temperature and large changes in temperature have been wholly or partly reversed during that time. However, it is difficult to make any other assumptions, except with modern instruments such as the CG-5 where internal temperature is recorded and compensated for automatically.

To correct manually for drift using the linear assumption, readings are first tidally corrected and the corrected initial reading at the drift base is then subtracted from every other reading in turn. The result of doing this to the final reading at the drift base gives the total drift. The *pro rata* corrections to the other stations must be calculated or estimated graphically to a final accuracy of 0.1 g.u. The sign of the correction is dictated by the requirement that, after correction, all drift base relative values should be zero.

Absolute observed gravities are obtained by adding the absolute value at the drift base to the drift-corrected gravity differences.

### 2.4.6 Elevation control

The elevations of gravity survey points can be determined in many different ways. If 1 g.u. contours are required, high-accuracy optical, radio-wave or DGPS techniques are essential, while barometric levelling or direct reference to sea-level and tide tables may be adequate for the 50 or 100 g.u. contours common in regional surveys. Measuring elevations is often the most expensive part of a gravity survey and advantage should be taken of any 'free' levelling that has been done for other purposes, e.g. surveyed seismic lines.

### 2.4.7 Field notebooks

At each station, the number, time and reading must be recorded. The most modern meters incorporate data loggers that do this at a key stroke, but all other information must be recorded in field notebooks. This may include positional information from GPS receivers and elevation data from barometers.

Any factors that might affect readings, such as heavy vibrations from machinery, traffic, livestock or people, unstable ground or the possible presence of underground cavities, should be noted in a *Remarks* column. Comments on weather conditions may also be useful, even if only as indicating the

observer's state of mind. Where local terrain corrections are only occasionally significant, estimates may also be entered as 'Remarks', but individual terrain-correction sheets may be needed for each station in rugged areas. Additional columns may be reserved for tidal and drift corrections, since drift should be calculated each day, but such calculations are now usually made on laptop PCs or programmable calculators and not manually in field notebooks.

Each loop should be annotated with the observer's name or initials, the gravity-meter serial number and calibration factor and the base-station number and gravity value. It is useful also to record the difference between local and 'Universal' time (GMT) on each sheet, since this will be needed when tidal corrections are calculated.

Gravity data are expensive to acquire and deserve to be treated with respect. The general rules of Section 1.4.2 should be scrupulously observed.

### 2.5 Field Interpretation

Gravity results are usually interpreted by calculating the fields produced by geological models and comparing these with the actual data. This requires a computer and until recently was only rarely done in the field. Even now, an appreciation of the effects associated with a few simple bodies can help an observer temporarily severed from his laptop to assess the validity and significance of the data being collected. This can sometimes lead to a vital decision to infill with additional stations being taken at a time when this can be done quickly and economically.

#### 2.5.1 The Bouguer plate

The Bouguer plate provides the simplest possible interpretational model. An easily memorized rule of thumb is that the gravity effect of a slab of material 1 km thick and  $1 \text{ Mg m}^{-3}$  denser than its surroundings is about 400 g.u. This is true even when the upper surface of the slab is some distance below the reading points (as in the case of the second layer in Figure 2.11), provided that the distance of the station from the nearest edge of the slab is large compared with the distance to the lower surface. The effect varies in direct proportion to both thickness and density contrast.

---

#### Example 2.1

In Figure 2.12, if the standard crustal density is taken to be  $2.67 \text{ Mg m}^{-3}$ , the effect of the upper sediment layer, 1.5 km thick, would be approximately  $1.5 \times 0.37 \times 400 = 220 \text{ g.u.}$  at the centre of the basin.

The effect of the deeper sediments, 1.6 km thick, would be approximately  $1.6 \times 0.27 \times 400 = 170 \text{ g.u.}$

The total (negative) anomaly would thus be about 390 g.u.

---

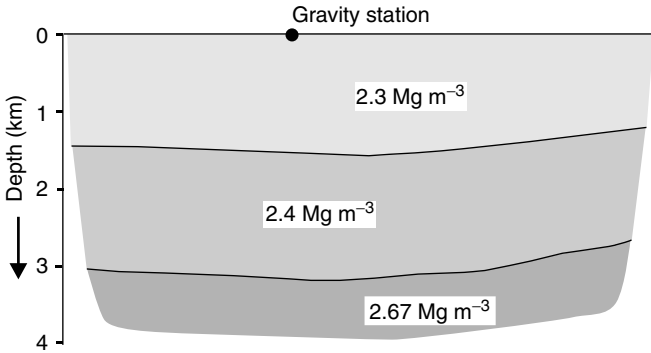


**Figure 2.11** Sedimentary basin model suitable for Bouguer plate methods of approximate interpretation. Basement is assigned the standard  $2.67 \text{ Mg m}^{-3}$  crustal density.

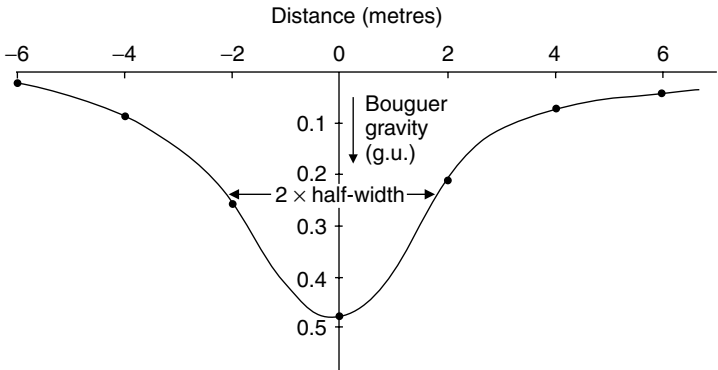


**Figure 2.12** Detailed Bouguer anomaly profile over a subsurface cavity.

## 2.5.2 Spheres and cylinders

Less-extensive bodies that produce anomalies similar to that in Figure 2.12 (or its inverse) can be modelled by homogeneous spheres or by homogeneous cylinders with circular cross-sections and horizontal axes. The field due to a sphere, radius  $r$  measured at a point immediately above its centre, is:

$$g = 4\pi\rho Gr^3/3h^2$$

The factor  $4\pi\rho G/3$  is about 280 g.u. for a density contrast of  $1 \text{ Mg m}^{-3}$  and lengths measured in kilometres, or 0.28 g.u. if lengths are measured in metres. The depth,  $h$ , of the centre of the sphere is roughly equal to four-thirds of the half-width of the anomaly.

For an infinite horizontal cylinder of circular cross-section (an example of a 2D source), the maximum field is:

$$g = 2\pi\rho Gr^2/h$$

The factor  $2\pi\rho G$  is about 400 g.u. for a density contrast of  $1 \text{ Mg m}^{-3}$  and lengths measured in kilometres, or 0.4 g.u. if lengths are measured in metres. The depth,  $h$ , of the axis of the cylinder is equal to the half-width of the anomaly.

---

### Example 2.2

Interpreting the anomaly of Figure 2.13 as due to a roughly spherical air-filled cavity in rock of density  $2.5 \text{ Mg m}^{-3}$  and working in metres:

Half-width of anomaly = 2 m

Therefore depth to sphere centre =  $2 \times 4/3 = 2.7 \text{ m}$

Amplitude of anomaly = 0.45 g.u.

$$\frac{(\text{gravity anomaly}) \times h^2}{0.28 \times (\text{density contrast})} = \frac{0.45 \times 2.7^2}{0.28 \times 2.5} \text{ i.e. } r = 1.7 \text{ m}$$

---

### Example 2.3

Interpreting the anomaly in Figure 2.13 as due to a roughly cylindrical air-filled cavity in rock of density  $2.5 \text{ Mg m}^{-3}$  and working in metres.

Half-width of anomaly = 2 m

Therefore depth to cylinder centre = 2 m

Amplitude of anomaly = 0.45 g.u.

$$\frac{(\text{gravity anomaly}) \times h}{0.4 \times (\text{density contrast})} = \frac{0.45 \times 2.0}{0.4 \times 2.5}$$

i.e.  $r = 0.8 \text{ m}$

---



### 2.5.3 Nettleton's method for direct determination of density

Density information is clearly crucial to understanding gravity anomalies, but is not easily obtained. Samples collected in the field may be more weathered, and so less dense, than the bulk of the rock mass they are assumed to represent, and the density reduction may be accentuated by the loss of some of the pore water. Estimates may also be obtained, rarely and expensively, from borehole gravity or from radiometric well logging, but such data will normally only be available where the work is being done in support of exploration for hydrocarbons.

There is, however, a method, due to Nettleton (1976) by which density estimates can be made directly from the gravity data. The bulk density of topography may be estimated by assuming that the correct value is the one which removes the effect of topography from the gravity map when corrections are made. This is true only if there is no real gravity anomaly associated with the topography and the method will fail if, for example, a hill is the surface expression of a dense igneous plug or a dipping limestone bed (Figure 2.13). The method may be applied to a profile or to all the gravity stations in an area. In the latter case, a computer may be used to determine the density value that produces the least correlation between topography and the corrected anomaly map. Even though the calculations are normally done by the interpreters, field observers should understand the technique since they may have opportunities to take additional readings for density control.

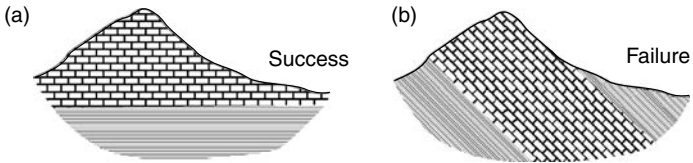


**Figure 2.13** Examples of cases in which the Nettleton (1976) method of density determination could be expected to (a) succeed and (b) fail.



# 3

## MAGNETIC METHOD

---

Compasses and dip needles were used in the Middle Ages to find magnetite ores in Sweden, making the magnetic method the oldest of all applied geophysical techniques. It is still one of the most widely used, even though significant magnetic effects are produced by only a very small number of minerals.

Magnetic field strengths are now usually measured in *nanoTesla* (nT). The pre-SI unit, the gamma, originally defined as  $10^{-5}$  gauss but numerically equal to the nT, is still often used.

### 3.1 Magnetic Properties

Although governed by the same fundamental equations, magnetic and gravity surveys are very different. The magnetic properties of adjacent rock masses may differ by several orders of magnitude rather than a few percent.

#### 3.1.1 Poles, dipoles and magnetization

An isolated magnetic pole would, if it existed, produce a field obeying the inverse-square law. In reality, the fundamental magnetic source is the dipole (Section 1.1.5) but, since a line of dipoles end-to-end produces the same effect as positive and negative poles isolated at opposite ends of the line (Figure 3.1), the pole concept is often useful.

A dipole placed in a magnetic field tends to rotate, and so is said to have a *magnetic moment*. The moment of the simple magnet of Figure 3.1, which is effectively a positive pole, strength  $m$ , at a distance  $2L$  from a negative pole  $-m$ , is equal to  $2Lm$ . The magnetization of a solid body is defined by

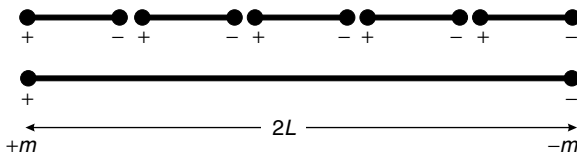


**Figure 3.1** Combination of magnetic dipoles to form an extended magnet. The positive and negative poles at the ends of adjacent dipoles cancel each other out. The pole strength of the magnet is the same as that of the constituent dipoles, but its magnetic moment is equal to its length multiplied by that pole strength.

its magnetic moment per unit volume and is a vector, having direction as well as magnitude.

### 3.1.2 Susceptibility

A body placed in a magnetic field acquires a magnetization which, if small, is proportional to the field:

$$M = kH$$

The *susceptibility*,  $k$ , is very small for most natural materials, and may be either negative (diamagnetism) or positive (paramagnetism). The fields produced by dia- and paramagnetic materials are usually considered to be too small to affect survey magnetometers, but modern high-sensitivity magnetometers are creating exceptions to this rule. Most observed magnetic anomalies are due to the small number of *ferro-* or *ferri-magnetic* substances in which the molecular magnets are held parallel by intermolecular *exchange forces*. Below the *Curie temperature*, these forces are strong enough to overcome the effects of thermal agitation. Magnetite, pyrrhotite and maghemite, all of which have Curie temperatures of about 600 °C, are the only important naturally occurring magnetic minerals and, of the three, magnetite is by far the most common. Hematite, the most abundant iron mineral, has a very small susceptibility and many iron ore deposits do not produce significant magnetic anomalies.

The magnetic properties of highly magnetic rocks tend to be extremely variable and their magnetization is not strictly proportional to the applied field. Quoted susceptibilities are for Earth-average field strengths.

### 3.1.3 Remanence

Ferro- and ferri-magnetic materials may have permanent as well as induced magnetic moments, so that their magnetization is not necessarily in the direction of the Earth's field. The *Konigsberger ratio* of the permanent moment to the moment that would be induced in an Earth-standard field of 50 000 nT, is generally large in highly magnetic rocks and small in weakly magnetic ones, but is occasionally extraordinarily high (>10 000) in hematite. Magnetic anomalies due entirely to remanence are sometimes produced by hematitic ores.

### 3.1.4 Susceptibilities of rocks and minerals

The *susceptibility* of a rock usually depends on its magnetite content. Sediments and acid igneous rocks have small susceptibilities whereas basalts, dolerites, gabbros and serpentinites are usually strongly magnetic. Weathering generally reduces susceptibility because magnetite is oxidized to hematite, but some laterites are magnetic because of the presence of maghemite and

**Table 3.1** *Magnetic susceptibilities of common rocks and ores*

<i>Common rocks</i>	
Slate	0–0.002
Dolerite	0.01–0.15
Greenstone	0.0005–0.001
Basalt	0.001–0.1
Granulite	0.0001–0.05
Rhyolite	0.00025–0.01
Salt	0.0–0.001
Gabbro	0.001–0.1
Limestone	0.00001–0.0001
<i>Ores</i>	
Hematite	0.001–0.0001
Magnetite	0.1–20.0
Chromite	0.0075–1.5
Pyrrhotite	0.001–1.0
Pyrite	0.0001–0.005

remanently magnetized hematite. The susceptibilities, in rationalized SI units, of some common rocks and minerals are given in Table 3.1.

## 3.2 The Magnetic Field of the Earth

The magnetic fields of geological bodies are superimposed on the background of the Earth's main field. Variations in magnitude and direction of this field influence both the magnitudes and shapes of local anomalies.

In geophysics, the terms *north* and *south* used to describe polarity are replaced by positive and negative. The direction of a magnetic field is conventionally defined as the direction in which a unit positive pole would move but, since all things are relative, geophysicists give little thought to whether it is the north or south magnetic pole that is positive.

### 3.2.1 The main field of the Earth

The Earth's main magnetic field originates in electric currents circulating in the liquid outer core, but can be largely modelled by a dipole source at the Earth's centre. Distortions in the dipole field extending over regions thousands of kilometres across can be thought of as caused by a relatively small number of subsidiary dipoles at the core–mantle boundary.

The variations with latitude of the magnitude and direction of an ideal dipole field aligned along the Earth's spin axis are shown in Figure 3.2. Note that near the equator the dip angles change almost twice as fast as

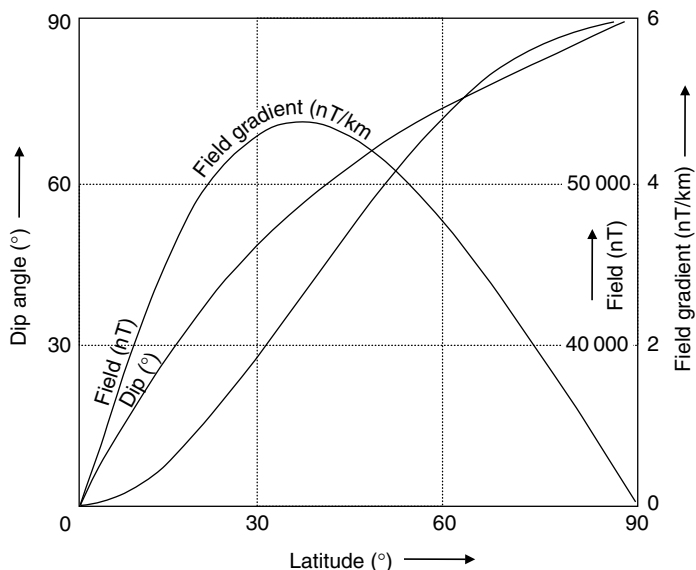


**Figure 3.2** Variation in intensity, dip and gradient for an ideal dipole aligned along the Earth's spin axis and producing a polar field of 60 000 nT.

the latitude angles. To explain the Earth's actual field, the main dipole would have to be inclined at about  $11^\circ$  to the spin axis, and thus neither the magnetic equator, which links points of zero magnetic dip on the Earth's surface, nor the magnetic poles coincide with their geographic equivalents (Figure 3.3). The North Magnetic Pole is in northern Canada and the South Magnetic Pole is not even on the Antarctic continent, but in the Southern Ocean at about  $65^\circ\text{S}$ ,  $138^\circ\text{E}$ . Differences between the directions of true and magnetic North are known as declinations, presumably because a compass needle *ought* to point north but *declines* to do so.

Dip angles estimated from the global map (Figure 3.3) can be used to obtain rough estimates of magnetic latitudes and hence (using Figure 3.2) of regional gradients. This approach is useful in determining whether a regional gradient is likely to be significant but gives only approximate correction factors, because of the existence of very considerable local variations. Gradients are roughly parallel to the local *magnetic* north arrow, so that corrections have E–W as well as N–S components. In ground surveys where anomalies of many tens of nT are being mapped, regional corrections, which generally amount to only a few nT per km, are often neglected.

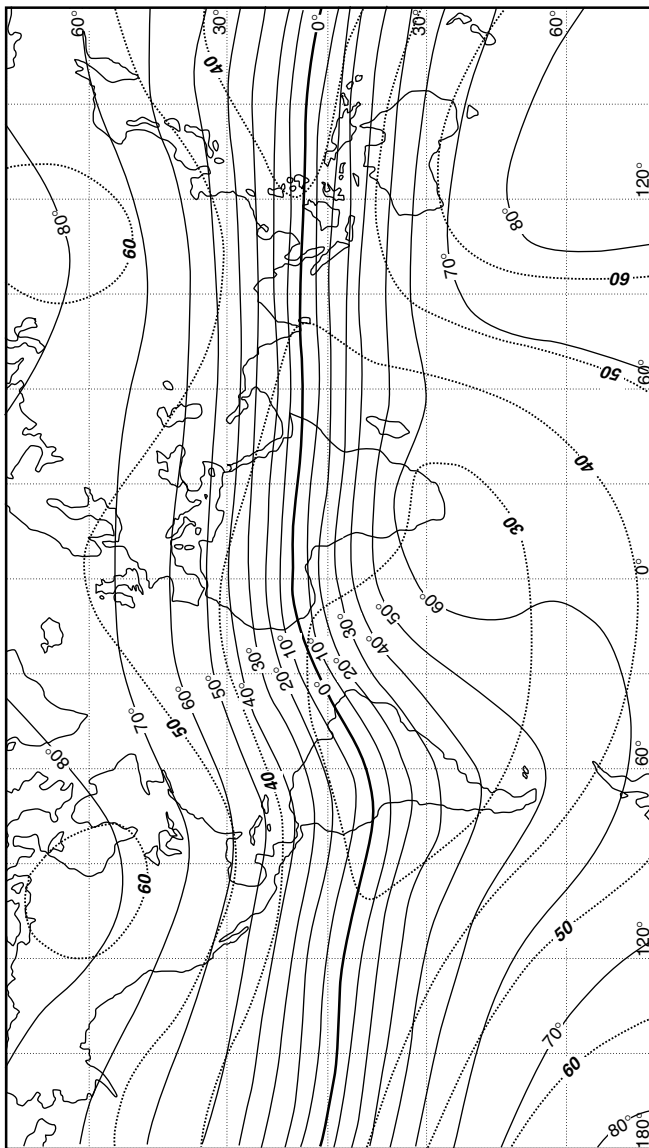


**Figure 3.3** Dip (continuous lines, values in degrees) and intensity (dotted lines, values in thousands of nT) of the Earth's magnetic field. The thick continuous line is the magnetic equator.

### 3.2.2 The International Geomagnetic Reference Field (IGRF)

The variations of the Earth's main field with latitude, longitude and time are described by experimentally determined International Geomagnetic Reference Field (IGRF) equations, defined by 120 spherical harmonic coefficients, to order  $N = 10$ , supplemented by a predictive secular variation model to order  $N = 8$ . The shortest wavelength present is about 4000 km. IGRFs provide reasonable representations of the actual regional fields in well-surveyed areas, where they can be used to calculate regional corrections, but discrepancies of as much as 250 nT can occur in areas from which little information was available at the time of formulation.

Because the long-term *secular* changes are not predictable except by extrapolation from past observations, the IGRF is updated every five years on the basis of observations at fixed observatories and is also revised retrospectively to give a definitive model (DGRF). GRF corrections are vital when airborne or marine surveys carried out months or years apart are being compared or combined but are less important in ground surveys, where base stations can be reoccupied.

### 3.2.3 Diurnal variations

The Earth's magnetic field also varies because of changes in the strength and direction of currents circulating in the ionosphere. In the normal *solar-quiet* (Sq) pattern, the background field is almost constant during the night but decreases between dawn and about 11 a.m., increases again until about

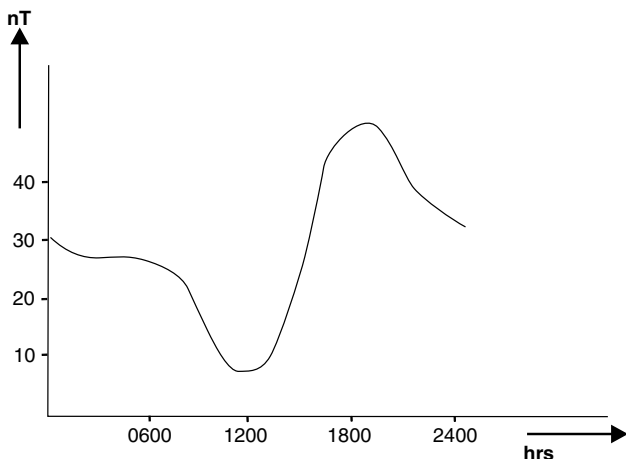


**Figure 3.4** Typical 'quiet day' magnetic field variation at mid-latitudes.



4 p.m. and then slowly declines to the overnight value (Figure 3.4). Peak-to-trough amplitudes in mid-latitudes are of the order of a few tens of nanoTesla. Since upper atmosphere ionization is caused by solar radiation, diurnal curves tend to be directly related to local solar time but amplitude differences of more than 20% due to differences in crustal conductivity may be more important than time dependency for points up to a few hundred kilometers apart. Short period, horizontally polarized and roughly sinusoidal *micropulsations* are significant only in surveys that are to be contoured at less than 5 nT.

Within about  $5^\circ$  of the magnetic equator the diurnal variation is strongly influenced by the *equatorial electrojet*, a band of high conductivity in the ionosphere about 600 km ( $5^\circ$  of latitude) wide. The amplitudes of the diurnal curves in the affected regions may be well in excess of 100 nT and may differ by 10 to 20 nT at points only a few tens of kilometres apart.

Many of the magnetic phenomena observed in polar regions can be explained by an *auroral electrojet* subject to severe short-period fluctuations. In both equatorial and polar regions it is particularly important that background variations be monitored continuously. Returning to a base station at intervals of one or two hours may be quite insufficient.

### 3.2.4 Magnetic storms

Short-term auroral effects are special cases of the irregular disturbances (Ds and Dst) known as *magnetic storms*. These are produced by sunspot and solar flare activity and, despite the name, are not meteorological, often occurring on clear, cloudless days. There is usually a sudden onset, during which the field may change by hundreds of nT, followed by a slower, erratic return to normality. Time scales vary widely but the effects can persist for hours and sometimes days. Micropulsations are generally at their strongest in the days immediately following a storm, when components with periods of a few tens of seconds can have amplitudes of as much as 5 nT.

Ionospheric prediction services in many countries give advance warning of the general probability of storms but not of their detailed patterns, and the field changes in both time and space are too rapid for corrections to be applied. Survey work must stop until a storm is over. Aeromagnetic data are severely affected by quite small irregularities and for contract purposes *technical magnetic storms* may be defined, sometimes as departures from linearity in the diurnal curve of as little as 2 nT in an hour. Similar criteria may have to be applied in archaeological surveys when only a single sensor is being used (rather than a two-sensor gradiometer).

### 3.2.5 Geological effects

The Curie points for all geologically important magnetic materials are in the range 500–600 °C. Such temperatures are reached in the lower part of normal

continental crust but below the Moho under the oceans. The upper mantle is only weakly magnetic, so that the effective base of local magnetic sources is the Curie isotherm beneath continents and the Moho beneath the oceans.

Massive magnetite deposits can produce magnetic fields of as much as 200 000 nT, which is several times the magnitude of the Earth's normal field. Because of the dipolar nature of magnetic sources these, and all other, magnetic anomalies have positive and negative parts and in extreme cases directional magnetometers may even record negative fields. Anomalies of this size are unusual, but basalt dykes and flows and some larger basic intrusions can produce fields of thousands and occasionally tens of thousands of nT. Anomalous fields of more than 1000 nT are otherwise rare, even in areas of outcropping crystalline basement. Sedimentary rocks generally produce changes of less than 10 nT, as do the changes in soil magnetization important in archaeology.

In some tropical areas, magnetic fields of tens of nT are produced by maghemite formed as nodular growths in laterites. The nodules may later weather out to form ironstone gravels which give rise to high noise levels in ground surveys. The factors that control the formation of maghemite rather than the commoner, non-magnetic form of hematite are not yet fully understood.

### 3.3 Magnetic Instruments

Early *torsion magnetometers* used compass needles mounted on horizontal axes (dip needles) to measure vertical fields. These were in use until about 1960, when they began to be replaced by fluxgate, proton precession and alkali vapour magnetometers. Instruments of all these three types are now marketed with built-in data loggers and can often be set to record automatically at fixed time intervals at base stations. All three can be used singly or in tandem as *gradiometers*, although care must then be taken with precession instruments to ensure that the polarizing field from one sensor does not affect the measurement at the other. Gradient measurements emphasize near surface sources (Figure 3.5) and are particularly useful in archaeological and environmental work.

#### 3.3.1 Proton precession magnetometer

The proton precession magnetometer makes use of the small magnetic moment of the hydrogen nucleus (proton). The sensing element consists of a bottle containing a low freezing-point hydrocarbon fluid about which is wound a coil of copper wire. Although many fluids *can* be used, the manufacturer's recommendation, usually for high-purity decane, should always be followed if the bottle has to be topped up. A *polarizing* current of the order of an amp or more is passed through the coil, creating a strong magnetic

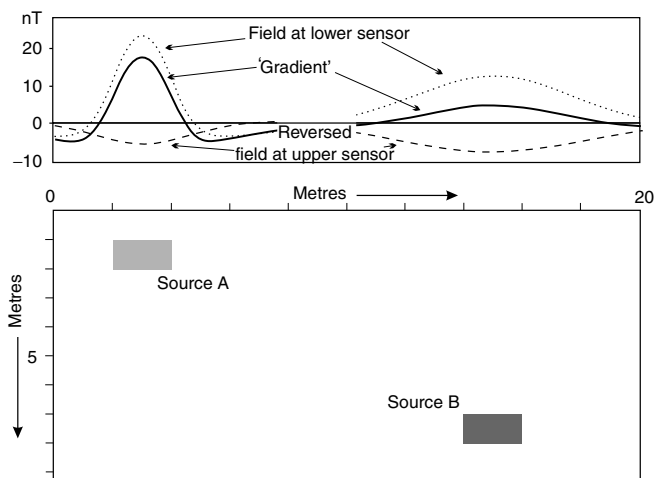


**Figure 3.5** Inverse-cube law effects in magnetic gradiometry. The dotted curves show the magnetic effects of the two bodies measured at the ground surface, the dashed curves show the effects (reversed) as measured one metre above the surface. The solid curves show the differential effect. In the case of Source A, the difference (gradient) anomaly has almost the same amplitude as the anomaly measured at ground level. In the case of the deep Source B, the total field anomaly amplitudes at the two sensors are similar and the gradient anomaly is correspondingly small.

field, along which the moments of the protons in the hydrogen atoms will tend to become aligned.

When the current is switched off, the protons realign to the direction of the Earth's field. Quantum theory describes this reorientation as occurring as an abrupt 'flip', with the emission of a quantum of electromagnetic energy. In classical mechanics, the protons are described as *precessing* about the field direction, as a gyroscope precesses about the Earth's gravity field, at a frequency proportional to the field strength, emitting an electromagnetic wave as they do so. Both theories relate the electromagnetic frequency to the external field via two of the most accurately known of all physical quantities, Planck's constant and the proton magnetic moment. In the Earth's field of about 50 000 nT, the precession frequency is about 2000 Hz. Sophisticated phase-sensitive circuitry is needed to measure such frequencies to the accuracies of one part in 50 000 (i.e. 1 nT) in the half or one second which is all that modern geophysicists will tolerate. Ultra-portable instruments are available

which read to only 10 nT, but these are only marginally easier to use and have not become popular.

In theory the proton magnetometer is capable of almost any desired accuracy, but in practice the need for short reading times and reasonable polarization currents sets the limit at about 0.1 nT.

Proton magnetometers may give erratic readings in strong field gradients and also because of interference from power lines and radio transmitters and even from eddy currents induced in nearby conductors by the termination of the polarizing current. Also, they can only measure total fields, which may cause problems in interpreting large anomalies where the direction of the field changes rapidly from place to place. However, these are only minor drawbacks and the 1 nT or 0.1 nT proton magnetometer is now the most widely used instrument in ground surveys. The self-orientating property allows the sensor to be supported on a staff well away from both the observer and from small magnetic sources at ground level (Figure 1.6). It is also an advantage that readings are obtained as drift-free absolute values in nT, even though corrections must still be made for diurnal variations.

### 3.3.2 High sensitivity (alkali vapour) magnetometers

Proton magnetometers can be made more sensitive using the Overhauser effect, in which a VHF radio wave acts on paramagnetic material added to the bottle fluid. This increases the precession signal by several orders of magnitude, considerably improving the signal/noise ratio. However, high sensitivity is now more commonly achieved using electrons, which have magnetic moments about 2000 times greater than those of protons. Effectively isolated electrons are provided by vapours of alkali metals (usually caesium), since the outer electron 'shell' of an atom of one of these elements contains only a single electron. The principle is similar to that of the proton magnetometer, in that transitions between energy states are observed, but the much higher energy differences imply much higher frequencies, which can be measured with much smaller percentage errors. The actual measurement process is quite complicated, involving the raising of electrons to a high energy state by a laser beam ('optical pumping') and then determining the frequency of the high frequency radio signal that will trigger the transition to a lower state. This is all, however, invisible to the user. Measurements are in principle discontinuous but measuring times are very small and 10 readings can routinely be taken every second. The effects of electrical interference and high field gradients are less serious than with proton precession instruments.

Alkali vapour magnetometers are slightly direction sensitive. Readings cannot be obtained if the sensor is oriented within a few degrees of either the direction of the magnetic field or the direction at right angles to it. This is not a significant limitation in most circumstances, and the rather slow

acceptance of these instruments for ground surveys has had more to do with their relatively high cost and the fact that in most geological applications the high sensitivity is of little use. Sensitivity is, however, essential in gradiometry (Figure 3.5), and field changes of less than 1 nT may be significant in archaeology, where rapid coverage (sometimes achieved using a non-magnetic trolley with a trigger actuated by the rotations of the wheels) demands virtually continuous readings.

### 3.3.3 The fluxgate magnetometer

The sensing element of a fluxgate magnetometer consists of one or more cores of magnetic alloy, around which are wound coils through which alternating current can be passed. Variations in the electrical properties of the circuits with magnetization of the cores can be converted into voltages proportional to the external magnetic field along the core axes. Measurements are thus of the magnetic field component in whichever direction the sensor is pointed. Vertical fields are measured in most ground surveys.

Fluxgates do not measure absolute fields and therefore require calibration. They are also subject to thermal drift, because the magnetic properties of the cores and, to a lesser extent, the electrical properties of the circuits vary with temperature. Early ground instruments sacrificed thermal insulation for portability and were often accurate to only 10 or 20 nT. In recognition of this, readings were displayed, rather crudely, by the position of a needle on a graduated dial. Despite claims to the contrary by some manufacturers, such sensitivity is quite inadequate for most ground survey work.

One problem with portable fluxgates is that because they require orientation at each station, the operator must be close to the sensor when the reading is taken. Ensuring the operator is completely non-magnetic is not easy, and most dry batteries now obtainable are steel-jacketed and very magnetic. They can make nonsense of readings if installed in the same housing as the sensor. External battery packs can be used but are clumsy and reduce rather than eliminate the effects. Lead-acid gel rechargeable batteries are not inherently magnetic but need to be checked for the presence of magnetic materials.

Fluxgates are now mainly used, either with internal memory or linked to data loggers, in archaeological surveys where the negligible reading times allow very large numbers of readings to be taken quickly within small areas. A survey of this type may require measurements to be made close to ground level and may not be possible with proton magnetometers because of their sensitivity to field gradients and electrical interference. Subtracting the readings from two similar and rigidly linked fluxgate sensors to obtain gradient information minimizes thermal drift effects, reduces the effect of errors in

orientation, emphasizes local sources (Figure 3.5) and virtually eliminates the effects of diurnal variations, including micropulsations.

Three-component fluxgate magnetometers can eliminate the need for precise orientation or, alternatively, can provide information on field direction as well as field strength.

### 3.4 Magnetic Surveys

Although absolute numerical readings are obtained (and can be repeated) at the touch of a button with proton and caesium magnetometers, faulty magnetic maps can still be produced if simple precautions are ignored. For example, all base locations, whether used for repeat readings or for continuous diurnal monitoring, should be checked for field gradients. A point should not be used as a base if moving the sensor a metre produces a significant change.

#### 3.4.1 Starting a survey

The first stage in any magnetic survey is to check the magnetometers (and the operators). Operators can be potent sources of magnetic noise, although the problems are much less acute when sensors are on 3 m poles than when, as with fluxgates, they must be held close to the body. Errors can also occur when the sensor is carried on a short pole or in a back-pack. Compasses, pocket knives and geological hammers are all detectable at distances below about a metre, and the use of high sensitivity magnetometers may require visits to the tailor (and cobbler) for non-magnetic clothing. Survey vehicles can affect results at distances of up to 20 m. The safe distance should be determined before starting survey work.

All absolute magnetometers should give the same reading at the same time in the same place. Differences were often greater than 10 nT between instruments manufactured prior to 1980 but are now seldom more than 1 or 2 nT. Sensors can be placed very close together and may even touch when checks are being made, but proton magnetometer readings cannot be precisely simultaneous because the two polarizing fields would interfere.

Large discrepancies and very variable readings with a proton magnetometer usually indicate that it is poorly tuned. The correct tuning range can be roughly identified using global maps (Figure 3.3) but final checks should be made in the field. Near-identical readings should be obtained if the setting is varied over a range of about 10 000 nT about its optimum position (e.g. 47 000 in Example 3.1). Manual versions are generally rather coarsely tunable in steps of a few thousand nT, but greater accuracy is possible with microprocessor control. It is partly this finer tuning that allows some proton magnetometers to be routinely read to 0.1 nT. Often, these instruments are programmed to warn of faulty tuning or high gradients by refusing to display the digit beyond the decimal point.

Example 3.1 also shows that repeatability alone is no guarantee of correct tuning. It is the range of settings over which the circuits can lock to the precession signal that provides the crucial evidence.

---

**Example 3.1: Proton magnetometer tuning (manual model)**


---

<i>Tuning setting</i>	<i>Readings</i>		
30 000	31 077	31 013	31 118
32 000	32 770	32 788	32 775
34 000	35 055	34 762	34 844
36 000	37 481	37 786	37 305
38 000	42 952	40 973	41 810
41 000	47 151	47 158	47 159
44 000	47 160	47 158	47 159
47 000	47 171	47 169	47 169
50 000	47 168	47 175	47 173
53 000	47 169	47 169	47 169
56 000	53 552	54 602	54 432
60 000	59 036	59 292	58 886
64 000	65 517	65 517	65 517

---

### 3.4.2 Monitoring diurnal variation

Diurnal corrections are essential in most field work, unless only gradient data are to be used. If only a single instrument is available, corrections have to rely on repeated visits to a base or sub-base, ideally at intervals of less than one hour. A more complete diurnal curve can be constructed if a second, fixed, magnetometer is used to obtain readings at 3 to 5 minute intervals. This need not be of the same type as the field instrument. A cheaper proton magnetometer can provide adequate diurnal control for surveys with a more expensive caesium vapour instrument.

In principle, it is possible to dispense with frequent base reoccupations when an automatic base station is operating. It is, however, poor practice to rely entirely on the base record, since recovery of field data will then be difficult, if not impossible, if the base instrument fails. Problems are especially likely with unattended automatic instruments because the battery drain is rather high and the transition from operational to unworkable can occur with little warning. Readings already stored are preserved by the action of a separate lithium battery, but diurnal control is lost for the rest of the day.

Obviously, bases should be remote from possible sources of magnetic interference (especially temporary sources such as traffic), and should be

describable for future use. Especial vigilance is needed if field and diurnal instruments are later linked by a data-exchange line and corrections are made automatically. Unless the diurnal curve is actually plotted and examined, absurdities in the diurnal data (as might be caused by an inquisitive passer-by driving up to the base) may be overlooked and may appear, in reverse, as anomalies in the field data.

### 3.4.3 Field procedures – total field surveys

At the start of each survey day the diurnal magnetometer must be set up. The first reading of the field magnetometer should be at a base or sub-base, and should be made at the same time as a reading is being made, either automatically or manually, at the base. This does not necessarily require the two instruments to be adjacent.

All field readings should be taken twice and the two readings should differ by no more than 1 nT. Greater differences may indicate high field gradients, which may need further investigation. Large differences between readings at adjacent stations call for *infill* at intermediate points. It is obviously desirable that the operator notices this, and infills immediately.

At each station the location, time and reading must be recorded, as well as any relevant topographic or geological information and details of any visible or suspected magnetic sources. Unless the grid is already well mapped, the notebook should also contain enough information for the lines to be positioned on maps or air-photos.

At the end of the day, a final reading should be made at the base first occupied. This should again be timed to coincide with a reading of the diurnal magnetometer. If readings in the field are being recorded manually, it is good practice to then transcribe the diurnal data for the times of the field readings into the field notebook, which then contains a complete record of the day's work.

### 3.4.4 Standard values

Diurnal curves record the way in which field strength has varied at a fixed base, and data processing is simplified if this base is at the same point throughout the survey. A *standard value* (SV) must be allocated to this point, preferably by the end of the first day of survey work. The choice is to some extent arbitrary. If the variation in measured values were to be between 32 340 nT and 32 410 nT, it might be convenient to adopt 32 400 nT as the SV, even though this was neither the mean nor the most common reading.

Unless the survey area is so small that a single reference base can be used, a number of sub-bases will have to be established (Section 1.4) and their SVs determined. The underlying principle is that if, at some given time, the base magnetometer reading is actually equal to the base SV, then identical



instruments at all other bases and sub-bases should record the SVs at those points. The field readings are then processed so that this is true of the values assigned to all survey points.

## 3.4.5 Processing magnetic data

During a survey, bases or sub-bases should be occupied at intervals of not more than two hours, so that data can be processed even if the diurnal record is lost or proves faulty. The way in which such readings might be used to provide diurnal control, with or without an automatically recorded diurnal curve, is shown in Figure 3.6.

The diurnal correction at any time is simply the difference between the SV at the diurnal station and the actual diurnal reading, but magnetic data can be corrected in two different ways using this fact. The most straightforward is to determine, by interpolation when necessary, the diurnal value at the time a given field reading was made and to subtract this from the reading. The

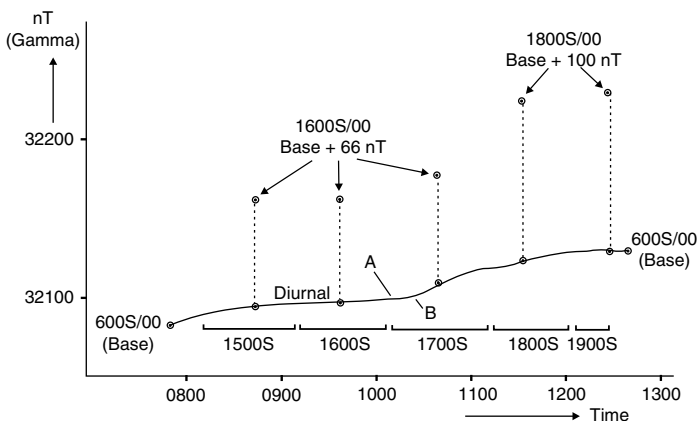


**Figure 3.6** Diurnal control, with variations monitored both by a memory instrument at the diurnal base and by repeat readings at various sub-bases. The greatest error introduced by using straight-line interpolation between diurnal values derived from the sub-bases would have been 5–10 nT and would have affected Line 1700S between points A and B. Interpolation using a smooth curve instead of straight lines would have significantly reduced this error. The shifts needed to make the sets of sub-base values fall on the diurnal curve provide estimates of the differences between the SVs at the diurnal base and at the sub-bases. The time periods during which individual survey lines were being read are also shown.

diurnal station SV can then be added to give the SV at the field station. If a computer is available, the whole operation can be automated.

This method is simple in principle and provides individual values at all field points but is tedious and error-prone if hundreds of stations have to be processed by hand each evening. If only a contour map is required, this can be based on profiles of uncorrected readings, as shown in Figure 3.7. Fewer calculations are needed and errors and peculiarities in the data are immediately obvious.

Even if no computer is available to do the hard work, plotting magnetic profiles should be a field priority since this provides the best way of assessing the significance, or otherwise, of diurnal effects and noise. For example, the profile in Figure 3.7 shows very clearly that, with 100 nT contours, the 5 nT discrepancy between the diurnal curves based on direct observation and on

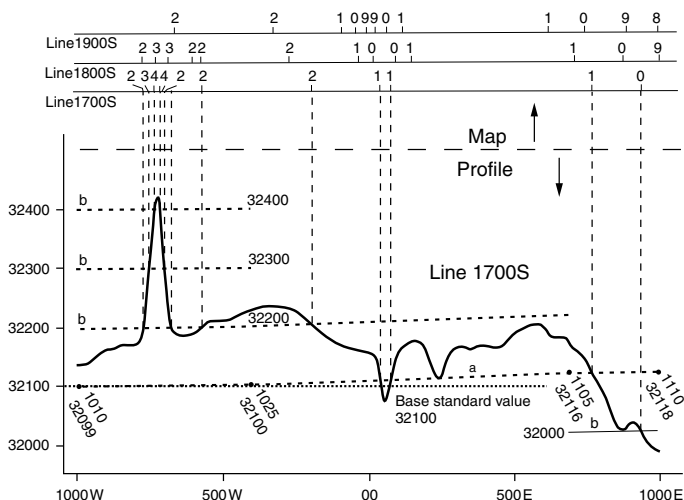


**Figure 3.7 PROFILE:** Contour cuts at 100 nT intervals on uncorrected profile 1700S, by diurnal curve and parallel curves. The reference base SV is 32 100 nT and the points at which the diurnal curve (dashed line 'a') intersects the profile therefore correspond to points on the ground where the corrected value of the magnetic field is also 32 100 nT. Parallel curves (dashed lines 'b') identify points at which the SVs differ from those at the diurnal base by integer multiples of 100 nT. MAP: Contour cut plot of 1700S and two adjacent lines. Only these contour cuts need be plotted on the map, and some may be omitted where they are very close together.

base reoccupations is unimportant. It also shows the extent to which such contours leave significant magnetic features undefined.

If a computer is used to calculate corrected values at each field point, profiles should still be produced but can then be of corrected rather than raw data.

### 3.4.6 Noise in ground magnetic surveys

Magnetic readings in populated areas are usually affected by stray fields from pieces of iron and steel (*cultural noise*). Even if no such materials are visible, profiles obtained along roads are usually very distorted compared to those obtained on parallel traverses through open fields only 10 or 20 m away. Since the sources are often quite small and may be buried within a metre of the ground surface, the effects are very variable.

One approach to the noise problem is to try to take all readings well away from obvious sources, noting in the field books where this has not been possible. Alternatively, the almost universal presence of ferrous noise can be accepted and the data can be filtered. For this method to be successful, many more readings must be taken than would be needed to define purely geological anomalies. The technique is becoming more popular with the increasing use of data loggers, which discourage note-taking but allow vast numbers of readings to be taken and processed with little extra effort, and is most easily used with alkali vapour and fluxgate instruments which read virtually continuously. The factors discussed in Section 1.3.10 in relation to continuous readings must all be taken into account. It is only safe to dispense with notebooks for comments on individual stations if the survey grid as a whole is well surveyed, well described and accurately located.

## 3.5 Simple Magnetic Interpretation

Field interpretation of magnetic data allows areas needing infill or checking to be identified and then revisited immediately and at little cost. Good interpretation requires profiles, which preserve all the detail of the original readings, and contour maps, which allow trends and patterns to be identified. Fortunately, the now almost ubiquitous laptop PC has reduced the work involved in contouring (providing the necessary programs have been loaded).

### 3.5.1 Forms of magnetic anomaly

The shape of a magnetic anomaly varies dramatically with the dip of the Earth's field, as well as with variations in the shape of the source body and its direction of magnetization. Simple sketches can be used to obtain rough visual estimates of the anomaly produced by any magnetized body.

Figure 3.8a shows an irregular mass magnetized by induction in a field dipping at about  $60^\circ$ . Since the field direction defines the direction in which a positive pole would move, the effect of the external field is to produce

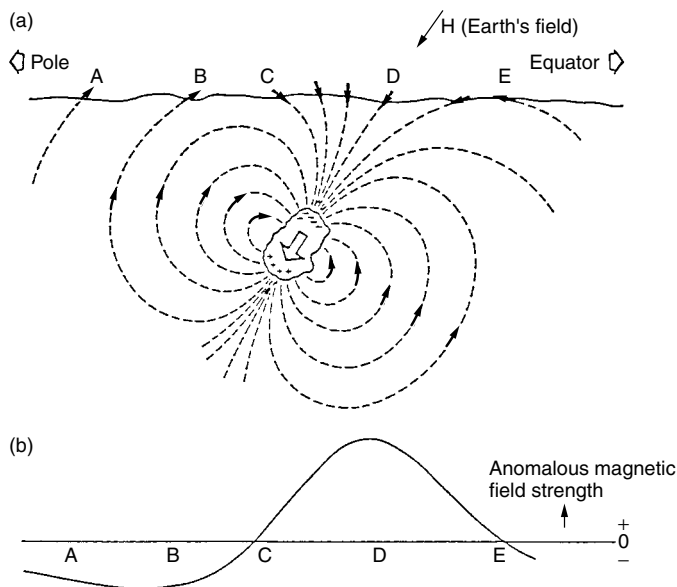


**Figure 3.8** Mid-latitude total field anomaly due to induced magnetization. (a) The induced field. (b) The anomaly profile, derived as described in the text.

the distribution of poles shown. The secondary field due to these poles is indicated by the dashed lines of force. Field direction is determined by the simple rule that like poles repel.

If the secondary field is small, the directions of the total and background fields will be similar and no anomalous field will be detected near C and E. The anomaly will be positive between these points and negative for considerable distances beyond them. The anomaly maximum will be near D, giving a magnetic profile with its peak offset towards the magnetic equator (Figure 3.8b). At the equator the total-field anomaly would be negative and centred over the body and would have positive side lobes to north and south, as can easily be verified by applying the method of Figure 3.8 to a situation in which the inducing field is horizontal.

Because each positive magnetic pole is somewhere balanced by a negative pole, the net flux involved in any anomaly is zero. Over the central parts of a uniform magnetized sheet the fields from positive and negative poles cancel out, and only the edges are detected by magnetic surveys. Strongly magnetized but flat-lying bodies thus sometimes produce little or no anomaly.

### 3.5.2 'Rule-of-thumb' depth estimation

Depth estimation is one of the main objectives of magnetic interpretation. Simple rules give depths to the tops of source bodies that are usually correct to within about 30%, which is adequate for preliminary assessment of field results.

In Figure 3.9a the part of the anomaly profile, on the side nearest the magnetic equator, over which the variation is almost linear is emphasized by a thickened line. The depths to the abruptly truncated tops of bodies of many shapes are approximately equal to the horizontal extent of the corresponding straight-line sections. This method is effective but is hard to justify since there is actually no straight segment of the curve and the interpretation relies on an optical illusion.

In the slightly more complicated *Peters' method*, a tangent is drawn to the profile at the point of steepest slope, again on the side nearest the equator, and lines with half this slope are drawn using the geometrical construction of Figure 3.9b. The two points at which the half-slope lines are tangents to the anomaly curve are found by eye or with a parallel ruler, and the horizontal distance between them is measured. This distance is divided by 1.6 to give a rough depth to the top of the source body.

Peters' method relies on model studies that show that the true factor generally lies between about 1.2 and 2.0, with values close to 1.6 being common for thin, steeply dipping bodies of considerable strike extent. Results are usually very similar to those obtained using the straight slope. In both cases the profile must either be measured along a line at right angles to the

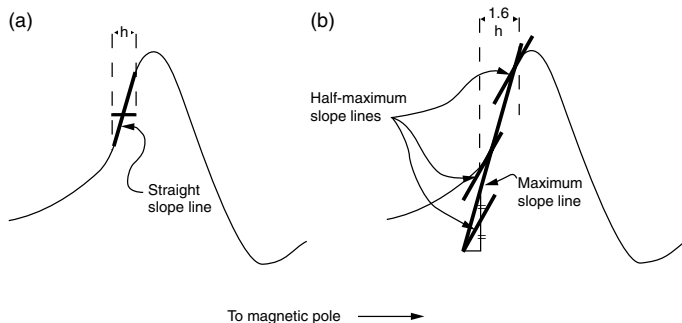


**Figure 3.9** Simple depth estimation: (a) Straight slope method. The distance over which the variation appears linear is (very) roughly equal to the depth to the top of the magnetized body. (b) Peters' method. The distance between the contact points of the half-slope tangents is (very) roughly equal to 1.6 times the depth to the top of the magnetized body.

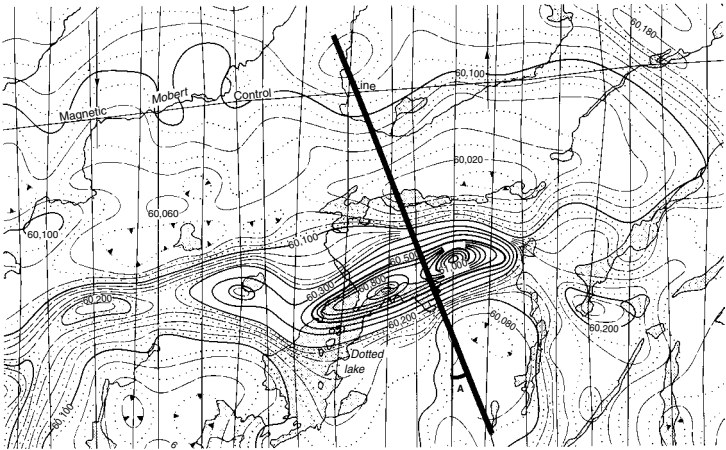


**Figure 3.10** *Effect of strike. A depth estimate on a profile recorded along a traverse line (i.e. one of the set of continuous, approximately straight lines) must be multiplied by the cosine of the angle A made with the line drawn at right angles to the magnetic contours. The example is from an aeromagnetic map (from northern Canada) but the same principle applies in ground surveys.*

strike of the anomaly or else the depth estimate must be multiplied by the cosine of the intersection angle (A in Figure 3.10).

# 4

## RADIOMETRIC SURVEYS

---

The radioactivity of rocks is monitored using gamma-ray scintillometers and spectrometers. Although most radiometric instruments were developed with uranium search in mind, other uses were soon found. Among these were regional geological mapping and correlation, exploration for some industrial minerals and *in situ* determinations of phosphates. The same instruments may also be used to track the movement of artificial radioactive *tracers* deliberately introduced into groundwater, and to assess health risks from natural and artificial radiation sources. Radon gas detectors, which monitor alpha particles, have some exploration uses but are most important in public health applications.

### 4.1 Natural Radiation

Spontaneous radioactive decay produces alpha, beta and gamma radiation. Alpha and beta ‘rays’ are actually particles; gamma rays are high-energy electromagnetic waves which, so quantum theory tells us, can be treated as if composed of particles.

#### 4.1.1 Alpha particles

An alpha particle consists of two protons held together by two neutrons to form a stable helium nucleus. Emission of alpha particles is the main process in radioactive decay, resulting in a decrease of four in atomic mass and two in atomic number. The particles have large kinetic energies but are rapidly slowed down by collisions with other atomic nuclei. At *thermal* energies they soon gain two orbital electrons and become indistinguishable from other helium atoms. The average distance travelled in solid rock before this occurs is measured in fractions of a millimetre.

#### 4.1.2 Beta particles

Beta particles are electrons ejected from atomic nuclei. They differ from other electrons only in having higher kinetic energies and so cease to be identifiable after being slowed down by multiple collisions. Energy is lost most rapidly in collisions with other electrons. In solids or liquids the average range of a beta particle is measured in centimetres.

#### 4.1.3 Gamma radiation

Gamma rays are electromagnetic waves with frequencies so high that they are best regarded as consisting of particles, known as *photons*, with energies

proportional to the frequencies. The energy range for gamma rays is generally considered to start at about 0.1 MeV (a frequency of about  $0.25 \times 10^{20}$  Hz).

Because they are electrically neutral, photons penetrate much greater thicknesses of rock than do either alpha or beta particles and are consequently the most geophysically useful form of radiation. Even so, approximately 90% of the gamma photons detected over bare rock will come from within 20–30 cm of the surface and even over soil only 10% will come from below about 50 cm. Water is almost equally effective, with one metre absorbing about 97% of the radiation travelling through it. On the other hand, 100 m of air will only absorb about half of a gamma-ray flux. Attenuation is frequency dependent and (for once) it is the higher frequency, higher energy radiation that has the greater penetrating power. Half of a 1 MeV flux is absorbed by about 90 m of air but it takes about 160 m of air to absorb half of a 3 MeV flux. In either case, these figures imply that atmospheric absorption can generally be ignored in ground surveys.

## 4.1.4 Radioactivity of rocks

Gamma rays provide information on the presence of unstable atomic nuclei. The average number of decays in a given time will be directly proportional to the number of atoms of the unstable element present. The rate of decrease in mass of a radioactive material therefore obeys an exponential law governed by a *half-life* (Section 1.1.6).

Elements with short half-lives can occur in nature because they are formed in decay series which originate with very long-lived isotopes, sometimes termed *primeval*, that are mainly concentrated in acid igneous rocks and in sediments deposited as evaporites or in reducing environments. The principal primeval isotopes are  $^{40}\text{K}$ ,  $^{232}\text{Th}$ ,  $^{235}\text{U}$  and  $^{238}\text{U}$ . Others, such as  $^{48}\text{Ca}$ ,  $^{50}\text{V}$  and  $^{58}\text{Ni}$ , are either rare or only very weakly radioactive.

## 4.1.5 Radioactive decay series

The main radioactive decay schemes are shown in Table 4.1.  $^{40}\text{K}$ , which forms about 0.0118% of naturally occurring potassium, decays in a single stage, either by beta emission to form  $^{40}\text{Ca}$ , or by electron capture (K-capture) to form  $^{40}\text{Ar}$ . The argon nucleus is left in an excited state but settles down with the emission of a 1.46 MeV photon. The half-life of  $^{40}\text{K}$  is 1470 m.y. for beta decay and 11 000 m.y. for K-capture.

The other important primeval radioisotopes decay into nuclei which are themselves unstable. As with  $^{40}\text{K}$ , there may be more than one possible decay mode, and the decay chains are quite complex. All, however, end in stable isotopes of lead. The decay series for  $^{238}\text{U}$  and  $^{232}\text{Th}$  are shown in Table 4.1.  $^{235}\text{U}$  makes up only 0.7114% of the naturally occurring element



# RADIOMETRIC SURVEYS

**Table 4.1** Natural radioactive decay of  $^{238}\text{U}$ ,  $^{232}\text{Th}$  and  $^{40}\text{K}$

Parent	Mode	Daughter	Half-life	$\gamma$ energy (MeV) and % yield <sup>†</sup>
$^{238}\text{U}$	$\alpha$	$^{234}\text{Th}$	$4.5 \times 10^9$ yr	0.09(15) 0.6(7) 0.3(7)
$^{234}\text{Th}$	$\alpha$	$^{234}\text{Pa}$	24.1 day	1.01(2) 0.77(1) 0.04(3)
$^{234}\text{Pa}$	$\beta$	$^{234}\text{U}$	1.18 min	0.05(28)
$^{234}\text{U}$	$\alpha$	$^{230}\text{Th}$	$2.6 \times 10^5$ yr	
$^{230}\text{Th}$	$\alpha$	$^{226}\text{Ra}$	$8 \times 10^4$ yr	
$^{226}\text{Ra}$	$\alpha$	$^{222}\text{Rn}$	1600 yr	0.19(4)
$^{222}\text{Rn}$	$\alpha$	$^{218}\text{Po}$	3.82 day	
$^{218}\text{Po}$	$\alpha$	$^{214}\text{Pb}$	3.05 min	
$^{214}\text{Pb}$	$\beta$	$^{214}\text{Bi}$	26.8 min	0.35(44) 0.24(11) 0.29(24) 0.05(2)
$^{214}\text{Bi}$	$\beta$	$^{214}\text{Po}$	17.9 min	2.43(2) 2.20(6) 1.76(19) 1.38(7)*
$^{214}\text{Po}$	$\alpha$	$^{210}\text{Pb}$	$1.6 \times 10^{-4}$ sec	
$^{210}\text{Pb}$	$\beta$	$^{210}\text{Bi}$	19.4 yr	
$^{210}\text{Bi}$	$\beta$	$^{210}\text{Po}$	5.0 day	0.04(4)
$^{210}\text{Po}$	$\alpha$	$^{206}\text{Pb}$	138.4 day	
$^{232}\text{Th}$	$\alpha$	$^{228}\text{Ra}$	$1.4 \times 10^{10}$ yr	0.06(24)
$^{228}\text{Ra}$	$\beta$	$^{228}\text{Ac}$	6.7 yr	
$^{228}\text{Ac}$	$\beta$	$^{228}\text{Th}$	6.1 hr	1.64(13) 1.59(12) 0.99(25) 0.97(18)*
$^{228}\text{Th}$	$\alpha$	$^{224}\text{Ra}$	1.9 yr	
$^{224}\text{Ra}$	$\alpha$	$^{220}\text{Rn}$	3.64 day	
$^{220}\text{Rn}$	$\alpha$	$^{216}\text{Po}$	54.5 sec	
$^{216}\text{Po}$	$\alpha$	$^{212}\text{Pb}$	0.16 sec	
$^{212}\text{Pb}$	$\beta$	$^{212}\text{Bi}$	10.6 hr	0.30(5) 0.24(82) 0.18(1) 0.12(2)*
$^{212}\text{Bi}$	$\beta$ (66%)	$^{212}\text{Po}$	40 min	1.18(1) 0.83(8) 0.73(10)
$^{212}\text{Po}$	$\alpha$	$^{208}\text{Pb}$	$0.3 \times 10^{-6}$ sec	
$^{212}\text{Bi}$	$\alpha$ (34%)	$^{208}\text{Tl}$	97.3 min	
$^{208}\text{Tl}$	$\beta$	$^{208}\text{Pb}$	3.1 min	2.62(100) 0.86(14) 0.58(83) 0.51(25)*
$^{40}\text{K}$	$\beta$ (89%)	$^{40}\text{Ca}$	$1.45 \times 10^9$ yr	
	K (11%)	$^{40}\text{Ar}$	$1.17 \times 10^{10}$ yr	1.46(11)

Notes: 1. The number of photons of the energy specified produced in each 100 decays is indicated as % yield (in parentheses). More than one photon may be produced in a single decay event <sup>†</sup>.

2. Decay branches that involve less than 10% of a parent element are not shown.

3. Photons of numerous other energies are emitted in events marked \*.

and, although its rather greater activity allows it to contribute nearly 5% of the overall uranium activity, it may for most practical purposes be ignored.

By no means all decay events are accompanied by significant gamma emission. The first stage in the decay of  $^{232}\text{Th}$  involves only weak gamma activity and the strongest radiation in the chain comes from the decay of  $^{208}\text{Tl}$ , near the end. This decay is accompanied by emission of a 2.615 MeV photon, the most energetic radiation to come from a terrestrial source.

In the  $^{238}\text{U}$  chain,  $^{214}\text{Bi}$  is notable for the numbers and energies of the gamma photons produced. Those at 1.76 MeV are taken as diagnostic of the presence of uranium but the gaseous radon isotope,  $^{222}\text{Rn}$ , which precedes  $^{214}\text{Bi}$  in the chain, has a half-life of nearly four days and so can disperse quite widely away from a primary uranium source. Gaseous dispersion has much less effect in thorium decay since the half-life of  $^{220}\text{Rn}$  is less than a minute.

### 4.1.6 Radioactive equilibria

If a large amount of a primeval isotope is present, and if all the daughter products remain where they are formed, an equilibrium will eventually be established in which the same number of atoms of each element are created as decay in a given time. Only the concentrations of the two end members of the series change.

In equilibrium decay, each member of the chain loses mass at the same rate, equal in each case to the mass of the element present multiplied by the appropriate decay constant. Equilibrium masses are therefore inversely proportional to decay constants. If more or less of an element is present than is required for equilibrium, decay will be respectively faster or slower than the equilibrium rate until equilibrium is re-established.

Equilibrium can be disrupted if any gaseous or soluble intermediate products have half-lives long enough to allow them to disperse before they decay. The exhalation of radon by uranium ores notably disrupts equilibrium and the primary source of a 'uranium' (actually  $^{214}\text{Bi}$ ) anomaly may be hard to find. *Roll-front* uranium ores are notorious for the separation between the uranium concentrations and the zones of peak radioactivity.

### 4.1.7 Natural gamma-ray spectra

Natural gamma rays range from cosmic radiation with energies above 3 MeV down to X-rays. A typical measured spectrum is shown in Figure 4.1. The individual peaks correspond to specific decay events, the energy of each photon falling somewhere within a small range determined by the nuclear kinetic energies at the time of the decay and by errors in measurement.

The background curve upon which the peaks are superimposed is due to *scattered* terrestrial and *cosmic* (mainly solar) radiation. Gamma photons can be scattered in three ways. Very energetic (cosmic) photons passing close to atomic nuclei may form electron-positron pairs, and the positrons soon interact with other electrons to produce more gamma rays. At lower energies, a gamma ray may eject a bound electron from an atom (*Compton scattering*). Some of the energy is transferred to the electron and the remainder continues as a lower-energy photon. At still lower energies, a photon may eject an electron from an atom and itself be totally absorbed (*photoelectric effect*).

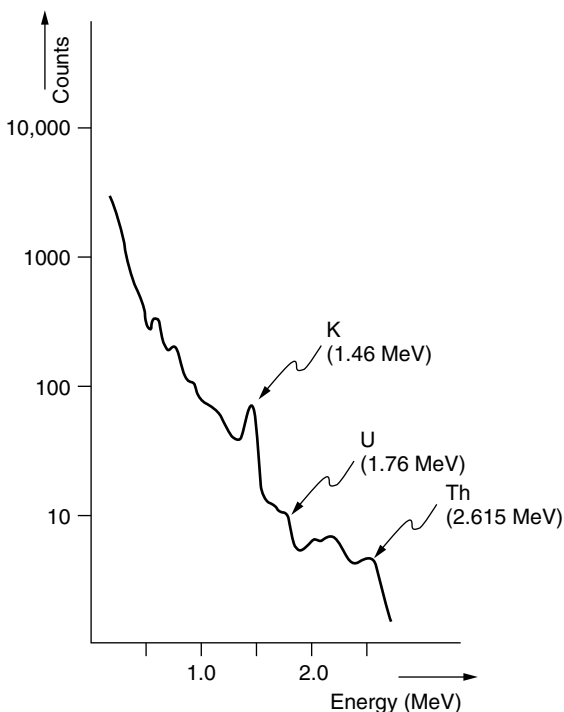


**Figure 4.1** A natural gamma-ray spectrum. Note that the vertical scale (numbers of counts) is logarithmic.

## 4.2 Radiation Detectors

The earliest detectors relied on the ability of radiation to ionize low-pressure gas and initiate electrical discharges between electrodes maintained at high potential differences. These *Geiger-Müller* counters are now considered obsolete. They responded mainly to alpha particles and suffered long ‘dead’ periods after each count, during which no new events could be detected.

### 4.2.1 Scintillometers

Gamma rays produce flashes of light when they are photoelectrically absorbed in sodium iodide crystals. Small amounts of thallium are added to the crystals, which are said to be *thallium activated*. The light can be detected by photomultiplier tubes (PMTs) which convert the energy into electric current. The whole sequence occupies only a few microseconds and corrections for

‘dead time’, which in some instruments are made automatically, are required only at very high count rates.

A scintillometer consists of a crystal, one or more PMTs, a power supply (which must provide several hundred volts for the PMTs), and some counting circuitry. The results may be displayed digitally but quite commonly are shown by a needle on an analogue *rate meter*. Some instruments produce an audible click each time a gamma photon is detected, or have alarms which are triggered when the count rate exceeds a predetermined threshold, so that the dial need not be continually observed.

Radioactive decay is a statistical process. The *average* number of events observed in a given area in a given time will be constant, but there will be some variation about the mean. The continuous averaging of a rate meter is controlled by a time constant, and if this is too short, the needle will be in continual motion and readings will be difficult to take. If it is too long, the response will be slow and narrow anomalies may be overlooked. Where a digital display is used, a fixed count time is selected which must be long enough to produce a statistically valid result (Section 4.3.1).

The sensitivity of a scintillometer depends almost entirely on crystal size; larger crystals record more events. Count rates are thus not absolute but depend on the instrument and the crystal. Many instruments are designed to be compatible with several different crystals, which can be chosen on the basis of cost, time available for survey work and accuracy required.

Similar instruments with similar crystals should read roughly the same in the same places, but even this needs to be checked carefully since radioactive contaminants near, and within, the crystals can cause readings to differ. Different scintillometers may record different count rates because crystals are usually shielded so that they detect radiation from one direction only, and even instruments of the same type may have quite different apertures. If it is essential that comparable data be obtained, portable radioactive sources can be used for calibration and also to check the extent of shielding. Such comparisons are, strictly speaking, valid only at the specific (usually fairly low) gamma-ray energy of the source used.

### 4.2.2 Gamma-ray spectrometers

The energy of a gamma photon that produces a scintillation event can be estimated if a *pulse-height analyser* is incorporated in the PMT circuitry. Events with energies within certain predetermined energy *windows* or above preselected energy *thresholds* can then be counted separately, and the entire gamma-ray flux can be observed at a series of narrow adjoining windows to obtain a curve similar to that shown in Figure 4.1.

Strictly, the term *spectrometer* should be reserved for those instruments, with 256 or more channels, that can record a complete spectrum, but in

practice it is applied to any multichannel instrument with some degree of energy discrimination. Usually there are only four channels, one for total count and one each for the  $^{208}\text{Tl}$  peak at 2.62 MeV (for thorium),  $^{214}\text{Bi}$  at 1.76 MeV (for uranium) and  $^{40}\text{K}$  at 1.46 MeV (for potassium). Typical windows for these peaks might extend from 2.42 to 2.82 MeV, from 1.66 to 1.86 MeV and from 1.36 to 1.56 MeV respectively. Concentrations of all three parent elements can thus be estimated, provided that the primeval radioelement is in equilibrium with its daughter products.

### 4.2.3 Stripping ratios

To estimate thorium, uranium and potassium abundances from spectrometer readings, corrections must be made for gamma rays scattered from other parts of the spectrum. The thorium peak must be corrected for cosmic radiation and for the 2.43 MeV radiation from  $^{214}\text{Bi}$  in the uranium decay chain, which overlaps into the commonly used 'thorium' window. The uranium count must be corrected for thorium, and the potassium count for thorium and uranium. The correction process is known as *stripping*.

Stripping factors vary from detector to detector, primarily with variations in crystal size. They are listed in instrument handbooks and in some cases can be applied by built-in circuitry so that the corrected results can be displayed directly. Equilibrium is assumed when automatic corrections are made, and interpretations will be wrong if it does not exist. It is generally better to record actual count rates in the field and make corrections later.

The characteristics of the measuring circuits vary slowly over time (and also, more rapidly, with temperature) and the positioning of spectrometer 'windows' or thresholds needs to be checked regularly, using portable sources producing gamma rays of a single energy. An additional form of calibration is needed if spectrometer results are to be converted directly into radioelement concentrations. In the USA, Canada, Australia and some other countries, calibration sites have been established where instrument performance can be checked over concrete pads containing known concentrations of various radioelements. 'Null' pads allow background to be estimated. Portable pads are also available in some countries. If, however, several instruments are to be used in a single survey, it is wise, even if they have all been calibrated, to compare them in the actual survey area before attempting to reduce all results to common equivalent readings. Bases at which this has been done should be described for the benefit of later workers.

### 4.2.4 Alpha-particle monitors

The radon content of soil gas can be estimated by monitoring alpha activity, which may exist even in areas without obvious gamma-ray anomalies. Radon diffuses readily through rocks and soil and the presence of otherwise 'blind'

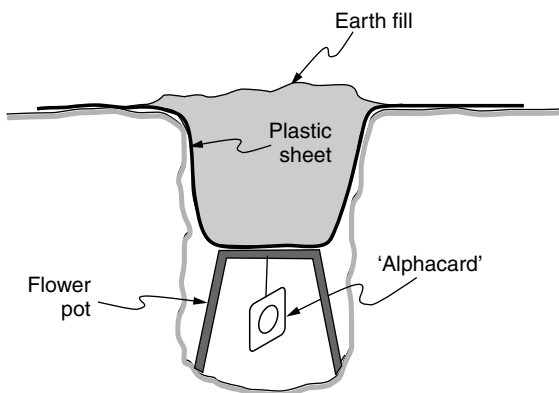


**Figure 4.2** *Alphacard radiation detector in its hole.*

uranium mineralization can sometimes be indicated by this method, although locating it may still be difficult. Radon gas is also a potential health hazard in some areas, particularly in cellars, and may need to be monitored for that reason.

One form of monitor is a thin metallic membrane mounted on a frame about the size of a 35-mm slide, on which radon daughter products can collect. For field surveys, this *alphacard* is suspended in an inverted flower pot or similar container in a hole about 0.5 m deep. The hole is covered with a plastic sheet and earth is poured on top until the ground surface is again level (Figure 4.2). The sheet should be sufficiently large for its edges to project, so that it can be lifted out, together with the overlying soil, to allow the card to be removed. The hole is left covered for at least 12 hours. This is long enough for equilibrium to be established and longer periods of burial will not alter the reading. In public health applications, the card is simply left for 12 hours within the area being monitored. It is then removed and placed in a special reader which is sensitive to alpha radiation.

Other types of alpha-particle detector include photographic emulsions that can be etched by ionizing radiation, and sealed units in which the reading and data storage units are contained in a single housing. For exploration use, these should be inserted in holes similar to those dug for alphacards.

## 4.3 Radiometric Surveys

Ground radiometric surveys tend to be rather frustrating operations. Because of the shielding effect of even thin layers of rock or soil, it is very easy to overlook radioactive minerals in rocks that are only patchily exposed at the

surface. Reliance on stations placed at uniform distances along a traverse may be unwise and the field observer needs to be more than usually aware of the environment.

### 4.3.1 Reading times

Accurate radiometric data can be obtained only by occupying stations long enough for the statistical variations to average out. What this implies will depend on the count levels themselves and must be determined by actual experiment. The percent statistical error is equal to about  $100/\sqrt{n}$ , where  $n$  is the number of counts, and so is about 30% for 10 counts and only 1% for 10 000. A period of time which is fully adequate for total count readings may not be sufficient for readings on the K, U and Th channels.

There is little point in wasting time obtaining statistically accurate data if areas where count rates are low are in any case of no interest. It may be sufficient to cover the ground at a slow walk with a ratemeter. The rate of progress should be such that the narrowest source of interest would not be crossed completely in a time equal to the time constant selected.

Even when a spectrometer is used, it is usual to record only total count in the first instance, reserving the more time-consuming spectral readings for areas of total-count anomaly. There are, of course, dangers in this approach, as one radioelement might decrease in concentration in the same region as another increased.

### 4.3.2 Radiometric assays

If a bare rock surface is available, a gamma-ray spectrometer can be used to assay quantitatively for thorium, uranium and potassium. The rock should be dry, so that absorption by moisture, either on or below the surface, is not a factor. Observations must be taken over a sufficiently long period for statistical fluctuations to be smoothed out, which in practice means accumulating at least 1000 counts. Each count takes a few microseconds and at 10 000 cps the instrument would be 'dead' for several tens of milliseconds in each second. Corrections are therefore needed for 'dead' time when working with very radioactive material.

Radioelement concentrations are determined by inserting the observed count rates into equations, provided by the manufacturers, which are specific to the instrument and crystal being used, or by comparison with 'pad' calibrations.

### 4.3.3 Geometrical considerations

Source *geometry* is important in all radiometric surveys and especially in assay work. Radiation comes from a very thin surface layer and only a small anomaly will be detected if the lateral extent of the source is small compared

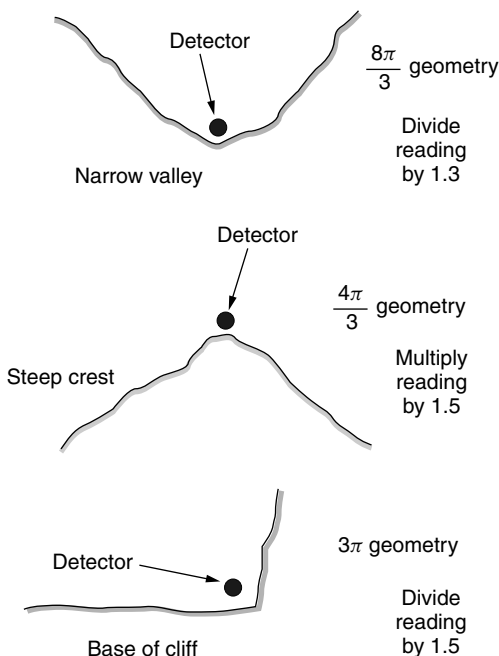


**Figure 4.3** Geometries and correction factors for radiometric surveys.

with the distance to the detector. If, on the other hand, the source is extensive and at the surface, the height of the detector should not greatly affect the count rate. Generally, this condition ( $2\pi$  geometry) is achieved if the lateral extent of the source is 10 or more times the height of the detector above it.

$2\pi$  geometry is often not possible in practice. Some other possible source geometries and factors for correction to standard  $2\pi$  values are shown in Figure 4.3.

## 4.3.4 Corrections for background variations

Atmospheric radon, cosmic radiation and radioactive particles attached to the instrument itself produce background radiation unrelated to survey objectives. The background contribution is usually less than 10% of the total count and is often ignored in ground surveys. If corrections are necessary, either because very subtle variations are being observed or precise assay work is being done, their magnitude can be estimated by taking readings either in the middle of a



body of water at least 1 m deep and at least 10 m across or with the detector shielded from the ground by a lead sheet. Neither of these methods is likely to be very convenient, and sometimes 'background' is defined simply (and possibly unreliably) as the lowest reading obtained anywhere in the survey area. Variations in background, mainly due to atmospheric humidity changes (wet air absorbs radiation far more efficiently than dry) can be monitored using a fixed detector in this location.

The level of background radiation due to radioactive material in the detector crystal and housing should be constant over long periods and can be measured by placing the detector in a totally shielded environment, but in practice this is likely to be difficult to arrange. The correction is usually trivial and it is far more important to ensure that no dirt, which might be contaminated, is smeared on the detector housing.

The observer is an important possible source of spurious radiation, especially if the sensor is carried in a back-pack. In these circumstances the absorption of radiation by the observer's body has also to be taken into account, usually by direct experiment. Watches with radioactive luminous dials are now rare, but compasses need to be carefully checked. Obviously, a calibration source should not be carried.

A small amount of radioactive material is included in the vacuum chambers of some quartz gravity meters to ionize the residual gas and prevent build-ups of static electricity on the spring systems. Radiometric and gravity surveys are occasionally done together, and absurd conclusions have been reached.

### 4.3.5 Recording radiometric data

Because gamma radiation is strongly absorbed by both rock and soil, comprehensive notes should be taken during radiometric surveys. Departures from  $2\pi$  geometry must be noted, together with details of soil cover. If bare rock cannot be seen, some attempt should be made to decide whether the overburden was transported into place or developed *in situ*, and to estimate its thickness. Weather conditions can also be important. In particular, since absorption is much greater in wet than in dry soil, recent rain and the presence of puddles of standing water should always be noted.

The ways in which readings are taken, including time constants or count periods, must be recorded. Field techniques should not be varied in the course of a survey and the location of the sensor (e.g. whether hand-held or in a back-pack) should be specified.



# 5

## ELECTRIC CURRENT METHODS – GENERAL CONSIDERATIONS

---

Many geophysical surveys rely on measurements of the voltages or magnetic fields associated with electric currents flowing in the ground. Some of these currents exist independently, being sustained by natural oxidation–reduction reactions or variations in ionospheric or atmospheric magnetic fields, but most are generated artificially. Current can be made to flow by direct injection, by capacitive coupling or by electromagnetic induction (Figure 5.1). Surveys involving direct injection via electrodes at the ground surface are generally referred to as direct current or *DC* surveys, even though in practice the direction of current is reversed at regular intervals to cancel some forms of natural background noise. Currents that are driven by electric fields acting either through electrodes or capacitatively (rather than inductively, by varying magnetic fields) are sometimes termed *galvanic*. Surveys in which currents are made to flow inductively are referred to as electromagnetic or *EM* surveys.

Relevant general concepts are introduced in this chapter. Direct current methods are considered in more detail in Chapter 6, which also describes the relatively little-used capacitive-coupled methods. Natural potential (*self-potential* or *SP*) and *induced polarization (IP)* methods are covered in Chapter 7. Chapter 8 deals with EM surveys using local sources and Chapter 9 with VLF and CSAMT surveys, which use plane waves generated by distant transmitters.

### 5.1 Resistivity and Conductivity

Metals and most metallic sulphides conduct electricity efficiently by flow of electrons, and electrical methods are therefore important in environmental investigations, where metallic objects are often the targets, and in the search for sulphide ores. Graphite is also a good ‘electronic’ conductor and, since it is not itself a useful mineral, is a source of noise in mineral exploration.

Most rock-forming minerals are very poor conductors, and ground currents are therefore carried mainly by ions in the pore waters. Pure water is ionized to only a very small extent and the electrical conductivity of pore waters depends on the presence of dissolved salts, mainly sodium chloride (Figure 5.2). Clay minerals are ionically active and clays conduct well if even slightly moist.

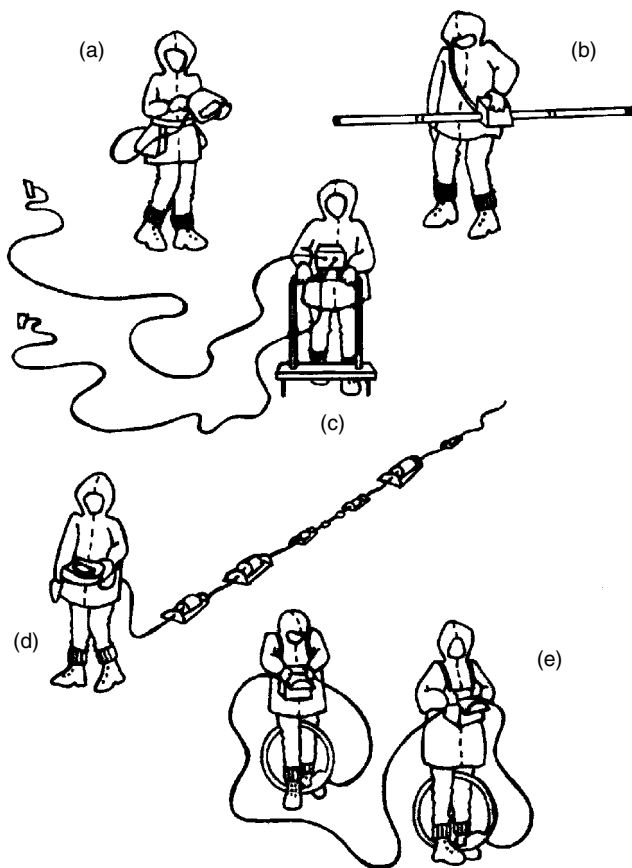


**Figure 5.1** Electrical survey methods for archaeology and site investigation. In (a) the operator is using an ABEM Wadi, recording waves from a remote VLF transmitter (Chapter 9). Local source electromagnetic surveys (Chapter 8) may use two-coil systems such as the Geonics EM31 (b) or EM37 (e). DC resistivity surveys (c) often use the two-electrode array (Section 5.2), with a data logger mounted on a frame built around the portable electrodes. Capacitive-coupling systems (d) do not require direct contact with the ground but give results equivalent to those obtained in DC surveys. There would be serious interference problems if all these systems were used simultaneously in close proximity, as in this illustration.

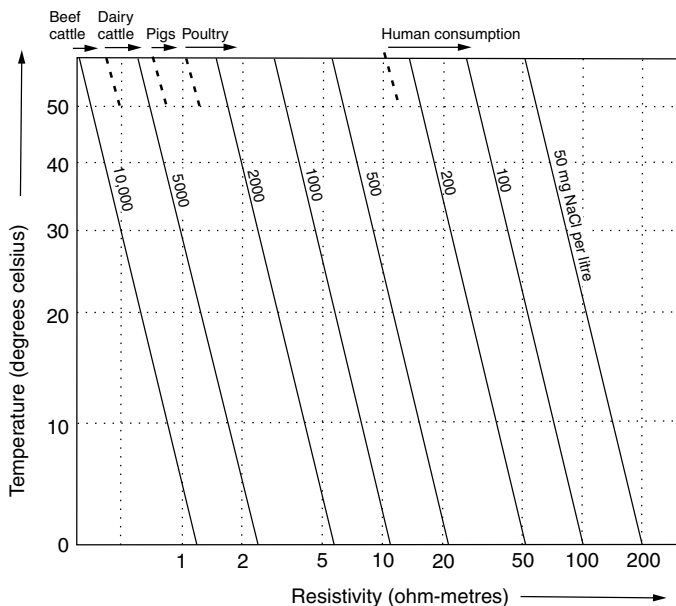


**Figure 5.2** Variation of water resistivity with concentration of dissolved NaCl. The uses that can be made of waters of various salinities are also indicated.

### 5.1.1 Ohm's law and resistivity

The current that flows in a conductor is in most cases proportional to the voltage across it, i.e.

$$V = IR$$

This is *Ohm's law*. The constant of proportionality,  $R$ , is known as the resistance and is measured in ohms when current ( $I$ ) is in amps and voltage ( $V$ ) is in volts. The reciprocal, conductance, is measured in siemens, also known as mhos.

The resistance of a unit cube to current flowing between opposite faces is known as its resistivity ( $\rho$ ) and is measured in ohm-metres ( $\Omega\text{m}$ ). The reciprocal, conductivity, is expressed in siemens per metre ( $\text{S m}^{-1}$ ) or mhos per metre. The resistance of a rectangular block measured between opposite faces is proportional to its resistivity and to the distance  $x$  between the faces, and inversely proportional to their cross-sectional area,  $A$ , i.e.

$$R = \rho(x/A)$$

*Isotropic* materials have the same resistivity in all directions. Most rocks are reasonably isotropic but strongly laminated slates and shales are more resistive across the laminations than parallel to them.

### 5.1.2 Electrical resistivities of rocks and minerals

The resistivity of many rocks is roughly equal to the resistivity of the pore fluids divided by the fractional porosity. *Archie's law*, which states that resistivity is inversely proportional to the fractional porosity raised to a power which varies between about 1.2 and 1.8 according to the shape of the matrix grains, provides a closer approximation in most cases. The departures from linearity are not large for common values of porosity (Figure 5.3).

Resistivities of common rocks and minerals are listed in Table 5.1. Bulk resistivities of more than 10 000  $\Omega\text{m}$  or less than 1  $\Omega\text{m}$  are rarely encountered in field surveys.

### 5.1.3 Apparent resistivity

A single electrical measurement tells us very little. The most that can be extracted from it is the resistivity value of a completely homogeneous ground (a homogeneous *half-space*) that would produce the same result when investigated in exactly the same way. This quantity is known as the *apparent resistivity*. Variations in apparent resistivity or its reciprocal, *apparent conductivity*, provide the raw material for interpretation in most electrical surveys.

Where electromagnetic methods are being used to detect very good conductors such as sulphide ores or steel drums, target location is more important than determination of precise electrical parameters. Since it is difficult to separate the effects of target size from target conductivity for small targets, results are sometimes presented in terms of the *conductivity–thickness product*.

### 5.1.4 Overburden effects

Build-ups of salts in the soil produce high conductivity in near-surface layers in many arid tropical areas. These effectively short-circuit current generated at the surface, allowing very little to penetrate to deeper levels. Conductive overburden thus presents problems for all electrical methods, with continuous wave electromagnetic surveys being the most severely affected.

Highly resistive surface layers are obstacles only in DC surveys. They may actually be advantageous when EM methods are being used, because attenuation is reduced and depth of investigation is increased.

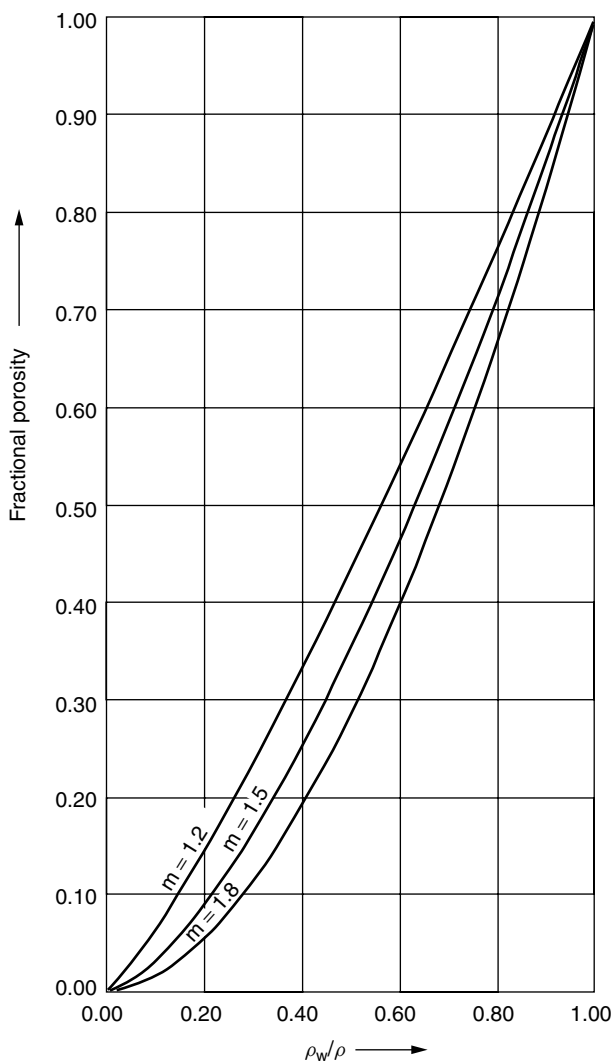


**Figure 5.3** Archie's law variation of bulk resistivity,  $\rho$ , for rocks with insulating matrix and pore-water resistivity  $\rho_w$ . The index,  $m$ , is about 1.2 for spherical grains and about 1.8 for platy or tabular materials.

**Table 5.1** Resistivities of common rocks and ore minerals (ohm-metres)

<i>Common rocks</i>	
Topsoil	50–100
Loose sand	500–5000
Gravel	100–600
Clay	1–100
Weathered bedrock	100–1000
Sandstone	200–8000
Limestone	500–10 000
Greenstone	500–200 000
Gabbro	100–500 000
Granite	200–100 000
Basalt	200–100 000
Graphitic schist	10–500
Slates	500–500 000
Quartzite	500–800 000
<i>Ore minerals</i>	
Pyrite (ores)	0.01–100
Pyrrhotite	0.001–0.01
Chalcopyrite	0.005–0.1
Galena	0.001–100
Sphalerite	1000–1 000 000
Magnetite	0.01–1000
Cassiterite	0.001–10 000
Hematite	0.01–1 000 000

## 5.2 DC Methods

The currents used in surveys described as ‘direct current’ or *DC* are seldom actually unidirectional. Reversing the direction of flow allows the effects of unidirectional natural currents to be eliminated by simply summing and averaging the results obtained in the two directions.

DC surveys require current generators, voltmeters and electrical contact with the ground. Cables and electrodes are cheap but vital parts of all systems, and it is with these that much of the noise is associated.

### 5.2.1 Metal electrodes

The electrodes used to inject current into the ground are nearly always metal stakes, which in dry ground may have to be hammered in to depths of more than 50 cm and be watered to improve contact. Where contact is very poor, salt water and multiple stakes may be used. In extreme cases, holes may have to be blasted through highly resistive caliche or laterite surface layers.



Metal stake electrodes come in many forms. Lengths of drill steel are excellent if the ground is stony and heavy hammering necessary. Pointed lengths of angle-iron are only slightly less robust and have larger contact areas. If the ground is soft and the main consideration is speed, large numbers of metal tent pegs can be pushed in along a traverse line by an advance party.

Problems can arise at voltage electrodes, because *polarization* voltages are generated wherever metals are in contact with the groundwater. However, the reversal of current flow that is routine in conventional DC surveys generally achieves acceptable levels of cancellation of these effects. Voltage magnitudes depend on the metals concerned. They are, for instance, small when electrodes are made of stainless steel.

### 5.2.2 Non-polarizing electrodes

Polarization voltages are potentially serious sources of noise in SP surveys, which involve the measurement of natural potentials and in induced polarization (IP) surveys (Chapter 7). In these cases, non-polarizing electrodes must be used. Their design relies on the fact that the one exception to the rule that a metallic conductor in contact with an electrolyte generates a contact potential occurs when the metal is in contact with a saturated solution of one of its own salts. Most non-polarizing electrodes consist of copper rods in contact with saturated solutions of copper sulphate. The rod is attached to the lid of a container or *pot* with a porous base of wood, or, more commonly, unglazed earthenware (Figure 5.4). Contact with the ground is made via the solution that leaks through the base. Some solid copper sulphate should be kept in the pot to ensure saturation and the temptation to ‘top up’ with fresh water must be resisted, as voltages will be generated if any part of the solution is less than saturated. The high resistance of these electrodes is not generally important because currents should not flow in voltage-measuring circuits.

In induced polarization surveys it may very occasionally be desirable to use non-polarizing *current* electrodes but not only does resistance then become a problem but also the electrodes deteriorate rapidly due to electrolytic dissolution and deposition of copper.

Copper sulphate solution gets everywhere and rots everything and, despite some theoretical advantages, non-polarizing electrodes are seldom used in routine DC surveys.

### 5.2.3 Cables

The cables used in DC and IP surveys are traditionally single core, multi-strand copper wires insulated by plastic or rubber coatings. Thickness is usually dictated by the need for mechanical strength rather than low resistance, since contact resistances are nearly always very much higher than cable resistance. Steel reinforcement may be needed for long cables.



**Figure 5.4** Porous-pot non-polarizing electrodes designed to be pushed into a shallow scraping made by a boot heel. Other types can be pushed into a hole made by a crowbar or geological pick.

In virtually all surveys, at least two of the four cables will be long, and the good practice in cable handling described in Section 1.2.2 is essential if delays are to be avoided. Multicore cables that can be linked to multiple electrodes are becoming increasingly popular since, once the cable has been laid out and connected up, a series of readings with different combinations of current and voltage electrodes can be made using a selector switch.

Power lines can be sources of noise, and it may be necessary to keep the survey cables well away from their obvious or suspected locations. The 50 or 60 Hz power frequencies are very different from the 2 to 0.5 Hz frequencies at which current is reversed in most DC and IP surveys but can affect the very sensitive modern instruments, particularly in time-domain IP work (Section 7.3). Happily, the results produced are usually either absurd or non-existent, rather than misleading.

Cables are usually connected to electrodes by crocodile clips, since screw connections can be difficult to use and are easily damaged by careless hammer blows. Clips are, however, easily lost and every member of a field crew should carry at least one spare, a screwdriver and a small pair of pliers.

#### 5.2.4 Generators and transmitters

The instruments that control and measure current in DC and IP surveys are known as *transmitters*. Most deliver square wave currents, reversing the

direction of flow with cycle times of between 0.5 and 2 seconds. The lower limit is set by the need to minimize inductive (electromagnetic) and capacitive effects, the upper by the need to achieve an acceptable rate of coverage.

Power sources for the transmitters may be dry or rechargeable batteries or motor generators. Hand-cranked generators (*Meggers*) have been used for DC surveys but are now very rare. Outputs of several kVA may be needed if current electrodes are more than one or two hundred metres apart, and the generators then used are not only not very portable but supply power at levels that can be lethal. Stringent precautions must then be observed, not only in handling the electrodes but also in ensuring the safety of passers-by and livestock along the whole lengths of the current cables. In at least one (Australian) survey, a serious grass fire was caused by a poorly insulated time-domain IP transmitter cable.

### 5.2.5 Receivers

The instruments that measure voltage in DC and IP surveys are known as *receivers*. The primary requirement is that negligible current be drawn from the ground. High-sensitivity moving-coil instruments and potentiometric (voltage balancing) circuits were once used but have been almost entirely replaced by units based on field-effect transistors (FETs).

In most of the low-power DC instruments now on the market, the transmitters and receivers are combined in single units on which readings are displayed directly in ohms. To allow noise levels to be assessed and SP surveys to be carried out, voltages can be measured even when no current is being supplied. In all other cases, current levels must be either predetermined or monitored, since low currents may affect the validity of the results. In modern instruments the desired current settings, cycle periods, numbers of cycles, read-out formats and, in some cases, voltage ranges are entered via front-panel key-pads or switches. The number of cycles used represents a compromise between speed of coverage and good signal-to-noise ratio. The reading is usually updated as each cycle is completed, and the number of cycles selected should be sufficient to allow this reading to stabilize.

Some indication will usually be given on the display of error conditions such as low current, low voltage and incorrect or missing connections. These warnings may be expressed by numerical codes that are meaningless without the handbook. If all else fails, read it.

### 5.3 Varying Current Methods

Alternating electrical currents circulating in wires and loops can cause currents to flow in the ground without actual physical contact, using either inductive or capacitive coupling. Non-contacting methods are obviously essential in

airborne work but can also be very useful on the ground, since making direct electrical contact is a tedious business and may not even be possible where the surface is concrete, asphalt, ice or permafrost.

### 5.3.1 Depth penetration

Currents that are caused to flow in the ground by alternating electrical or magnetic fields obtain their energy from the fields and so reduce their penetration. Attenuation follows an exponential law (Section 1.1.6) governed by an attenuation constant ( $\alpha$ ) given by:

$$\alpha = \omega[\mu_a \epsilon_a \{(\sqrt{1 + \sigma^2/\omega^2 \epsilon_a^2}) - 1\}/2]^{1/2}$$

$\mu_a$  and  $\epsilon_a$  are the absolute values of, respectively, magnetic permeability and electrical permittivity and  $\omega$  ( $=2\pi f$ ) is the *angular frequency*. The reciprocal of the attenuation constant is known as the *skin depth* and is equal to the distance over which the signal falls to  $1/e$  of its original value. Since  $e$ , the base of natural logarithms, is approximately equal to 2.718, signal strength decreases by almost two-thirds over a single skin depth.

The rather daunting attenuation equation simplifies considerably under certain limiting conditions. Under most survey conditions, the ground conductivity,  $\sigma$ , is much greater than  $\omega \epsilon_a$  and  $\alpha$  is then approximately equal to  $\sqrt{(\mu_a \sigma \omega)}$ . If, as is usually the case, the variations in magnetic permeability are small, the skin depth ( $=1/\alpha$ ), in metres, is approximately equal to 500 divided by the square roots of the frequency and the conductivity (Figure 5.5).

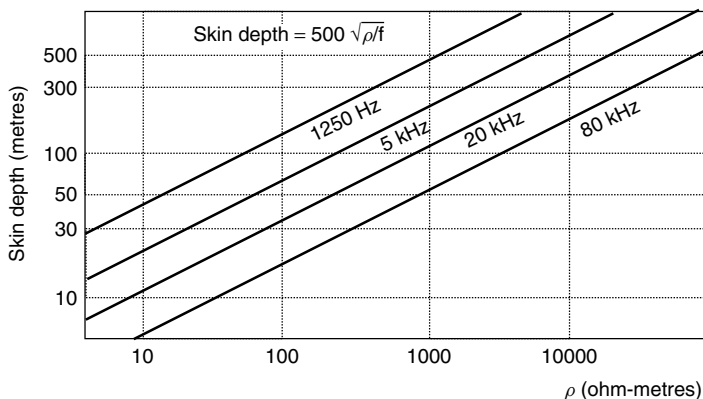


**Figure 5.5** Variation in skin depth,  $d$ , with frequency and resistivity.

The depth of investigation in situations where skin depth is the limiting factor is commonly quoted as equal to the skin depth divided by  $\sqrt{2}$ , i.e. to about  $350 \sqrt{(\rho/f)}$ . However, the separation between the source and the receiver also affects penetration and is the dominant factor if smaller than the skin depth.

### 5.3.2 Induction

The varying magnetic field associated with an electromagnetic wave will induce a voltage (electromotive force or *emf*) at right-angles to the direction of variation, and currents will flow in any nearby conductors that form parts of closed circuits. The equations governing this phenomenon are relatively simple but geological conductors are very complex and for theoretical analyses the induced currents, known as *eddy currents*, are approximated by greatly simplified models.

The magnitudes of induced currents are determined by the rates of change of currents in the inducing circuits and by a geometrical parameter known as the *mutual inductance*. Mutual inductances are large, and conductors are said to be *well coupled* if there are long adjacent conduction paths, if the magnetic field changes are at right-angles to directions of easy current flow and if magnetic materials are present to enhance field strengths.

When current changes in a circuit, an opposing emf is induced in that circuit. As a result, a tightly wound coil strongly resists current changes and is said to have a high *impedance* and a large *self-inductance*.

### 5.3.3 Phase

In most continuous wave systems, the energizing current has the form of a sine wave, but may not, as a true sine wave should, be zero at zero time. Such waves are termed *sinusoidal*. The difference between time zero and the zero point on the wave is usually measured as an angle related to the  $360^\circ$  or  $2\pi$  radians of a complete cycle, and is known as the *phase angle* (Figure 5.6).

Induced currents and their associated secondary magnetic fields differ in phase from the primary field and can, in accordance with a fundamental property of sinusoidal waves, be resolved into components that are in-phase and  $90^\circ$  out of phase with the primary (Figure 5.6). These components are sometimes known as *real* and *imaginary* respectively, the terms deriving originally from the mathematics of complex numbers. The *out-of-phase* component is also (more accurately and less confusingly) described as being in *phase quadrature* with the primary signal.

Since electromagnetic waves travel at the speed of light and not instantaneously, their phase changes with distance from the transmitter. The small distances between transmitters and receivers in most geophysical surveys ensure that these shifts are negligible and can be ignored.

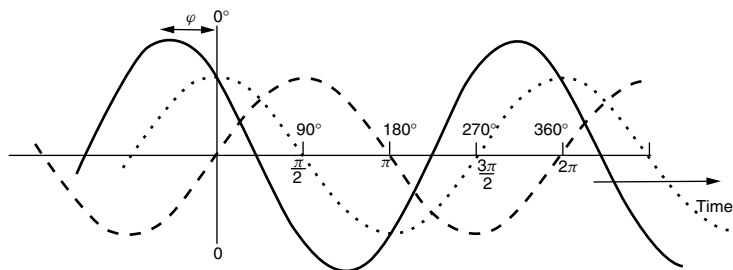


**Figure 5.6** Phase in sinusoidal waves. The wave drawn with a solid line is sinusoidal, with a phase angle  $\phi$ , as compared to the 'zero phase' reference (cosine) sinusoid (dotted curve). The phase difference between the dashed (sine) and dotted waves is  $90^\circ$  or  $\pi/2$  radians and the two are therefore in phase quadrature. The amplitudes are such that subtracting the sine wave from the cosine wave would reconstitute the solid-line wave.

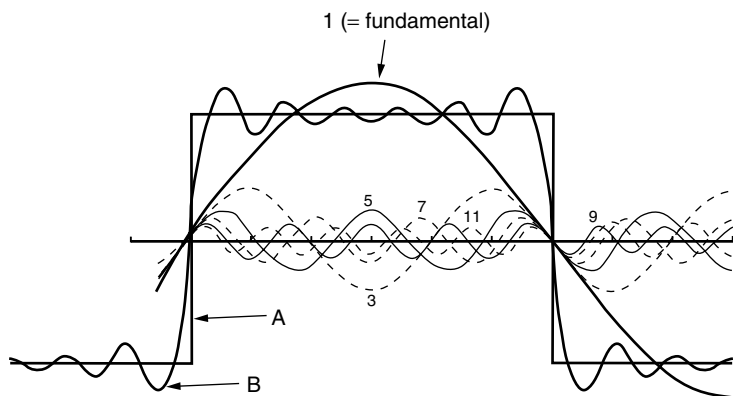


**Figure 5.7** The square wave as a multi-frequency sinusoid. A reasonable approximation to the square wave, A, can be obtained by adding the first five odd harmonics (integer multiples 3, 5, 7, 9 and 11) of the fundamental frequency to the fundamental. Using the amplitudes for each of these component waves determined using the techniques of Fourier analysis, this gives the summed wave B. The addition of higher odd harmonics with appropriate amplitudes would further improve the approximation.

### 5.3.4 Transients

Conventional or *continuous wave* (CW) electromagnetic methods rely on signals generated by sinusoidal currents circulating in coils or grounded wires. Additional information can be obtained by carrying out surveys at two or more different frequencies. The skin-depth relationships (Figure 5.5) indicate that penetration will increase if frequencies are reduced. However, resolution of small targets will decrease.

As an alternative to sinusoidal signals, currents circulating in a transmitter coil or wire can be terminated abruptly. These *transient electromagnetic* (TEM) methods are effectively multi-frequency, because a square wave contains elements of all the odd harmonics of the fundamental up to theoretically infinite frequency (Figure 5.7). They have many advantages over CW methods, most of which derive from the fact that the measurements are of the effects of currents produced by, and circulating after, the termination of the primary current. There is thus no possibility of part of the primary field ‘leaking’ into secondary field measurements, either electronically or because of errors in coil positioning.





# 6

## RESISTIVITY METHODS

---

Nomenclature is a problem in electrical work. Even in the so-called *direct current* (DC) surveys, current flow is usually reversed at intervals of one or two seconds. Moreover, surveys in which high frequency alternating current is made to flow in the ground by capacitive coupling (c-c) have more in common with DC than with electromagnetic methods, and are also discussed in this chapter.

### 6.1 DC Survey Fundamentals

#### 6.1.1 Apparent resistivity

The ‘obvious’ method of measuring ground resistivity by simultaneously passing current and measuring voltage between a single pair of grounded electrodes does not work, because of contact resistances that depend on such things as ground moisture and contact area and which may amount to thousands of ohms. The problem can be avoided if voltage measurements are made between a second pair of electrodes using a high-impedance voltmeter. Such a voltmeter draws virtually no current, and the voltage drop through the electrodes is therefore negligible. The resistances at the current electrodes limit current flow but do not affect resistivity calculations. A geometric factor is needed to convert the readings obtained with these four-electrode *arrays* to resistivity.

The result of any single measurement with any array could be interpreted as due to homogeneous ground with a constant resistivity. The geometric factors used to calculate this *apparent resistivity*,  $\rho_a$ , can be derived from the formula:

$$V = \rho I / 2\pi a$$

for the electric potential  $V$  at a distance  $a$  from a point electrode at the surface of a *uniform half-space* (homogeneous ground) of resistivity  $\rho$  (referenced to a zero potential at infinity). The current  $I$  may be positive (if into the ground) or negative. For arrays, the potential at any voltage electrode is equal to the sum of the contributions from the individual current electrodes. In a four-electrode survey over homogeneous ground:

$$V = I\rho(1/[Pp] - 1/[Np] - 1/[Pn] + 1/[Nn])/2\pi$$

where  $V$  is the voltage difference between electrodes P and N due to a current  $I$  flowing between electrodes p and n, and the quantities in square brackets represent inter-electrode distances.

Geometric factors are not affected by interchanging current and voltage electrodes but voltage electrode spacings are normally kept small to minimize the effects of natural potentials.

### 6.1.2 Electrode arrays

Figure 6.1 shows some common electrode arrays and their geometric factors. The names are those in general use and may upset pedants. A dipole, for example, *should* consist of two electrodes separated by a distance that is negligible compared to the distance to any other electrode. Application of the term to the dipole–dipole and pole–dipole arrays, where the distance to the next electrode is usually from 1 to 6 times the ‘dipole’ spacing, is thus formally incorrect. Not many people worry about this.

The distance to a fixed electrode ‘at infinity’ should be at least 10, and ideally 30, times the distance between any two mobile electrodes. The long cables required can impede field work and may also act as aerials, picking up stray electromagnetic signals (inductive noise) that can affect the readings.

---

#### Example 6.1

Geometrical factor for the Wenner array (Figure 6.1a).

$$Pp = a \quad Pn = 2a \quad Np = 2a \quad Nn = a$$

$$V = I\rho\left(1 - \frac{1}{2} - \frac{1}{2} + 1\right) / 2\pi a = I\rho / 2\pi a$$

$$\text{i.e.} \quad \rho = 2\pi a \cdot V / I$$


---

### 6.1.3 Array descriptions (Figure 6.1)

*Wenner array*: very widely used, and supported by a vast amount of interpretational literature and computer packages. The ‘standard’ array against which others are often assessed.

*Two-electrode (pole–pole) array*: Theoretically interesting since it is possible to calculate from readings taken along a traverse the results that would be obtained from any other type of array, providing coverage is adequate. However, the noise that accumulates when large numbers of results obtained with closely spaced electrodes are added prevents any practical use being made of this fact. The array is very popular in archaeological work because it lends itself to rapid one-person operation (Section 6.2.2). As the *normal* array, it is one of the standards in electrical well logging.

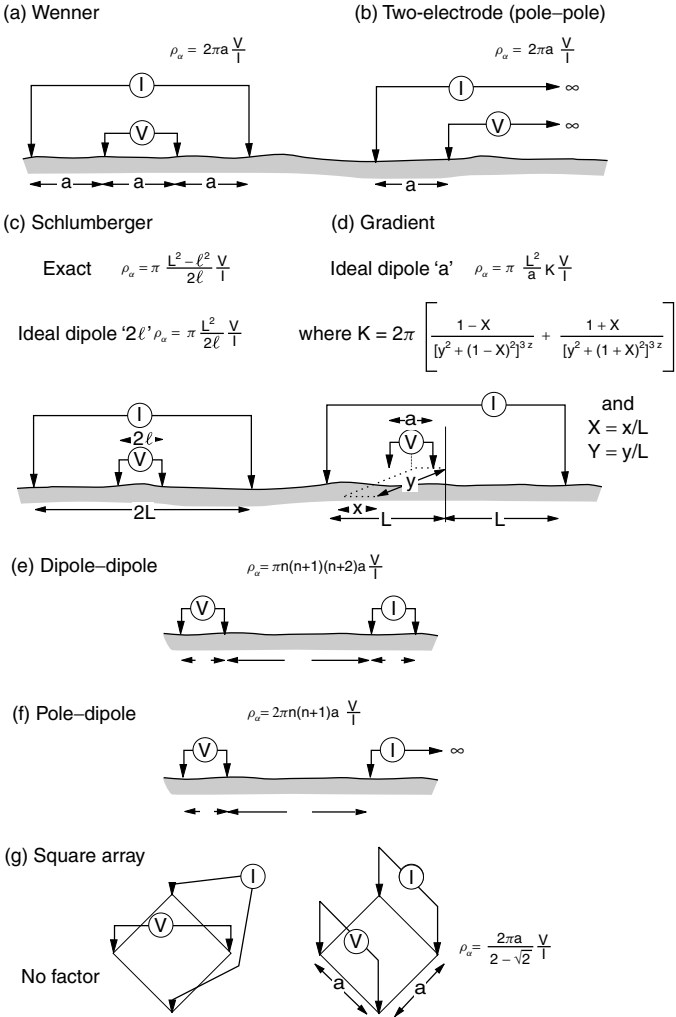


**Figure 6.1** Some common electrode arrays and their geometric factors. (a) Wenner; (b) Two-electrode; (c) Schlumberger; (d) Gradient; (e) Dipole-dipole; (f) Pole-dipole; (g) Square array; (left) Diagonal; (right) Broadside. There is no geometrical factor for the diagonal square array, as no voltage difference is observed over homogeneous ground.

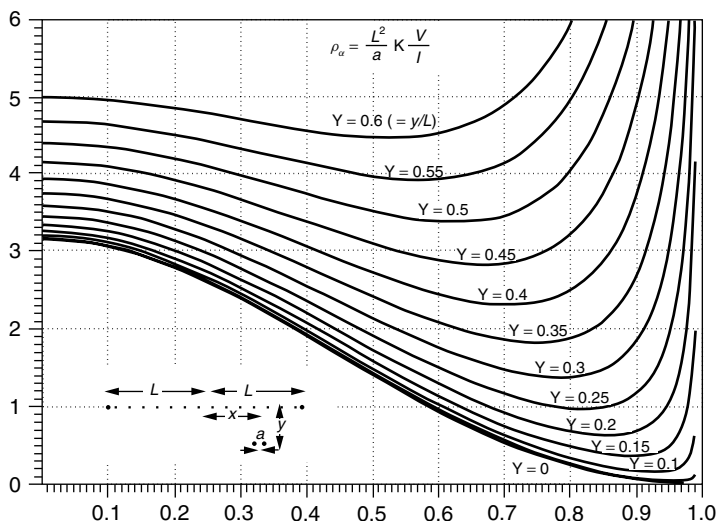


**Figure 6.2** Variation in gradient array geometric factor with distance along and across line. Array total length  $2L$ , voltage dipole length  $a$ .

*Schlumberger array:* the only array to rival the Wenner in availability of interpretational material, all of which relates to the 'ideal' array with negligible distance between the inner electrodes. Favoured, along with the Wenner, for electrical depth-sounding work.

*Gradient array:* widely used for reconnaissance. Large numbers of readings can be taken on parallel traverses without moving the current electrodes if powerful generators are available. Figure 6.2 shows how the geometrical factor given in Figure 6.1d varies with the position of the voltage dipole.

*Dipole-dipole (Eltran) array:* popular in induced polarization (IP) work because the complete separation of current and voltage circuits reduces the vulnerability to inductive noise. A considerable body of interpretational material is available. Information from different depths is obtained by changing  $n$ . In principle, the larger the value of  $n$ , the deeper the penetration of the current path sampled. Results are usually plotted as pseudo-sections (Section 7.5.2).

*Pole-dipole array:* produces asymmetric anomalies that are consequently more difficult to interpret than those produced by symmetric arrays. Peaks are displaced from the centres of conductive or chargeable bodies and electrode positions have to be recorded with especial care. Values are usually plotted at the point mid-way between the moving voltage electrodes but this is not

a universally agreed standard. Results can be displayed as pseudo-sections, with depth penetration varied by varying  $n$ .

*Square array:* four electrodes positioned at the corners of a square are variously combined into voltage and current pairs. Depth soundings are made by expanding the square. In traversing, the entire array is moved laterally. Inconvenient, but can provide an experienced interpreter with vital information about ground anisotropy and inhomogeneity. Few published case histories or type curves.

*Multi-electrode arrays (not shown).*

*Lee array:* resembles the Wenner array but has an additional central electrode. The voltage differences from the centre to the two 'normal' voltage electrodes give a measure of ground inhomogeneity. The two values can be summed for application of the Wenner formula.

*Offset Wenner:* similar to the Lee array but with all five electrodes the same distance apart. Measurements made using the four right-hand and the four left-hand electrodes separately as standard Wenner arrays are averaged to give apparent resistivity and differenced to provide a measure of ground variability.

*Focused arrays:* multi-electrode arrays have been designed which supposedly focus current into the ground and give deep penetration without large expansion. Arguably, this is an attempt to do the impossible, and the arrays should be used only under the guidance of an experienced interpreter.

#### 6.1.4 Signal-contribution sections

Current-flow patterns for one and two layered earths are shown in Figure 6.3. Near-surface inhomogeneities strongly influence the choice of array. Their effects are graphically illustrated by contours of the *signal contributions* that are made by each unit volume of ground to the measured voltage, and hence to the apparent resistivity (Figure 6.4). For linear arrays the contours have the same appearance in any plane, whether vertical, horizontal or dipping, through the line of electrodes (i.e. they are semicircles when the array is viewed end on).

A reasonable first reaction to Figure 6.4 is that useful resistivity surveys are impossible, as the contributions from regions close to the electrodes are very large. Some disillusioned clients would endorse this view. However, the variations in sign imply that a conductive near-surface layer will in some places increase and in other places decrease the apparent resistivity. In homogeneous ground these effects can cancel quite precisely.

When a Wenner or dipole–dipole array is expanded, all the electrodes are moved and the contributions from near-surface bodies vary from reading to reading. With a Schlumberger array, near-surface effects vary much less, provided that only the outer electrodes are moved, and for this reason

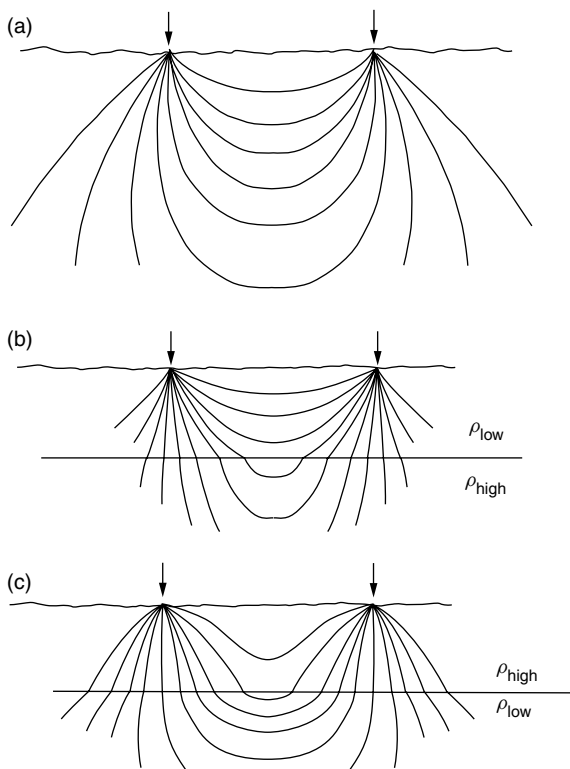


**Figure 6.3** Current flow patterns for (a) uniform half-space; (b) two-layer ground with lower resistivity in upper layer; (c) two-layer ground with higher resistivity in upper layer.

the array is often preferred for depth sounding. However, offset techniques (Section 6.3.3) allow excellent results to be obtained with the Wenner.

Near-surface effects may be large when a gradient or two-electrode array is used for profiling but are also very local. A smoothing filter can be applied.

### 6.1.5 Depth penetration

Arrays are usually chosen at least partly for their depth penetration, which is almost impossible to define because the depth to which a given fraction of current penetrates depends on the layering as well as on the separation between the current electrodes. Voltage electrode positions determine which

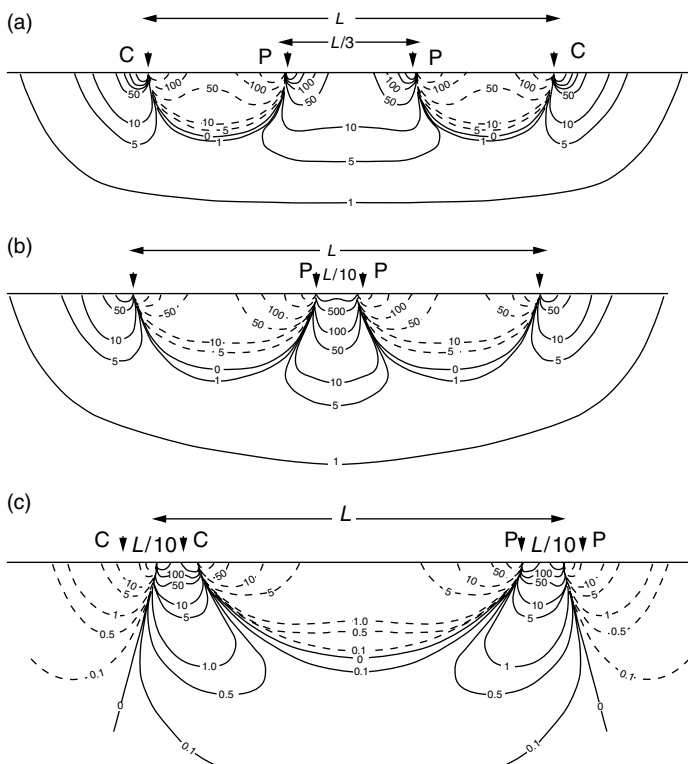


**Figure 6.4** Signal contribution sections for (a) Wenner; (b) Schlumberger and (c) dipole-dipole arrays. Contours show relative contributions to the signal from unit volumes of homogeneous ground. Dashed lines indicate negative values. (Reproduced by permission of Dr R. Barker.)

part of the current field is sampled, and the penetrations of the Wenner and Schlumberger arrays are thus likely to be very similar for similar total array lengths. For either array, the expansion at which the existence of a deep interface first becomes evident depends on the resistivity contrast (and the levels of background noise) but is of the order of half the spacing between the outer electrodes (Figure 6.5). Quantitative determination of the resistivity change would, of course, require much greater expansion.

For any array, there is also an expansion at which the effect of a thin horizontal layer of different resistivity in otherwise homogeneous ground is

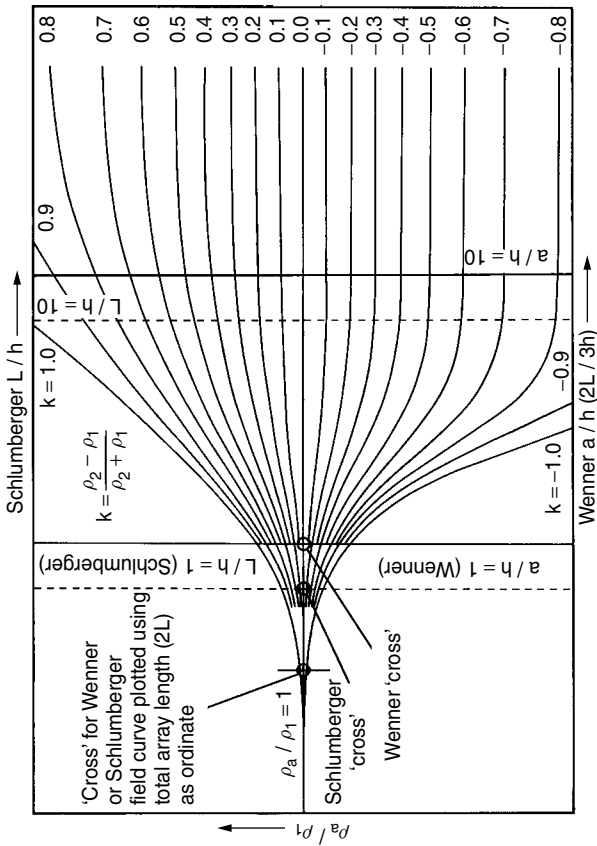


**Figure 6.5** Two-layer apparent resistivity type curves for the Wenner array, plotted on log-log paper. When matched to a field curve obtained over a two-layer earth, the line  $a/h = 1$  points to the depth of the interface and the line  $\rho_a / \rho_1 = 1$  points to the resistivity of the upper layer. The value of  $k$  giving the best fit to the field curve allows the value  $\rho_2$  of the lower layer resistivity to be calculated. The same curves can be used, to a good approximation, for Schlumberger depth sounding with the depth to the interface given by the line  $L/h = 1$ .



a maximum. It is, perhaps, to be expected that much greater expansion is needed in this case than is needed simply to detect an interface, and the plots in Figure 6.6, for the Wenner, Schlumberger and dipole–dipole arrays, confirm this. By this criterion, the dipole–dipole is the most and the Wenner is the least penetrative array. The Wenner peak occurs when the array is 10

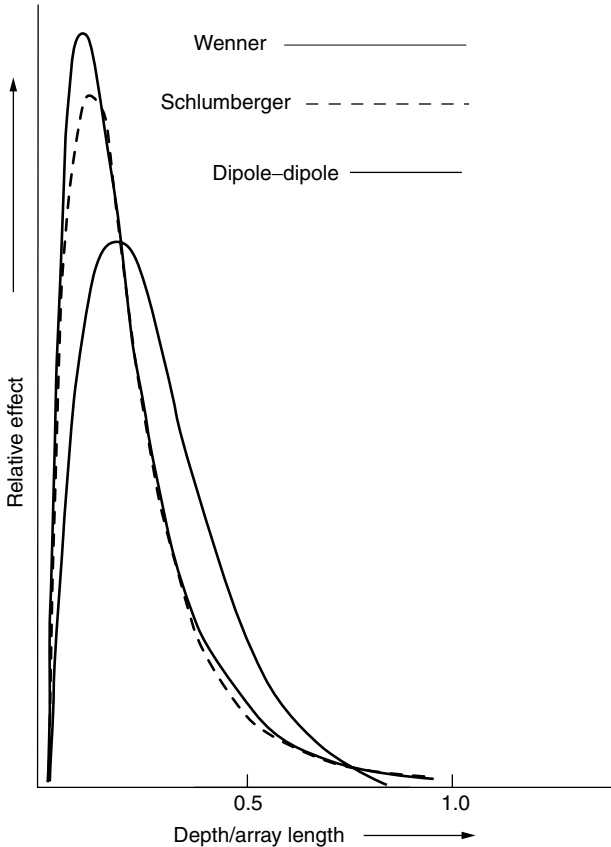


**Figure 6.6** Relative effect of a thin, horizontal high-resistance bed in otherwise homogeneous ground. The areas under the curves have been made equal, concealing the fact that the voltage observed using the Schlumberger array will be somewhat less, and with the dipole–dipole array very much less, than with the Wenner array.

times as broad as the conductor is deep, and the Schlumberger is only a little better. Figure 6.5 suggests that at these expansions a two-layer earth would be interpretable for most values of resistivity contrast.

Figure 6.6 also shows the Wenner curve to be the most sharply peaked, indicating superior vertical resolving power. This is confirmed by the signal-contribution contours (Figure 6.4), which are slightly flatter at depth for the Wenner than for the Schlumberger, indicating that the Wenner locates flat-lying interfaces more accurately. The signal-contribution contours for the dipole-dipole array are near vertical in some places at considerable depths, indicating poor vertical resolution and suggesting that the array is best suited to mapping lateral changes.

### 6.1.6 Noise in electrical surveys

Electrodes may in principle be positioned on the ground surface to any desired degree of accuracy (although errors are always possible and become more likely as separations increase). Most modern instruments provide current at one of a number of preset levels and fluctuations in supply are generally small and unimportant. Noise therefore enters the apparent resistivity values almost entirely via the voltage measurements, the ultimate limit being determined by voltmeter sensitivity. There may also be noise due to induction in the cables and also to natural voltages, which may vary with time and so be incompletely cancelled by reversing the current flow and averaging. Large separations and long cables should be avoided if possible, but the most effective method of improving signal/noise ratio is to increase the signal strength. Modern instruments often provide observers with direct readings of  $V/I$ , measured in ohms, and so tend to conceal voltage magnitudes. Small ohm values indicate small voltages but current levels also have to be taken into account. There are physical limits to the amount of current any given instrument can supply to the ground and it may be necessary to choose arrays that give large voltages for a given current flow, as determined by the geometric factor. The Wenner and two-electrode arrays score more highly in this respect than most other arrays.

For a given input current, the voltages measured using a Schlumberger array are always less than those for a Wenner array of the same overall length, because the separation between the voltage electrodes is always smaller. For the dipole-dipole array, the comparison depends upon the  $n$  parameter but even for  $n = 1$  (i.e. for an array very similar to the Wenner in appearance), the signal strength is smaller than for the Wenner by a factor of three.

The differences between the gradient and two-electrode reconnaissance arrays are even more striking. If the distances to the fixed electrodes are 30 times the dipole separation, the two-electrode voltage signal is more than 150 times the gradient array signal for the same current. However, the gradient array voltage cable is shorter and easier to handle, and less vulnerable to

inductive noise. Much larger currents can safely be used because the current electrodes are not moved.

## **6.2 Resistivity Profiling**

Resistivity traversing is used to detect lateral changes. Array parameters are kept constant and the depth of penetration therefore varies only with changes in subsurface layering. Depth information can be obtained from a profile if only two layers, of known and constant resistivity, are involved since each value of apparent resistivity can then be converted into a depth using a two-layer type-curve (Figure 6.6). Such estimates should, however, be checked at regular intervals against the results from expanding-array soundings of the type discussed in Section 6.3.

### **6.2.1 Targets**

The ideal traverse target is a steeply dipping contact between two rock types of very different resistivity, concealed under thin and relatively uniform overburden. Such targets do exist, especially in man-modified environments, but the changes in apparent resistivity due to geological changes of interest are often small and must be distinguished from a background due to other geological sources. Gravel lenses in clays, ice lenses in Arctic tundra and caves in limestone are all much more resistive than their surroundings but tend to be small and rather difficult to detect. Small bodies that are very good conductors, such as (at rather different scales) oil drums and sulphide ore bodies, are usually more easily detected using electromagnetic methods (Chapter 8).

### **6.2.2 Choice of array**

The preferred arrays for resistivity traversing are those that can be most easily moved. The gradient array, which has only two mobile electrodes separated by a small distance and linked by the only moving cable, has much to recommend it. However, the area that can be covered with this array is small unless current is supplied by heavy motor generators. The two-electrode array has therefore now become the array of choice in archaeological work, where target depths are generally small. Care must be taken in handling the long cables to the electrodes 'at infinity', but large numbers of readings can be made very rapidly using a rigid frame on which the two electrodes, and often also the instrument and a data logger, are mounted (Figure 5.1). Many of these frames now incorporate multiple electrodes and provide results for a number of different electrode combinations.

With the Wenner array, all four electrodes are moved but since all inter-electrode distances are the same, mistakes are unlikely. Entire traverses of cheap metal electrodes can be laid out in advance. Provided that DC or very low frequency AC is used, so that induction is not a problem, the work can

be speeded up by cutting the cables to the desired lengths and binding them together, or by using purpose-designed multicore cables.

The dipole–dipole array is mainly used in IP work (Chapter 7), where induction effects must be avoided at all costs. Four electrodes have to be moved and the observed voltages are usually very small.

### 6.2.3 Traverse field-notes

Array parameters remain the same along a traverse, and array type, spacing and orientation, and very often current settings and voltage ranges can be noted on page headers. In principle, only station numbers, remarks and  $V/I$  readings need be recorded at individual stations, but any changes in current and voltage settings should also be noted since they affect reading reliability.

Comments should be made on changes in soil type, vegetation or topography and on cultivated or populated areas where non-geological effects may be encountered. These notes will usually be the responsibility of the instrument operator who will generally be in a position to personally inspect every electrode location in the course of the traverse. Since any note about an individual field point will tend to describe it in relation to the general environment, a general description and sketch map should be included. When using frame-mounted electrodes to obtain rapid, closely spaced readings, the results are usually recorded directly in a data logger and the description and sketch become all-important.

### 6.2.4 Displaying traverse data

The results of resistivity traversing are most effectively displayed as profiles, which preserve all the features of the original data. Profiles of resistivity and topography can be presented together, along with abbreviated versions of the field notes. Data collected on a number of traverses can be shown by plotting *stacked* profiles on a base map (Section 1.3.10), but there will usually not then be much room for annotation.

Strike directions of resistive or conductive features are more clearly shown by contours than by stacked profiles. Traverse lines and data-point locations should always be shown on contour maps. Maps of the same area produced using arrays aligned in different directions can be very different.

## 6.3 Resistivity Depth-sounding

Resistivity depth-soundings investigate layering, using arrays in which the distances between some or all of the electrodes are increased systematically. Apparent resistivities are plotted against expansion on log-log paper and matched against type curves (Figure 6.5). Although the introduction of multicore cables and switch selection has encouraged the use of simple doubling (Section 6.3.3), expansion is still generally in steps that are approximately

or accurately logarithmic. The half-spacing sequence 1, 1.5, 2, 3, 5, 7, 10, 15... is convenient, but some interpretation programs require exact logarithmic spacing. The sequences for five and six readings to the decade are 1.58, 2.51, 3.98, 6.31, 10.0, 15.8... and 1.47, 2.15, 3.16, 4.64, 6.81, 10.0, 14.7... respectively. Curves drawn through readings at other spacings can be resampled but there are obvious advantages in being able to use the field results directly. Although techniques have been developed for interpreting dipping layers, conventional depth-sounding works well only where the interfaces are roughly horizontal.

### 6.3.1 Choice of array

Since depth-sounding involves expansion about a centre point, the instruments generally stay in one place. Instrument portability is therefore less important than in profiling. The Wenner array is very popular but for speed and convenience the Schlumberger array, in which only two electrodes are moved, is often preferred. Interpretational literature, computer programs and type curves are widely available for both arrays. Local near-surface variations in resistivity nearly always introduce noise with amplitudes greater than the differences between the Wenner and Schlumberger curves.

Array orientation is often constrained by local conditions, i.e. there may be only one direction in which electrodes can be taken a sufficient distance in a straight line. If there is a choice, an array should be expanded parallel to the probable strike direction, to minimize the effect of non-horizontal bedding. It is generally desirable to carry out a second, orthogonal expansion to check for directional effects, even if only a very limited line length can be obtained.

The dipole-dipole and two-electrode arrays are not used for ordinary DC sounding work. Dipole-dipole *depth pseudo-sections*, much used in IP surveys, are discussed in Section 7.4.2.

### 6.3.2 Using the Schlumberger array

Site selection, extremely important in all sounding work, is particularly critical with the Schlumberger array, which is very sensitive to conditions around the closely spaced inner electrodes. A location where the upper layer is very inhomogeneous is unsuitable for an array centre and the offset Wenner array (Section 6.3.3) may therefore be preferred for land-fill sites.

Apparent resistivities for the Schlumberger array are usually calculated from the approximate equation of Figure 6.1c, which strictly applies only if the inner electrodes form an ideal dipole of negligible length. Although more accurate apparent resistivities can be obtained using the precise equation, the interpretation is not necessarily more reliable since all the type curves are based on the ideal dipole.

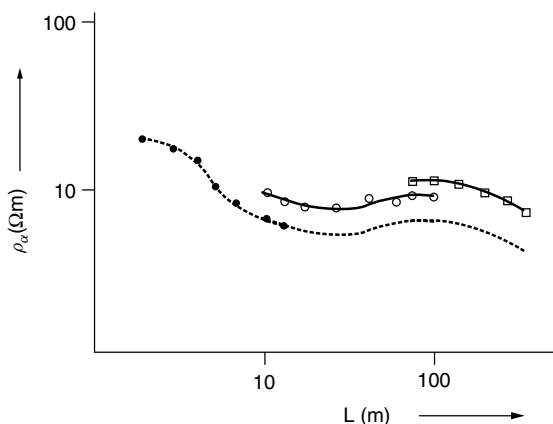


**Figure 6.7** Construction of a complete Schlumberger depth-sounding curve (dashed line) from overlapping segments obtained using different inner-electrode separations.

In principle a Schlumberger array is expanded by moving the outer electrodes only, but the voltage will eventually become too small to be accurately measured unless the inner electrodes are also moved farther apart. The sounding curve will thus consist of a number of separate segments (Figure 6.7). Even if the ground actually is divided into layers that are perfectly internally homogeneous, the segments will not join smoothly because the approximations made in using the dipole equation are different for different  $l/L$  ratios. This effect is generally less important than the effect of ground inhomogeneities around the potential electrodes, and the segments may be linked for interpretation by moving them in their entirety parallel to the resistivity axis to form a continuous curve. To do this, overlap readings must be made. Ideally there should be at least three of these at each change, but two are more usual (Figure 6.7) and one is unfortunately the norm.

### 6.3.3 Offset Wenner depth sounding

Schlumberger interpretation is complicated by the segmentation of the sounding curve and by the use of an array that only approximates the conditions assumed in interpretation. With the Wenner array, on the other hand, near-surface conditions differ at all four electrodes for each reading, risking a high noise level. A much smoother sounding curve can be produced with an *offset* array of five equi-spaced electrodes, only four of which are used for any one reading (Figure 6.8a). Two readings are taken at each expansion and

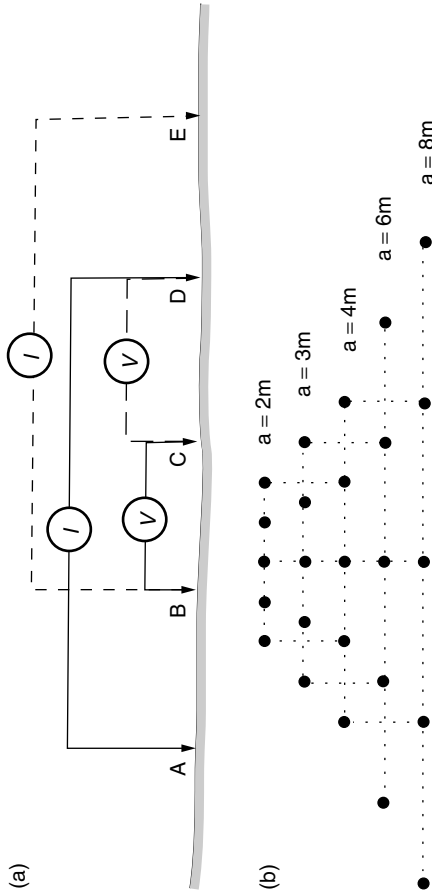


**Figure 6.8** Offset Wenner sounding. (a) Voltage readings are obtained between B and C when current is passed between A and D, and between C and D when current is passed between B and E. (b) An expansion system allowing reuse of electrode positions and efficient operation with multicore cables.

are averaged to produce a curve in which local effects are suppressed. The differences between the two readings provide a measure of the significance of these effects.

The use of five electrodes complicates field work, but if expansion is based on doubling the previous spacing (Figure 6.8b), very quick and efficient operation is possible using multicore cables designed for this purpose.

### 6.3.4 Depth-sounding notebooks

In field notebooks, each sounding should be identified by location, orientation and array type. The general environment should be clearly described and any peculiarities, e.g. the reasons for the choice of a particular orientation, should be given. Generally, and particularly if a Schlumberger array is used, operators are able to see all the inner electrode locations. For information on the outer electrode positions at large expansions, they must either rely on second-hand reports or personally inspect the whole length of the line. Considerable variations in current strengths and voltage levels are likely, and range-switch settings should be recorded for each reading.

### 6.3.5 Presentation of sounding data

There is usually time while distant electrodes are being moved to calculate and plot apparent resistivities. Minor delays are in any case better than returning with uninterpretable results, and field plotting should be routine. All that is needed is a pocket calculator and a supply of log-log paper. A laptop in the field is often more trouble than it is worth, since all are expensive, most are fragile and few are waterproof.

Simple interpretation can be carried out using two-layer type curves (Figure 6.5) on transparent material. Usually an exact two-layer fit will not be found and a rough interpretation based on segment-by-segment matching will be the best that can be done in the field. Ideally, this process is controlled using auxiliary curves to define the allowable positions of the origin of the two-layer curve being fitted to the later segments of the field curve (Figure 6.9). Books of three-layer curves are available, but a full set of four-layer curves would fill a library.

Step-by-step matching was the main interpretation method until about 1980. Computer-based interactive modelling is now possible, even in field camps, and gives more reliable results, but the step-by-step approach is still often used to define initial computer models.

### 6.3.6 Pseudo-sections and depth sections

The increasing power of small computers now allows the effects of lateral changes in resistivity to be separated from changes with depth. For this to be done, data must be collected along the whole length of a traverse at a number



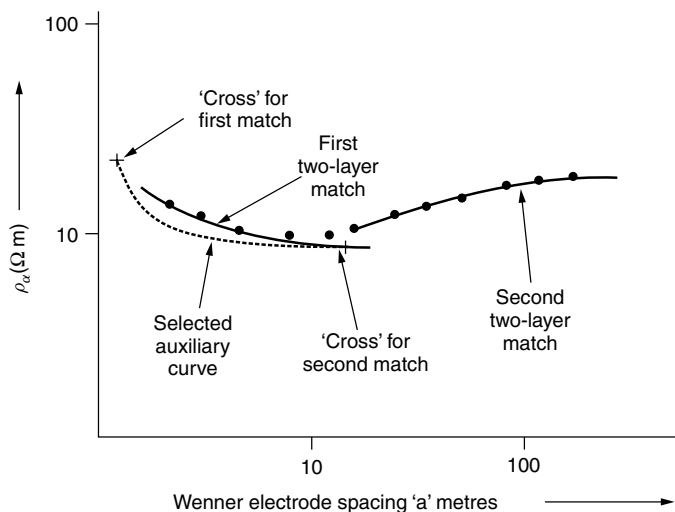


**Figure 6.9** Sequential curve matching. The curve produced by a low-resistivity layer between two layers of higher resistivity is interpreted by two applications of the two-layer curves. In matching the deeper part of the curve, the intersection of the  $a/h = 1$  and  $r_a/r_1 = 1$  lines (the 'cross') must lie on the line defined by the auxiliary curve.

of different spacings that are multiples of a fundamental spacing. The results can be displayed as contoured *pseudo-sections* that give rough visual impressions of the way in which resistivity varies with depth (Figure 6.10a, b). The data can also be *inverted* to produce revised sections with vertical scales in depth rather than electrode separation, which give greatly improved pictures of actual resistivity variations (Figure 6.10c). As a result of the wide use of these techniques in recent times, the inadequacies of simple depth sounding have become much more widely recognized. The extra time and effort involved in obtaining the more complete data are almost always justified by results.

## 6.4 Capacitive Coupling

A number of instruments have been introduced, relatively recently, in which electrical fields due to currents in insulated conductors cause currents to flow in the ground without direct contact. Because the *aerials* can be dragged along the ground, either manually or mechanically, resistivity can be measured continuously.

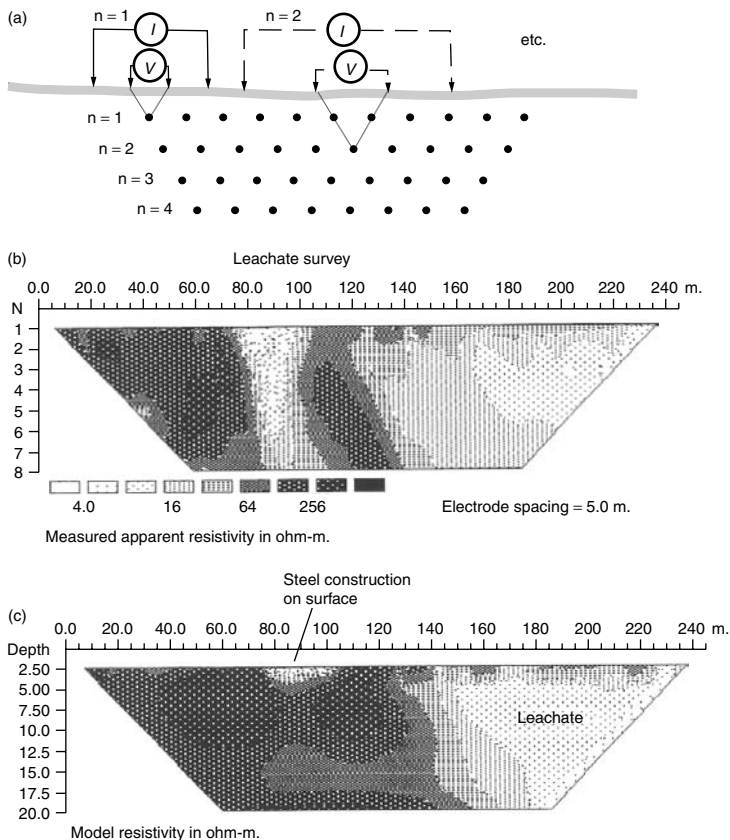


**Figure 6.10** Wenner array pseudo-sections. (a) Plotting system; (b) 'raw' pseudo-section; (c) pseudo-section after inversion. The low-resistivity (white) area at about 90 m was produced by a metal loading bay and railway line, i.e. by a source virtually at the ground surface. (Pseudo-sections reproduced by permission of Dr R. Barker.)

## 6.4.1 Capacitative principles

If the current electrodes in a conventional electrical survey were to be removed from the ground and placed on insulating pads, and then connected to a power source, current would flow only until the electrical potential produced by the charges on the electrodes was equal and opposite to that produced by the

current source. The ability of a system to store charge in this way is termed its electrical *capacity* and is measured in farads.

The fact that the electrodes would be charged, even when insulated from the ground, implies the existence of an electric field between them that can cause charged particles in the ground to move. Again, this current flow would be brief, persisting only until equal and opposite reverse potentials had been established. If, however, polarity is reversed, there will be further flow of charge until a new equilibrium is established. An alternating voltage of sufficiently high frequency will thus cause alternating current to flow in the ground, despite the presence of the insulators. This is capacitive coupling.

### 6.4.2 Instrumentation

The Geometrics 'OhmMapper' (Figure 5.1d) is typical of the instruments now exploiting the advantages of capacitive coupling. Alternating current is supplied at a frequency of 16.6 kHz to a dipole aerial that, in standard configurations, is made up of 2 m or 5 m lengths of cable. The signal is received at a second, similar aerial towed behind the first and separated from it by a non-conductive linkage, also usually several metres long. Transmitter and receiver electronics and power sources are enclosed in nacelles situated at the midpoints of their respective aerials. The entire system is designed to be dragged or towed along the ground. Results are recorded at fixed time intervals in a data logger that, when the system is being dragged, is strapped to the operator's belt. The belt also takes the strain on the cable. The logger display can show the resistivity profile as it develops, and several parallel profiles simultaneously. The precautions discussed in Section 1.3.3 need to be observed to ensure data validity.

The OhmMapper utilizes only signal amplitudes, but there will generally also be a difference in phase between the currents circulating in the receiving and transmitting aerials, and this can provide additional useful information. Instruments are under development, notably by the British Geological Survey, that make use of this fact.

### 6.4.3 Depth of investigation

The depth of investigation in a DC survey is determined mainly by the separation between the electrodes. Similarly, in c-c systems, it is determined by the separation between the aerials and by their lengths. A rough rule of thumb is that the investigation depth is equal to the distance between the centre points of the two aerials.

The use of high-frequency alternating fields introduces an additional factor. The currents in the ground obtain their energy from the varying field and so reduce its strength. Attenuation follows an exponential law (Section 1.1.6),

governed by the attenuation constant ( $\alpha$ ) of Section 5.3.1. The depth of investigation will be determined, or at least influenced, by the skin depth unless this is significantly greater than the distance between receiver and transmitter. The graph in Figure 5.5 suggests that, at the frequencies and separations characteristic of the OhmMapper, there will usually be some element of skin-depth limitation.

#### 6.4.4 Advantages and disadvantages of capacitive coupling

Capacitive coupling allows resistivity data to be obtained very rapidly even in areas where ground contact via electrodes would be difficult or impossible. Traverses can be repeated with different separations between the aerals, and commercially available inversion programs allow resistivity cross-sections to be constructed from multispaced data. However, as with all geophysical methods, there are problems, both practical and theoretical.

Capacitive results will be reliable only if the coupling between the ground and the aerals remains reasonably constant, and this limits the acceptable variations in the insulating gap between ground and aerial. Changes in coupling due to surface irregularities thus introduce a form of noise. Noise is minimized by weighting the aerals but this has obvious disadvantages in one-person operations. Considerable effort may be needed to pull the system over anything but the smoothest terrain, and especially uphill. Even more effort may be needed with later versions of the OhmMapper, which use two receiver aerals to obtain data at two different spacings.

Readings are obtained essentially continuously, and intervals at which they are recorded can be made very small. This does not, however, imply an ability to resolve very small targets, since resolution is determined by aerial length and separation.

Natural, unidirectional currents flow in the ground and produce voltage (self-potential or SP) anomalies that can amount to several hundreds of millivolts between points on the ground surface. They have applications in exploration for massive sulphides, and in some other situations.

Artificial currents flowing in the ground can cause some parts of the rock mass to become electrically polarized. The process is analogous to charging a capacitor or a car battery, and both capacitive and electrochemical effects are involved. If the current suddenly ceases, the polarization cells discharge over periods of several seconds, producing currents, voltages and magnetic fields that can be detected at the surface. Disseminated sulphide minerals produce large polarization effects and *induced polarization (IP)* techniques are therefore widely used in exploring for base metals. Arrays are similar to those used in conventional resistivity work. The gradient and dipole–dipole arrays are especially popular (for reconnaissance and detailed work, respectively) because current and voltage cables can be widely separated to minimize electromagnetic induction.

## 7.1 SP Surveys

SP surveys were at one time popular in mineral exploration because of their low cost and simplicity. They are now little used because some near-surface ore bodies that are readily detected by other electrical methods produce no SP anomaly.

### 7.1.1 Origins of natural potentials

Natural potentials of as much as 1.8 V have been observed where alunite weathers to sulphuric acid, but the negative anomalies produced by sulphide ore bodies and graphite are generally less than 500 mV. The conductor should extend from the zone of oxidation near the surface to the reducing environment below the water table, thus providing a low-resistance path for oxidation–reduction currents (Figure 7.1).

Small potentials, seldom exceeding 100 mV and usually very much less, may accompany groundwater flow. Polarity depends on rock composition and on the mobilities and chemical properties of the ions in the pore waters but most commonly the region towards which groundwater is flowing becomes more electropositive than the source area. These *streaming potentials* are

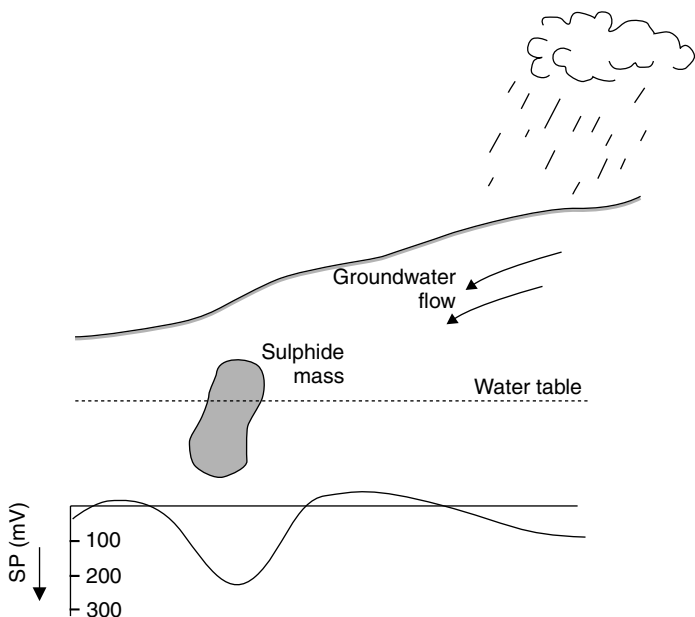


**Figure 7.1** Sources of SP effects. The sulphide mass straddling the water table concentrates the flow of oxidation–reduction currents, producing a negative anomaly at the surface. The downslope flow of groundwater after rain produces a temporary SP, in this case inversely correlated with topography.

sometimes useful in hydrogeology but can make mineral exploration surveys inadvisable for up to a week after heavy rain.

Movements of steam or hot water can explain most of the SPs associated with geothermal systems, but small ( $<10$  mV) voltages, which may be positive or negative, are produced directly by temperature differences. Geothermal SP anomalies tend to be broad (perhaps several kilometres across) and have amplitudes of less than 100 mV, so very high accuracies are needed.

Small alternating currents are induced in the Earth by variations in the ionospheric component of the magnetic field and by thunderstorms (Section 9.4). Only the long-period components of the associated voltages, seldom amounting to more than 5 mV, are detected by the DC voltmeters used in SP surveys. If, as is very occasionally the case, such voltages are significant, the survey should be repeated at different times of the day so that results can be averaged.

### 7.1.2 SP surveys

Voltmeters used for SP work must have millivolt sensitivity and very high impedance so that the currents drawn from the ground are negligible. Copper/copper-sulphate 'pot' electrodes (Section 5.2.2) are almost universal, linked to the meter by lengths of insulated copper wire.

An SP survey can be carried out by using two electrodes separated by a small constant distance, commonly 5 or 10 m, to measure average field gradients. The method is useful if cable is limited, but errors tend to accumulate and coverage is slow because the voltmeter and both electrodes must be moved for each reading. More commonly, voltages are measured in relation to a fixed base. One electrode and the meter remain at this point and only the second electrode is moved. Sub-bases must be established if the cable is about to run out or if distances become too great for easy communication. Voltages measured from a base and a sub-base can be related provided that the potential difference between the two bases is accurately known.

Figure 7.2 shows how a secondary base can be established. The end of the cable has almost been reached at field point B, but it is still possible to obtain a reading at the next point, C, using the original base at A. After differences have been measured between A and both B and C, the field electrode is left at C and the base electrode is moved to B. The potential difference between A and B is thus estimated both by direct measurement and by subtracting the B to C voltage from the directly measured A to C voltage. The average difference can be added to values obtained with the base at B to obtain values relative to A.

### 7.1.3 Errors and precautions

If two estimates of a base/sub-base difference disagree by more than one or two millivolts, work should be stopped until the reason has been determined. Usually it will be found that copper sulphate solution has either leaked away or become undersaturated. Electrodes should be checked every two to

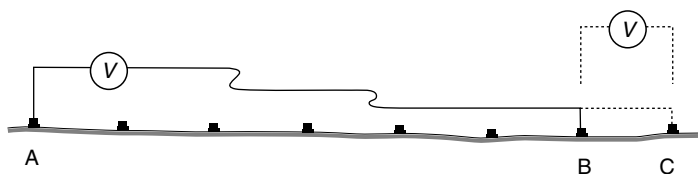


**Figure 7.2** Moving base in an SP survey. The value at the new base (B) relative to A is measured directly and also indirectly by measurements of the voltage at the field point C relative to both bases. The two estimates of the voltage difference between A and B are then averaged.

three hours by placing them on the ground a few inches apart. The voltage difference should not exceed 1 or 2 mV.

Accumulation of errors in large surveys can be minimized by working in closed and interconnecting loops around each of which the voltages should sum to zero (Section 1.4.3).

## 7.2 Polarization Fundamentals

IP surveys are perhaps the most useful of all geophysical methods in mineral exploration, being the only ones responsive to low-grade disseminated mineralization. There are two main mechanisms of rock polarization and three main ways in which polarization effects can be measured. In theory the results obtained by the different techniques are equivalent but there are practical differences.

### 7.2.1 Membrane polarization

The surfaces of clays and some other platy or fibrous minerals are negatively charged and cause *membrane polarization* in rocks with small pore spaces. Positive ions in the formation waters in such rocks congregate near the pore walls, forming an *electrical double layer*. If an electric field is applied, the positive ion clouds are distorted and negative ions move into them and are trapped, producing concentration gradients that impede current flow. When the applied field is removed, a reverse current flows to restore the original equilibrium.

### 7.2.2 Electrode polarization

The static *contact potentials* between metallic conductors and electrolytes were discussed in Section 5.2.2. Additional *over-voltages* are produced whenever currents flow. This *electrode polarization* occurs not merely at artificial electrodes but wherever grains of electronically conducting minerals are in contact with the groundwater. The degree of polarization is determined by the surface area, rather than the volume, of the conductor present, and polarization methods are thus exceptionally well suited to exploration for disseminated *porphyry* ores. Strong anomalies are also usually produced by massive sulphide mineralization, because of surrounding disseminated haloes.

Although, for equivalent areas of active surface, electrode polarization is the stronger mechanism, clays are much more abundant than sulphides and most observed IP effects are due to membrane polarization.

### 7.2.3 The square wave in chargeable ground

When a steady current flowing in the ground is suddenly terminated, the voltage  $V_0$  between any two grounded electrodes drops abruptly to a small



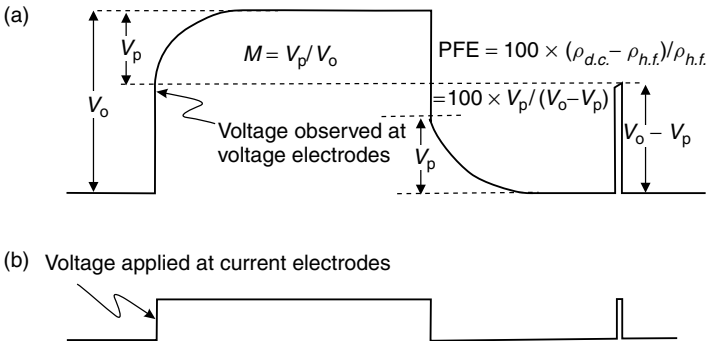


**Figure 7.3** Ground response to a square-wave signal and to a spike impulse. The ratio of  $V_0$  to  $V_p$  is seldom more than a few percent. Input voltage waveform is for reference only. In practice its amplitude will be many times greater than the measured voltage, the exact values depending on the array being used.

polarization voltage  $V_p$  and then declines asymptotically to zero. Similarly, when current is applied to the ground, the measured voltage first rises rapidly and then approaches  $V_0$  asymptotically (Figure 7.3). Although in theory  $V_0$  is never reached, in practice the difference is not detectable after about a second.

*Chargeability* is formally defined as the polarization voltage developed across a unit cube energized by a unit current and is thus in some ways analogous to magnetic susceptibility. The *apparent chargeability* of an entire rock mass is defined, in terms of the square wave shown in Figure 7.3, as the ratio of  $V_p$  to  $V_0$ . This is a pure number but in order to avoid very small values it is generally multiplied by a thousand and quoted in millivolts per volt.

The ratio of  $V_p$  to  $V_0$  cannot be measured directly since electromagnetic transients are dominant in the first tenth of a second after the original current ceases to flow. The practical definition of time-domain chargeability, which is in terms of the decay voltage at some specified delay time, is only tenuously linked to the theoretical definition. Not only do different instruments use different delays, but also it was originally essential and is still quite common to measure an area under the decay curve using integrating circuitry, rather than an instantaneous voltage. The results then depend on the length of the integration period as well as on the delay and are quoted in milliseconds.

#### 7.2.4 Frequency effects

Figure 7.3 also shows that if a current were to be terminated almost immediately after being introduced, a lower apparent resistivity, equal to  $(V_0 - V_p)/I$

multiplied by the array geometrical factor, would be calculated. The IP frequency effect is defined as the difference between the 'high frequency' and 'DC' resistivities, divided by the high-frequency value. This is multiplied by 100 to give an easily handled whole number, the *percent frequency effect* (PFE). The origin of the theoretical relationship between the PFE and the chargeability:

$$M = [PFE]/(100 + [PFE])$$

is illustrated in Figure 7.3.

Because of electromagnetic transients, the theoretical PFE cannot be measured and the practical value depends on the frequencies used. To cancel telluric and SP noise, 'DC' measurements are taken with current reversed at intervals of the order of a few seconds, while the 'high' frequencies are usually kept below 10 Hz to minimize electromagnetic induction.

### 7.2.5 Metal factors

A PFE can be divided by the DC resistivity to give a quantity which, multiplied by 1000, 2000 or  $2000\pi$ , produces a number of convenient size known as the *metal factor*. Metal factors emphasize rock volumes that are both polarizable and conductive and which may therefore be assumed to have a significant sulphide (or graphite) content. Although this may be useful when searching for massive sulphides, low resistivity is irrelevant and can be actually misleading in exploration for disseminated deposits. As usual when factors that should be considered separately are combined, the result is confusion, not clarification.

### 7.2.6 Phase

The square-wave of Figure 7.3 can be resolved by Fourier analysis into sinusoidal components of different amplitudes and frequencies. The asymmetry of the voltage curve implies frequency-dependent phase shifts between the applied current and the measured voltage. In *spectral* IP surveys, these shifts are measured, in milliradians, over a range of frequencies.

## 7.3 Time-domain IP Surveys

Large primary voltages are needed to produce measurable IP effects. Current electrodes can be plain metal stakes but non-polarizing electrodes must be used to detect the few millivolts of transient signal.

### 7.3.1 Time-domain transmitters

A time-domain transmitter requires a power source, which may be a large motor generator or a rechargeable battery. Voltage levels are usually selectable within a range of from 100 to 500 V. Current levels, which may be controlled

through a current limiter, must be recorded if apparent resistivities are to be calculated as well as IPs.

Current direction is alternated to minimize the effects of natural voltages, and cycle times can generally be varied from 2 to 16 seconds. One second each for energization and reading is not generally sufficient for reliable results, while cycles longer than 8 seconds unreasonably prolong the survey.

### 7.3.2 Time-domain receivers

A time-domain receiver measures primary voltage and one or more decay voltages or integrations. It may also be possible to record the SP, so that chargeability, resistivity and SP data can be gathered together.

Early *Newmont* receivers integrated from 0.45 to 1.1 secs after current termination. The SP was first balanced out manually and the primary voltage was then *normalized* by adjusting an amplifier control until a galvanometer needle swung between defined limits. This automatically ratioed  $V_p$  to  $V_o$  for the  $M$  values recorded by a second needle. Experienced operators acquired a 'feel' for the shape of the decay curve from the rates of needle movement and were often able to recognize electromagnetic transients where these persisted into the period used for voltage sampling.

With purely digital instruments, the diagnostic information provided by a moving needle is lost and enough cycles must be observed for statistical reduction of noise effects. Digital systems allow more parameters to be recorded and very short integration periods, equivalent to instantaneous readings. Natural SPs are now compensated (*backed-off* or *bucked-out*) automatically rather than manually. Memory circuits store data and minimize note taking.

The receiver must be tuned to the cycle period of the transmitter so that it can lock on to the transmissions without use of a reference cable (which could carry inductive noise). Cycle times of 4, 8 or 16 seconds are now generally favoured. Changing the cycle time can produce quite large differences in apparent chargeability, even for similar delay times, and chargeabilities recorded by different instruments are only vaguely related.

### 7.3.3 Decay-curve analysis

With readings taken at several different delay times, curve analysis can be attempted. A method suggested for use with Hunttec receivers assumed that each decay curve was a combination of two exponential decays, corresponding to electrode and membrane polarizations, which could be isolated mathematically. This is far too drastic a simplification and the separation, using a limited number of readings, of two exponential functions that have been added together is in any case virtually impossible in the presence of even small amounts of noise. Nonetheless, research continues into the controls

on decay-curve shapes, and chargeabilities should be recorded at as many decay times as are conveniently possible in areas of interesting anomaly. In non-anomalous areas a single value generally suffices.

## **7.4 Frequency-domain Surveys**

Quite small currents and voltages can be used for resistivity measurements, and frequency-domain transmitters can therefore be lighter and more portable than their time-domain equivalents. Especial care has to be taken in positioning cables to minimize electromagnetic coupling. Coupling is increased by increasing the spacing within or between dipoles, by increasing frequency and by conductive overburden. Unfortunately, field crews have very limited control over this final factor in many areas. They may also be forced to use large electrode separations if deep targets are being sought.

### **7.4.1 Frequency-domain transmitters**

Square waves are commonly used for work in the frequency as well as in the time domain, and most modern IP transmitters can be used for both. Measuring resistivity at two frequencies in separate operations is time consuming and does not allow precise cancellation of random noise. Transmitters may therefore be designed to permit virtually simultaneous readings on complex waveforms made up of two frequencies. Simple square waves may be used if the receiver can analyse the voltage waveform to extract the high-frequency effects.

### **7.4.2 Frequency/phase receivers**

Sophisticated receivers are needed to analyse waveforms and extract frequency effects from either single- or dual-frequency transmissions but this sophistication is normally not apparent to an operator recording PFEs from a front panel display.

To measure phase differences for multi-frequency (spectral) IP surveys, a common time reference for transmitter and receiver is essential. Because a reference cable could increase inductive coupling and might also be operationally inconvenient, crystal clocks are used. These can be synchronized at the start of a day's work and should drift no more than a fraction of a millisecond in 24 hours.

### **7.4.3 Phase measurements**

A typical spectral IP plot is shown in Figure 7.4. The frequency at which the maximum phase shift occurs is dependent on grain size, being higher for fine-grained conductors. The sharper the peak, the more uniform the grain size. Most attempts to distinguish between different types of IP source are now based on analysis of these spectral curves, since grain size may be correlated

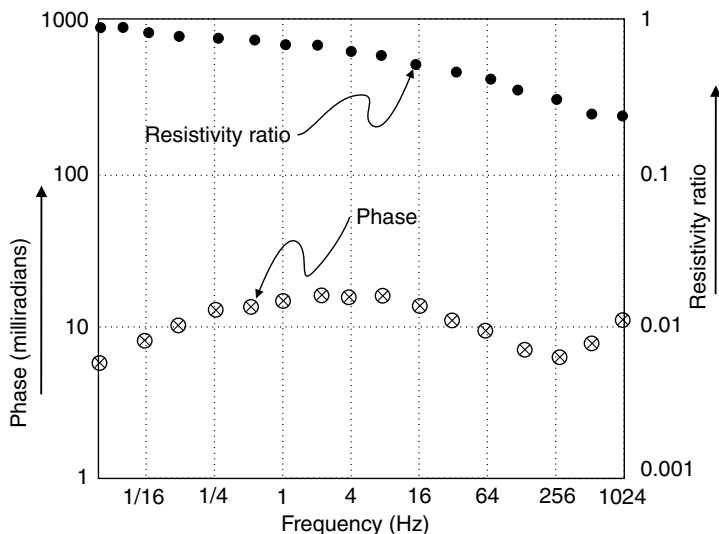


**Figure 7.4** Typical plot of IP phase and amplitude against frequency.

with mineral type. However, exploration programs soon reach the point at which further theoretical analysis of IP curves is less effective than drilling a few holes.

The general pattern of increasing phase shift at high frequencies is caused by electromagnetic coupling. Simple *decoupling* calculations involve readings at three different frequencies and assume a quadratic relationship (i.e.  $\varphi = A + Bf + Cf^2$ ) between phase-shift and frequency. The three readings allow this equation to be solved for A, the *zero-frequency* phase shift value. At most survey points only the value of A will be worth recording, but at points that are clearly anomalous an entire phase spectrum, using many more than the three basic frequencies, may be stored for further processing.

#### 7.4.4 Comparison of time- and frequency-domain methods

The relationship between polarization and current is not precisely linear. This not only limits the extent to which time, frequency and phase measurements can be interrelated, but can also affect comparisons between different surveys of the same type. The effects generally do not exceed a few percent, but provide yet another reason for the very qualitative nature of most IP interpretation.

The relative merits of time- and frequency-domain IP have long been argued, especially by rival instrument manufacturers. Time-domain surveys are essentially multi-frequency and the shapes of decay curves provide information equivalent to that obtained by measurements at several different frequencies in frequency-domain or phase work. It is, moreover, generally conceded that PFEs and phase shifts are more vulnerable to electromagnetic interference than are time-domain chargeabilities, and that the additional readings needed if correction factors are to be calculated take additional time and demand more sophisticated instruments. However, frequency-domain surveys require smaller currents and voltages and may be preferred as safer and involving more portable instruments. The final choice between the two usually depends on personal preference and instrument availability.

## 7.5 IP Data

The methods used to display IP data vary with the array. Profiles or contour maps are used for gradient arrays, while dipole–dipole data are almost always presented as pseudo-sections. In surveys with either array, the spacing between the voltage electrodes should not be very much greater than the width of the smallest target that would be of interest.

### 7.5.1 Gradient array data

Current paths are roughly horizontal in the central areas investigated using gradient arrays, and chargeable bodies will be horizontally polarized. Profiles can be interpreted by methods analogous to those used for magnetic data, with approximate depths estimated using the techniques of Section 3.5.2.

### 7.5.2 Dipole–dipole data

Dipole–dipole traverses at a single  $n$  value can be used to construct profiles but multispaced results are almost always displayed as pseudo-sections (Figure 7.5). The relationships between the positions of highs on pseudo-sections and source body locations are even less simple with dipole–dipole than with Wenner arrays (Section 6.3.6). In particular, the very common *pant's leg* anomaly (Figure 7.5) is usually produced by a near-surface body with little extent in depth; every measurement made with either the current or the voltage dipole near the body will record high chargeability. Anomaly shapes are thus very dependent on electrode positions, and the directions of apparent dip are not necessarily the directions of dip of the chargeable bodies. Even qualitative interpretation requires considerable experience as well as familiarity with model studies.

Pseudo-sections are nearly always plotted in relation to horizontal baselines, even in rugged terrain. Referencing them to topographic profiles (using construction lines similar to those of Figure 7.5 but at  $45^\circ$  to the actual ground

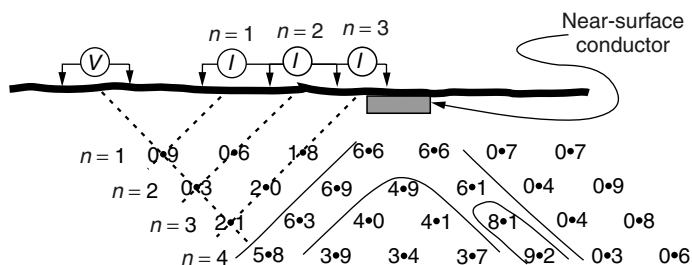


**Figure 7.5** Pseudo-section construction. The three different positions of the current dipole correspond to three different multiples of the basic spacing. Measured values (of IP or resistivity) are plotted at the intersections of lines sloping at  $45^\circ$  from the dipole centres. The plotting ‘point’ often doubles as a decimal point for IP values. The pant’s leg anomaly shown is typical of those produced by small, shallow bodies.

surface) has its dangers, since it might be taken as implying much closer correlation with true sub-surface distributions of resistivity and chargeability than actually exist. However, steep and varied slopes do influence dipole–dipole results and it is better that they be displayed than ignored.

### 7.5.3 Negative IPs and masking

Negative IP effects can be caused by power or telephone cables or, as shown, by signal contribution sections (Figure 6.4), or by lateral inhomogeneities. Layering can also produce negative values, and can conceal deeper sources, most readily if both the surface and target layers are more conductive than the rocks in between. In these latter circumstances, the penetration achieved may be very small and total array lengths may need to be 10 or more times the desired exploration depth.

Interactions between conduction and charge in the earth are very complex, and interpreters generally need more reliable resistivity data than is provided by the dipole–dipole array, which performs poorly in defining layering. A small number of Wenner or Schlumberger expansions, carried out specifically to map resistivity, may prove invaluable. Also, any changes in surface conditions that might correlate with changes in surface conductivity should be noted. The detectability of ore is likely to be quite different beneath bare rock ridges and under an intervening swamp.





Electromagnetic (EM) induction, which is a source of noise in resistivity and IP surveys (Chapters 6 and 7), is the basis of a number of geophysical methods. These were originally mainly used in the search for conductive sulphide mineralization but are now being increasingly used for area mapping and depth sounding. Because a small conductive mass within a poorly conductive environment has a greater effect on induction than on 'DC' resistivity, discussions of EM methods tend to focus on conductivity ( $\sigma$ ), the reciprocal of resistivity, rather than on resistivity itself. Conductivity is measured in mhos per metre or, more correctly, in siemens per metre ( $\text{S m}^{-1}$ ).

There are two limiting situations. In the one, eddy currents are induced in a small conductor embedded in an insulator, producing a discrete anomaly that can be used to obtain information on conductor location and conductivity. In the other, horizontal currents are induced in a horizontally layered medium and their effects at the surface can be interpreted in terms of apparent conductivity. Most real situations involve combinations of layered and discrete conductors, making greater demands on interpreters, and sometimes on field personnel.

Wave effects are important only at frequencies above about 10 kHz, and the methods can otherwise be most easily understood in terms of varying current flow in conductors and varying magnetic fields in space. Where the change in the inducing primary magnetic field is produced by the flow of sinusoidal alternating current in a wire or coil, the method is described as continuous wave (CWEM). Alternatively, transient electromagnetic (TEM) methods may be used, in which the changes are produced by abrupt termination of current flow.

## 8.1 Two-coil CW Systems

A current-carrying wire is surrounded by circular, concentric lines of magnetic field. Bent into a small loop, the wire produces a magnetic dipole field (Figure 1.4) that can be varied by alternating the current. This varying magnetic field causes currents to flow in nearby conductors (Section 5.3.2).

### 8.1.1 System descriptions

In CW (and TEM) surveys, sources are (usually) and receivers are (virtually always) wire loops or coils. Small coil sources produce dipole magnetic fields that vary in strength and direction as described in Section 1.1.5. Anomaly

amplitudes depend on the coil magnetic moments, which are proportional to the number of turns in the coil, the coil areas and the current circulating. Anomaly shapes depend on system geometry as well as on the nature of the conductor.

Coils are described as horizontal or vertical according to the plane in which the windings lie. 'Horizontal' coils have vertical axes and are alternatively described as *vertical dipoles*. Systems are also characterized by whether the receiver and transmitter coils are *co-planar*, *co-axial* or *orthogonal* (i.e. at right angles to each other), and by whether the coupling between them is a maximum, a minimum or variable (Figure 8.1).

Co-planar and co-axial coils are maximum-coupled since the primary flux from the transmitter acts along the axis of the receiver coil. Maximum-coupled systems are only slightly affected by small relative misalignments but, because a strong in-phase field is detected even in the absence of a conductor, are very sensitive to changes in coil separation. Orthogonal coils are minimum-coupled. The primary field is not detected and small changes in separation have little effect. However, large errors are produced by slight misalignments. In the field it is easier to maintain a required coil separation than a relative orientation, and this is one reason for favouring maximum coupling.

*Dip-angle* systems, in which the receiver coil is rotated to determine the dip of the resultant field, were once very popular but are now generally limited to the *shoot-back* instruments used in rugged terrain. Shoot-back receiver and transmitter coils are identical and are linked to electronic units that can both transmit and receive. Topographic effects are cancelled by measuring and averaging the receiver coil dip angles with first one and then the other coil held horizontal and used as transmitter.

### 8.1.2 Slingram

Most ground EM systems use horizontal co-planar coils ('horizontal loops'), usually with a shielded cable carrying a phase-reference signal from transmitter to receiver. The sight of two operators, loaded with bulky apparatus and linked by an umbilical cord, struggling across rough ground and through thick scrub, has provided light entertainment on many surveys. Very sensibly, some instruments allow the reference cable to be also used for voice communication. Fortunately, memory units have not (yet) been added to record the conversations.

The Swedish term *Slingram* is often applied to horizontal-loop systems but without any general agreement as to whether it is the fact that there are two mobile coils, or that they are horizontal and co-planar, or that they are linked by a reference cable, that makes the term applicable.

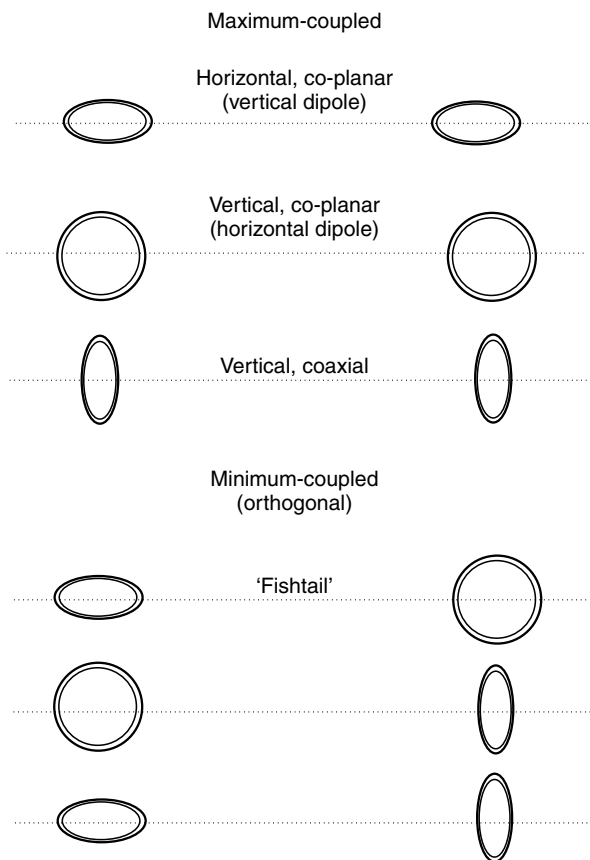


**Figure 8.1** Coil systems for electromagnetic surveys. The Geonics standard descriptions, in terms of magnetic dipole direction rather than loop orientation, are given in brackets. Relative orientation is variable in dip-angle systems, although usually the transmitter coil is held horizontal and the receiver coil is rotated to locate the direction for minimum signal.

### 8.1.3 Response functions

In a Slingram survey, the electromagnetic *response* of a body is proportional to its mutual inductances with the transmitter and receiver coils and inversely proportional to its self-inductance,  $L$ , which limits eddy current

flow. Anomalies are generally expressed as percentages of theoretical primary field and are therefore also inversely proportional to the mutual inductance between transmitter and receiver, which determines the strength of the primary field. The four parameters can be combined in a single *coupling factor*,  $M_{ts}M_{sr}/M_{tr}L$ .

Anomalies also depend on a *response parameter* which involves frequency, self-inductance (always closely related to the linear dimensions of the body) and resistance. Response curves (Figure 8.2) illustrate simultaneously how responses vary over targets of different resistivity using fixed-frequency systems and over a single target as frequency is varied. Note that the quadrature field is very small at high frequencies, where the distinction between good and merely moderate conductors tends to disappear.

Most single-frequency systems (except, as discussed in Section 8.1.8, those used for conductivity mapping) operate below 1000 Hz, and even the multi-frequency systems that are now the norm generally work entirely below 5000 Hz. Narrow poor-quality conductors may produce measurable anomalies only at the highest frequency or not at all (see Figure 9.10).

#### 8.1.4 Slingram practicalities

The coil separation in a Slingram survey should be adjusted to the desired depth of penetration. The greater the separation, the greater the effective

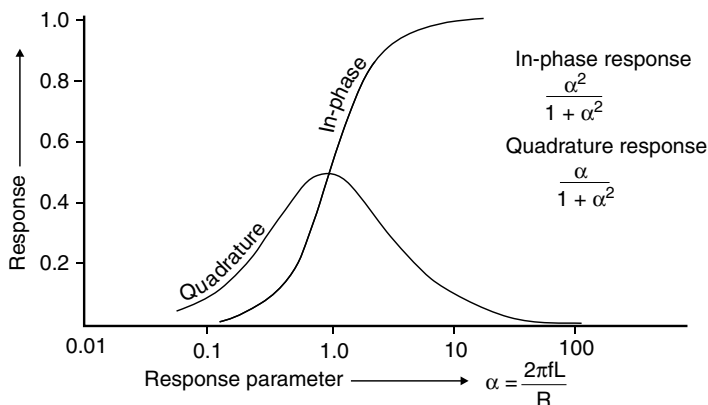


**Figure 8.2** Response of a horizontal-loop EM system to a vertical loop target, as a function of the response parameter ( $\alpha$ ). Note that the Response Parameter scale is logarithmic.  $L$  is the loop self-inductance,  $R$  its resistance and  $f$  is the frequency. The curves for more complex targets would have the same general form.

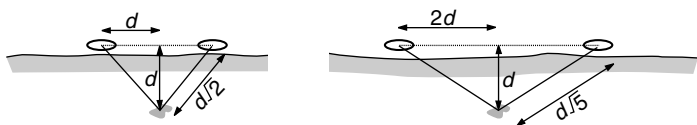


**Figure 8.3** *Spacing and penetration. When the two coils are moved apart, the fractional change in distance between them is greater than between either and the conductor at depth. The increased separation thus increases the anomalous field as a percentage of the primary. In the example, doubling the separation increases the coil to target distances by about 60%.*

penetration, because the primary field coupling factor  $M_{tr}$  is more severely affected by the increase than are either  $M_{ts}$  or  $M_{sr}$  (Figure 8.3). The maximum depth of investigation of a Slingram system is often quoted as being roughly equal to twice the coil separation, provided that this is less than the skin depth (Figure 5.5) but this ignores the effects of target size and conductivity and may be unduly optimistic.

Because signals in Slingram surveys are referenced to primary field strengths, the 100% level should be verified at the start of each day by reading at the standard survey spacing on ground which is level and believed to be non-anomalous. This check has to be carried out even with instruments that have fixed settings for allowable separations, because drift is a continual problem.

A check must also be made for any leakage of the primary signal into the quadrature channel (*phase mixing*). Instrument manuals describe how to test for this condition and how to make any necessary adjustments. Receivers and transmitters must, of course, be tuned to the same frequency for sensible readings to be obtained, but care is needed. A receiver can be seriously damaged if a transmitter tuned to its frequency is operated close by.

Figure 8.4 shows the horizontal-loop system anomaly over a thin, steeply dipping conductor. No anomaly is detected by a horizontal receiving coil immediately above the body because the secondary field there is horizontal. Similarly, there will be no anomaly when the transmitter coil is vertically above the body because no significant eddy currents will be induced. The greatest (negative) secondary field values will be observed when the conductor lies mid-way between the two coils. Coupling depends on target orientation and lines should be laid out across the expected strike. Oblique intersections produce poorly defined anomalies that may be difficult to interpret.

Readings obtained with mobile transmitter and receiver coils are plotted at the mid-points. This is reasonable because in most cases where relative coil orientations are fixed, the anomaly profiles over symmetrical bodies are also symmetrical and are not affected by interchanging receiver and transmitter.

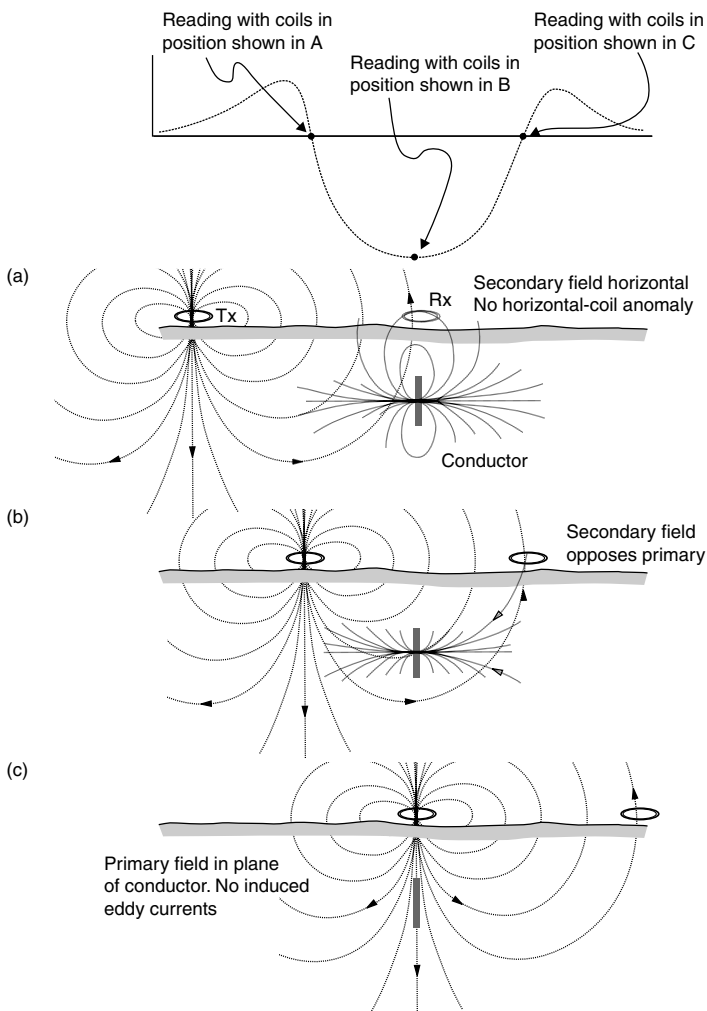


**Figure 8.4** Horizontal loop anomaly across a steeply dipping conductive sheet. Over a dipping sheet, the area between the side lobe and the distance axis would be greater on the down-dip side. Anomaly width is largely determined by coil separation, not by target width.

Even where this is not completely true, recording mid-points is less likely to lead to confusion than recording either transmitter or receiver coil positions.

In all EM work, care must be taken to record any environmental variations that might affect the results. These include obvious actual conductors and also features such as roads, alongside which artificial conductors are often buried. Power and telephone lines cause special problems since they broadcast noise which, although different in frequency, is often strong enough to pass through the rejection (*notch*) filters. It is important to check that these filters are appropriate to the area of use (60 Hz in most of the Americas and 50 Hz nearly everywhere else).

Ground conditions should also be noted, since variations in overburden conductivity can drastically affect anomaly shapes as well as signal penetration. In hot, dry countries, salts in the overburden can produce surface conductivities so high that CW methods are ineffective and have been superseded by TEM.

### 8.1.5 Effects of coil separation

Changes in coupling between transmitter and receiver can produce spurious in-phase anomalies. The field at a distance  $r$  from a coil can be described in terms of radial and tangential components  $F(r)$  and  $F(t)$  (Figure 8.5). The amplitude factor  $A$  depends on coil dimensions and current strength.

For co-planar coils,  $F(r)$  is zero because  $\phi$  is zero and the measured field,  $F$ , is equal to  $F(t)$ . The inverse cube law for dipole sources then implies

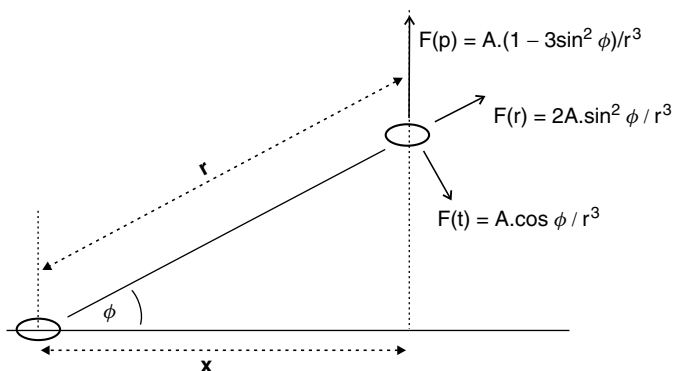


**Figure 8.5** Field components due to a current-carrying loop acting as a magnetic dipole source.  $F(r)$  and  $F(t)$  are radial and tangential components, respectively.  $F(p)$ , obtained by adding the vertical components of both, is the primary field measured by a horizontal receiver coil.

that, for a fractional change  $x$ :

$$F = F_0/(1 + x)^3$$

where  $F_0$  is the field strength at the intended spacing. If  $x$  is small, this can be written as:

$$F = F_0(1 - 3x)$$

Thus, for small errors, the percentage error in the in-phase component is three times the percentage error in distance. Since real anomalies of only a few percent can be important, separations must be kept very constant.

### 8.1.6 Surveys on slopes

On sloping ground, the distances between survey pegs may be measured either horizontally (*secant chaining*) or along slope (Figure 8.6). If along-slope distances are used in reasonably gentle terrain, coil separations should be constant but it is difficult to keep coils co-planar without a clear line of sight and simpler to hold them horizontal. The field  $F(p)$  along the receiver axis is then equal to the co-planar field multiplied by  $(1 - 3 \sin^2 \theta)$ , where  $\theta$  is the slope angle (Figure 8.7). The correction factor  $1/(1 - 3 \sin^2 \theta)$  is always greater than 1 (coils really are maximum-coupled when co-planar) and becomes infinite when the slope is  $35^\circ$  and the primary field is horizontal (Figure 8.7).

If secant-chaining is used, the distances along slope between coils are proportional to the secant ( $=1/\cosine$ ) of the slope angle. For co-planar (tilted) coils the ratio of the 'normal' to the 'slope' field is therefore  $\cos^3 \theta$  and

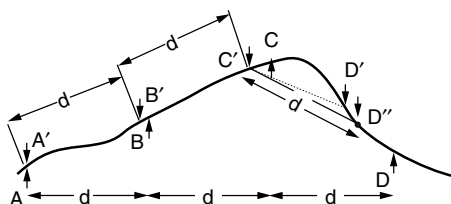


**Figure 8.6** Secant chaining and slope chaining. Down arrows show locations of stations separated by intervals of  $d$  metres measured along slope. Up arrows show locations of secant-chained stations, separated by  $d$  metres horizontally. Between  $C$  and  $D$ , where topographic 'wavelength' is less than the station spacing, the straight line distance from  $C'$  to  $D'$  (for which separation was measured as the sum of short along-slope segments), is less than  $d$ . The 'correct' slope position is at  $D''$ .



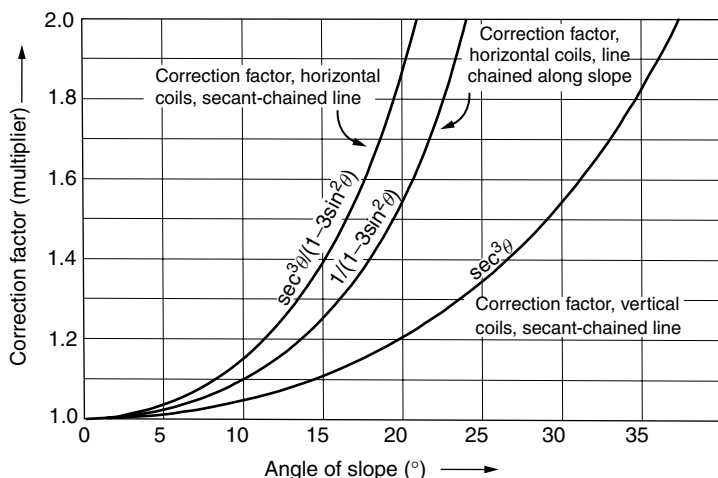


**Figure 8.7** Slope corrections for a two-coil system calibrated for use in horizontal, co-planar mode. Readings should be multiplied by the appropriate factors.

the correction factor is  $\sec^3 \theta$ . If the coils were to be held horizontal, the combined correction factor would be  $\sec^3 \theta / (1 - 3 \sin^2 \theta)$  (Figure 8.7).

Separations in rugged terrain can differ from their nominal values if the coil separation is greater than the distances over which slopes have been measured (Figure 8.6). Accurate surveying is essential in such areas and field crews may need to carry lists of the coil tilts required at each station. Instruments which incorporate tilt meters and communication circuits are virtually essential and even so errors are depressingly common and noise levels tend to be high.

### 8.1.7 Applying the corrections

For any coupling error, whether caused by distance or tilt, the in-phase field that would be observed with no conductors present can be expressed as a percentage of the maximum-coupled field  $F_0$ .

A field calculated to be 92% of  $F_0$  because of non-maximum coupling can be converted to 100% *either* by adding 8% *or* by multiplying the actual reading by 100/92. If the reading obtained actually were 92%, these two operations would produce identical results of 100%. If, however, there were a superimposed secondary field (e.g. if the actual reading were 80%), adding 8% would correct only the primary field (converting 80% to 88% and

indicating the presence of a 12% anomaly). Multiplication would apply a correction to the secondary field also and would indicate a 13% anomaly. Neither procedure is actually 'right', but the principles illustrated in Figure 8.3 apply, i.e. the deeper the conductor, the less the effect of a distance error on the secondary field. Since any conductor that can be detected is likely to be quite near the surface, correction by multiplication is generally more satisfactory, but in most circumstances the differences will be trivial.

Coupling errors cause fewer problems if only quadrature fields are observed, since these are anomalous by definition (although, as Figure 8.2 shows, they may be small for very good as well as poor conductors). Rough corrections can be made using the in-phase multipliers but there is little point doing this in the field. The detailed problems caused by changes in coupling between a transmitter, a receiver and a third conductor can, thankfully, be left to the interpreter, provided the field notes describe the system configurations and topography precisely.

### 8.1.8 Ground conductivity measurement

Slingram-style systems are now being used for rapid conductivity mapping. At low frequencies and low conductivities, eddy currents are small, phase shifts are close to  $90^\circ$  and the bulk apparent resistivity of the ground is roughly proportional to the ratio between the primary (in-phase) and secondary (quadrature phase) magnetic fields. Relatively high frequencies are used to ensure a measurable signal in most ground conditions. If the *induction number*, equal to the transmitter–receiver spacing divided by the skin depth, is significantly less than unity, the depth of investigation is determined mainly by coil spacing.

Induced current flow in a homogeneous earth is entirely horizontal at low induction numbers, regardless of coil orientation, and in a horizontally layered earth the currents in one layer hardly affect those in any other. Figure 8.8 shows how current flow varies with depth for horizontal and vertical inducing coils in these circumstances. One reason for preferring horizontal coils (i.e. vertical dipoles) is obvious. The response for vertical co-planar coils, and hence the apparent conductivity estimate, is dominated by the surface layer.

The independence of current flows at different levels implies that the curves of Figure 8.8, which strictly speaking are for a homogeneous medium, can be used to calculate the theoretical apparent resistivity of a layered medium (Figure 8.9). Using this principle, layering can to some extent be investigated by raising or lowering the coils within the zero-conductivity air 'layer'. In principle it could also be investigated by using a range of frequencies, but the range would have to be very wide and inherently *broad-band* methods such as TEM (Section 8.4) or CSAMT/MT (Section 9.4) are preferable.

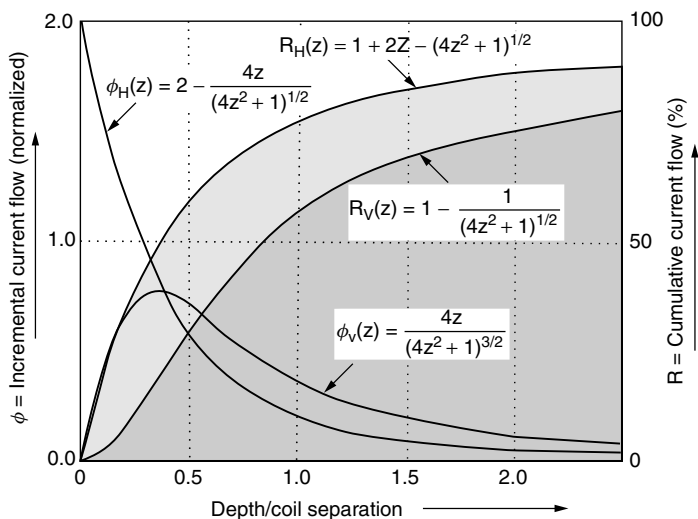


**Figure 8.8** Variation of induced current with depth in homogeneous ground, for co-planar coil systems operating at low induction numbers. ‘Filled’ curves show total current flowing in the region between the surface and the plane at depth, as a fraction of total current flow. Incremental curves are normalized. Subscripts ‘h’ and ‘v’ refer to horizontal and vertical dipoles, following the Geonics terminology used with the EM-31 and EM-34.

The Geonics EM-31 (Figure 8.10) is an example of a co-planar coil instrument that can be used, at some risk to life and limb on difficult sites, by one operator to obtain rapid estimates of apparent resistivity (manmade conductors such as buried drums and cables may also be detected). Normally the coils are held horizontal giving, at low induction numbers, a penetration of about 6 m and a radius of investigation of about 3 m with the fixed 3.7 m coil spacing. This compares very favourably with the 20–30 m total length of a Wenner array with similar penetration (Section 6.1.3). Figure 8.11 shows the results of a very detailed EM-31 survey for sinkholes in chalk, carried out on top of a plastic membrane forming the lining of a small reservoir. Measurements can also be made (although not easily), with the coils vertical, halving the penetration. A shorter, and therefore more manoeuvrable version, the EM-31SH, is only 2 m long and therefore provides better resolution but only about 4 m of penetration.

Both versions of the EM-31 operate at 9.8 kHz. The more powerful, two-person, Geonics EM-34-3 (Figure 5.1e) uses frequencies of 0.4, 1.6 and

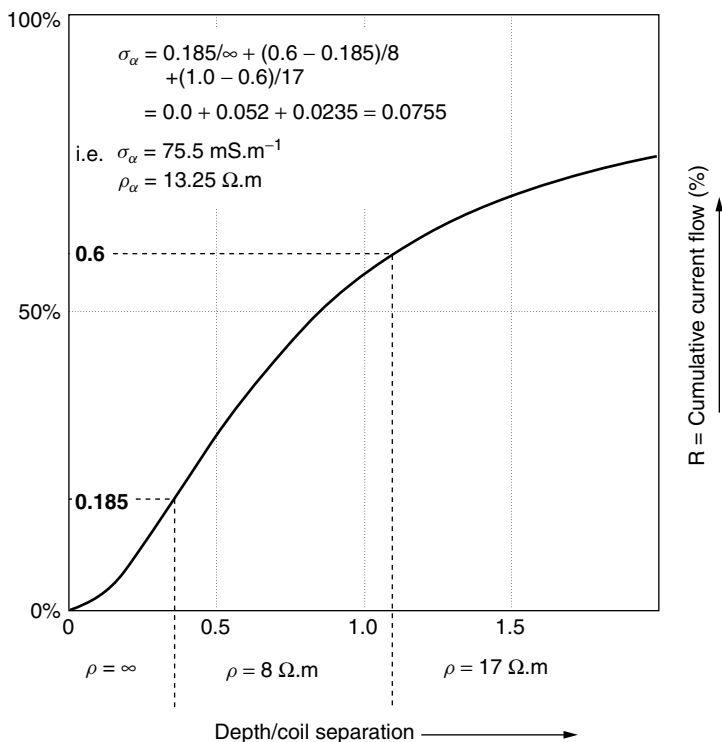


**Figure 8.9** Calculation of 'low induction number' apparent resistivity for a layered earth. The thickness of the first layer is determined by the height of the coils above the ground. This introduces an air layer with infinite resistivity and (in this example) a thickness of 1 m.

6.4 kHz with spacings of 40, 20 and 10 m respectively. The frequency is quadrupled each time the coil separation is halved, so the induction number remains constant. Coil separation is monitored using the in-phase signal. Penetrations are 15, 30 and 60 m for horizontal coils and 7.5, 15 and 30 m for vertical coils. As with the EM-31, the EM-34-3 is calibrated to read apparent conductivity directly in  $\text{mS m}^{-1}$ .

## 8.2 Other CWEM Techniques

CWEM surveys can be carried out using long-wire sources instead of coils and many different system geometries. These can only be considered very briefly.



**Figure 8.10** *EM-31 in use in open country.*

### 8.2.1 Fixed-source methods

The fields produced by straight, current-carrying wires can be calculated by repeated applications of the *Biot–Savart law* (Figure 8.12). The relationship for four wires forming a rectangular loop is illustrated in Figure 8.13. If the measurement point is outside the loop, vectors that do not cut any side of the loop have negative signs.

The Slingram anomaly of Figure 8.4 was symmetrical because the receiver and transmitter coil were moved over the body in turn. If the source, whether a coil or a straight wire, were to be fixed, there would be a zero when a horizontal receiver coil was immediately above a steeply dipping body and the anomaly would be anti-symmetrical (Figure 8.14). Fixed-source systems often measure dip angles or (which is effectively the same thing) ratios of vertical to horizontal fields.

*Turam* (Swedish: ‘two coil’) methods use fixed extended sources and two receiving coils separated by a distance of the order of 10 m. Anomalies are assessed by calculating *reduced ratios* equal to the actual ratios of the signal amplitudes through the two coils divided by the *normal* ratios that would have been observed over non-conductive terrain. Phase differences are measured between the currents in the two receiver coils and any non-zero value is

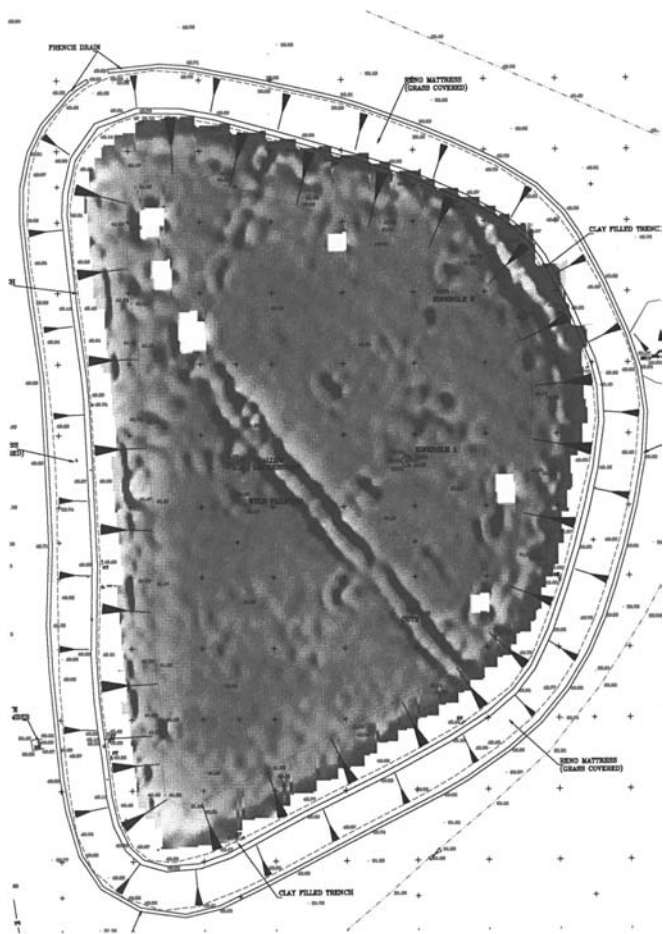


**Figure 8.11** Results of detailed EM-31 resistivity survey, plotted as an image. (Reproduced by permission of Geo-services International (UK) Ltd.)

anomalous. There is no reference cable between receivers and transmitter, but absolute phases and ratios relative to a single base can be calculated provided that each successive reading is taken with the trailing coil placed in the position just vacated by the leading coil. CWEM Turam is now little used, but large fixed sources are common in TEM work.

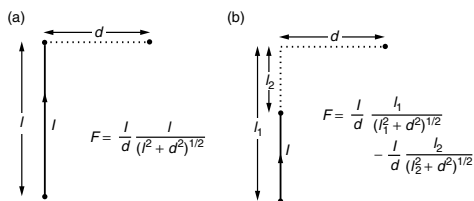


**Figure 8.12** The Biot–Savart law. Any long-wire transmitter can be regarded as made up of elements of the type shown in (a). Two such elements, with currents in opposite directions, can be used to calculate cases such as (b) where the observation point is beyond the end of the wire.

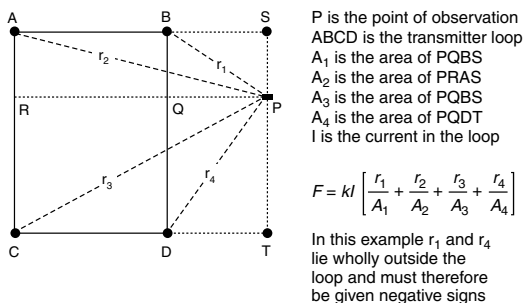


**Figure 8.13** Primary field due to a fixed, rectangular loop carrying a current  $I$ . If  $I$  is measured in amps and distances are in metres,  $k = 10^{-7}$  for  $F$  in  $\text{Weber} \cdot \text{m}^{-2}$ .

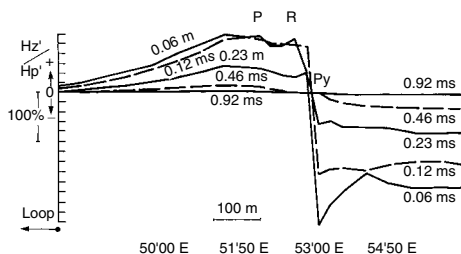


**Figure 8.14** Fixed-loop UTEM vertical component anomaly at *Que River*, Tasmania. Reading interval 25 m. The weak anomaly at *P* indicates economic mineralization, whereas the large anomaly at *R* is produced by barren pyrite. (Reproduced by permission of the Australian Society of Exploration Geophysicists.)

### 8.3 Transient Electromagnetics

TEM systems provide multi-frequency data by repeated sampling of the transient magnetic fields that persist after a transmitter current is terminated. A modified square wave of the type shown in Figure 8.15 flows in the transmitter circuits, and transients are induced in the

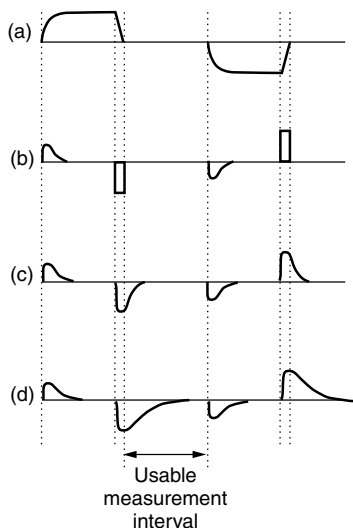


**Figure 8.15** TEM waveforms. (a) Transmitter waveform. Note the taper on the up ramp. The slope on the down ramp is drawn deliberately shallow, for clarity. (b) Signal induced in receiver due to primary field. (c) Signal induced in receiver due to currents circulating in a poor conductor. (d) Signal induced in receiver due to currents circulating in a good conductor. The beginning of the usable measurement interval is defined by the termination of the current induced by the primary, and the end by the beginning of the following up ramp.

ground both on the upgoing and downgoing ramps. Observations are made on currents induced during the downgoing ramps only, since it is only these that can be measured in the absence of the primary field. It is therefore desirable that the up-ramp transients should be small and decay quickly, and the up-ramp is often tapered, reducing induction. In contrast, the current flow is terminated as quickly as possible, in order to maximize induction in the ground. This means that transmitter self-induction must be minimized, and single-turn loops are preferred to multi-turn coils.

#### 8.3.1 TEM survey parameters

A system in which the primary field is not present when secondary fields are being measured can use very high powers, and TEM systems are popular in areas where overburden conductivities are high and penetration is skin-depth limited. Since measurements are made when no primary field is present, the transmitter loop, which may have sides of 100 m or more, can also be used to receive the secondary field. Alternatively, a smaller receiver coil can be positioned within the loop. This technique can be used in CWEM surveys only with very large transmitter loops because of the strong coupling to the primary field.



It is also possible to carry out TEM 'Slingram' surveys, and most commercial systems can employ several different loop configurations. They differ in portability and, in detail, in sampling programs. The SIROTEM may be taken as typical. It produces a square-wave current with equal on and off times in the range from 23 to 185 msec. The voltage in the receiver coil can be recorded at 32 different times during eddy-current decay, and signals can be averaged over as many as 4096 cycles.

An alternative approach is provided by the UTEM system, in which current with a precisely triangular waveform and a fundamental frequency of between 25 and 100 Hz is circulated in a large rectangular loop. In the absence of ground conductivity, the received signal, proportional to the time derivative of the magnetic field, is a square wave. Deviations from this in the vertical magnetic and horizontal electric fields are observed by sampling at eight time delays.

In mineral exploration, TEM data are usually presented as profiles for individual delay times (Figure 8.14). The results at short delay times are dominated by eddy currents in large volume, relatively poor conductors. These attenuate quite rapidly, and the later parts of the decay curves are dominated by currents circulating in any very good conductors that may be present.

### 8.3.2 TEM depth sounding

TEM methods were originally developed to overcome some of the disadvantages of CWEM methods in mineral exploration but are now also being widely used for depth sounding. In homogeneous or horizontally layered ground, termination of current flow in the transmitter loop induces a similar current loop or ring in the adjacent ground. This current then decays, inducing a further current ring with a slightly greater radius at a slightly greater depth. The induced current thus progresses through the subsurface as an expanding 'smoke ring' (Figure 8.16), and the associated magnetic fields at progressively later times are determined by current flow (and hence by resistivity) at progressively greater depths. TEM surveys with 100 m transmitter loops have been used to obtain estimates of resistivity down to depths of several hundred metres, something requiring arrays several kilometres in length if conventional DC methods are used.

If localized good conductors, whether buried oil drums or sulphide orebodies, are present, the effects of the eddy currents induced in them will dominate the late parts of decay curves and may prevent valid depth-sounding data from being obtained. A relatively minor shift in position of the transmitter and receiver loops may be all that is needed to solve the problem.

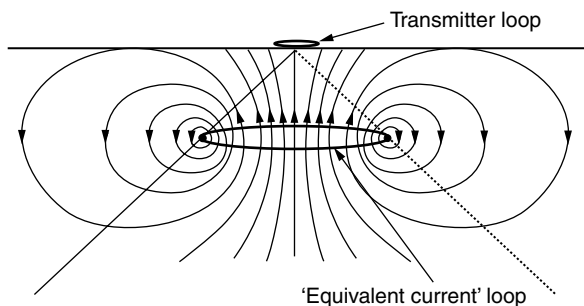


**Figure 8.16** The TEM 'expanding smoke ring' in a layered medium. The 'equivalent current loop' defines the location of maximum circulating current at some time after the termination of current flow in the transmitter loop. The slant lines define the cone within which the loop expands. Arrows are on lines of magnetic field.

### 8.3.3 TEM and CWEM

CWEM and TEM methods are theoretically equivalent but have different advantages and disadvantages because the principal sources of noise are quite different.

Because noise in CWEM surveys arises mainly from variations in the coupling between transmitter and receiver coils, the separations and the relative orientations of the coils must either be kept constant or, if this is not possible, must be very accurately measured. The receiver circuitry must also be very precisely stabilized, but even so it is difficult to ensure that the initial 100% (for the in-phase channel) and 0% (for the quadrature channel) levels do not drift significantly during the course of the day. Because all these possible sources of noise are associated with the primary field, their effects cannot be reduced merely by increasing transmitter power. On the other hand, in TEM surveys the secondary fields due to ground conductors are measured at times when no primary field exists, and coupling noise is therefore negligible. The very sharp termination of transmitter current provides a timing reference that is inherently easier to use than the rather poorly defined maxima or zero-crossings of a sinusoidal wave, and the crystal-controlled timing circuits drift very little.

The most important sources of noise in TEM surveys are external natural and artificial field variations. The effect of these can be reduced by increasing the strength of the primary field and by  $N$ -fold repetition to achieve a  $\sqrt{N}$  improvement in signal-to-noise ratio (Section 1.3.6). There are, however, practical limits to these methods of noise reduction. Transmitter loop

magnetic moments depend on current strengths and loop areas, neither of which can be increased indefinitely. Safety and generator power, in particular, set fairly tight limits on usable current magnitudes. The large loops that are necessary for deep penetration are inevitably difficult to use and can be moved only slowly. Multiple repetitions are not a problem in shallow work, where virtually all the useful information is contained in the first few milliseconds of the decay curve, but can be time consuming in deep work, where measurements have to be extended to time delays of as much as half a second. Moreover, repetition rates must be adjusted so that power-line noise (which is systematic) is cancelled and not enhanced, and the number of repetitions must be adequate for this purpose. It may take more than 10 minutes to obtain satisfactory data at a single point when sounding to depths of more than 100 m (this does, of course, compare very favourably with the time needed to obtain soundings to similar depths with Wenner or Schlumberger arrays).

In Slingram CWEM systems, resolution is determined by the spacing between the transmitter and receiver coils. Because the two coils can be superimposed in a TEM survey, the resolving power can be very high. TEM is thus much more suitable than CWEM for precise location of very small targets. Most modern metal detectors, including 'super metal detectors' such as the Geonics EM-63, which was designed specifically to detect unexploded ordnance (UXO) at depths of a few metres, use TEM principles.

#### 8.3.4 TEM and IP

TEM superficially resembles the time-domain IP methods discussed in Chapter 7. The most obvious difference is that currents in most IP surveys are injected directly into the ground and not induced by magnetic fields. However, at least one IP method does use induction and a more fundamental difference lies in the time scales.

Time-domain IP systems usually sample after delays of between 100 msec and 2 sec, and so avoid most EM effects. There is a small region of overlap, from about 100 to 200 msec, between the two systems and some frequency-domain or phase IP units are designed to work over the whole range of frequencies from DC to tens of kHz to obtain conductivity spectra. However, it is usually possible in mineral exploration to regard the EM and IP phenomena as completely separate and to avoid working in regions, either of frequency or time delay, where both are significant.



Some geophysical instruments make use of high-power military communications transmissions in the 15–25 kHz band. Termed *very low frequency* (VLF) by radio engineers, these waves have frequencies higher than those used in conventional geophysical work, but allow electromagnetic surveys to be carried out without local transmitters.

Natural electromagnetic radiation covers a much broader range of frequencies. Longer wavelengths (lower frequencies) are generally due to ionospheric micropulsations, while much of the radiation in the audible range is generated by distant thunderstorm activity. These latter signals, known as *sferics*, form the basis of audiomagnetotelluric (AMT) methods in mineral exploration and resistivity depth sounding. Because sferic signal strengths vary considerably with time, methods have been developed of producing signals similar to the natural ones using controlled sources (CSAMT). Instruments such as the Geometrics Stratagem allow both natural and CSAMT signals to be used at the same time but over different frequency ranges.

## 9.1 VLF Radiation

An electromagnetic wave consists of coupled alternating electrical and magnetic fields, directed at right angles to each other and to the power vector defining the direction of propagation (Figure 9.1). Electric field vectors will always align themselves at right angles to perfectly conductive surfaces and a wave can therefore be *guided* by enclosing conductors. The extent to which this is possible is governed by the relationship between the wavelength of the radiation and the dimensions of the guide. Waves at VLF frequencies propagate very efficiently over long distances in the waveguide formed by the ground surface and the ionosphere.

### 9.1.1 VLF transmissions

Neither the Earth nor the ionosphere is a perfect conductor, and some VLF energy penetrates the ground surface or is lost into space. Without this penetration, there would be neither military nor geophysical uses. As it is, the waves can be detected tens of metres below the sea surface and are ideal for communicating with submarines. Amplitudes decrease exponentially with depth and the secondary fields produced in subsurface conductors are similarly attenuated on their way to the surface, i.e. VLF surveys are *skin-depth limited* (Figure 5.5).

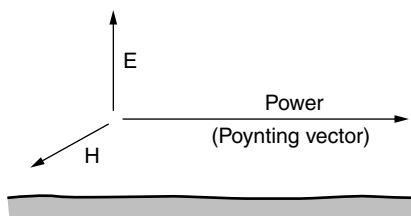


**Figure 9.1** Electromagnetic wave vectors close to a perfect conductor. The magnetic ( $H$ ) and electric ( $E$ ) fields are at right angles to each other and to the power or Poynting vector that defines the direction of propagation.

There are more than a score of stations around the world transmitting VLF signals continuously for military purposes (Figure 9.2). The message content is generally superimposed by frequency modulation on a sinusoidal carrier wave, but occasionally the transmission is chopped into dots and dashes resembling Morse code. Making geophysical use of these *quenched-carrier* signals is extremely difficult. Transmission patterns and servicing schedules vary widely but the makers of VLF instruments are usually aware of the current situation and provide information on their websites.

### 9.1.2 Detecting VLF fields

A geophysical user of a VLF signal has control over neither the amplitude nor the phase of the signal. Readings of a single field component at a single point are therefore meaningless; one component must be selected as a reference with which the strengths and phases of other components can be compared. The obvious choices are the horizontal magnetic and vertical electric fields, since these approximate most closely to the primary signals.

VLF magnetic fields are detected by coils in which currents flow in proportion to the number of turns in the coil, the core permeability and the magnetic field component along the coil axis. No signal will be detected if the magnetic field is at right angles to this axis.

A VLF electric field will induce alternating current in an aerial consisting of a straight conducting rod or wire. The signal strength is roughly proportional to the amplitude of the electric-field component parallel to the aerial, and to the aerial length.

### 9.1.3 Magnetic field effects

Eddy currents induced by a VLF magnetic field produce secondary magnetic fields with the same frequency as the primary but generally with different phase. Any vertical magnetic component is by definition anomalous, and

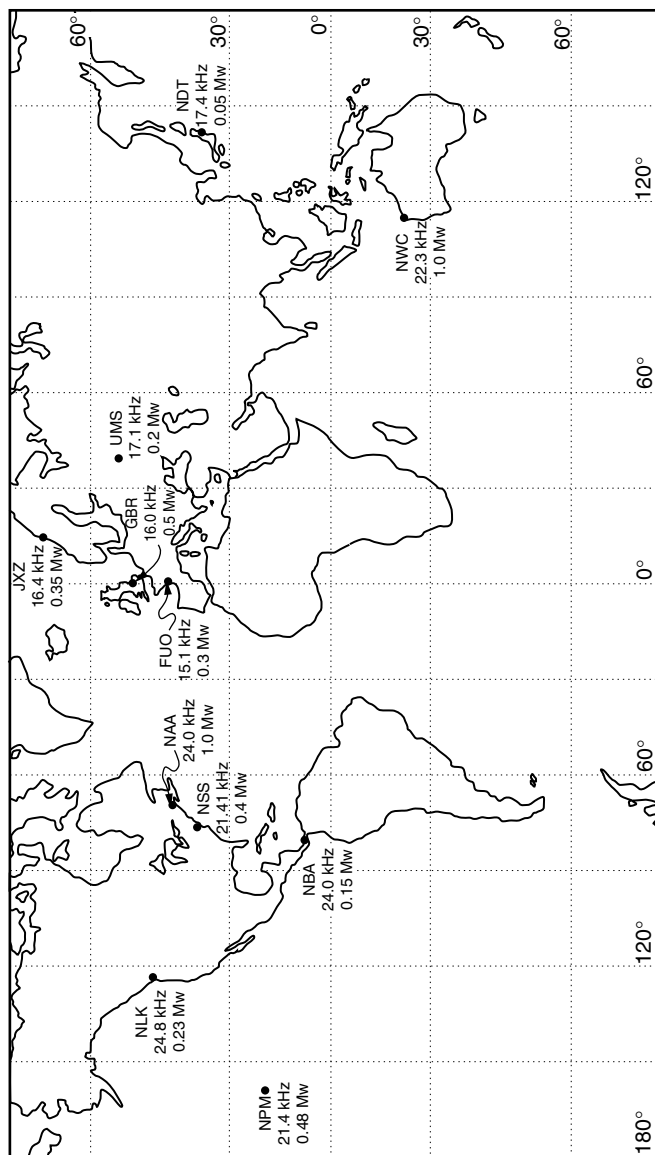


**Figure 9.2** Major VLF transmitters. Data blocks identify station codes (e.g. NAA), frequencies in kHz and power in Megawatts. Frequencies and powers are liable to change without much notification.

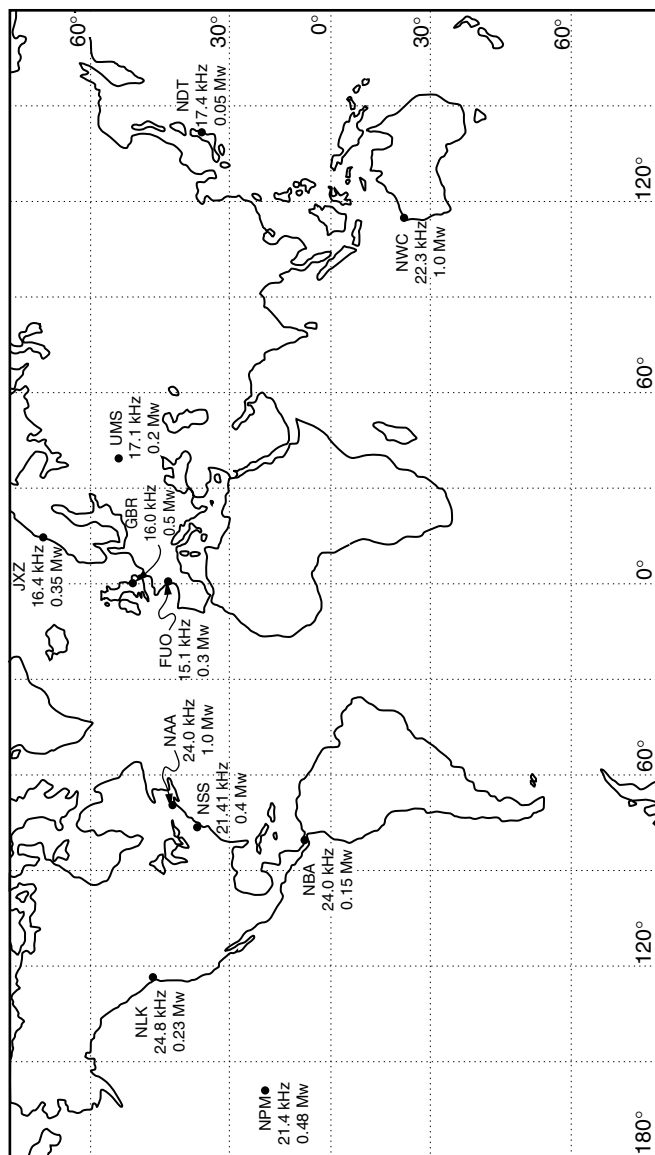


**Figure 9.2** Major VLF transmitters. Data blocks identify station codes (e.g. NAA), frequencies in kHz and power in Megawatts. Frequencies and powers are liable to change without much notification.



most VLF instruments compare vertical with horizontal magnetic fields, either directly or by measuring tilt angles.

The directions of the changes in the secondary magnetic fields are always in opposition to the changes in the primary field. Directly above a steeply dipping sheet-like conductor this secondary field may be strong but will be horizontal and will not be detected by most systems. On either side there will be detectable vertical fields, in opposite directions, defining an anti-symmetric anomaly (Figure 9.3).

Steeply dipping contacts also produce VLF anomalies, which are positive or negative depending upon the sign convention (Figure 9.4). The classical anti-symmetric ‘thin conductor’ anomaly can be looked upon as being produced by two contacts very close together.

Two steeply dipping conductors close to each other produce a resultant anomaly that is generally similar to the sum of the anomalies that would have been produced by each body singly. Where, however, one of the bodies is steeply dipping and the other flat lying, the results are more difficult to

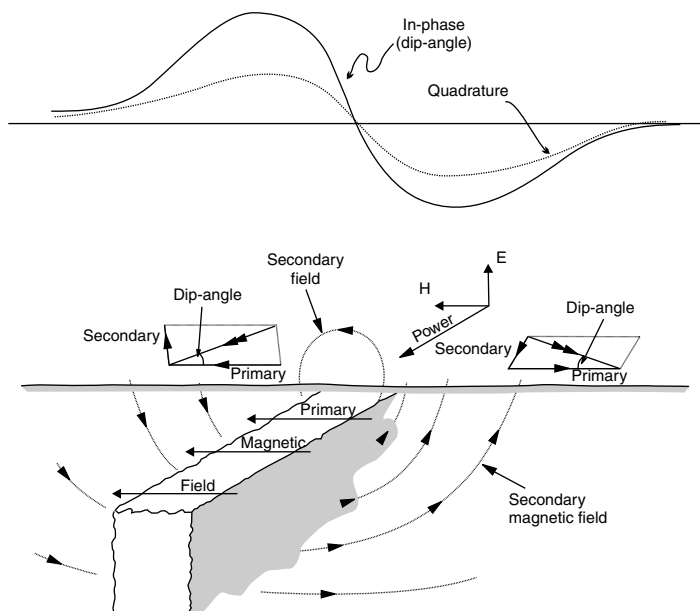


**Figure 9.3** VLF magnetic component anomaly over a vertical conducting sheet striking towards the transmitter. Note the need for a sign convention.

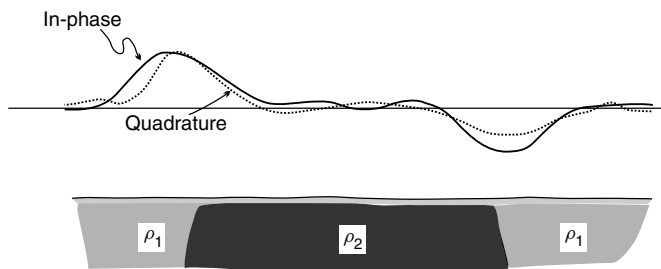


**Figure 9.4** VLF magnetic field anomalies at the margins of an extended conductor. Sign convention as for Figure 9.3.

anticipate. Conductive overburden affects, and can actually reverse, the phase of the secondary field.

### 9.1.4 Electric field effects

Because the Earth is not a perfect conductor, VLF electric vectors near its surface are tilted, not vertical, having horizontal components. Above homogeneous ground the horizontal field would differ in phase from the primary (vertical) field by  $45^\circ$ , would lie in the direction of propagation and would be proportional to the square root of the ground resistivity. Over a layered earth, the magnitude of the horizontal electric field (or tilt of the total field) records average (apparent) resistivity, strongly biased towards the resistivity of the ground within about half a skin depth of the surface. The phase angle will be greater than  $45^\circ$  if resistivity increases with depth in a layered earth and less than  $45^\circ$  if it decreases. Sharp lateral resistivity changes distort this simple picture and very good (usually artificial) conductors produce secondary fields that invalidate the assumptions upon which the resistivity calculations are based.

### 9.1.5 Elliptical polarization

If horizontal primary and secondary fields that differ in phase are combined, the resultant is also horizontal but differs from the two components in both magnitude and phase. A secondary field that is vertical and in phase with the primary produces a resultant which has the same phase but is tilted and stronger. A vertical secondary field in phase quadrature with the primary produces an elliptically polarized wave (Figure 9.5).

These are special cases. In the general case of an inclined secondary field that is neither in phase nor in phase quadrature with the primary, a tilted, elliptically polarized wave is produced. Because the secondary field has a horizontal component, the tangent of the tilt angle is not identical to the

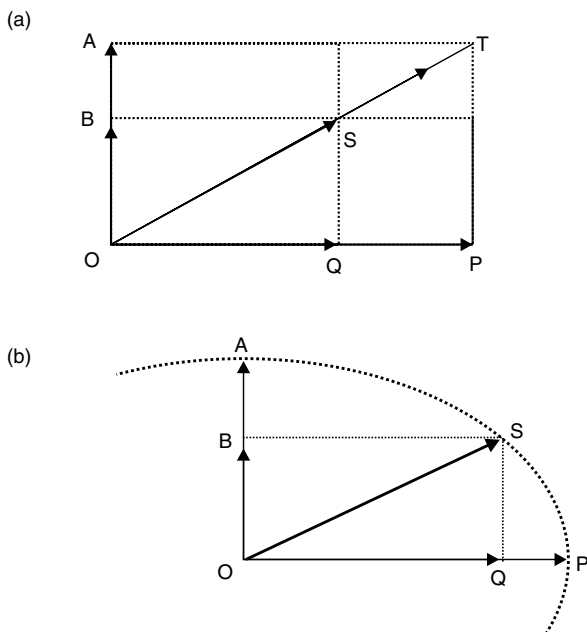


**Figure 9.5** Combination of alternating vertical and horizontal magnetic field vectors. (a) Horizontal and vertical fields in-phase: the vertical vector has its maximum value  $OA$  when the horizontal vector has its maximum value  $OP$  and the resultant has its maximum value  $OT$ . At any other time (as when the vertical field has value  $OB$  and the horizontal field has value  $OQ$ ), the resultant ( $OS$ ) is directed along  $OT$  but with lesser amplitude. All three are zero at the same time. (b) Phase-quadrature: the vertical vector is zero when the horizontal vector has its maximum value  $OP$ , and has its maximum value  $OA$  when the horizontal vector is zero. At other times, represented by  $OB$ ,  $OQ$  and  $OS$ , the tip of the resultant lies on an ellipse.

ratio of the vertical secondary field to the primary and, because of the tilt, the quadrature component of the vertical secondary field does not define the length of the minor axis of the ellipse. This seems complicated, but VLF dip-angle data are usually interpreted qualitatively and such factors, which are only significant for strong anomalies, are usually ignored. Quantitative interpretations are based on physical or computer model studies, the results of which can be expressed in terms of any quantities measured in the field.

### 9.1.6 Coupling

The magnetic-component response of a good conductor depends critically on its orientation. This is also true in conventional EM surveys but EM traverses are usually laid out at right angles to the probable geological strike, automatically ensuring good coupling. In VLF work the traverse direction is almost irrelevant, the critical parameter being the relationship between the strike of the conductor and the bearing of the transmitting station. A body that strikes towards the transmitter is said to be *well coupled*, since it is at right angles to the magnetic vector and eddy currents can flow freely. Current flow will otherwise be restricted, reducing the strength of the secondary field. If the probable strike of the conductors in a given area is either variable or unknown, two transmitters, bearing roughly at right angles to each other, should be used to produce separate VLF maps.

A Mercator projection map such as Figure 9.2 is of only limited use in determining the true bearings of VLF transmitters. The all-important *Great Circle* paths can be found using a computer program or a globe and a piece of string.

## 9.2 VLF Instruments

The first commercially available geophysical VLF instrument, the Ronka-Geonics EM-16, used only magnetic fields, although horizontal electric fields can now be measured with the EM-16R add-on module. The EM-16 is still widely used and serves to illustrate principles which, in some other instruments, are concealed by processing software.

### 9.2.1 The EM-16

The EM-16 consists of a housing containing the electronics, to which is attached a conventional sighting clinometer, and a T-shaped handle containing two coils at right angles (Figure 9.6). Controls include a two-position station-selector switch, a calibrated quadrature control and a knob that amplifies an audio tone which, although often extremely irritating, can be almost inaudible in areas such as forests on windy days, where other noises compete.

With the phase control at zero, the strength of the tone is determined by the setting of the volume control and by the component of the VLF magnetic field parallel to the axis of the main coil. Measurements are made by finding orientations of this coil that produce nulls (minima). This is easiest if the volume control is set so that at the 'null' the tone is only just audible.

Before reading, the direction of the minimum horizontal component (the direction of the power vector) must be determined. Unless there is a significant secondary field, this also gives the bearing of the transmitter. The instrument is held with both coils horizontal, most conveniently with the short coil at right angles to the stomach (Figure 9.7). The observer turns



*Figure 9.6 EM-16 in normal reading position.*



*Figure 9.7 Searching for the station with the EM-16.*

until a null is found, at which stage the magnetic field is at right angles to the main coil and parallel to the short coil. It is occasionally necessary to adjust the quadrature control during this process; it should be reset to zero before attempting to observe the vertical field. There is no way of telling, and no importance in knowing, whether the transmitter is to the left or right of the observer.

Without changing position, the observer then rotates the instrument *about the short coil as axis* into the upright position and then tilts it in the plane of the clinometer (which should now be at eye level). The signal minimum occurs when the long coil is at right angles to the major axis of the polarization ellipse. The null will be poorly defined if the quadrature component (minor axis field) is large or if the plane of the polarization ellipse is not vertical. Definition can be improved by using the quadrature control to subtract a measured percentage of the phase-shifted major-axis field, detected by the short coil, from the quadrature field detected by the long coil. At the null, with the instrument held in the tilted position, the quadrature reading gives the ratio of the ellipse axes and the tangent of the tilt angle defines the in-phase anomaly.

### 9.2.2 EM-16 sign conventions

At a null, the long handle of the EM-16 points towards the region of higher conductivity. An observer with the conductor to the front will have to lean backwards to obtain a null and will see a positive reading on the clinometer. Viewed from the opposite direction, the reading would be negative. To avoid confusion, all readings should be taken facing the same direction and this should be recorded in the field notes even if, as is recommended, a standard range of directions (e.g. N and E rather than S or W) is adopted on all surveys.

Quadrature anomalies usually show the same polarity as in-phase anomalies but may be reversed by conductive overburden. Reversed in-phase anomalies can be caused by steeply dipping insulators enclosed in conductive country rock, which are rare, or by active sources such as live power lines.

### 9.2.3 The EM-16R

With the additional circuitry contained in the EM-16R plug-in module and a 2 m length of shielded cable acting as an aerial, the EM-16 can be used to measure horizontal electric fields. The cable is stretched out towards the transmitter and the two ends are pegged down. The long coil must point towards the transmitter and, for convenience, the instrument is usually laid on the ground. The short coil then detects the maximum magnetic-field component. A null is obtained by rotating the 16R control, giving a reading directly in ohm-metres. Phase shifts are also monitored.

EM-16R resistivities, which use the horizontal magnetic field as a phase reference, assume a fixed ratio between the horizontal magnetic and vertical electric components. This is not the case if significant secondary magnetic fields are present, and use of the more stable vertical electric field as a reference is to be preferred in instruments that provide this option.

### 9.2.4 Other VLF instruments

Most of the alternatives to the EM-16 also record magnetic field variations but measure field components and their ratios rather than dip angles. Major advances include direct recording of data, often into a memory as well as to a front panel display, and elimination of the use of an audible tone. Some instruments can measure natural magnetic and two-transmitter VLF fields simultaneously, and some have been made self-orientating to increase speed of coverage. Amplitudes may also be measured but a base instrument is then needed to correct for amplitude variations caused by meteorological changes along the long transmission paths. Horizontal magnetic field directions are occasionally recorded but are generally less sensitive and less diagnostic than changes in tilt angle and require a directional reference.

Many instruments rely, as does the EM-16, on crystal-controlled tuning to lock to the desired station but others use high-Q tuning circuits. The ABEM Wadi scans the entire VLF band and presents the user with a plot of signal strength against frequency, allowing an informed choice of station.

## 9.3 Presentation of VLF Results

Dip-angle data can be awkward to contour and dip-angle maps, on which conductors are indicated by steep gradients, may be difficult to assess visually. Large artificial conductors produce classic anti-symmetric anomalies but geological conductors are often indicated merely by gradients (Figure 9.8). VLF results tend to be rather noisy, being distorted by minor anomalies due to small local (usually artificial) conductors and electrical interference.

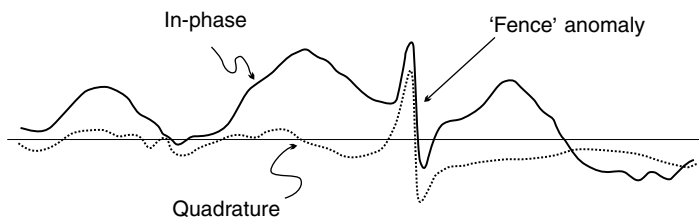


**Figure 9.8** Typical EM-16 profile in area of high geological noise, with superimposed anomaly due to rabbit-proof fence.

### 9.3.1 Filtering

Noise can be reduced by adding together results recorded at closely spaced stations and plotting the sum at the mid-point of the station group. This is the simplest form of low-pass filter. The asymmetry inherent in dip-angle data may be removed by differencing adjacent readings to obtain average horizontal gradients.

Two filters designed to carry out both these operations are in common use (Figure 9.9). The *Fraser filter* uses four equispaced consecutive readings. The first two are added together and halved. The same is done with the second two and the second average is then subtracted from the first. The more complicated *Karous-Hjelt* filter utilizes six readings, three on either side of a central reading that is not itself used. The ABEM Wadi instrument (Figure 5.1a) automatically displays K-H filtered data unless ordered not to do so.

Filtered data are usually easy to contour, especially if, as is normal practice with the Fraser filter, negative values are discarded. Steeply dipping

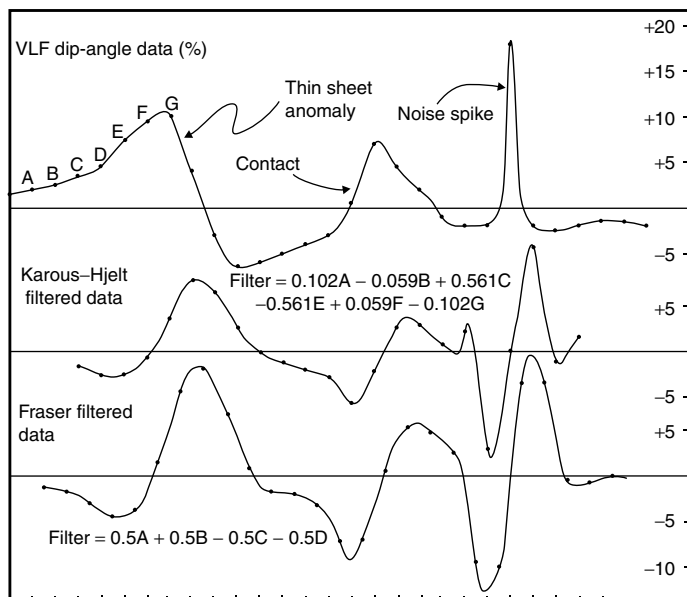


**Figure 9.9** EM-16 profile showing typical 'thin-sheet' and 'contact' anomalies and a noise spike, with Fraser and K-H filtered equivalents. The filters convert the thin-sheet anomaly to a peak but render the other anomalies almost unrecognizable.



conductors produce positive anomalies and are very obvious. However, it is a geophysical axiom that processing degrades data. Filters can destroy subtle but possible significant features and, more importantly, will distort anomalies due to sources other than simple, conductive sheets. For example, an isolated peak or trough due to a steeply dipping interface between materials of differing conductivity will be transformed by both the Fraser and K–H filters into an anti-symmetric anomaly (Figure 9.9). If negative values are then ignored, this feature will be interpreted as indicating a steeply dipping conductor some distance from the region of actual conductivity change.

It is suggested in the Wadi manual that the K–H filter can be used to compute current-density pseudo-sections. However, VLF data cannot be used to determine patterns of simultaneous current flow at different depths. What can be provided are the magnitudes of the currents that would have to flow at single selected depths to produce a given anomaly. The results of calculations for a number of depths are then presented using a variable density display, and the depths of the sources can then be roughly estimated.

### 9.3.2 Displaying VLF data

Since raw dip-angle data are difficult to contour and there are valid objections to filtering, VLF dip-angle data are most effectively presented as stacked profiles. These display all the original data, correctly located on the map, and sections of profile on which there are gradients indicating a conductor can be emphasized by thickened lines.

In order for a map to be interpreted, even qualitatively, the direction to the transmitter must be shown so that the degree of coupling can be assessed. Conductors striking at right angles to this direction will not be well coupled and may not be seen. The map must also show which of the two possible reading directions has been used, since it is otherwise not possible to distinguish ‘normal’ gradients in which values decrease in the facing direction from ‘reversed’ gradients which may be due to active sources such as power and telephone lines.

### 9.3.3 VLF/EM comparisons

VLF systems operate at relatively high frequencies at which most conductors appear good (Figure 8.2) and usually locate many more anomalies than do CWEM surveys over the same ground (Figure 9.10). The method is best suited to mapping near-vertical contacts and fractures. Conductive mineralization may be detected, but the magnitudes of anomalies associated with very good conductors may be no greater than those produced by unmineralized but water-filled fractures, which are likely to occupy larger volumes.

VLF measurements can be made quickly and conveniently by a single operator, and are therefore sometimes used to assess the electromagnetic

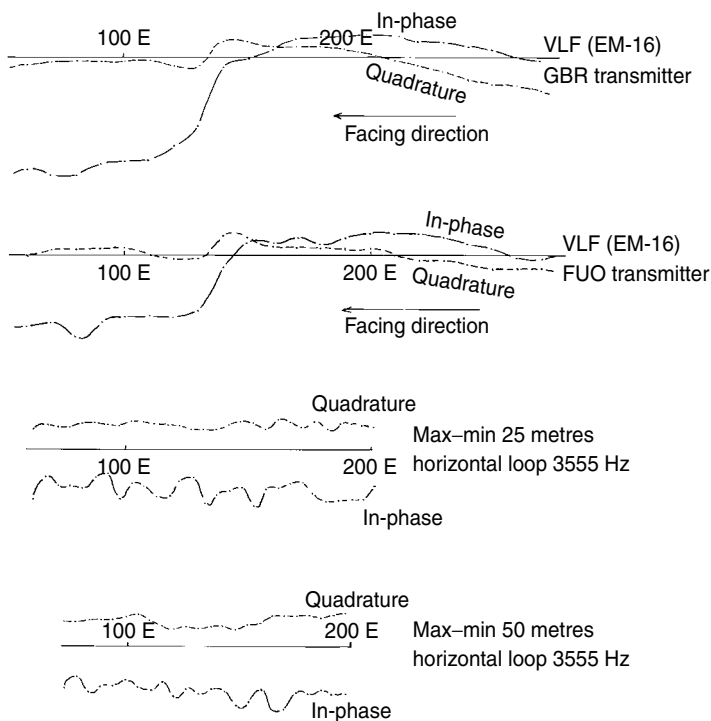


**Figure 9.10** Comparison of EM-16 and horizontal loop EM results across a shear zone in granite. The in-phase variations on the EM profiles are due to small errors in coil separation, which are more serious when actual separations are small. Note that the source of the strong VLF anomaly was detected by the EM system only in the quadrature channel and then only at the 50 m spacing and the highest frequency of which the instrument was capable.

characteristics of an area before the expense of a conventional EM survey is incurred. This is especially useful in populated areas where noise from manmade electrical sources is to be expected. VLF surveys are becoming increasingly popular in hydrogeology. The targets (steeply dipping water-bearing fractures in basement rocks) are important in parts of Africa where the military signals are weak or poorly coupled to the dominant conductors. Portable transmitters are now marketed that allow the method to be used in these areas.

## 9.4 Natural and Controlled-source Audio-magnetotellurics

A broad band of naturally occurring electromagnetic radiation exists and can be used geophysically. These *magnetotelluric* fields are partly sourced by ionospheric currents and partly by thunderstorm activity (*sferics*). The most useful signals, in the frequency range from 1 Hz to about 20 kHz, are commonly referred to as *audio-magnetotelluric* (AMT). These propagate down into the Earth as roughly planar wavefronts oriented parallel to the Earth's surface.

The broad AMT frequency band allows conductivity variations to be investigated over a correspondingly wide range of depths, from a few metres to several kilometres. However, the signals, like so many other things that come for free, are not always reliable. Short- and long-term amplitude fluctuations cause many problems, and unacceptably long times may be needed to obtain satisfactory readings because of low signal strengths. In particular, signals tend to be very weak in the 1–5 kHz range that is crucial for exploration of the upper 100 m of the ground. It is therefore now common to generate similar signals from controlled sources (CSAMT), and to use these to either supplement or replace the natural signals.

### 9.4.1 CSAMT principles

The source for a CSAMT survey is usually a long (2 km or more) grounded wire in which current is 'swept' through a range of frequencies that may extend from as low as 0.1 Hz to as high as 100 kHz. A variety of parameters can be measured, but the horizontal electrical field parallel to the source wire ( $E_x$ ) and the horizontal magnetic field at right angles to it ( $H_y$ ) are the most commonly used. Magnetic fields are measured using small vertical coils, electric fields using short grounded electrode pairs (dipoles) set out parallel to the transmitter. Provided that the transmitter wire is laid out parallel to the regional strike, the magnetic field usually varies comparatively slowly, and reconnaissance CSAMT surveys are often made using measurements at between five and 10 electric dipoles, short distances apart, for every magnetic measurement.

At the *far-field* distances of several kilometres at which AMT equations can be applied to CSAMT data, both magnetic and electric field strengths decrease as the inverse cube of distance from the transmitter. Signals are inevitably weak and, despite the inevitable loss of resolution, it may be impractical to use receiver dipoles less than 20 m in length. Even so, noise may exceed signal by a factor of 10 or more, and long recording times may have to be used during which large numbers of records are obtained to allow very high folds of stacking.

### 9.4.2 CSAMT data

The parameters most commonly measured in CSAMT surveys are the ratios of  $E_x$  to  $H_y$  and the phase differences (the *impedance phases*) between them.

The amplitude ratio is used to calculate a quantity known as the *Cagniard resistivity*, which is given by

$$\rho_a = (E_x/H_y)^2/5f$$

The Cagniard resistivity is often regarded as an estimate of average resistivity down to a depth equal to the skin depth divided by  $\sqrt{2}$ , i.e. to approximately  $350 \sqrt{(\rho_a/f)}$ . The range of frequencies used in CSAMT surveys allows this average to be estimated at depths from a few metres to several kilometres. Plots prepared in the field are usually of Cagniard resistivity and phase difference against frequency. At a single point the variation may be illustrated by a curve (Figure 9.11), but it is usual to plot pseudo-sections for CSAMT traverses (Figure 9.12).

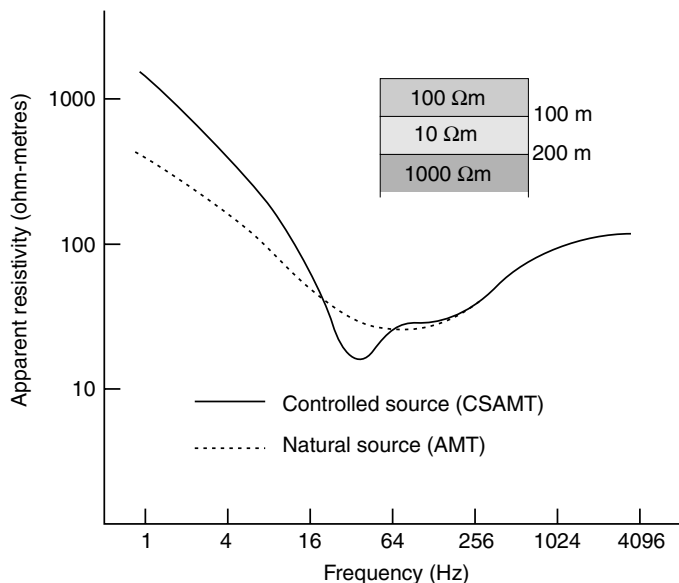


**Figure 9.11** Comparison of the results of AMT and CSAMT soundings over a simple layered earth (overburden, resistivity 100 Ωm, thickness 100 m, overlying low resistivity substrate, resistivity 10 Ωm, thickness 100 m, on bedrock of 1000 Ωm resistivity). The AMT signal provides a plane wavefront at all frequencies. The CSAMT wavefront, from a grounded wire 2 km long, 8 km from the measurement point, ceases to be effectively planar at a frequency of between 100 and 200 Hz (after van Blaricom, 1992).

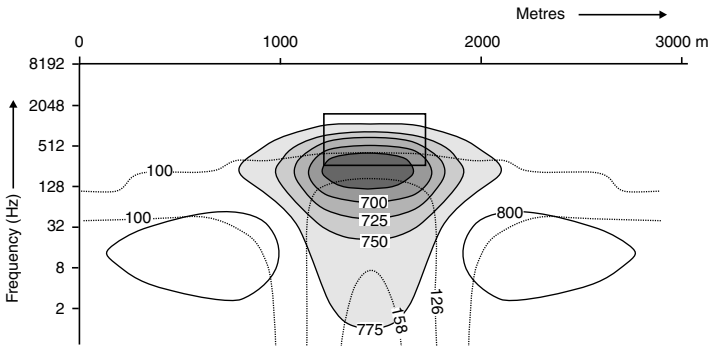


**Figure 9.12** AMT response of a resistive ( $5000 \Omega\text{m}$ ) prism buried in a  $100 \Omega\text{m}$  medium. Solid contours and shading are  $E_x/H_y$  phase difference ('impedance phase') in milliradians (contour interval 25 milliradians). Dotted lines are apparent resistivity, in  $\Omega\text{m}$ . The vertical scale is in frequency, not depth, and the prism (black solid outline) could be made to coincide with the phase anomaly peak by an arbitrary adjustment of scale. The phase anomaly indicates a body with limited extent in depth, something not apparent from the resistivity contours (after van Blaricom, 1992).

Programs can be run on laptop PCs to carry out one-dimensional (horizontal layering) and two-dimensional inversions of Cagniard resistivities to actual resistivities. To estimate the resistivity at a given depth, the Cagniard resistivities must be obtained down to at least three times that depth. However, the fact that the depth of investigation is itself dependent on resistivity implies a degree of circularity in the calculations and the modelling process is inherently ambiguous.

Phase differences are used mainly for investigating small sources, rather than layering. It may, for example, be possible to see both the top and the base of a buried source using phase measurements, even though only the top is visible on the corresponding resistivity plots (Figure 9.12).

### 9.4.3 CSAMT practicalities

The use of controlled sources eliminates some of the problems associated with natural fields but introduces others. Very high currents are required if long-wire sources are to generate sufficiently strong signals at the kilometre distances required by the far-field approximation, and it is seldom easy to find sites where kilometres of wire carrying many amperes of current can be laid out on the ground safely (or even at all). Even where this can be done, topographic irregularities may create significant distortions in the signal. Closed

loop sources can be considerably smaller but require currents even larger (by factors of as much as 10) than those needed for line sources.

The far field for CSAMT measurements is commonly considered to begin at a distance of three skin depths from a long-wire source, and is therefore frequency dependent. On a single sounding plot, the onset of intermediate-field conditions can usually be recognized by an implausibly steep gradient in the sounding curve (Figure 9.11). A simple rule of thumb that can be used in planning surveys is that, to ensure far-field conditions, the distance from source to receiver should be at least six times the required depth of investigation. The layout may, however, have to be modified in the light of actual field conditions. In principle, quite different equations must be used in intermediate and near-field interpretation, but quality control in the field is usually carried out using only the far-field approximations.



Radar methods use the reflections of short bursts of electromagnetic energy (*chirps*) spanning a range of frequencies from about 50% below to 50% above some specified central frequency. A typical 100 MHz signal thus has a significant content of frequencies as low as 50 MHz and as high as 150 MHz. The radar frequencies of from one to several thousand MHz were originally thought to be too high for useful ground penetration, and *ground penetrating radar* (GPR) is a relatively new geophysical tool.

Historically, the development of GPR derives from the use of radio echosounding to determine ice thickness, from which it was only a short step to studies of permafrost. It was soon realized that some penetration was being achieved into the deeper, unfrozen, ground, and that the depth of investigation, although unlikely to ever amount to more than a few tens of metres, could be increased by processing techniques virtually identical to those applied to seismic reflection data. GPR is now widely used to study the very shallow subsurface at landfill, construction and archaeological sites.

## 10.1 Radar Fundamentals

### 10.1.1 Decibels

Radar systems are often described in terms of processes involving amplifications and attenuations (*gains* and *losses*) measured in *decibels* (dB). If the power input to a system is  $I$  and the output is  $J$ , then the gain, in dB, is equal to  $10 \cdot \log_{10}(J/I)$ . A 10 dB gain thus corresponds to a tenfold, and a 20 dB gain to a hundredfold, increase in signal power. Negative values indicate losses. The logarithmic unit allows the effect of passing a signal through a number of stages to be obtained by straightforward addition of the gains at each stage.

$\log_{10}2$  is equal to 0.301 and doubling the power is thus almost exactly equivalent to a gain of 3 dB. This convenient approximation is so widely quoted that it sometimes seems to have become the (apparently totally arbitrary) definition of the decibel. Almost equally confusing is the popular use of decibels to measure absolute levels of sound. This conceals a seldom-stated threshold (dB = 0) level of  $10^{-12} \text{ W m}^{-2}$ , the commonly accepted minimum level of sound perceptible to the human ear. This *acoustic decibel* is, of course, irrelevant in radar work.



### 10.1.2 Radar parameters

The electromagnetic wave attenuation equation (Section 5.3.1) applies in radar work. Permittivity ( $\epsilon$ ) and conductivity ( $\sigma$ ) are usually both important and low frequency approximations cannot be used. Permittivity was originally known as *dielectric constant* and was defined in terms of the ratio of the capacities of otherwise identical parallel-plate capacitors with vacuum or the material in question filling the space between the plates. Changes in units of measurement have made it necessary to assign a value (equal to  $8.854 \times 10^{-12}$  farad  $\text{m}^{-1}$ ) to the permittivity  $\epsilon_0$  of empty (*free*) space, but it is convenient to retain the symbol  $\epsilon$  and the old values, renamed *relative permittivities*, as multipliers of  $\epsilon_0$  instead of assigning an absolute value to every material.  $\epsilon$  is close to one for most common substances, and the relative permittivities of rocks and soils are dominated by  $\epsilon_{\text{water}}$ , which, remarkably, is about 80.

Relative magnetic *permeability* ( $\mu$ ) also affects radar propagation but the relative permeabilities of most materials encountered in GPR surveys are close to one and absolute permeabilities close to the free space value ( $\mu_0 = 4\pi \cdot 10^{-7}$ ).

The velocity of an electromagnetic wave in an insulator is equal to  $c/\sqrt{\epsilon\mu}$ , where  $c$  is the velocity of light in empty (*free*) space. In conducting media, there are further complications. These can be described in terms of a *complex permittivity* ( $K = \epsilon + j\sigma/\omega$ ) and a *loss tangent* ( $\tan \alpha = \sigma/\omega\epsilon$ ), where  $\omega (=2\pi f)$  is the *angular frequency*. Large loss tangents imply high signal attenuation.

Table 10.1 lists typical values of radar parameters for some common materials. Velocities are generally well below the  $0.30 \text{ m ns}^{-1}$  ( $300\,000 \text{ km s}^{-1}$ ) velocity of light in free space. Electrical conductivities at radar frequencies differ, sometimes very considerably, from DC values, often increasing with frequency at roughly log-linear rates (Figure 10.1).

The radar wavelength in any material is equal to the radar wave velocity divided by the frequency, i.e.  $c/f\sqrt{\epsilon}$  if  $\mu$  can be taken as unity. The calculations should be straightforward but because GPR velocities are usually quoted in  $\text{m ns}^{-1}$  and frequencies in MHz (Table 10.1), it is easy to lose a few powers of ten unless orders of magnitude are appreciated. The wavelength of a 100 MHz signal in air is 3 m, in rock with velocity  $0.1 \text{ m ns}^{-1}$  is 10 cm and in salt water, where  $V = 0.01 \text{ m ns}^{-1}$ , only 1 cm.

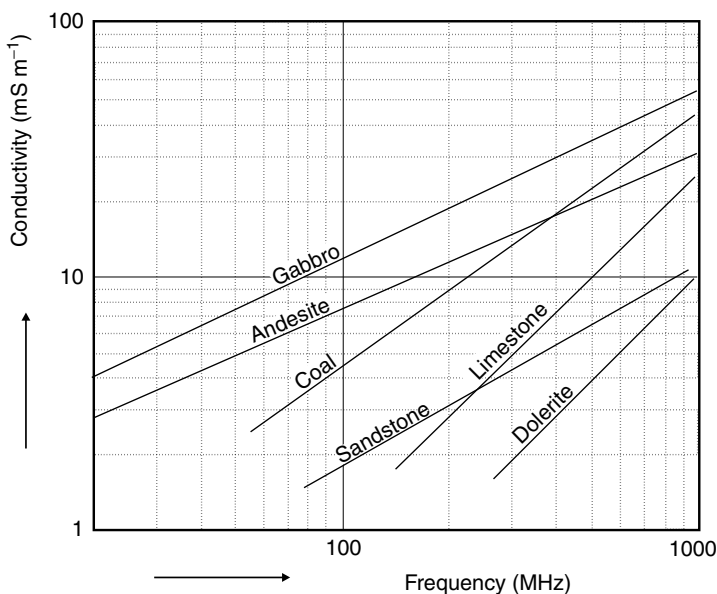
### 10.1.3 Reflection of radar pulses

The percentage of incident radar energy reflected from an interface is governed by the size of the target and by the *amplitude reflection coefficient* which for normal incidence on an infinite interface is given by the equation:

$$RC = (\sqrt{K_1} - \sqrt{K_2})/(\sqrt{K_1} + \sqrt{K_2})$$

**Table 10.1** Typical values of radar parameters for some common materials

Material	$\epsilon$	$\sigma$ mS/m	$V$ m/ns	$\alpha$ dB/m
Air	1	0	0.30	0
Ice	3–4	0.01	0.16	0.01
Fresh water	80	0.05	0.033	0.1
Salt water	80	3000	0.01	1000
Dry sand	3–5	0.01	0.15	0.01
Wet sand	20–30	0.01–1	0.06	0.03–0.3
Shales and clays	5–20	1–1000	0.08	1–100
Silts	5–30	1–100	0.07	1–100
Limestone	4–8	0.5–2.0	0.12	0.4–1
Granite	4–6	0.01–1	0.13	0.01–1
(Dry) salt	5–6	0.01–1	0.13	0.01–1

**Figure 10.1** Approximate rates of change in conductivity with frequency at radar frequencies for some common rock types, after Turner et al. (1993).

$K_1$  and  $K_2$  are the complex permittivities of the host and target material, respectively. The *power reflection coefficient*,  $(RC)^2$ , is also sometimes used but conceals the fact that there is a phase change of  $180^\circ$  on reflection from a boundary at which permittivity increases (and velocity therefore decreases). Reflection amplitudes from most geological materials are determined almost entirely by variations in water content but the conductive term dominates in metallic materials.

Reflection power is also governed by the area of the reflector and the nature of its surface. The strongest responses come from smooth surfaces at which specular reflection occurs, i.e. the angles of incidence and reflection are equal. Rough surfaces scatter energy, reducing reflection amplitudes, and small targets generate only weak reflections. Success with GPR generally requires at least 1% of the incident wave to be reflected (i.e.  $RC > 0.01$ ) and the smallest lateral dimension of the target should be not less than a tenth of its depth.

### 10.1.4 The radar range equation

Predicting, without an on-site test survey, whether useful results are likely to be obtained is probably no more difficult with GPR than with any other geophysical method (which means that it is very difficult) but, because the method is relatively new, the principles are less widely understood. The constraints can be divided into those related to instrument performance and those dependent on site conditions. Performance is dominated by the ratio between the signal power supplied by the transmitter and the minimum level of signal resolvable by the receiver. The signal loss during transmission through the ground is the most important factor but losses in the links between transmitters and receivers and their respective aerials and due to the directional characteristics of the aerials are also significant. These are considered separately because they depend on the frequencies and aerials used, which can be changed in virtually all GPR units. If the sum, in dB, of all the instrumental factors is equal to  $F$ , then the *radar range equation* can be written as:

$$F = -10 \cdot \log_{10}[A\lambda^2 e^{-4\alpha r} / 16\pi^2 r^4]$$

where  $\lambda$  is the radar wavelength,  $\alpha$  is the attenuation constant,  $A$  is a shape factor, with the dimensions of area, that characterizes the target and  $r$  is the *range*, i.e. the theoretical maximum depth at which the target can be detected. The factor  $\log_{10}[\lambda^2/4\pi]$  is often taken out of this expression and included in the system parameters. If this is done, the quantity within the brackets has dimensions and care must be taken in choosing units.

For specular reflection from a smooth plane and a rough surface, respectively, the shape factors are equal to  $\pi r^2 (RC)^2$  and  $\pi \lambda r (RC)^2$  and the range

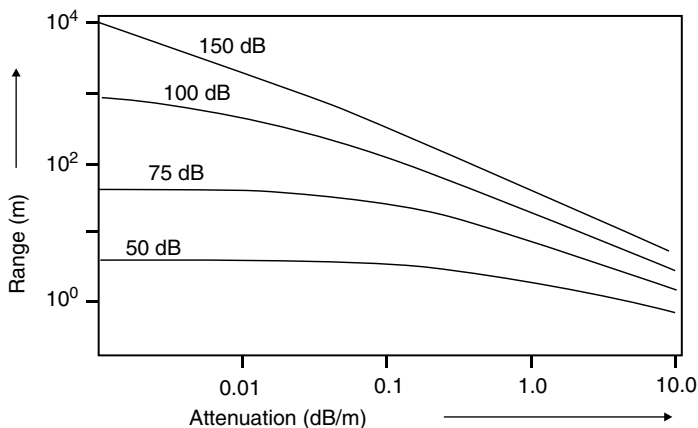


**Figure 10.2** 'Typical' nomogram relating radar range to attenuation constant for various fixed values of system gain and spreading and attenuation losses.

equations reduce to:

$$F = -10 \cdot \log_{10}[(RC)^2 \lambda^2 e^{-4\alpha r} / 16\pi r^2] \quad \text{and}$$

$$F = -10 \cdot \log_{10}[(RC)^2 \lambda^3 e^{-4\alpha r} / 32\pi r^3]$$

Neither equation can be solved directly for the range, which appears in both the exponent and the divisor. Computers can obtain numerical solutions but graphs provide another practical way of dealing with the problem (Figure 10.2). A rough rule that is sometimes applied where conductivity and attenuation are known is that the maximum depth of investigation will be somewhat less than 30 divided by the attenuation or 35 divided by the conductivity.

## 10.2 GPR Surveys

### 10.2.1 Instrumentation

A GPR system consists of a control and recorder unit (CRU) linked to receiver and transmitter units, each of which is in turn linked to an aerial or *antenna* (Figure 10.3). Metal wires are inefficient conductors of alternating current at radar frequencies, and signals to and from the CRU are normally transmitted by optical fibres. These have the great advantage of immunity from electrical interference, but are more delicate than wires and less easily repaired when



**Figure 10.3** PulsEKKO radar unit in field use. The aerials are to the right, the CRU is in the foreground on the left. (Reproduced by permission of Dr C. Bristow.)

damaged. Unfortunately, most commercially available fibre cables are protected by black sleeving which makes them almost invisible when laid out on the ground. Plenty of spares need to be taken into the field.

The settings on the CRU determine the radar frequency, the time period (*window*) during which data are to be recorded and the number of individual traces to be stacked. Typical values of available central frequencies would be 25, 50, 100 and 200 MHz. Recordings might be made over time windows of between 32 and 2048 ns and up to 2048 separate traces might be stacked. Modern CRUs are equivalent to powerful personal computers and many signal processing operations can be carried out in the field. In some systems the CRU functions can be performed by any suitable laptop PC loaded with appropriate software. This has obvious advantages, but few laptops can cope with being rained on.

Receiver and transmitter antennae may be separate or integrated into a single module. Separability is desirable even if the spacing is to be kept constant because its optimum value depends on environment and target depth as well as on frequency and transmitter size. A single housing does, however, have advantages, since it allows continuous profiling with the antenna pack towed along the ground behind a slowly moving vehicle.

Physically, antennae resemble short (and extremely expensive) planks. Their sizes and weights decrease as frequency increases, e.g. from 3.5 m

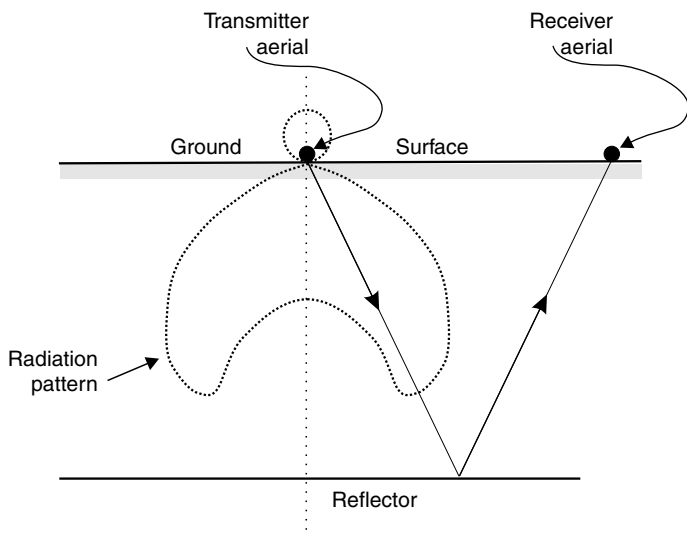


**Figure 10.4** Radiation pattern from a dipole aerial (viewed end on) at the surface of ground of moderate conductivity and relative permittivity. The optimum antenna separation occurs when the ray (slant line) through the radiation peak reaches the target interface mid-way between the antennae.

long and 4 kg weight at 25 MHz to less than half a metre long and 1 kg weight at 200 MHz (**pulseEKKO IV**). Most are simple dipoles, although the triangular dipole or *loaded bow-tie* is also used. The radiation from a dipole in space has cylindrical symmetry and zero intensity along the dipole axis. This simple pattern is modified, sometimes drastically, by the surrounding media. The angle to the surface at which the energy maximum occurs depends on ground permittivity and conductivity (Figure 10.4).

### 10.2.2 Survey types

Most GPR surveys use a constant antenna spacing; this is *common-offset profiling* (Figure 10.5a). The alternative is to vary the distances of the two antennae from a fixed mid-point to obtain *multi-fold common mid-point (CMP) coverage* (Figure 10.5b). CMP surveys have the advantage of allowing velocities to be calculated from the variations in reflection time with offset (see Section 12.1.2) but are very slow, and therefore rare, in GPR work. They are routine in seismic reflection, where cheap detectors known as *geophones* can be laid out in large numbers.

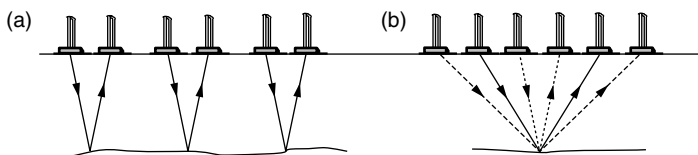


**Figure 10.5** (a) Fixed offset profiling. (b) Common mid-point sounding.

### 10.2.3 Selecting survey parameters

Frequency, antenna spacing, station spacing, record length and sampling frequency can all be varied to some extent in most GPR work. Frequency is the most important single variable, since it constrains the values of many other parameters. If  $d$ , the desired spatial resolution, is measured in metres, an initial estimate of a suitable frequency, in MHz, is given by:

$$f = 150/d\sqrt{\epsilon}$$

A useful rule of thumb is that for the spatial resolution to be equal to 25% of the target depth, the product of depth and frequency should be about 500. Resolution optimization may, and usually does, conflict with penetration requirements and field operators should at least know the extent to which, for the instruments in use, the trade-off between penetration and resolution can be compensated for in processing.

Resolution is also affected by station spacing. Targets that would otherwise be resolvable will not be properly defined if the distance between adjacent stations in a common offset profile is more than one-quarter of the wavelength in the ground, i.e. approximately  $75/f\sqrt{\epsilon}$ .

Dipolar transmitter and receiver antennae are most commonly set out side by side, but end-on and even broadside configurations are also used. Antennae should be oriented parallel to the target strike direction where this is known. Ideally, lines drawn from the transmitter and receiver antennae at the angle of maximum power radiation should meet at the target depth (Figure 10.4). A separation equal to about one-fifth of this depth usually gives good results but smaller spacings are often used for operational convenience.

Radar signals are recorded digitally and must be sampled sufficiently often to ensure that waveforms are fully defined. If there are under two samples in each wave cycle, a form of distortion known as *aliasing* will occur. The maximum frequency present in GPR signals is approximately twice the nominal central frequency, so the sampling rate should be at least four times the central frequency. A safety factor of two is usually added, giving a sampling frequency of 800 MHz for a 100 MHz signal and a sample interval of 1.25 ns.

### 10.2.4 Mobility

GPR systems are now light and portable. Control, transmitter and receiver units weigh only a few kg each, including batteries, and the fibre-optic cables are light (although delicate). Continuous coverage can be obtained if the antennae are mounted on a sled towed behind a vehicle and the CRU is triggered by an odometer to provide readings at uniform intervals. In areas where vehicle access is difficult, impossible or simply inconvenient, the transmitter and receiver units may be secured to frames to which the appropriate antennae are also attached and which can be positioned by a single fieldhand, as in Figure 10.3. For such work the most useful accessory can be a light, all-terrain (i.e. ball rather than wheel) plastic wheelbarrow in which the CRU, batteries and any other necessary items can be transported.

### 10.2.5 Interference in GPR surveys

Even when depth penetration, reflectivity and resolution seem satisfactory, environmental problems can prevent success in a GPR survey. Radio transmitters are potential sources of interference and powerful radio signals can overwhelm (saturate) receiver electronics. Mobile phones are now particularly ubiquitous forms of interference (and there are moves by phone companies to restrict GPR operations because, at their highest frequencies, GPR signals overlap into a band that they wish to use). The presence of metal objects can also be disastrous if these are not the survey targets. Reflections can come from objects away to the side (*sideswipe*) and may be very strong if metallic reflectors are involved. Features actually at the surface can produce strong sideswipe because there is substantial radiation of energy along the ground/air interface if ground conductivity is high.

## 10.3 Data Processing

GPR data are recorded digitally and need extensive processing. The reduction in size and increase in capacity of small computers has made it possible to process in the field, sometimes using the field instruments themselves.

### 10.3.1 Processing techniques

The high repetition rates possible with radar systems allow large numbers of signals to be recorded at each transmitter/receiver set-up and to be stacked to reduce the effects of random noise. The decision as to how many repetitions should be used is one that, inevitably, must be made in the field. A good initial rule of thumb is to use the maximum number of repetitions possible before reading time begins to significantly affect productivity.

After stacking, the data are passed through a low-cut filter to remove noise due to inductive effects and limitations in instrument frequency response, and



a high-cut filter to eliminate noise spikes. The decrease in signal amplitude with time is then reversed by time-variant amplification. *Automatic gain control* (AGC) is used to do this in the field, producing records for quality control, but data are normally stored in unmodified form. Compensation for propagation effects by SEC (*spherical and exponential compensation*) filters based on physical models of the subsurface is usually left to the processing laboratory.

Most of the processing techniques now being used resemble those developed for handling seismic data, and seismic processing software has been used almost unmodified to enhance GPR results. There are differences in emphasis, largely because of the well-controlled nature of the radar pulse and the general use of single-fold rather than CMP coverage, but these need not concern the operator in the field.

### 10.3.2 Display of GPR data

A raw or processed GPR *trace* is recorded as a series of digital values equally spaced in time. It can be displayed either as a simple curve (*wiggle trace*), or by the *variable area* method in which excursions on one side of the zero line are shaded (Figure 10.6). Colour is also sometimes used, either to shade excursions of one polarity in red and of the other in blue, or to shade an elongated rectangle according to signal amplitude and polarity. An ideal *variable area* trace would consist of a flat line punctuated by occasional ‘events’ produced by energy arriving at the surface after reflection from points vertically below the mid-point between receiver and transmitter aerials.

A GPR *section* is created by plotting traces side by side, producing a record on which the horizontal axis represents distance and the vertical scale is in two-way reflection time. With most instruments, a section formed by lightly processed traces is displayed on a screen in ‘real time’ as the



**Figure 10.6** SIR System-3 variable area GPR record showing sigmoidal oblique reflectors in the Lower Greensand. (Reproduced by permission of Dr C. Bristow.)

antennae are moved along traverse, making GPR one of the most interesting geophysical methods to actually use. The resemblance between radar and seismic reflection sections is extremely close (compare Figures 10.6 and 12.8), and it is sometimes only the fact that the two-way time scale is in nanoseconds rather than milliseconds that shows that the section was produced by electromagnetic rather than seismic waves.

The water table and sedimentary layering appear on GPR sections as continuous events (Figure 10.6). Pipes, cables, drums and UXO are usually indicated by curved, upwardly convex *diffraction patterns* created by a form of sideswipe. The root cause of the problem is the vertical plotting of the traces to form the section, which causes all events to be recorded vertically below the surface antennae positions, even when they derive from reflection along a slant path. Small reflectors or sharp angles in continuous reflectors can reflect radar waves at many angles, producing the diffraction patterns (Figure 10.7a). Less dramatic distortions affect the positions of dipping reflectors, since reflection from these also travel along slant paths (Figure 10.7b).

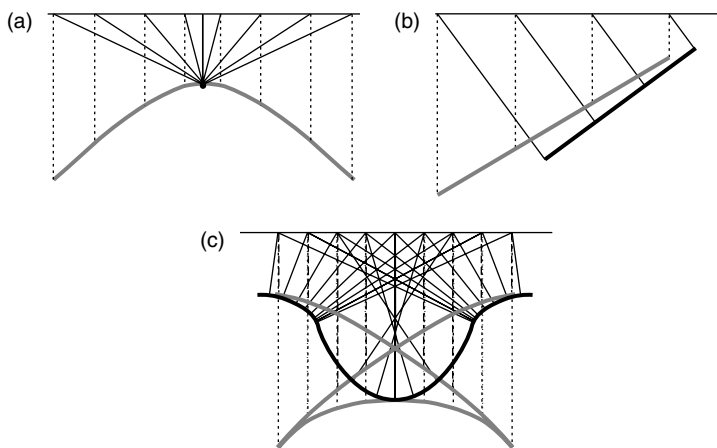


**Figure 10.7** Geometric distortion on radar sections. In each case continuous lines show the actual reflection paths (for near-coincident receiver and transmitter antennae) and the dashed and dotted lines show the plotted traces recording the event. Thick grey lines show the plotted image, assuming no major velocity changes: (a) diffraction pattern caused by a point reflector (b) reduction in dip and lateral displacement of a dipping bed (c) bow-tie from a tight syncline. Examples of some of these features can be identified on the seismic section of Figure 12.8.

Tight, upwardly concave *synclines* can produce three reflections at a single surface point, giving rise to the peculiar features known as *bow-ties* (Figure 10.7c). All these distortions can be corrected by the *migration* programs first developed for use with seismic data, but these must work on numerous traces simultaneously and cannot easily be applied in the field.

Diffraction patterns are hyperbolic curves, provided velocities vary only with depth. Their sources, provided that the traverse line actually passes over them (i.e. sideswipe is not involved) are located at their tops. It can almost be said of radar applications that they are divided into two distinct groups. In the first, layered structures are imaged and mapped. In the second, diffraction patterns are sought that may reveal the presence of limited, usually highly conductive, targets.

## SEISMIC METHODS – GENERAL CONSIDERATIONS

---

Seismic methods are the most effective, and the most expensive, of all the geophysical techniques used to investigate layered media. Features common to reflection and refraction surveys are discussed in this chapter. Chapter 12 is concerned with the special features of small-scale reflection work and Chapter 13 with shallow refraction. Deep reflection surveys, which involve large field crews, bulky equipment and complex data processing, are beyond the scope of this book.

### 11.1 Seismic Waves

A seismic wave is acoustic energy transmitted by vibration of rock particles. Low-energy waves are approximately elastic, leaving the rock mass unchanged by their passage, but close to a seismic source the rock may be shattered and permanently distorted.

#### 11.1.1 Types of elastic wave

When a sound wave travels in air, the molecules oscillate backwards and forwards in the direction of energy transport. This *pressure* or ‘push’ wave thus travels as a series of compressions and rarefactions. The pressure wave in a solid medium has the highest velocity of any of the possible wave motions and is therefore also known as the *primary* wave or simply the *P wave*.

Particles vibrating at right angles to the direction of energy flow (which can only happen in a solid) create an *S (shear, ‘shake’ or, because of its relatively slow velocity, secondary) wave*. The velocity in many consolidated rocks is roughly half the P-wave velocity. It depends slightly on the plane in which the particles vibrate but these differences are not significant in small-scale surveys.

P and S waves are *body waves* and expand within the main rock mass. Other waves, known as *Love waves*, are generated at interfaces, while particles at the Earth’s surface can follow elliptical paths to create *Rayleigh waves*. Love and Rayleigh waves may carry a considerable proportion of the source energy but travel very slowly. In many surveys they are simply lumped together as the *ground roll*.

#### 11.1.2 Seismic velocities

The ‘seismic velocities’ of rocks are the velocities at which wave motions travel through them. They are quite distinct from the continually varying velocities of the individual oscillating rock particles.

Any elastic-wave velocity ( $V$ ) can be expressed as the square root of an elastic modulus divided by the square root of density ( $\rho$ ). For P waves the elongational elasticity,  $j$  is appropriate, for S waves the shear modulus,  $\mu$ . The equations:

$$V_p = \sqrt{j/\rho} \quad V_s = \sqrt{\mu/\rho}$$

suggest that high density rocks should have low seismic velocities, but because elastic constants normally increase rapidly with density, the reverse is usually true. Salt is the only common rock having a high velocity but a low density.

If the density and P and S wave velocities of a rock mass are known, all the elastic constants can be calculated, since they are related by the equations:

$$(V_p/V_s)^2 = 2(1 - \sigma)/(1 - 2\sigma) \quad \sigma = [2 - (V_p/V_s)^2]/2[1 - (V_p/V_s)^2]$$

$$j = q(1 - \sigma)/(1 + \sigma)(1 - 2\sigma) \quad \mu = q/2(1 + \sigma) \quad K = q/3(1 - 2\sigma)$$

where  $\sigma$  is the Poisson ratio,  $q$  is the Young's modulus and  $K$  is the bulk modulus. It follows that  $j = K + 4\mu/3$  and that a P wave always travels faster than an S wave in the same medium. The Poisson ratio is always less than 0.5. At this limit,  $V_p/V_s$  is infinite.

Most seismic surveys provide estimates only of P-wave velocities, which are rather rough guides to rock quality. Figure 11.1 shows ranges of velocity for common rocks and also their *rippabilities*, defined by whether they can be ripped apart by a spike mounted on the back of a bulldozer.

### 11.1.3 Velocities and the time-average equation

Within quite broad limits, the velocity of a mixture of different materials can be obtained by averaging the transit times (the reciprocals of velocities) through the pure constituents, weighted according to the relative amounts present. The principle can be used even when, as in Example 11.1, one of the constituents is a liquid.

---

#### Example 11.1

$$V_p \text{ (quartz)} = 5200 \text{ m s}^{-1}$$

$$V_p \text{ (water)} = 1500 \text{ m s}^{-1}$$

P-wave velocity in a sandstone, 80% quartz, 20% water-filled porosity, is given by:

$$1/V_p = 0.8/5200 + 0.2/1500$$

$$= 0.000287$$

$$\text{i.e. } V_p = 3480 \text{ m s}^{-1}$$


---

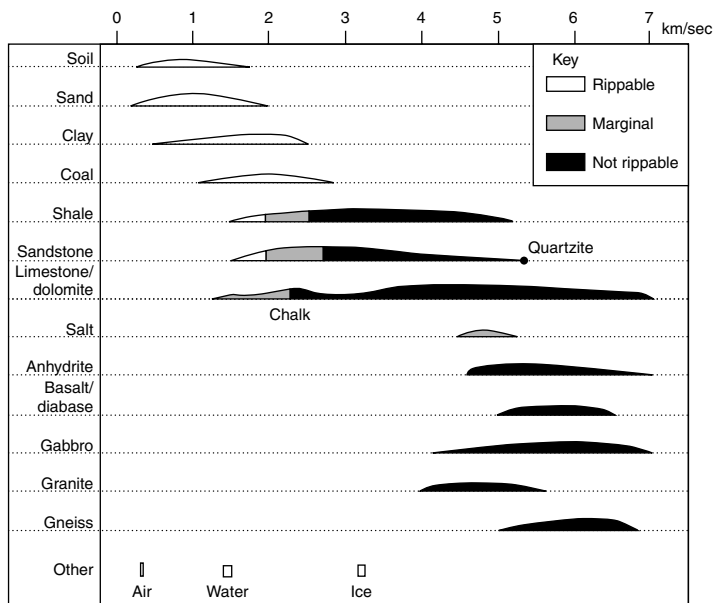


**Figure 11.1** Ranges of P-wave velocities and rippabilities in common rocks. The vertical axis, for each rock type, is intended to show approximately the relative numbers of samples that would show a given velocity.

In dry rocks, the pore spaces are filled with air ( $V = 330 \text{ m s}^{-1}$ ) rather than water. Time averaging cannot be applied quantitatively to gas-filled pores, but dry materials generally have very low P-wave velocities. If they are poorly consolidated and do not respond elastically, they may also strongly absorb S waves. Poorly consolidated water-saturated materials generally have velocities slightly greater than that of water, and the water table is often a prominent seismic interface.

Weathering normally increases porosity, and therefore reduces rock velocities. This fact underlies the rippability ranges shown in Figure 11.1. Few fresh, consolidated rocks have velocities of less than about  $2200 \text{ m s}^{-1}$ , and rocks that are rippable are generally also at least partly weathered.

#### 11.1.4 Ray-path diagrams

A seismic wave is properly described in terms of *wavefronts*, which define the points that the wave has reached at a given instant. However, only a small part of a wavefront is of interest in any geophysical survey, since only

a small part of the energy returns to the surface at points where detectors have been placed. It is convenient to identify the important travel paths by drawing seismic *rays*, to which the laws of geometrical optics can be applied, at right angles to the corresponding wavefronts. Ray-path theory works less well in seismology than in optics because the most useful seismic wavelengths are between 25 and 200 m, and thus comparable with survey dimensions and interface depths. Wave effects can be significant under these circumstances but field interpretation can nonetheless be based on ray-path approximations.

### 11.1.5 Reflection and refraction

When a seismic wave encounters an interface between two different rock types, some of the energy is reflected and the remainder continues on its way at a different angle, i.e. is *refracted*. The law of reflection is very simple; the angle of reflection is equal to the angle of incidence (Figure 11.2a). Refraction is governed by *Snell's law*, which relates the angles of incidence and refraction to the seismic velocities in the two media:

$$\sin i / \sin r = V_1 / V_2$$

If  $V_2$  is greater than  $V_1$ , refraction will be towards the interface. If  $\sin i$  equals  $V_1/V_2$ , the refracted ray will be parallel to the interface and some of its energy will return to the surface as a *head wave* that leaves the interface at the original angle of incidence (Figure 11.2b). This is the basis of the refraction methods discussed in Chapter 12. At greater angles of incidence there can be no refracted ray and all the energy is reflected.

When drawing ray paths for either reflected or critically refracted waves, allowance must be made for refraction at all shallower interfaces. Only the *normal-incidence* ray, which meets all interfaces at right angles, is not refracted.

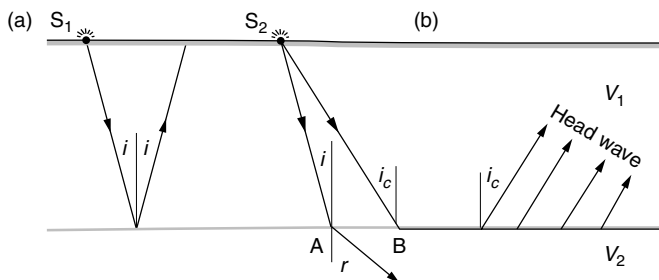


**Figure 11.2** (a) Reflection and (b) refraction. Simple refraction occurs at A, critical refraction at B.

### 11.2 Seismic Sources

The traditional seismic source is a small charge of dynamite. Impact and vibratory sources are now more popular but explosives are still quite commonly used.

#### 11.2.1 Hammers

A 4- or 6-pound sledgehammer provides a versatile source for small-scale surveys. The useful energy produced depends on ground conditions as well as on strength and skill. Hammers can nearly always be used in refraction work on spreads 10 to 20 m long but very seldom where energy has to travel more than 50 m.

The hammer is aimed at a flat plate, the purpose of which is not so much to improve the pulse (hitting the ground directly can sometimes provide more seismic energy) but to stop the hammer abruptly and so provide a definite and repeatable shot instant. Inch-thick aluminium or steel plates used to be favoured, but are now being replaced by thick rubber discs that last longer and are less painfully noisy. The first few hammer blows are often rather ineffective, as the plate needs to 'bed down' in the soil. Too much enthusiasm may later embed it so deeply that it has to be dug out.

#### 11.2.2 Other impact sources

More powerful impact sources must be used in larger surveys. Weights of hundreds of kilograms can be raised by portable hoists or cranes and then dropped (Figure 11.3). The minimum release height is about 4 m, even if a shorter drop would provide ample energy, since rebound of the support when the weight is released creates its own seismic wavetrain. A long drop allows these vibrations to die away before the impact occurs. Tractor-mounted post-hole drivers, common in farming areas, are also convenient sources. The weight drops down a guide and is raised by a pulley system connected to the tractor power take-off.

Relatively small (70 kg) weights falling in evacuated tubes have sometimes been used. The upper surface of the weight is exposed to the air, and effectively several hundred extra kilograms of atmosphere are also dropped. The idea is elegant but the source is difficult to transport because the tube must be strong and therefore heavy and must be mounted on a trailer, together with a motor-driven compressor to pump out the air.

Vibration sources are widely used in large-scale reflection surveys but produce data that need extensive and complex processing.

#### 11.2.3 Explosives

Almost any type of (safe) explosive can be used for seismic work, particularly if the shot holes are shallow and the charges will not be subject to





**Figure 11.3** *Impact source. A half-ton weight being dropped from a portable crane during a survey of the low-velocity layer.*

unusual temperatures or pressures. Cord explosives, used in quarry blasting to introduce delays into firing sequences, are rather safer to handle than normal gelignite and can be fed into shot holes prepared by driving metal rods or crowbars into the ground. Detonators used on their own are excellent sources for shallow reflection surveys where high resolution is needed.

Often, much of the energy delivered by an explosion is wasted in shattering rock near the shot point, and seismic waves are produced much more efficiently by shots fired in a metre or so of water. This effect is so marked that, if shot position is not critical, it can be worth going tens or even hundreds

of metres away from the recording spread in order to put the charge in a river. In dry areas, significant improvements can be obtained by pouring water down shot holes.

Electrical firing is normal when using explosives but with ordinary detonators there is a short delay between the instant at which the filament burns through, which provides a time reference, and the time at which the main charge explodes. *Zero-delay* detonators should be used for seismic work and total delays through the entire system, including the recorders, should be routinely checked using a single detonator buried a few inches away from a geophone.

Explosives involve problems with safety, security and bureaucracy. They must be used in conformity with local regulations, which usually require separate secure and licensed stores for detonators and gelignite. In many countries the work must be supervised by a licensed shot-firer, and police permission is required almost everywhere. Despite these disadvantages, and despite the headaches that are instantly produced if gelignite comes into contact with bare skin, explosives are still used. They represent potential seismic energy in its most portable form and are virtually essential if signals are to be detected at distances of more than 50 m.

A variety of explosive-based methods are available which reduce the risks. Seismic waves can be generated by devices which fire lead slugs into the ground from shotgun-sized cartridges, but the energy supplied is relatively small, and a firearms certificate may be needed, at least in the UK. Another approach is to use blank shotgun cartridges in a small auger which incorporates a firing chamber, combining the shot hole and the shot. Even this seldom provides more energy than a blow from a well-swung hammer, and is less easily repeated.

### 11.2.4 Safety

Large amounts of energy must be supplied to the ground if refractions are to be observed from depths of more than a few metres or reflections from depths of more than a few tens of metres, and such operations are inherently risky. The dangers are greatest with explosives but nor is it safe to stand beneath a half-ton weight dropping from a height of 4 m.

Explosives should only be used by experienced (and properly licensed) personnel. Even this does not necessarily eliminate danger, since experts in quarry blasting often lack experience in the special conditions of seismic surveys. If there is an accident, much of the blame will inevitably fall on the party chief who will, if he is wise, keep his own eye on safety.

The basic security principle is that the shot-firer must be able to see the shot point. Unfortunately, some seismographs have been designed so that the shot is triggered by the instrument operator, who can seldom see anything

and who is in any case preoccupied with checking noise levels. If such an instrument is being used, it must at least be possible for firing to be prevented by someone who is far enough from the shotpoint to be safe but close enough to see what is happening. This can be achieved if, after the shot hole has been charged, the detonator is first connected to one end of an expendable cable 20 or 30 m long. Only when the shotpoint is clear should the other end of this cable be connected to the cable from the firing unit. Firing can then be prevented at any time by pulling the two cables apart.

Unless ‘sweaty’ gelignite is being used (and the sight of oily nitroglycerine oozing out of the packets should be sufficient warning to even the least experienced), modern explosives are reasonably insensitive to both heat and shock. Detonators are the commonest causes of accidents. Although their explosive power is small, they have caused loss of fingers and even hands. If fired on their own as low energy sources, they should always be placed in well-tamped holes, since damage or serious injury can be caused by fragments of the metal casing.

It is possible (although not common) for a detonator to be triggered by currents induced by power lines or radio transmissions but this is less likely if the leads are twisted together. Triggering by static electricity is prevented if the circuit is closed. The shorted, twisted, ends of detonator leads should be parted only when the time comes to make the connection to the firing cable, which should itself be shorted at the far end. Explosives should not be handled at all when thunderstorms are about.

Explosive charges need to be matched to the holes available. Large charges may be used in deep holes with little obvious effect at the surface, but a hole less than 2 m deep will often blow out, scattering debris over a wide area. Only experience will allow safe distances to be estimated, and even experienced users can make mistakes; safety helmets should be worn and physical shelter such as a wall, a truck or a large tree should be available. Heavy blasting mats can reduce blow-outs, but their useful lives tend to be short and it is unwise to rely on them alone.

A point where a shot has been fired but no crater has formed should be regarded with suspicion. The concealed cavity may later collapse under the weight of a person, animal or vehicle, leading to interesting litigation.

### 11.2.5 Time breaks

In any seismic survey, the time at which the seismic wave is initiated must be known. In some instruments this appears on the record as a break in one of the traces (the *shot break* or *time break*). On most modern instruments it actually defines the start of the record.

Time-break pulses may be produced in many different ways. A geophone may be placed close to the source, although this is very hard on the geophone.

Explosive sources are usually fired electrically, and the cessation of current flow in the detonator circuit can provide the required signal. Alternatively, a wire can be looped around the main explosive charge, to be broken at the shot instant. This technique can be used on the rare occasions when charges are fired using lit fuses.

Hammer surveys usually rely on making rather than breaking circuits. One method is to connect the hammer head to one side of the trigger circuit and the plate (assuming it is metal, not rubber) to the other. Although this sounds simple and foolproof, in practice the repeated shocks suffered by the various connections are too severe for long-term reliability. In any case, the plates themselves have rather short lives, after which new connections have to be made. It is more practical to mount a relay on the back of the hammer handle, just behind the head, that closes momentarily when the hammer hits the plate (Figure 11.4). It will close late, or not at all, if the hammer is used the wrong way round. Solid-state switches sold by some seismograph manufacturers give more repeatable results but are expensive and rather easily damaged.

The cable linking the trigger switch on a hammer to the recorder is always vulnerable, tending to snake across the plate just before impact. If it is cut, the culprit is traditionally required both to repair the damage and ease the thirst of all the witnesses!

Where the source is a heavy weight dropped from a considerable height, a relay switch can be attached to its top surface but may not trigger if the drop is not absolutely straight. A crude but more reliable home-made device which can be attached to any dropping weight is shown in Figure 11.5.

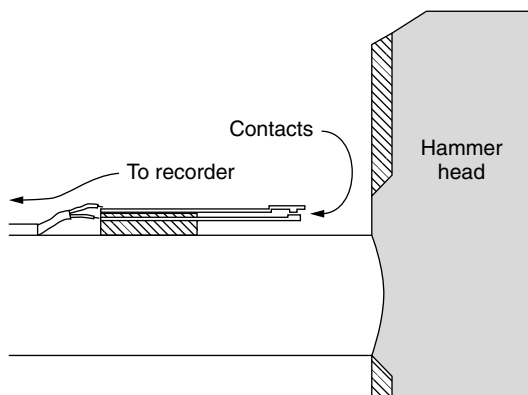


**Figure 11.4** 'Post-office relay' impact switch on the back of a sledgehammer handle.

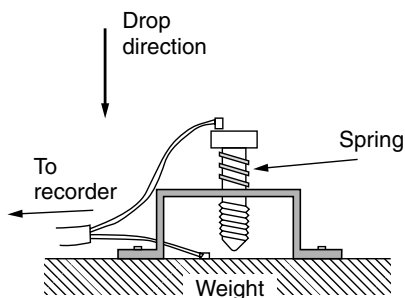


**Figure 11.5** Weight-drop contact switch. On impact the inertia of the bolt compresses the spring and contact is made with the upper surface of the weight.

Time-break pulses may be strong enough to produce interference on other channels (*cross-talk*; Section 11.3.5). Trigger cables and circuits should therefore be kept well away from data lines.

### 11.3 Detection of Seismic Waves

Land seismic detectors are known as *geophones*, marine detectors as *hydrophones*. Both convert mechanical energy into electrical signals. Geophones are usually positioned by pushing a spike screwed to the casing firmly into the ground but it may be necessary to unscrew the spike and use some form of adhesive pad or putty when working on bare rock.

#### 11.3.1 Geophones

A geophone consists of a coil wound on a high-permeability magnetic core and suspended by leaf springs in the field of a permanent magnet (Figure 11.6). If the coil moves relative to the magnet, voltages are induced and current will flow in any external circuit. The current is proportional to the velocity of the coil through the magnetic field, so that ground movements are recorded, not ground displacements. In most cases the coil is mounted so that it is free to vibrate vertically, since this gives the maximum sensitivity to P waves rising steeply from subsurface interfaces, i.e. to reflected and refracted (but not direct) P waves. P-wave geophones that have been normally connected give negative first-arrival pulses (*breaks*) for refractions and reflections, but may break either way for direct waves.

In reflection work using large offsets, or in refraction work where the velocity contrasts between overburden and deeper refractors are small, the rising wavefronts make relatively large angles with the ground surface and the discrimination by the geophones between S waves and P waves will be less good.

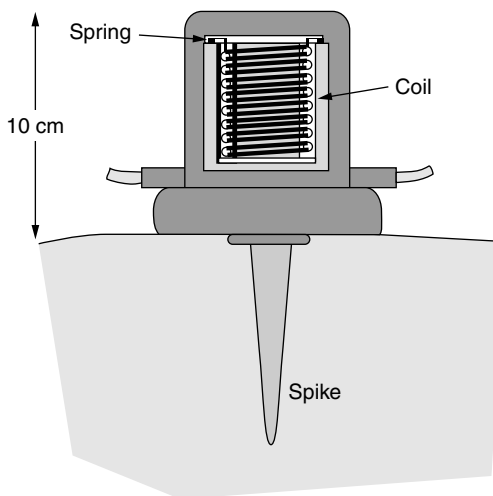


**Figure 11.6** *Moving coil geophone.*

Geophone coils have resistances of the order of 400 ohms and damping is largely determined by the impedance of the circuits to which they are linked. The relative motion between coil and casing is also influenced by the natural vibration frequency of the suspended system. At frequencies above resonance, the response approximately replicates the ground motion, but signals below the resonant frequency are heavily attenuated. Standard geophones usually resonate at or below 10 Hz, i.e. well below the frequencies useful in small-scale surveys. Response curves for a typical 10 Hz phone are shown in Figure 11.7.

Geophones are remarkably rugged, which is just as well considering the ways in which they are often treated. Even so, their useful lives will be reduced if they are dumped unceremoniously from trucks into tangled heaps on the ground. Frames can be bought or made to which they can be clipped for carrying (Figure 11.8) and these can be good investments, but only if actually used.

### 11.3.2 Detection of S waves

Although S waves are regarded as noise in most seismic work, there are occasions when S-wave information is specifically sought. For example, both S- and P-wave velocities are required to determine elastic properties (see Section 11.1.2).

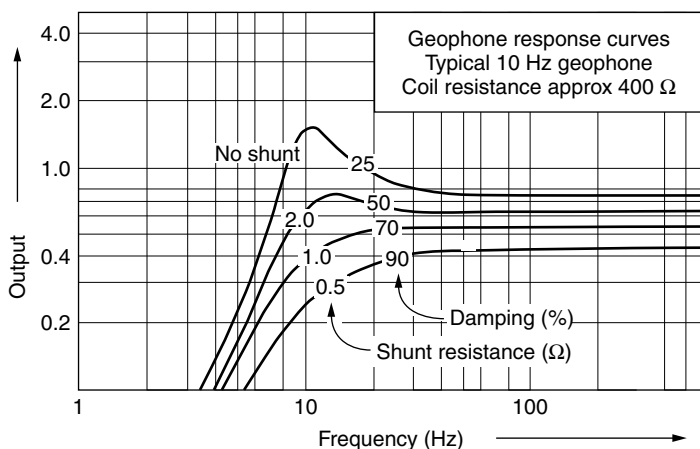


**Figure 11.7** Frequency response of a typical moving-coil geophone. The degree of damping depends on the value of the shunt resistance connected in parallel with the geophone, and also on the input resistance of the recorder. 'No shunt' corresponds to infinite shunt resistance.



**Figure 11.8** Geophone carrying frame in use, Papua New Guinea.

‘S-wave’ geophones have coils that move horizontally rather than vertically, the assumption being that wavefronts of interest will be rising more or less vertically and the S-wave vibrations will therefore be in the plane of the ground surface. Because direct waves travel parallel to the ground surface, S-wave geophones are more sensitive to direct P waves than direct S waves, just as P-wave geophones are sensitive to vertically polarized direct S waves.

### 11.3.3 Detection in swamps and water

Normal geophones are rainproof rather than waterproof, and are connected to cables by open crocodile clips. Geophones are also available that are completely enclosed and sealed into waterproof cases, for use in swamps. These do not have external spikes but are shaped so that they can be easily pushed into mud.

Motion-sensitive instruments cannot be used in water. Piezo-electric hydrophones respond to variations in pressure rather than motion and are equally sensitive in all directions. Discrimination between P and S waves is not required since S waves cannot travel through fluids.

### 11.3.4 Noise

Any vibration that is not part of the signal is *noise*. Noise is inevitable and *coherent* noise is generated by the shot itself. S waves, Love and Rayleigh waves and reflections from surface irregularities are all forms of coherent noise. In shallow refraction work these slow, and therefore late-arriving, waves usually prevent the use of any event other than the first arrival of energy.

Noise which is not generated by the shot is termed *random*. Movements of traffic, animals and people all generate random noise and can, to varying extents, be controlled. It should at least be possible to prevent the survey team contributing, by giving warning using a whistle or hooter.

Random noise is also produced by vegetation moving in the wind and disturbing the ground. The effects can be reduced by siting geophones away from trees and bushes, and sometimes by clearing away smaller plants. Significant improvements can often be achieved by moving particularly noisy geophones a few inches. Placement is also important. It may not be easy to push a spike fully home in hard ground but a geophone an inch above the ground vibrates in the wind.

### 11.3.5 Seismic cables

Seismic signals are carried from geophones to recorders as varying electric currents, in cables which must contain twice as many individual wires as there are geophones. Wires are necessarily packed very closely and not only can external current carriers such as power and telephone cables induce currents,



but a very strong signal in one wire can be passed inductively to all the others. *Cross-talk* can be particularly severe from the strong signals produced by geophones close to the shot point, and it may even be necessary to disconnect these to obtain good records on other channels.

The amount of cross-talk generally increases with the age of the cable, probably because of a gradual build-up of moisture inside the outer insulating cover. Eventually the cable has to be discarded.

Cables and plugs are the most vulnerable parts of a seismic system and are most at risk where they join. It is worthwhile being very careful. Resoldering wires to a plug with 24 or more connections is neither easy nor interesting.

Most cables are double-ended, allowing either end to be connected to the receiver. If a wire is broken, only the connection to one end will be affected and the 'dead' channel may revive if the cable is reversed. All too often, however, other dead channels are discovered when this is done.

## 11.4 Recording Seismic Signals

Instruments that record seismic signals are known as *seismographs*. They range from timers which record only single events to complex units which digitize, filter and store signals from a number of detectors simultaneously.

### 11.4.1 Single-channel seismographs

Most single-channel seismographs have graphic displays, although rudimentary seismic 'timers' which simply displayed the arrival time of the first significant energy pulse numerically were once popular. On a visual display, the time range is switch or key-pad selected and the left-hand edge of the screen defines the shot or impact instant. Hard copy is not usually obtainable and times are measured directly. In some models a cursor can be moved across the screen while the time corresponding to its position is displayed. Noise levels can be monitored by observing the trace in the absence of a source pulse.

Modern single-channel instruments use enhancement principles. A digital version of the signal is stored in solid-state memory, as well as being displayed on the screen. A second signal can either replace this or be added to it. Any number  $n$  of signals can be summed (*stacked*) in this way for a theoretical  $\sqrt{n}$  improvement in signal/noise ratio.

Seismographs that allow signals to be displayed and summed are obviously superior to mere timers, and can be used to study events other than first arrivals. However, they are generally only useful in shallow refraction work since it is difficult to distinguish between direct waves, refractions and reflections on a single trace. Hammer sources are universal, since it would be expensive and inefficient to use an explosive charge to obtain such a small amount of data.

### 11.4.2 Multi-channel seismographs

Seismographs with 12 or 24 channels are generally used in shallow surveys, whereas a minimum of 48 channels is now the norm in deep reflection work. With multiple channels, both refraction and reflection work can be done and explosives can reasonably be used since the cost per shot is less important when each shot produces many traces. Enhancement is used very widely and most instruments now provide graphic displays, optional hard copy and digital recording.

The enhancement seismographs now in use (Figure 11.9) are very sophisticated and versatile instruments. Display formats can be varied and individual traces can be selected for enhancement, replacement or preservation. Traces can be amplified after as well as before storage in memory, and time offsets can be used to display events that occur after long delay times. Digital recording has virtually eliminated the need for amplification before recording, because of the inherently very large *dynamic range* associated with storage of data as fixed precision numbers plus exponents (Example 11.2). Filters can also be applied, to reduce both high frequency random noise and also the long-period noise, of uncertain origin, that sometimes drives the traces from one or two geophones across the display, obscuring other traces.



**Figure 11.9** Enhancement seismographs. The instrument on the right is the now obsolete knob and switch controlled Geometrics 1210F. The instrument on the left is one of its successors, the Smartseis, which is entirely menu-driven. Note the hard-copy record just emerging from the Smartseis, and the much greater size of the display 'window'.

**Example 11.2**

*Dynamic range* is concerned with the range over which data can be recorded with roughly uniform *percentage* accuracies. When seismic amplitudes were recorded in ‘analogue’ form on magnetic tape, in which magnetization was proportional to signal strength, the dynamic range was limited at low amplitudes by tape noise and at high amplitudes by magnetic saturation. Automatic gain control (AGC) was therefore applied before recording, and inevitably distorted the signals.

In digital systems, data are recorded as numerical values plus *exponents*, which are the powers of some other number by which the numerical value must be multiplied. Thus, the values

$$46\,789 \quad \text{and} \quad 0.0000046789$$

can be written in the familiar engineering notation, which uses powers of 10, as:

$$4.6789\text{E} + 4 \quad \text{and} \quad 4.6789\text{E} - 6$$

The two quantities are thus recorded to the same percentage accuracy. In digital systems, data are usually recorded in binary formats and the exponent uses powers of 2. It is commonly allowed to range between  $-128$  and  $+127$ , which is roughly equivalent to a range from  $10^{-38}$  to  $10^{+38}$ .

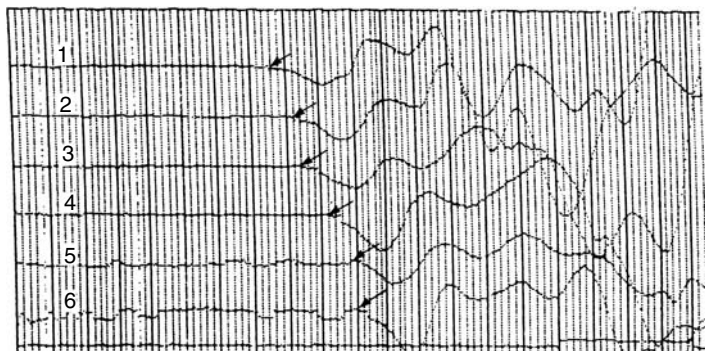


**Figure 11.10** Six-channel refraction record showing refraction ‘picks’. Noise prior to these picks is increasingly obvious as amplification is increased to record signals from the further geophones.

The refraction survey example in Figure 11.10 shows the signals recorded by six geophones at points successively further from the source, with the traces from distant geophones amplified more to compensate for attenuation. Inevitably, amplifying the signal also amplifies the noise.

In the field, arrival times can be estimated from the screen but this is never easy and seldom convenient. On the other hand, hard copies produced directly from the instrument are often of rather poor quality. This is especially true of dot-matrix outputs, because the matrix size causes irregularities in what should be smooth curves (Figure 11.10). Where these are the built-in printers, and assuming the instrument also has the capacity to store data digitally, it is worthwhile having a separate lap-top computer coupled to a reasonable printer at the field base. It would be foolhardy, however, not to produce, and preserve, the field hard-copy.

Powerful microcomputers are incorporated into most modern instruments, with high-capacity hard drives for data storage. Bewildering numbers of acquisition and processing options are available via menu-driven software. So versatile are these instruments that it is sometimes difficult, or at least time consuming, to persuade them to carry out routine, straightforward survey work.



# 12

## SEISMIC REFLECTION

---

The seismic reflection method absorbs more than 90% of the money spent world-wide on applied geophysics. Most surveys are aimed at defining oil-bearing structures at depths of thousands of metres using hundreds or even thousands of detectors. However, some reflection work is done by small field crews probing to depths of, at most, a few hundred metres. The instruments used in these surveys were originally very simple but may now have as much in-built processing power as the massive processing laboratories of 20 years ago. Field operators need to have some understanding of the theory behind the options available.

### 12.1 Reflection Theory

Ray-path diagrams, as used in Chapter 11, provide useful insights into the timing of reflection events but give no indication of amplitudes.

#### 12.1.1 Reflection coefficients and acoustic impedances

The *acoustic impedance* of a rock, usually denoted by  $I$ , is equal to its density multiplied by the seismic P-wave velocity. If a seismic wavefront strikes a planar interface between two rock layers with impedances  $I_1$  and  $I_2$  at right angles (*normal incidence*), the amplitude of the reflected wave, as a percentage of the amplitude of the incident wave (the *reflection coefficient*,  $RC$ ) is given by:

$$RC = (I_2 - I_1)/(I_2 + I_1)$$

If  $I_1$  is greater than  $I_2$ , the coefficient is negative and the wave is reflected with phase reversed, i.e. a negative pulse will be returned where a positive pulse was transmitted and vice versa.

The amount of energy reflected first decreases and then increases as the angle of incidence increases. If the velocity is greater in the second medium than in the first, there is ultimately total reflection and no transmitted wave (Section 11.1.5). However, most small-scale surveys use waves reflected at nearly normal incidence.

#### 12.1.2 Normal moveout

The true normal-incidence ray cannot be used in survey work, since a detector at the shot point would probably be damaged and would certainly be set into such violent oscillation that the whole record would be unusable. Geophones

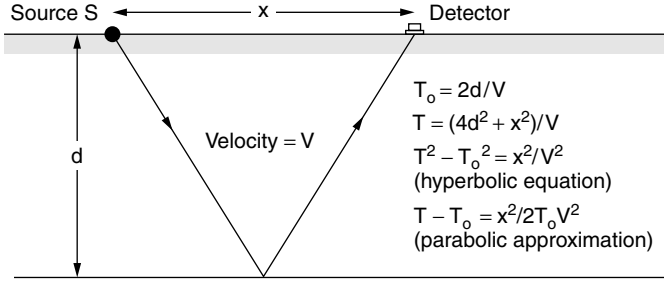


**Figure 12.1** Derivation of the normal moveout equation for a horizontal reflector.  $T_0$  is the normal incidence time.

are therefore offset from sources and geometric corrections must be made to travel times.

Figure 12.1 shows reflection from a horizontal interface, depth  $d$ , to a geophone at a distance  $x$  from the source. The exact *hyperbolic* equation linking the travel time  $T$  and the normal incidence time  $T_0$  is established by application of the Pythagoras theorem. For small offsets, the exact equation can be replaced by the *parabolic* approximation, which gives the *normal moveout* (NMO),  $T - T_0$ , directly as a function of velocity, reflection time and offset.

$$T - T_0 = x^2/2V^2T_0$$

Since  $V$  usually increases with depth and  $T_0$  always does, NMO decreases (i.e. NMO curves flatten) with depth.

Curved alignments of reflection events can be seen on many multi-channel records (Figure 12.2). Curvature is the most reliable way of distinguishing shallow reflections from refractions.

### 12.1.3 Dix velocity

If there are several different layers above a reflector, the NMO equation will give the ‘root-mean-square’ (*RMS*) velocity defined as:

$$V_{RMS}^2 = (V_1^2 t_1 + V_2^2 t_2 \cdots + \cdots V_n^2 t_n)/\mathbf{T}_n$$

where  $t_n$  is the transit time through the  $n$ th layer, velocity  $V_n$ , and  $\mathbf{T}_n$  is the total transit time to the base of the  $n$ th layer. Interval velocities can be calculated from RMS velocities using the *Dix formula*:

$$V_{DIX}^2 = (V_{n-1}^2 \mathbf{T}_{n-1} - V_n^2 \mathbf{T}_n)/(\mathbf{T}_{n-1} - \mathbf{T}_n)$$

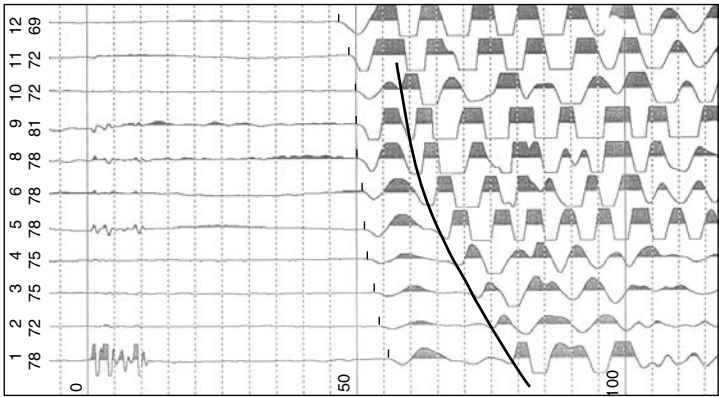


**Figure 12.2** Enhancement seismograph record showing curved alignment of reflections (thick line). The earlier events were produced by refractions. Note that on Channels 11 and 12 the strong refracted wave completely overwrites the reflection. The variable area presentation used is popular for reflection work since it emphasizes trace-to-trace correlations, although some information is lost where traces overlap.

The subscripts  $n - 1$  and  $n$  denote, respectively, the top and bottom of the  $n$ th layer. RMS velocities are normally slightly higher than true average velocities, since squaring the high velocities increases their influence on the average. Significant errors can arise if RMS velocities are used directly to make depth estimates but these are generally less than the errors introduced by the use of the NMO equation to estimate velocity using reflections from interfaces that may well not be horizontal. Dix conversion may not help very much in these cases.

#### 12.1.4 Effect of dip

If the source is placed at the centre of the geophone spread, the curves obtained over horizontal interfaces will be symmetrical about the source point. If, however, the reflector has a uniform dip  $\alpha$ , the reduction in travel path on the updip side of the shot compensates to some extent for the offset, and some travel times will be less than the normal-incidence time (Figure 12.3). The minimum time  $2d \cdot \cos(\alpha)/V$  is recorded at a distance  $2d \cdot \sin(\alpha)$  from the shot, on the updip side. The reflected ray rises vertically to this point, about which the moveout curve is symmetrical. Dip effects in shallow reflection surveys are detectable only for very large dips or very long spreads.



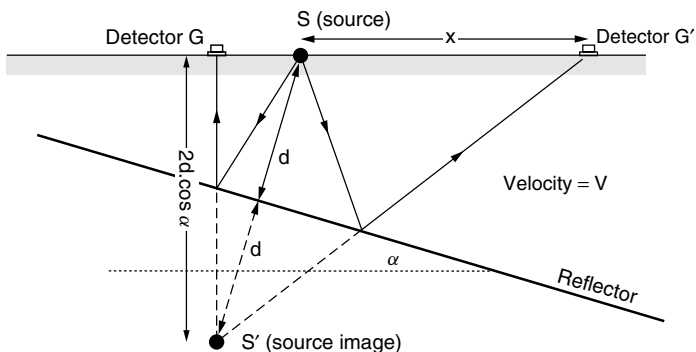


**Figure 12.3** Effect of dip on a single-fold record. Rays are reflected from the dipping interface as if derived from the image point  $S'$  at depth  $2d \cdot \cos \alpha$  below the surface, where  $d$  is the perpendicular distance from the shotpoint to the interface. The normal incidence travel time is  $2d/V$  but the shortest travel time is for the ray which is vertical after reflection. An identical moveout hyperbola would be produced by a shot at point  $G$  and a horizontal interface at depth  $d \cdot \cos \alpha$ .

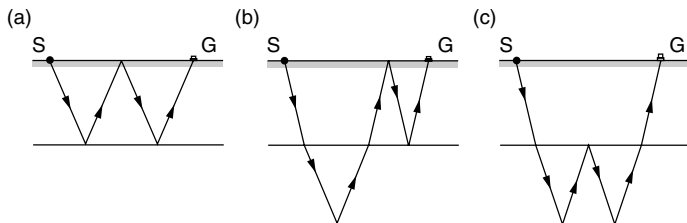


**Figure 12.4** Paths for multiple reflections. (a) Simple multiple. (b) Peg-leg. (c) Intra-formational multiple.

### 12.1.5 Multiple reflections

A wave reflected upwards with high amplitude from a subsurface interface can be reflected down again from the ground surface and then back from the same interface. This is a simple *multiple*. Two strong reflectors can generate *peg-leg* and *intraformational* multiples (Figure 12.4).

Multiples are difficult to identify with certainty on single traces. They can sometimes be recognized on multi-channel records because they have moveouts appropriate to shallow reflectors and simple time relationships with their primaries.

## 12.2 Reflection Surveys

Reflected waves are never first arrivals, so clear-cut reflection events are seldom seen. Oil-industry techniques for improving signal-to-noise ratios can be used for shallow work and simple versions of the programs used are incorporated in the software supplied with the latest generation of 12- and 24-channel seismographs.

### 12.2.1 Spread lengths

The distance from the source to the nearest geophone in a shallow reflection survey is usually dictated by the strength of the source (and the need to protect the geophone) and may be as little as 2 m when a hammer is being used. Even with explosives or heavy weight drops, minimum offsets of more than about 10 m are unusual when observing shallow reflections.

A reflection spread can be much shorter than a refraction spread used to probe to similar depths, but with powerful sources and multi-channel recording, the furthest geophone may be more than 100 m from the source. The optimum spread length can be determined only by experiment, since the most important factors are the arrival times of the noise trains associated with the direct wave and any strong refracted waves. Field work should begin with tests specifically designed to examine these arrivals, generally by using elongated spreads.

### 12.2.2 Arrays

Ideally, reflected energy should arrive after the near-surface waves (ground-roll and refractions) have passed but this may not be possible if the depth of investigation is very small. In such cases, geophones may be connected in arrays to each recording channel. Reflected waves, which travel almost vertically, will reach all the geophones in an array almost simultaneously but the direct waves will arrive at different times and produce signals that can interfere destructively.

The efficiency with which a wave is attenuated by an array is defined by its *relative effect* (RE) compared to the effect of the same number of geophones placed together at the array centre. The variation of the RE with *apparent wavelength* (which for the direct wave is equal to the true wavelength), for a linear array of five geophones equally spaced on a line directed towards the shot point, is shown in Figure 12.5. Non-linear arrays produce more complex curves.

Simple arrays are preferred in the field, since mistakes are easily made in setting out complicated ones. The range of frequencies over which attenuation of the direct wave occurs is proportional to array length and it may be necessary to overlap the geophones in adjacent arrays. It would be unusual in a shallow survey to use more than five geophones per array.

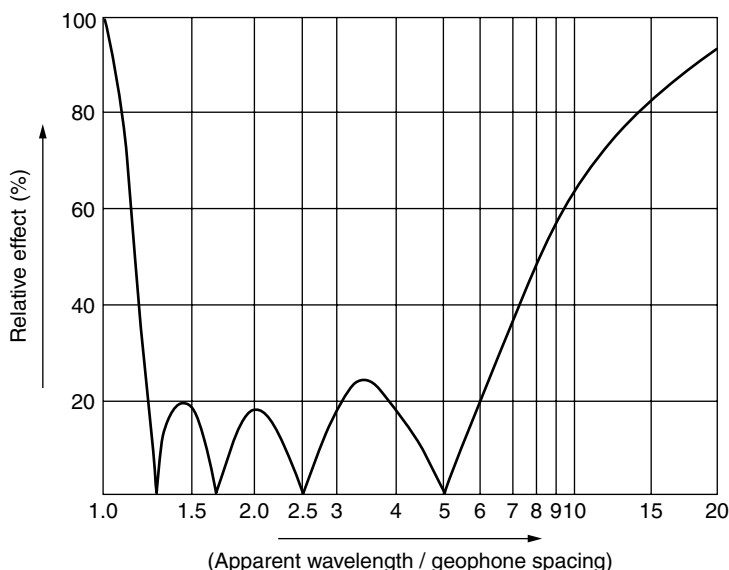


**Figure 12.5** Relative effect (RE) of an array of five equispaced in-line geophones. The 100% level would be attained with zero spacing between the geophones. The apparent wavelength is equal to the actual wavelength divided by the sine of the angle between the wavefront and the ground surface, and is infinite for a wave rising vertically and equal to the true wavelength for the direct wave. Attenuation is concentrated between values of apparent wavelength divided by geophone spacing of about 1.2 and 7. With 2 m spacing, a  $500 \text{ m}\cdot\text{s}^{-1}$  wave would be attenuated at frequencies of between about 35 and 200 Hz.

### 12.2.3 Shot arrays

Seismic cables for use with only 12 or 24 channels are not designed with arrays in mind, and non-standard connectors may have to be fabricated to link the geophones to each other and to the cable. It may be easier to use arrays of shots instead.

A shot array using explosives usually involves simultaneous detonation of charges laid out in a pattern resembling that of a conventional geophone array. If an impact source is used with an enhancement instrument, the same effect can be obtained by adding together results obtained with the impact at different points. This is the simplest way of reducing the effects of surface waves when using a hammer.

### 12.2.4 Common mid-point shooting

Improving signal-to-noise ratios by adding together several traces (*stacking*) is fundamental to deep reflection surveys. In shallow surveys this technique is normally used only to stack (enhance) results obtained with identical source and detector positions. If, however, the data are recorded digitally, NMO corrections can be made (although not in the field) to traces produced with different source–receiver combinations. The technique normally used is to collect together a number of traces that have the same mid-point between source and receiver (*common midpoint* or CMP traces), apply the corrections and then stack.

The number of traces gathered together in a CMP stack defines the *fold* of coverage. Three traces forming a single synthetic zero-offset trace constitute a 3-fold stack and are said to provide *300% cover*. The maximum fold obtainable, unless the shot point and geophone line are moved together by fractions of a geophone interval, is equal to half the number of data channels.

Figure 12.6 shows the successive geophone and source positions when a six-channel instrument is used to obtain 300% cover. Special cables and switching circuits are available for use in deep reflection surveys, but CMP fieldwork with the instruments used for shallow surveys is very slow and laborious. The need to combine traces from several different shots makes it difficult to do CMP processing in the field.

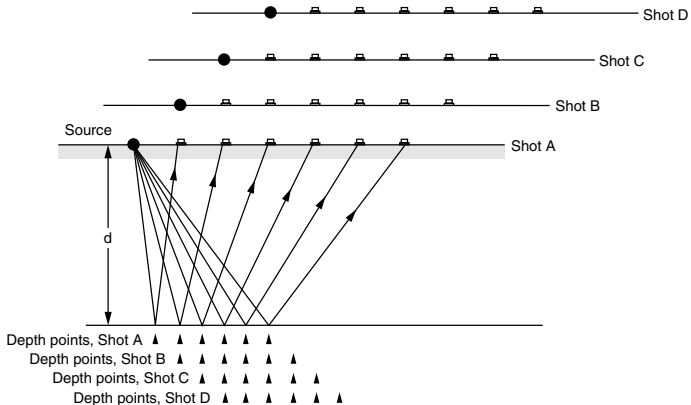


**Figure 12.6** CMP schematic, for 3-fold cover with a 6-channel system. Shot points A, B, C and D are progressively one geophone group interval further to the right. Note that the distance between reflection points (depth points) on the interface is only half that between geophone groups on the surface. Shots A and D have no depth points in common.

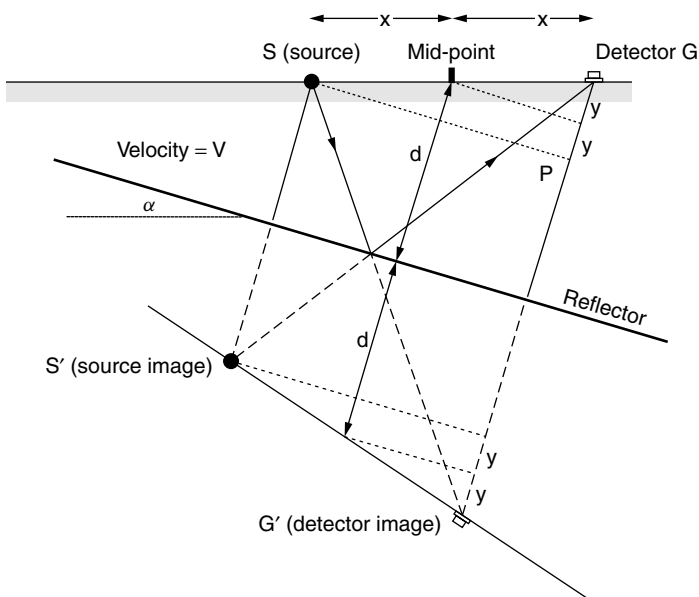


**Figure 12.7** Effect of dip in CMP shooting. In contrast to single-fold shooting (Figure 12.3), the shot points as well as the geophone locations are different for the different traces. Shot points and detector locations are equivalent and the 'depth point' on the reflector moves up dip as the offset increases. The moveout equation is most easily derived by noting that the path from source to detector is equal in length to the path  $SG'$  from the source to the detector 'image point', and that the geometric relationships between similar triangles imply the equality of all the lengths marked 'y'. The Pythagoras relationship can be applied to the triangle  $SG'P$ , and the times can be obtained by dividing the distances by  $V$ . Thus,  $T_0 = 2d/V$  and  $T = SG'/V$ .

The geometry of a CMP shoot differs from that for single-fold coverage, and the effect of dip is therefore different (Figure 12.7). If the interface dips at an angle  $\alpha$ , the velocity deduced from a CMP stack is equal to  $V/\cos \alpha$  and the 'depth' is equal to the length of the normal incidence ray from the common mid-point to the interface. In contrast to the single-fold gather of Section 12.1.4, the minimum time is associated with the normal incidence ray. The aim of stacking is to produce a noise-reduced seismic trace that approximates to the normal incidence trace, i.e. to the trace that would have been produced had the source and detector been coincident.

The initials CMP replaced an earlier acronym, CDP (*common depth point*) used for the same method. Referring to depth points (reflection points) as ‘common’ implies that all the reflections in a gather have come from the same point on the subsurface interface, which is true only for horizontal interfaces.

### 12.2.5 Depth conversion

Reflection events are recorded not in depth but in *two-way time* (TWT). Velocities are needed to convert times into depths, but the Dix velocities (Section 12.1.3) obtained from NMO curves may be 10–20% in error, even

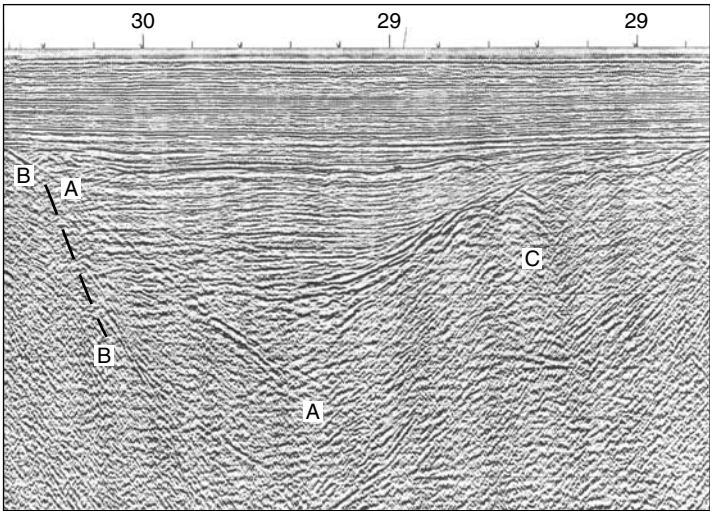


**Figure 12.8** Geometric distortion on seismic sections. The image is of a small graben structure beneath an unconformity. The position of the true fault plane *BB* (indicated by the dashed line) can be estimated from the positions of the terminations of the sub-horizontal reflectors representing the sediment fill within the graben (although care must be exercised because many of the deeper sub-horizontal events are multiples). The event *AA* is the seismic image of *BB*. It is displaced because the techniques used to display the data assume that reflections are generated from points vertically beneath the surface points, whereas they are actually generated by normal-incidence rays that are inclined to the vertical if reflected from dipping interfaces (Section 10.3.2). The reflections from the fault and the opposite side of the graben cross over near the lower symbol ‘A’, forming a ‘bow-tie’. Convex-upward reflections near point *C* are diffraction patterns generated by faulting.

for horizontal reflectors. Interpretations should be calibrated against borehole data wherever possible, and field crews should always be on the lookout for opportunities to measure vertical velocities directly.

### 12.2.6 Geometric distortion

Seismic reflection data are normally presented as sections prepared by playing out, next to each other and vertically down the sheet of paper, the traces from adjacent CMP gathers. Such sections are subject to geometric distortion. Artefacts such as displaced reflectors, diffraction patterns and 'bow-ties', described in Section 10.3.2 as affecting radar sections, also appear on seismic imagery, as is shown in Figure 12.8.

# 13

## SEISMIC REFRACTION

---

Refraction surveys are widely used to study the water table and, for engineering purposes, the poorly consolidated layers near the ground surface, and also in determining near-surface corrections for deep reflection traces. Travel times are usually only a few tens of milliseconds and there is little separation between arrivals of different types of wave or of waves that have travelled by different paths. Only the first arrivals, which are always of a P wave, can be 'picked' with any confidence.

### 13.1 Refraction Surveys

Ideally the interfaces studied in a small refraction survey should be shallow, roughly planar and dip at less than  $15^\circ$ . Velocity must increase with depth at each interface. The first arrivals at the surface will then come from successively deeper interfaces as distance from the shot point increases.

#### 13.1.1 The principal refractors

P-wave velocities for common rocks were shown in Figure 11.1. In shallow refraction work it is often sufficient to consider the ground in terms of dry overburden, wet overburden and weathered and fresh bedrock. It is very difficult to deal with more than three interfaces.

The P-wave velocity of dry overburden is sometimes as low as  $350 \text{ m s}^{-1}$ , the velocity of sound in air, and is seldom more than  $800 \text{ m s}^{-1}$ . There is usually a slow increase with depth, which is almost impossible to measure, followed by an abrupt increase to  $1500\text{--}1800 \text{ m s}^{-1}$  at the water table.

Fresh bedrock generally has a P-wave velocity of more than  $2500 \text{ m s}^{-1}$  but is likely to be overlain by a transitional weathered layer where the velocity, which may initially be less than  $2000 \text{ m s}^{-1}$ , usually increases steadily with depth and the accompanying reduction in weathering.

#### 13.1.2 Critical refraction and the head wave

Snell's law (Section 11.1.5) implies that if, in Figure 11.2,  $V_2$  is greater than  $V_1$  and if  $\sin i = V_1/V_2$ , the refracted ray will travel parallel to the interface at velocity  $V_2$ . This is *critical refraction*.

After critical refraction, some energy will return to the ground surface as a *head wave* represented by rays which leave the interface at the critical angle. The head wave travels through the upper layer at velocity  $V_1$  but, because of its inclination, appears to move across the ground at the  $V_2$  velocity with



which the wavefront expands below the interface. It will therefore eventually overtake the direct wave, despite the longer travel path. The *cross-over* or *critical* distance for which the travel times of the direct and refracted waves are equal is:

$$x_c = 2d\sqrt{[(V_2 + V_1)/(V_2 - V_1)]}$$

This equation forms the basis of a simple method of refraction interpretation.  $x_c$  is always more than double the interface depth and is large if the depth is large or the difference in velocities is small. The *critical time*, obtained by dividing the critical distance by the direct-wave velocity, is also sometimes used.

The term ‘critical distance’ is also sometimes used for the minimum distance at which refractions return to the surface, i.e. the distance from the shot point at which energy arrives after reflection at the critical angle. This usage is not common amongst field crews since the refractions arrive after the direct wave at this point, and for some distance beyond, and are difficult to observe.

If more than one interface is involved (as in Figure 13.1), the ray that is critically refracted at the lowermost interface leaves the ground surface at an angle  $i_n$  given by:

$$\sin i_n = V_1/V_n$$

Thus, the angle at which energy leaves the ground surface for ultimate critical refraction at a deep interface depends only on the velocities in the uppermost

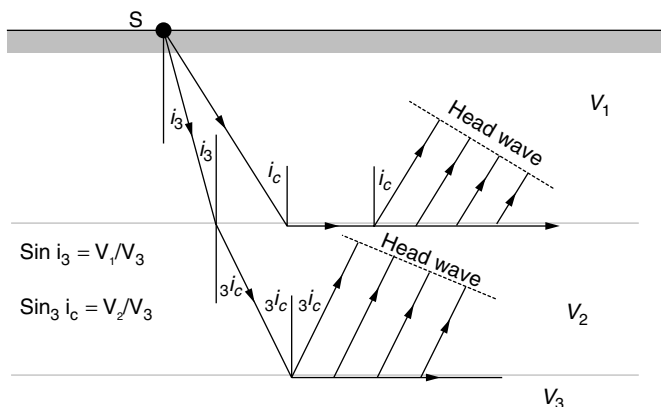


**Figure 13.1** Critical refraction at two interfaces:  $\sin i_c = V_1/V_2$ .

and lowermost layers involved, and not on the velocities in between. Even though this is a surprisingly simple result, cross-over interpretation becomes rather complicated for multiple layers and the intercept-time method discussed below (Section 13.2) is generally preferred.

### 13.1.3 Lengths of refraction spreads

A line of geophones laid out for a refraction survey is known as a *spread*, the term *array* being reserved for geophones feeding a single recording channel. Arrays are common in reflection work but are almost unknown in refraction surveys where the sharpest possible arrivals are needed.

Sufficient information on the direct wave and reasonable coverage of the refractor is obtained if the length of the spread is about three times the cross-over distance. A simple but often inaccurate rule of thumb states that the spread length should be eight times the expected refractor depth.

### 13.1.4 Positioning shots

In most refraction surveys, *short shots* are fired very close to the ends of the spread. Interpretation is simplified if these shots are actually at the end-geophone positions so that travel times between shot points are recorded directly. If this system is used, the geophone normally at the short shot location should be moved half-way towards the next in line before the shot is actually fired (and replaced afterwards). Damage to the geophone is avoided and some extra information is obtained on the direct wave.

*Long shots* are placed sufficiently far from the spread for all first arrivals to have come via the refractor, and short-shot data may therefore be needed before long-shot offsets can be decided. Distances to long shots need be measured accurately only if continuous coverage is being obtained and the long-shot to one spread is to be in the same place as a short or centre shot to another. If explosives are being used, it may be worthwhile using a very long offset if this will allow firing in water (see Section 11.2.1).

### 13.1.5 Centre shots

The information provided by a conventional four-shot pattern may be supplemented by a centre shot. Centre shots are especially useful if there are considerable differences in interpretation at opposite ends of the spread, and especially if these seem to imply different numbers of refractors. They may make it possible to obtain a more reliable estimate of the velocity along an intermediate refractor or to monitor the thinning of an intermediate layer that is hidden, at one end of the spread, by refractions from greater depths. An additional reliable depth estimate is obtained that does not depend on assumptions about the ways in which the thicknesses of the various layers vary along the spread, and there will be extra data on the direct wave velocity.

Centre shots are used less than they deserve. The extra effort is generally trivial compared to the work done in laying out the spread, and the additional and possibly vital information is cheaply obtained.

### 13.1.6 Annotation of field records

Hard-copy records can be (and should be) produced in the field from most of the seismographs now used for shallow refraction surveys. The several dozen records produced in a day's work that includes repeats, checks and tests as well as the completion of a number of different spreads must be carefully annotated if confusion is to be avoided. Annotations should obviously include the date and the name of the observer-in-charge, along with the survey location and spread number. Orientation should be noted, and the position of Geophone 1 should be defined. Unless the geophone spacing is absolutely uniform, a sketch showing shot and geophone locations should be added. If the interval between timing lines on the records can be varied and/or variable time offsets can be applied, these settings must also be noted. In many cases this is now done automatically.

Other items are optional. Amplifier gains and filter settings are not often recorded but such information may be useful. The number of shots or impacts combined in a single record can also be important with enhancement instruments. And, of course, features such as the use of S-wave geophones at some points or peculiarities in the locations of some of the geophones should always be noted.

Many of the items listed above can be printed directly on to the hard-copy record, provided they are first entered into the machine. This is often a more tedious, and more error-prone, process than simply writing the information on each record by hand.

### 13.1.7 Picking refraction arrivals

Picking first arrivals on refraction records relies on subjective estimates of first break positions (Figure 13.2) and may be difficult at remote geophones where the signal-to-noise ratio is poor. Some of the later peaks and troughs in the same wave train are likely to be stronger, and it is sometimes possible to work back from these to estimate the position of the first break. However, because high frequencies are selectively absorbed in the ground, the distance between the first break and any later peak gradually increases with increasing distance from the source. Furthermore, the trace beyond the first break is affected by many other arrivals as well as by later parts of the primary wave train, and these will modify peak and trough locations. Using later features to estimate first-arrival times should always be regarded as a poor substitute for direct picking.

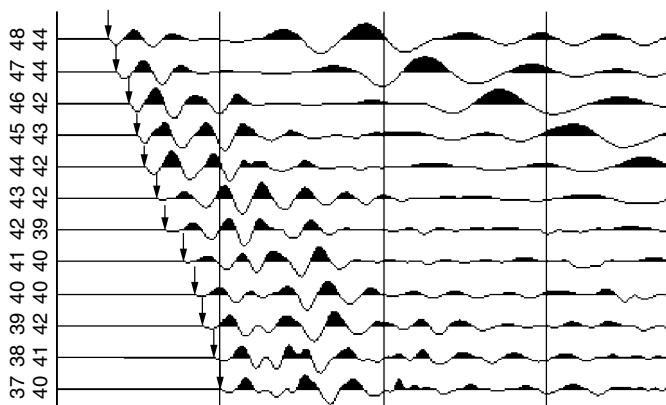


**Figure 13.2** Portion of a multi-channel refraction record, with first-break 'picks' identified by arrows. These become more difficult to make as signal-to-noise ratio worsens. This record would be considered good, and much more difficult decisions usually have to be made.

### 13.1.8 Time–distance plots

The data extracted from a refraction survey consist of sets of times (usually first-arrival times) measured at geophones at various distances from the source positions. Since these are plotted against vertical time axes and horizontal distance axes, the gradient of any line is equal to the reciprocal of a velocity, i.e. steep slopes correspond to slow velocities. All the data for a spread are plotted on a single sheet that has a working area covering only the ground where there are actually geophones (see Figure 13.8 accompanying Example 13.1). It is not necessary to show the long-shot positions. Since as many as five sets of arrivals may have to be plotted, as well as a set of time differences, different colours or symbols are needed to distinguish between data sets.

If the arrival times lie on a number of clearly defined straight-line segments, best-fit lines may be drawn. These are not actually necessary if the intercept-time interpretation method described below is used, and will be difficult to define if the arrival times are irregular because of variations in refractor depth. It is often best to draw lines through only the direct-wave arrivals (which should plot on straight lines), leaving refracted arrivals either unjoined or linked only by faint lines between adjacent points.

## 13.2 Field Interpretation

Interpretation is an essential part of refraction fieldwork because the success of a survey depends on parameters such as line orientation, geophone spacing,

shot positions and spread lengths, that can be varied almost at will. Only if analysis keeps pace with data collection will the right choices be made. Field interpretation has been made easier by computer programs that can be implemented on portable PCs or on the seismographs themselves but such programs are based on very simple models and are no substitute for actually thinking about the data.

### 13.2.1 Intercept times

The intercept time  $t_i$  is defined as the time at which the back-extrapolated refracted arrival line cuts the time axis. For a single refractor, it is related to the velocities and the refractor depth by the equation:

$$t_i = 2d\sqrt{(V_2^2 - V_1^2)}/V_1 V_2 = 2d/V_{1,2}$$

The quantity  $V_{1,2}$  is defined by this equation. It has the units of a velocity and is approximately equal to  $V_1$  if  $V_2$  is very much larger than  $V_1$ . The critical angle is then almost  $90^\circ$  and the delay suffered by the refracted ray in travelling between the surface and the refractor is close to double the vertical travel time. If the difference between  $V_1$  and  $V_2$  is small,  $V_{1,2}$  can be very large.

Intercept times are conventionally obtained by drawing best-fit lines through the refracted arrival times but even a very good fit is no guarantee that the depth of the refractor does not change in the region near the shot point, from which no refractions are observed. If, however, a long shot is used, there should be a constant difference between long-shot and short-shot arrival times at points towards the far end of the spread (Figure 13.3). An intercept time can then be obtained by subtracting this difference from the long-shot

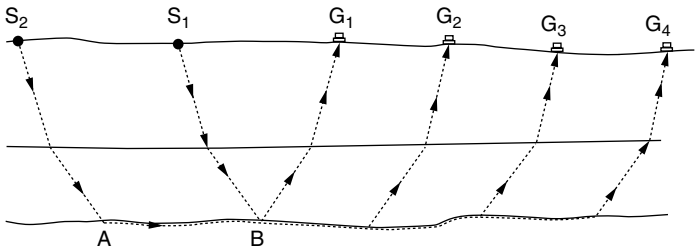


**Figure 13.3** Long-shot and short-shot travel paths for a three-layer case. The paths for energy travelling to the geophones from  $S_1$  and  $S_2$  via the lower refractor are identical from point B onwards. Upper refractor paths have been omitted for clarity.

arrival time at the short-shot location, and this can be done exactly if there is a geophone in this position when the long shot is fired (Example 13.1). Otherwise, use of the nearest long-shot arrival at least reduces the distance over which extrapolation must be made.

### 13.2.2 Multiple layers

The intercept-time equation can be extended to cases involving a number of critically refracting layers. If the intercept time associated with the  $n$ th refractor is  $t_n$ , then:

$$t_n = 2d_1/V_{1,n+1} + 2d_2/V_{2,n+1} \cdots + \cdots 2d_n/V_{n,n+1}$$

where  $d_n$  is the thickness of the  $n$ th layer, which overlies the  $n$ th refracting interface, at which velocity increases from  $V_n$  to  $V_{n+1}$ . The definition of the various quantities  $V_{m,n}$  is exactly analogous to the definition of  $V_{1,2}$  cited above. The presence of intermediate layers may be recognized by comparing long- and short-shot data, but at least two points are needed to define a velocity and three for any confidence to be placed in the estimate. At best, therefore, only four layers can be easily investigated with a 12-channel system.

Complicated field procedures can be devised to overcome this limitation; geophones may, for example, be moved one half-interval after a shot has been fired and the same shot-point can then be reused. Progress is extremely slow, and the problems presented by refractor topography, hidden layers and blind zones (Section 13.3) still exist. In most circumstances, firing multiple shots into modified spreads represents an attempt to extract more from the method than is really obtainable.

### 13.2.3 Effect of dip

Depths estimated from refraction surveys are related to geophone and shot-point elevations, which must therefore be measured to obtain a true picture of the subsurface refractor. Furthermore, the 'depths' determined are the perpendicular, not the vertical, distances to interfaces from shot points or geophones. With this proviso, 'horizontal' formulae can be applied without modification wherever the ground surface and the refractor are parallel. More usually their slopes will be different. Formulae are then most commonly quoted in terms of a horizontal ground and dipping refractors, but can equally well be applied if the ground slopes above, for example, a horizontal water table.

The intercept-time equations require the true value of  $V_2$  to be used. However, a wave that travels down-dip not only has to travel further at velocity  $V_2$  to reach more distant geophones, but also further at the slow velocity  $V_1$  in the upper layer (Figure 13.4). It therefore arrives late, with a low *apparent velocity*. The reverse is true shooting up-dip, when arrivals at

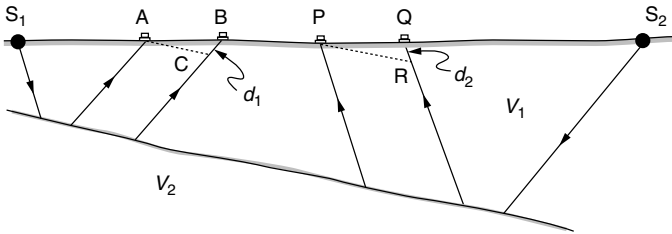


**Figure 13.4** Refraction at a dipping interface. The refracted energy from  $S_1$  arrives later at  $B$  than at  $A$  not only because of the greater distance travelled along the refractor but also because of the extra distance  $d_1$  travelled in the low velocity layer. Energy from  $S_2$  arrives earlier at  $P$  than would be predicted from the time of arrival at  $Q$ , by the time taken to travel  $d_2$  at velocity  $V_1$ . The lines  $AC$  and  $PR$  are parallel to the refractor.

further geophones may actually precede those at nearer ones. The slope of the line through the refracted arrivals on a time–distance plot depends on the dip angle,  $\alpha$ , according to:

$$V_{\text{app}} = V_2 / (1 + \sin \alpha)$$

If shots are fired from both ends of the spread, different apparent velocities will be measured because the sign of the dip angle will differ. For dips of less than about  $10^\circ$ , the true velocity is given by the dip-velocity equation:

$$2/V_2 = 1/V_{\text{up}} + 1/V_{\text{down}}$$

### 13.2.4 Refractor relief and true velocities

Most refractors, except the water table, are irregular.

If there were only a single local depression in an otherwise flat refractor, refracted arrivals from shots in opposite directions would plot on straight lines of equal slope, and the differences between the two arrival times at each geophone would plot on a line with double this slope. The exception to this rule would seem to be the geophone immediately above the depression. However, both waves would arrive late at this point (Figure 13.5) and, for small dips, the delays would be very similar. The difference between the arrival times would thus be almost the same as if no depression existed, plotting on the straight line generated by the horizontal parts of the interface. The argument can be extended to a refractor with a series of depressions and highs. Provided that the dip angles are low, the difference points will plot along a straight line with slope corresponding to half the refractor velocity. Where a refractor has a constant dip, the slope of the difference line will equal

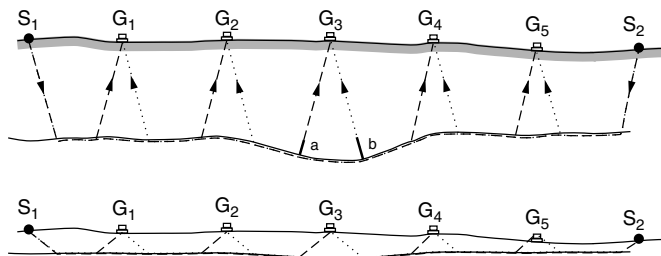


**Figure 13.5** Effect on travel times of a bedrock depression. The arrivals at  $G_3$  of energy from  $S_1$  and  $S_2$  are delayed by approximately the same amounts ('a' and 'b'). Note that, as in all the diagrams in this chapter, vertical exaggeration has been used to clarify travel paths. The lower version gives a more realistic picture of the likely relationships between geophone spacing and refractor depths and gradients.

the sum of the slopes of the individual lines, giving a graphical expression to the dip-velocity equation.

The approach described above generally works far better than the very qualitative 'proof' (and the rather contrived positioning of the geophones in Figure 13.5) might suggest. Changes in slopes of difference lines correspond to real changes in refractor velocity, so that zones of weak bedrock can be identified.

The importance of long shots is obvious, since the part of the spread over which the first arrivals from the short shots at both ends have come via the refractor is likely to be rather short and may not even exist. It is even sometimes possible, especially when centre shots have been used, for the differencing technique to be applied to an intermediate refractor.

Differences are easily obtained directly from the plot using dividers, or a pencil and a straight-edged piece of paper. They are plotted using an arbitrary time zero line placed where it will cause the least confusion with other data (see Figure 13.8).

### 13.2.5 Reciprocal time interpretation

The *reciprocal time*,  $t_R$ , is defined as the time taken for seismic energy to travel between the two long-shot positions. The difference between  $t_R$  and the sum of the travel times  $t_A$  and  $t_B$  from the two long-shots to any given geophone,  $G$ , is:

$$t_A + t_B - t_R = 2D/F$$

where  $D$  is the depth of the refractor beneath  $G$  and  $F$  is a *depth conversion factor* (Figure 13.6). If there is only a single interface,  $D$  is equal to the



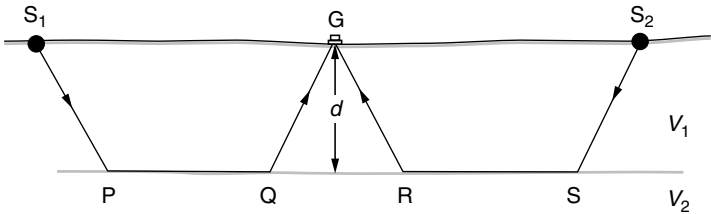


**Figure 13.6** Reciprocal time interpretation. The sum of the travel times from  $S_1$  and  $S_2$  to  $G$  differs from the reciprocal time,  $t_R$ , taken to travel from  $S_1$  to  $S_2$  by the difference between the times taken to travel  $QR$  at velocity  $V_2$  and  $QGR$  at velocity  $V_1$ .

thickness,  $d$ , of the upper layer and  $F$  is equal to  $V_{1,2}$ . If there are more interfaces,  $F$  is a composite of all the velocities involved, weighted according to the layer thicknesses. At the short shots  $2D/F = t_i$  (the intercept time) and the  $F$  values can be calculated. The ways in which  $F$  varies between these points may be very complex, but linear interpolation is usually adequate in the field (Example 13.1).

Although  $t_R$  can be measured directly, it is more convenient to calculate it from the equation above using the intercept times. This can be done provided that geophones are located at the short-shot points when the long shots are fired (so that  $t_A + t_B$  at those points can be measured). The estimates of  $t_R$  made using the data from the two ends should agree within the limits of error of the method (i.e. within 1–2 msec). If they are not, the raw data and the calculations should be thoroughly checked to find the reason for the discrepancy.

Short-shot reciprocal times are measured directly if short-shots are fired at end-geophone positions, and the fact that they should be equal may help in picking arrivals. However, they have little interpretational significance.

### 13.3 Limitations of the Refraction Method

First-arrival refraction work uses only a small proportion of the information contained in the seismic traces, and it is not surprising that interpretation is subject to severe limitations. These are especially important in engineering work; in low-velocity-layer studies only a time delay estimate is sought and short shots alone are often sufficient.

#### 13.3.1 Direct waves

The *ground roll* consists of a complex of P and S body waves and Love and Rayleigh surface waves travelling with different but generally slow velocities.

There is often some doubt as to which component actually produces the first break, since conventional geophones respond only poorly to the horizontal ground motions of direct P-waves. Close to the source, enough energy is associated with the P-waves for the response to be measurable, but at greater distances the first breaks may record the arrival of S-waves, surface waves or even the air wave.

The complex character of the direct wave may be among the reasons for the commonly observed failure of the best-fit arrival line to pass through the origin. Delays in the timing circuits may also play a part but can be determined by direct experiment, with a detonator or a light hammer blow close to a geophone. A more important reason may be that the amplifier gains at geophones close to the shot point have been set so low that the true first arrivals have been overlooked (Figure 13.7). Full digital storage of the incoming signals should allow the traces to be examined individually over a range of amplifications, but if this is not possible, then the most reliable velocity estimates will be those that do not treat the origin as a point on the line.

### 13.3.2 Vertical velocities

However much care is taken to obtain valid direct-wave or refracted-wave velocities, the refraction method is fundamentally flawed in that the depth equations require vertical velocities but what are actually measured are horizontal velocities. If there is significant anisotropy, errors will be introduced.

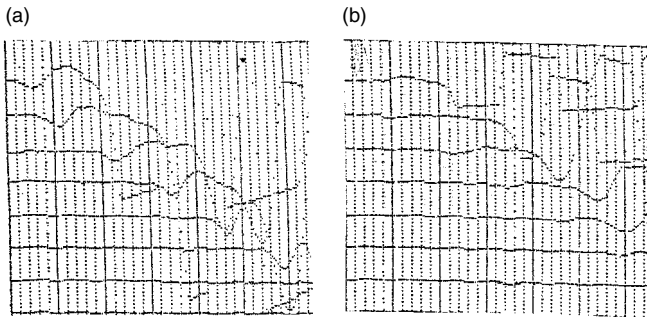


**Figure 13.7** Hard copy of a single stored data set played back at two different amplifications. The first arrivals clearly visible on (a) would probably be overlooked or dismissed as noise on (b). A direct wave velocity based on (b) would be roughly correct provided that the best-fit line was not forced through the origin. The cross-over distance would also be wrong but the intercept time would not be affected, provided that the refracted arrivals were amplified sufficiently.

This is a problem for interpreters rather than field observers but the latter should at least be aware of the importance of using any boreholes or recent excavations for calibration or to measure vertical velocities directly.

### 13.3.3 Hidden layers

A refractor that does not give rise to any first arrivals is said to be *hidden*. A layer is likely to be hidden if it is much thinner than the layer above and has a much lower seismic velocity than the layer below. Weathered layers immediately above basement are often hidden.

The presence of a hidden layer can sometimes be recognized from second arrivals but this is only occasionally possible, in part because refracted waves are strongly attenuated in thin layers.

A layer may also be hidden even if the head wave that it produces does arrive first over some part of the ground surface, if there are no appropriately located geophones. Concentrating geophones in the critical region can sometimes be useful (although never convenient) but the need to do so will only be recognized if preliminary interpretations are being made on a daily basis.

### 13.3.4 Blind zones

If velocity decreases at an interface, critical refraction cannot occur and no refracted energy returns to the surface. Little can be done about these *blind* interfaces unless vertical velocities can be measured directly.

Thin high-velocity layers such as perched water tables and buried terraces often create blind zones. The refracted waves within them lose energy rapidly with increasing distance from the source and ultimately become undetectable. Much later events may then be picked as first arrivals, producing discontinuities in the time–distance plot. A similar effect is seen if the layer itself ends abruptly.

### 13.3.5 Limitations of drilling

Despite the limitations of refraction surveys, interpretations are not always wrong when they disagree with drill hole data. Only a very small subsurface volume is sampled by the drill, and many drill tests of drift thickness have been terminated in isolated boulders some distance above the true top of bedrock. It is always important that explanations are found for any differences between drilling and seismic results.

---

#### Example 13.1

Field interpretation of a four-shot refraction spread with long shot (LS) and short shot (SS) arrivals from west (W) and east (E) ends plotted on same set

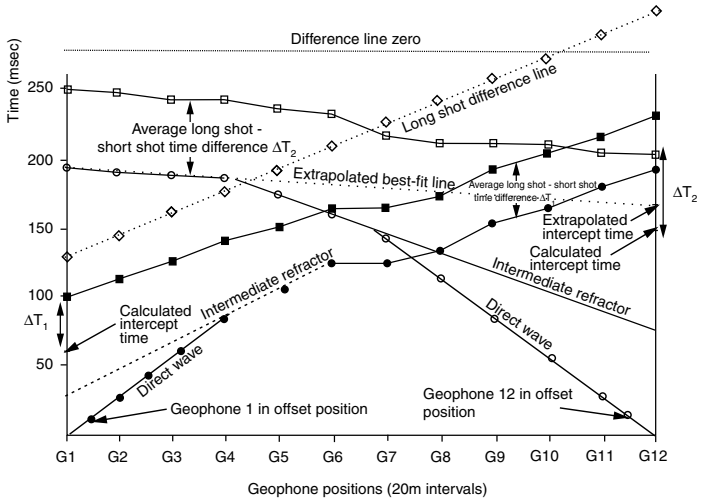


**Figure 13.8** Time–distance plot for a four-shot refraction spread. The long-shot difference times, indicated by open circles, are referred to a zero line arbitrarily placed at  $t = 280 \text{ m s}^{-1}$ . Note the difference between the intercept time obtained by extrapolation of short-shot data and by using long-shot–short-shot difference times, for the G12 position. Extrapolation of the refracted arrival line back to zero time would be even more difficult for the G1 position and could lead to an even more erroneous interpretation. West is to the left of the plot (Example 13.1).

of axes (Figure 13.8). After plotting the data, interpretation proceeds in the following stages.

#### Stage 1 Base refractor intercept times

**Measure LS(W)–SS(W) time differences.** These are roughly constant and close to 41 ms from G6 to G12, indicating that in this region the SS(W) arrivals have come from base refractor. Similarly, LS(E)–SS(E) time differences are close to 59 ms, from G1 to G4.

**Intercept times:** LS(W) time at W end = 101 ms.  
Intercept time =  $101 - 41 = 60 \text{ ms}$ .  
LS(E) time at E end = 208 ms.  
Intercept time =  $208 - 59 = 149 \text{ ms}$ .

Note the LS(E) difference from the extrapolated intercept time of about 170 ms.

## Stage 2 Velocities

### Direct-wave velocity:

Straight line from W origin through nearby SS(W) arrivals extends 60 m to G4.

$$\text{Velocity } V_1 = 60/0.079 = 759 \text{ m s}^{-1}$$

Straight line from E origin through nearby SS(E) arrivals extends 100 m to G7.

$$\text{Velocity } V_1 = 100/0.134 = 746 \text{ m s}^{-1} \quad \text{Average } V_1 \text{ value} = 750 \text{ m s}^{-1}$$

### Intermediate refractor:

Arrivals at G5 from SS(W) and at G5 and G6 from SS(E) do not belong to the 'base refractor' sets (see Stage 1) nor do they fall on the direct-wave arrival line, suggesting the presence of an intermediate, 'V<sub>2</sub>', refractor. The V<sub>2</sub> velocity is poorly controlled but the arrivals lines should pass above all direct wave (V<sub>1</sub>) and base refractor first arrivals. For the most likely positions, as shown;

$$\text{SS(W): } V_2 = 1470 \text{ m s}^{-1} \quad \text{Intercept time} = 29 \text{ ms}$$

$$\text{SS(E): } V_2 = 1560 \text{ m s}^{-1} \quad \text{Intercept time} = 77 \text{ ms}$$

These velocities suggest that the interface is probably the water table, with a velocity of about 1500 m s<sup>-1</sup>.

### Base refractor velocity:

Plot LS(W)–LS(E) time differences at each geophone, using a convenient (280 ms) line as time zero.

$$V_3 = 2/(\text{slope of difference line}) = 2 \times 220/0.182 = 2420 \text{ m s}^{-1}$$

### Velocity functions:

$$\begin{aligned} V_{1,2} &= V_1 \times V_2 / \sqrt{(V_2^2 - V_1^2)} = 750 \times 1500 / \sqrt{(1500^2 - 750^2)} \\ &= 870 \text{ m s}^{-1} \end{aligned}$$

$$\begin{aligned} V_{1,3} &= V_1 \times V_3 / \sqrt{(V_3^2 - V_1^2)} = 750 \times 2420 / \sqrt{(2420^2 - 750^2)} \\ &= 790 \text{ m s}^{-1} \end{aligned}$$

$$\begin{aligned} V_{2,3} &= V_2 \times V_3 / \sqrt{(V_3^2 - V_2^2)} = 1500 \times 2420 / \sqrt{(2420^2 - 1500^2)} \\ &= 1910 \text{ m s}^{-1} \end{aligned}$$

*Stage 3 Depths at shot points*

**Depths to intermediate refractor ( $d_1 = \frac{1}{2}t_i V_{1,2}$ ):**

$$\text{W end: } d_1 = \frac{1}{2} \times 0.029 \times 870 = 12.6 \text{ m}$$

$$\text{E end: } d_1 = \frac{1}{2} \times 0.077 \times 870 = 33.5 \text{ m}$$

**Thickness of intermediate layer ( $d_2 = \frac{1}{2}[t_i - 2d_1/V_{1,3}] \times V_{2,3}$ ):**

$$\text{W end: } d_2 = \frac{1}{2} \times \{0.060 - 25.2/790\} \times 1910 = 26.8 \text{ m}$$

$$D = 26.8 + 12.6 = 39.4 \text{ m}$$

$$\text{E end: } d_2 = \frac{1}{2} \times \{0.149 - 67.0/790\} \times 1910 = 61.3 \text{ m}$$

$$D = 33.5 + 61.3 = 94.8 \text{ m}$$

*Stage (4) Reciprocal time interpretation (example using Geophone 8)*

**Reciprocal time ( $t_A + t_B - t_i$ )**

$$\text{W end: } t_R = 101 + 254 = 295 \text{ ms}$$

$$\text{E end: } t_R = 233 + 208 - 149 = 292 \text{ ms}$$

$$\text{Average} = 293 \text{ ms}$$

**Depth conversion factors at short shots ( $F = 2 \times D/t_i$ )**

$$\text{W end: } F = 2 \times 39.4/0.060 = 1310 \text{ m s}^{-1}$$

$$\text{E end: } F = 2 \times 94.8/0.149 = 1270 \text{ m s}^{-1}$$

$$F \text{ at G8 (by interpolation)} = 1280 \text{ m s}^{-1}$$

**Depth at G8 ( $D = t_A + t_B - t_R$ )**

$$D = \frac{1}{2} \times (0.174 + 0.213 - 0.293) \times 1280 = 60.2 \text{ m}$$


---



## APPENDIX

---

Terrain corrections for Hammer zones B to M, in SI gravity units. Row R lists the inner and outer radii of the zones, in metres up to and including Zone G and in kilometres thereafter. Row N lists the number of compartments into which each zone is divided.

Zone:	B	C	D	E	F	G	
R (m):	2	166	53.3	170	390	895	1530
N	4	6	6	8	8	12	
0.01	0.5	1.9	3.3	7.6	11.5	24.9	
0.02	0.7	2.6	4.7	10.7	16.3	35.1	
0.03	0.8	3.2	5.8	13.1	19.9	43.3	
0.04	1.0	3.8	6.7	15.2	23.0	49.8	
0.05	1.1	4.2	7.5	17.0	25.7	55.6	
0.06	1.2	4.6	8.2	18.6	28.2	60.9	
0.07	1.3	5.0	8.9	20.1	30.4	65.8	
0.08	1.4	5.4	9.5	21.5	32.6	70.4	
0.09	1.5	5.7	10.1	22.9	34.5	74.7	
0.10	1.6	6.0	10.6	24.1	36.4	78.7	
0.20	2.4	8.7	15.1	34.2	51.6	111.6	
0.30	3.2	10.9	18.6	42.1	63.3	136.9	
0.40	3.9	12.9	21.7	48.8	73.2	158.3	
0.50	4.6	14.7	24.4	54.8	82.0	177.4	
0.60	5.3	16.5	26.9	60.2	90.0	194.7	
0.70	6.1	18.2	29.3	65.3	97.3	210.7	
0.80	6.9	19.9	31.5	70.1	104.2	225.6	
0.90	7.8	21.6	33.7	74.7	110.8	239.8	
1.00	8.7	23.4	35.7	79.1	117.0	253.2	

Effect      Height differences (metres)  
(g.u.):



# APPENDIX

Zone:	H	I	J	K	L	M	
R (km):	1.53	2.61	4.47	6.65	99	14.7	21.9
N:	12	12	16	16	16	16	
0.01	32	42	72	88	101	125	
0.02	46	60	101	124	148	182	
0.03	56	74	125	153	186	225	
0.04	65	85	144	176	213	262	
0.05	73	95	161	197	239	291	
0.06	80	104	176	216	261	319	
0.07	86	112	191	233	282	346	
0.08	92	120	204	249	303	370	
0.09	96	127	216	264	322	391	
0.10	103	134	228	278	338	413	
0.20	146	190	322	394	479	586	
0.30	179	233	396	483	587	717	
0.40	206	269	457	557	679	828	
0.50	231	301	511	624	759	926	
0.60	253	330	561	683	832	1015	
0.70	274	357	606	738	899	1097	
0.80	293	382	648	790	962	1173	
0.90	311	405	688	838	1020	1244	
1.00	328	427	726	884	1076	1312	

Effect      Height differences (metres)  
(g.u.):

These tables list the exact height differences which, assuming a density of  $2.0 \text{ Mg m}^{-3}$ , will produce the tabulated terrain effects. Thus a height difference of 32 m between the gravity station elevation and the average topographic level in one compartment of Zone E (between 170 and 390 m from the gravity station) would be associated with a terrain effect of about 0.18 g.u. Most commercial gravity meters have sensitivities of only 0.1 g.u. but an additional decimal point is used in the tabulation to avoid the accumulation of 'rounding off' errors when summing the contributions from large numbers of compartments.

## BIBLIOGRAPHY

---

### 1 Books

- Clark, A.** (1996) *Seeing Beneath the Soil – Prospecting Methods in Archaeology* (Second Edition), Routledge, London, 192 pp.
- Dentith, M.C., Frankcombe, K.F., Ho, S.E., Shepherd, J.M., Groves, D.I. and Trench, A.** (eds) (1995) *Geophysical Signatures of Western Australian Mineral Deposits*, Geology and Geophysics Department (Key Centre) and UWA Extension, University of Western Australia, Publication 26, and Australian Society of Exploration Geophysicists, Special Publication 7, 454 pp.
- Emerson, D.W., Mills, K.J., Miyakawa, K., Hallett, M.S. and Cao, L.Q.** (1993) *Case Study, Koongarra NT*, Australian Society of Exploration Geophysicists, Special Publication 8, 71 pp.
- Hoover, D.B., Heran, W.D. and Hill, P.L.** (Eds) (1992) *The Geophysical Expression of Selected Mineral Deposit Models*, United States Department of the Interior, Geological Survey Open File Report 92-557, 128 pp.
- Kearey, P., Brooks, M. and Hill, I.** (2002) *An Introduction to Geophysical Exploration* (Third Edition), Blackwell Science, Oxford, 262 pp.
- McCann, D.M., Fenning, P. and Cripps, J.** (Eds) (1995) *Modern Geophysics in Engineering Geology*, Engineering Group of the Geological Society, London, 519 pp.
- Mussett, A.E. and Khan, M.A.** (2000) *Looking into the Earth: An Introduction to Geological Geophysics*, Cambridge University Press, Cambridge, 470 pp.
- Nettleton, L.L.** (1976) *Gravity and Magnetism in Oil Prospecting*, McGraw-Hill, New York, 464 pp.
- Parasnis, D.S.** (1996) *Principles of Applied Geophysics* (Fifth Edition), Chapman & Hall, London, 456 pp.
- Reynolds, J.M.** (1997) *An Introduction to Applied and Environmental Geophysics*, Wiley, Chichester, 796 pp.
- Sharma, P.V.** (1997) *Environmental and Engineering Geophysics*, Cambridge University Press, Cambridge, 475 pp.
- Telford, W.M., Geldart, L.P., Sheriff, R.E. and Keys, D.A.** (1990) *Applied Geophysics* (Second Edition), Cambridge University Press, Cambridge, 770 pp.
- Van Blaricom, R.** (1992) *Practical Geophysics II*, Northwest Mining Association, Spokane, 570 pp.
- Whitely, R.J.** (Ed.) (1981) *Geophysical Case Study of the Woodlawn Orebody, New South Wales, Australia*, Pergamon Press, Oxford, 588 pp.

## 2 Papers

- Barker, R.D.** (1981) The offset system of electrical resistivity sounding and its use with a multicore cable. *Geophysical Prospecting*, **29**, 128–43.
- Bhattacharya, B.B. and Sen, M.K.** (1981) Depth of investigation of collinear electrode arrays over an homogeneous anisotropic half-space in the direct current method. *Geophysics*, **46**, 766–80.
- Corwin, R.F. and Hoover, D.B.** (1979) The self-potential method in geothermal exploration. *Geophysics*, **44**, 226–45.
- Fraser, D.C.** (1969) Contouring of VLF data. *Geophysics*, **34**, 958–67.
- Hammer, S.** (1939) Terrain corrections for gravimeter stations. *Geophysics*, **4**, 184–94.
- Hawkins, L.V.** (1961) The reciprocal method of routine shallow seismic refraction investigations. *Geophysics*, **26**, 806–19.
- IGA Division V, Working Group 8** (1995) International Geomagnetic Reference Field, 1995 Revision. *Preview*, **58**, 27–30.
- Longman, I.M.** (1959) Formulas for computing the tidal accelerations due to the moon and sun. *Journal of Geophysical Research*, **64**, 2351–5.
- Morelli, C., Gantar, C., Honkasalo, T., McConnell, R.K., Szabo, B., Tanner, J.G., Uotila, U. and Whalen, C.T.** (1974) *The International Gravity Standardization Net 1974*, International Association of Geodesy, Special Publication 4.
- Quick, D.H.** (1974) The interpretation of gradient array chargeability anomalies. *Geophysical Prospecting*, **19**, 551–67.
- Scollar, I., Weidner, B. and Segeth, K.** (1986) Display of archaeological data. *Geophysics*, **51**, 623–33.
- Staltari, G.** (1986) The Que River TEM case-study. *Exploration Geophysics*, **17**, 125–128.
- Turner, G., Siggins, A.F. and Hunt, L.D.** (1993) Ground penetrating radar – will it clear the haze at your site? *Exploration Geophysics*, **24**, 819–32.

## 3 Websites

### (a) Instrument manufacturers

ABEM	<a href="http://www.abem.com/">http://www.abem.com/</a>
Geometrics	<a href="http://www.geometrics.com">http://www.geometrics.com</a>
Geometrics (UK) (now Geomatrix)	<a href="http://www.georentals.co.uk">http://www.georentals.co.uk</a>
Geonics	<a href="http://www.geonics.com/">http://www.geonics.com/</a>
Electromagnetic Instruments Inc.	<a href="http://www.emiinc.com">http:// www.emiinc.com</a>
Scintrex	<a href="http://www.scintrexltd.com/">http://www.scintrexltd.com/</a>
Zonge	<a href="http://www.zonge.com">http:// www.zonge.com</a>

### (b) Organizations

European Association of Geoscientists  
& Engineers (EAGE)

<http://www.eage.nl/>

Environmental and Engineering Geophysical Society (EEGS)	<a href="http://www.eegs.org/">http://www.eegs.org/</a>
Society of Exploration Geophysicists (SEG)	<a href="http://www.seg.org/">http://www.seg.org/</a>
Australian Society of Exploration Geophysicists (ASEG)	<a href="http://www.aseg.org.au">http:// www.aseg.org.au</a>
Canadian Society of Exploration Geophysicists (CSEG)	<a href="http://www.cseg.ca/">http://www.cseg.ca/</a>

## 4 Notes

### IGSN71

Descriptions of IGSN71 international base stations can be obtained from the Bureau Gravimetrique International, CNES, 18, Avenue Edouard Belin, 31055 Toulouse Cedex, France. National and state geological surveys usually maintain subsidiary base networks within their areas of responsibility.

### WGS84 Ellipsoidal Gravity Formula

The basic formula is

$$g_{\text{norm}} = \frac{978032.67714(1 + 0.00193185138639 \cdot \sin^2 L)}{\sqrt{(1 - 0.00669437999013 \cdot \sin^2 L)}}$$

To this there has to be added a correction for the gravitational effect of the atmosphere, given by

$$\delta g = 0.87 \cdot \exp(-0.116h^{1.047})$$

Application of this correction brings the normal sea-level gravity values back to values similar to those given by IGF1967.

### IGRF

ASCII files of IGRF coefficients and computer programs for synthesizing field components are available from World Data Center A, Solid Earth Geophysics, National Geophysical Data Center, NOAA, Code EICCI, 325 Broadway, Boulder, CO 80303-3328, USA or World Data Centre CI (Geomagnetism), British Geological Survey, Murchison House, West Mains Road, Edinburgh EH9 3LA, UK.



# INDEX

---

- accuracy, defined 12
- alkali-vapour magnetometers 20, 60–61
- Alphacard 78
- alpha particles 71, 77–78
- anomalies 15–17
- Archie's Law 86, 87
- arrays
  - electrical 98–101
  - seismic 201–202
- assays, radiometric 79
- attenuation constant 5, 168
- audiomagnetotellurics (AMT) 162
- base stations 22–25, 42, 119
- beta particles 71
- Biot-Savart Law 143
- blind zones (seismic) 218
- Bouguer correction 39–40
- Bouguer plate 4, 46–47
- bow-tie (processing artefact) 205
- cables 7, 89–90, 107, 171–172, 191–192
- caesium vapour
  - magnetometers 20, 60–61
- capacitive coupling 97, 113–116
- chargeability 121–122
- coil systems, electromagnetic 129–130, 131, 144
- common depth-point (CDP)
  - methods 205
- common mid-point (CMP)
  - methods 173, 203–205
- conductivity, electrical 85, 138–140, 168–169
- connectors 8, 90, 192
- contact resistance 89, 97
- continuous profiling 19–22, 115
- controlled source
  - audiomagnetotellurics (CSAMT) 162–165
- contours
  - by intercepts 66
  - by computer program 18, 20–22
- coupling
  - in e.m. surveys 130, 135–137
  - in VLF surveys 152, 155
  - as noise in IP surveys 124–125
- critical distance 208
- cross-talk 7, 188, 192
- crossover distance 208
- Curie temperature 52, 57–58
- data loggers 7, 12, 19–22
- decay constant, radioactive 5
- decay curve, induced
  - polarization 120–121
- decay series, radioactive 72–74
- decibel 167
- declination, magnetic 54
- densities 30–31

- 
- |                         |                            |                                 |                        |
|-------------------------|----------------------------|---------------------------------|------------------------|
| depth penetration       |                            | fluxgate magnetometer           | 61–62                  |
| electrical methods      | 92–93,<br>102–106, 115–116 | Fraser filter                   | 159–160                |
| electromagnetic methods | 92–93, 138, 145            | free-air correction             | 38                     |
| radar                   | 170–171, 174               | frequency-domain IP             | 124                    |
| seismic refraction      | 209                        |                                 |                        |
| depth-sounding          |                            | gamma (nT)                      | 51                     |
| CWEM                    | 138                        | gamma rays                      | 71–72,                 |
| DC                      | 108–113                    | Gaussian distribution           | 14                     |
| TEM                     | 145, 146                   | Geiger counters                 | 75                     |
| dielectric constant     | 168, 169                   | geomagnetic field               | 53–56                  |
| diffraction patterns    | 177–178, 205, 206          | geophones                       | 188–189, 190, 191      |
| differential GPS        |                            | global positioning satellites   |                        |
| (DGPS)                  | 25, 26                     | (GPS)                           | 20, 25–26, 27, 28      |
| dipole aerial           | 172–173                    | gravitational constant (G)      | 29                     |
| dipole-dipole array     | 99,<br>100, 103, 127       | gravity meters                  | 31–38                  |
| dipole field            | 4                          | gravity unit (g.u.)             | 29                     |
| direct waves            | 179, 216–217               | ground radar (GPR)              | 167–178                |
| diurnal changes,        |                            | ground roll                     | 179                    |
| magnetic                | 56–57, 63–64               |                                 |                        |
| Dix velocity            | 198–199                    | half-life, radioactive          | 5, 72–74               |
| drift, instrumental     | 13,<br>22–23, 45, 61       | half-width                      | 16, 17, 47–48          |
| dynamic range           | 194                        | Hammer chart                    | 40,<br>41, 43, 223–224 |
|                         |                            | hammer sources                  |                        |
| Earth gravity field     | 29, 30                     | (seismic)                       | 183, 187               |
| Earth magnetic field    | 53–56                      | heading errors                  | 20–21                  |
| Earth tides             | 44–45                      | head-wave                       | 207–208                |
| eddy currents           | 60,<br>93, 129, 145, 151   | hidden layers (seismic)         | 218                    |
| elastic constants       | 180                        | hydrophones                     | 191                    |
| electrodes              | 88–89                      |                                 |                        |
| electrode polarization  | 120                        | IGRF (international geomagnetic |                        |
| electron volt (eV)      | 71–72                      | reference field)                | 56, 227                |
| elliptical polarization | 153–155                    | IGF (international gravity      |                        |
| explosives              | 183–186                    | formula)                        | 29, 227                |
| exponential decay       | 4, 5, 92                   | IGSN71                          | 29, 227                |
|                         |                            | image processing                | 18                     |
|                         |                            | induced polarization            |                        |
|                         |                            | (IP)                            | 120–127                |
|                         |                            | induction, electromagnetic      |                        |
|                         |                            |                                 | 93, 144–146            |

# INDEX

induction number	138	numbering systems	11
intercept times	212–213	offset Wenner array	101, <i>111</i>
interpretation		Overhauser effect	
gravity	46–49	magnetometer	60
magnetic	67–70	ohm-metre	85
resistivity	<i>104, 114</i>	P-waves	179, 207
seismic refraction	217–221	permeability (magnetic)	2, 168
interval velocity,		permittivity (electrical)	168, 169
seismic	198–199	Peters' method	69–70
inverse-square law	2–4	percent frequency effect	
isotopes	72–74	(PFE)	121–122
Karous-Hjelt (K-H)		phase	
filter	159–160	in electromagnetics	93,
Konigsberger ratio	52	<i>94, 153–155, 162, 164</i>	
latitude correction,		in induced polarization	93,
gravity	29, 38	<i>94, 122, 124–125</i>	
levelling errors	36–37	pixel	18
loss tangent	168	plugs	8, 192
magnetic storms	26, 57	Poisson ratio	180
magnetometers	<i>9, 20, 58–62</i>	Poynting vector	<i>150</i>
magnetometer tuning	63	power supplies	6, 122
magnetotellurics	162	precision, defined	12
membrane polarization	120	profiles	<i>16, 17–18, 108</i>
metal factor	122	profiling, electrical	107–108
migration	178	proton precession magnetometer	
milligal (mGal)	29	<i>9, 58–60, 63</i>	
multiple reflections	200	pseudo-sections	18,
mutual inductance	132	<i>112–113, 114, 126–127</i>	
nanoTesla (nT)	51	quadrature (phase)	93,
Nettleton's method	49	<i>94, 153–155</i>	
networks	24–25	radar	167–178
noise	7, 13–14, 67,	radioactive decay	5, 72–74
<i>106, 175, 188, 192, 191</i>		rain	8–10, 117–118
normal moveout		ray-paths	181–182
(NMO)	197–198	reciprocal time interpretation	
notebooks	11–12,	<i>215–216</i>	
<i>45–46, 64–67, 81, 108</i>			



- reflection coefficient
  - radar 168–169
  - seismic 197
- relative effect, in geophone
  - arrays 202
- remanence 52
- resistivity 85–88, 97–98
- response function 131–132
- response parameter 132
- rippability 181
- root-mean-square (RMS)
  - velocity 198
- S-waves 179, 189, 191
- SP (Self-Potential)
  - method 117–120
- safety 185–186
- Schlumberger array 99, 100, 103–106, 109–110
- scintillometers 75–76
- secant-chaining 136
- self-inductance 131
- seismographs 192–195
- sensitivity, defined 12, 194
- sferics 149, 162
- shoot-back EM system 130
- signal-contribution
  - sections 101–102, 103
- skin-depth 5, 92, 165
- Slingram 130–135, 145
- Snell's Law 182
- spectrometers (gamma ray) 76–77
- stacking 14, 18
- standard deviation 14
- streaming potentials 117–118
- stripping ratios, radiometric 77
- susceptibility, magnetic 52–53
- terrain corrections,
  - gravity 39, 40, 43–44
- time-break 186–188
- time-domain EM (TEM) 144–147
- time-domain IP 122–124, 147
- toolkits 10
- torsion magnetometers 58
- transient electromagnetics (TEM) 95, 144–147
- Turam 141–143
- two- $\pi$  geometry 4, 79–80
- two-way times (TWT) 176, 205
- type curves, electrical 65, 112
- variance 14
- vector addition 1–2
- velocities
  - seismic waves 180–181, 207
  - radar waves 168–169
- VLF (very low frequency)
  - waves 149–150
- VLF transmitters 149–150, 151
- weight-drop (seismic) 183, 184, 188
- Wenner array 98, 99, 103–106, 111, 114